

Green Chemistry

Cutting-edge research for a greener sustainable future

www.rsc.org/greenchem

Volume 10 | Number 2 | February 2008 | Pages 141–256



ISSN 1463-9262

Perchyonok *et al.*
Recent advances in C–H bond
formation in aqueous media
Christensen *et al.*
Aerobic oxidation of aldehydes



1463-9262(2008)10:2;1-G

RSC Publishing

Covering the complete spectrum

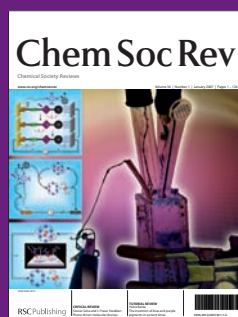
Multidisciplinary chemical sciences



For communications...

ChemComm is a weekly high impact blend of quality research from across the chemical sciences, offering exceptionally fast publication times.

www.rsc.org/chemcomm



For reviews...

Chem Soc Rev provides highly cited, succinct and reader friendly review articles each month, covering topics of international, multidisciplinary and social interest.

www.rsc.org/chemsocrev



For full papers...

The home of quality, original and significant work of wide general appeal, the monthly issue of *New Journal of Chemistry* is the perfect place to publish your research.

www.rsc.org/njc



For the latest news...

The award-winning *Chemistry World* is a lively and informative guide to the latest developments across the chemical sciences. Daily web updates ensure you'll always be kept informed of the science hitting the headlines.

www.chemistryworld.org

RSC Publishing

www.rsc.org/publishing

Registered Charity Number 207890

Green Chemistry

Cutting-edge research for a greener sustainable future

www.rsc.org/greenchem

RSC Publishing is a not-for-profit publisher and a division of the Royal Society of Chemistry. Any surplus made is used to support charitable activities aimed at advancing the chemical sciences. Full details are available from www.rsc.org

IN THIS ISSUE

ISSN 1463-9262 CODEN GRCHFJ 10(2) 141–256 (2008)



Cover

See Perchyonok *et al.*, pp. 153–163.

Recent advances in free radical chemistry in water have expanded the versatility and flexibility of carbon–hydrogen bond formation in aqueous media. This review highlights the substantial progress which has been made in the last decade to “tame” the reactive free radical species in aqueous phase reactions and highlights choices, reasons and applications of the methodology. Images reproduced with permission from V. Tamara Perchyonok from *Green Chem.*, 2008, 10, 153.

CHEMICAL TECHNOLOGY

T9

Drawing together research highlights and news from all RSC publications, *Chemical Technology* provides a ‘snapshot’ of the latest applications and technological aspects of research across the chemical sciences, showcasing newsworthy articles and significant scientific advances.

Chemical Technology

February 2008/Volume 5/issue 2

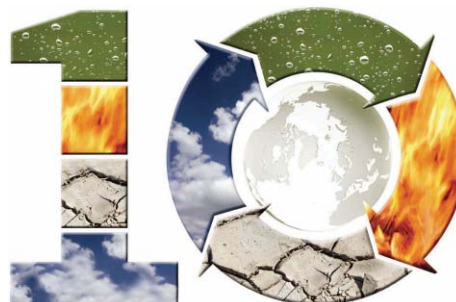
www.rsc.org/chemicaltechnology

EDITORIAL

151

Green chemistry, green solvents, and free radical reactions in aqueous media

Chao-Jun Li discusses the ideas behind green chemistry and green solvents and introduces the tutorial review on radical reactions that appears in this issue.



EDITORIAL STAFF

Editor

Sarah Ruthven

Assistant editor

Sarah Dixon

Publishing assistant

Ruth Bircham

Team leader, serials production

Stephen Wilkes

Technical editor

Edward Morgan

Production administration coordinator

Sonya Spring

Administration assistantsClare Davies, Donna Fordham, Kirsty Lunnon,
Julie Thompson**Publisher**

Emma Wilson

Green Chemistry (print: ISSN 1463-9262; electronic: ISSN 1463-9270) is published 12 times a year by the Royal Society of Chemistry, Thomas Graham House, Science Park, Milton Road, Cambridge, UK CB4 0WF.

All orders, with cheques made payable to the Royal Society of Chemistry, should be sent to RSC Distribution Services, c/o Portland Customer Services, Commerce Way, Colchester, Essex, UK CO2 8HP. Tel +44 (0) 1206 226050; E-mail sales@rscdistribution.org

2008 Annual (print + electronic) subscription price: £947; US\$1799. 2008 Annual (electronic) subscription price: £852; US\$1695. Customers in Canada will be subject to a surcharge to cover GST. Customers in the EU subscribing to the electronic version only will be charged VAT.

If you take an institutional subscription to any RSC journal you are entitled to free, site-wide web access to that journal. You can arrange access via Internet Protocol (IP) address at www.rsc.org/ip. Customers should make payments by cheque in sterling payable on a UK clearing bank or in US dollars payable on a US clearing bank. Periodicals postage paid at Rahway, NJ, USA and at additional mailing offices. Airfreight and mailing in the USA by Mercury Airfreight International Ltd., 365 Blair Road, Avenel, NJ 07001, USA.

US Postmaster: send address changes to Green Chemistry, c/o Mercury Airfreight International Ltd., 365 Blair Road, Avenel, NJ 07001. All despatches outside the UK by Consolidated Airfreight.

PRINTED IN THE UK

Advertisement sales: Tel +44 (0) 1223 432246; Fax +44 (0) 1223 426017; E-mail advertising@rsc.org

Green Chemistry

Cutting-edge research for a greener sustainable future

www.rsc.org/greenchem

Green Chemistry focuses on cutting-edge research that attempts to reduce the environmental impact of the chemical enterprise by developing a technology base that is inherently non-toxic to living things and the environment.

EDITORIAL BOARD

Chair

Professor Martyn Poliakoff
Nottingham, UK

Scientific Editor

Professor Walter Leitner
RWTH-Aachen, Germany

Associate Editors

Professor C. J. Li
McGill University, Canada

Members

Professor Paul Anastas
Yale University, USA
Professor Joan Brennecke
University of Notre Dame, USA
Professor Mike Green
Sasol, South Africa
Professor Buxing Han
Chinese Academy of Sciences,
China

Dr Alexei Lapkin
Bath University, UK
Dr Janet Scott
Unilever, UK
Professor Tom Welton
Imperial College, UK

ADVISORY BOARD

James Clark, York, UK
Avelino Corma, Universidad
Politécnica de Valencia, Spain
Mark Harmer, DuPont Central
R&D, USA
Herbert Hugl, Lanxess Fine
Chemicals, Germany
Roshan Jachuck,
Clarkson University, USA
Makato Misono, nite,
Japan

Colin Raston,
University of Western Australia,
Australia
Robin D. Rogers, Centre for Green
Manufacturing, USA
Kenneth Seddon, Queen's
University, Belfast, UK
Roger Sheldon, Delft University of
Technology, The Netherlands
Gary Sheldrake, Queen's
University, Belfast, UK

Pietro Tundo, Università ca
Foscari di Venezia, Italy

INFORMATION FOR AUTHORS

Full details of how to submit material for publication in Green Chemistry are given in the Instructions for Authors (available from <http://www.rsc.org/authors>). Submissions should be sent *via* ReSource: <http://www.rsc.org/resource>.

Authors may reproduce/republish portions of their published contribution without seeking permission from the RSC, provided that any such republication is accompanied by an acknowledgement in the form: (Original citation) – Reproduced by permission of the Royal Society of Chemistry.

© The Royal Society of Chemistry 2008. Apart from fair dealing for the purposes of research or private study for non-commercial purposes, or criticism or review, as permitted under the Copyright, Designs and Patents Act 1988 and the Copyright and Related Rights Regulations 2003, this publication may only be reproduced, stored or transmitted, in any form or by any means, with the prior permission in writing of the Publishers or in the case of reprographic reproduction in accordance with the terms of licences issued by the Copyright Licensing Agency in the UK. US copyright law is applicable to users in the USA.

The Royal Society of Chemistry takes reasonable care in the preparation of this publication but does not accept liability for the consequences of any errors or omissions.

Ⓢ The paper used in this publication meets the requirements of ANSI/NISO Z39.48-1992 (Permanence of Paper).

Royal Society of Chemistry: Registered Charity No. 207890

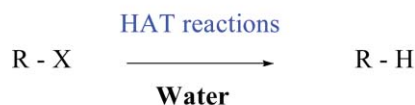
TUTORIAL REVIEW

153

Recent advances in C–H bond formation in aqueous media: a mechanistic perspective

V. Tamara Perchyonok,* Ioannis N. Lykakis* and Kellie L. Tuck*

This review highlights progress made in the last decade to “tame” reactive free-radical species in aqueous-phase reactions.



Choices

Reasons

Applications

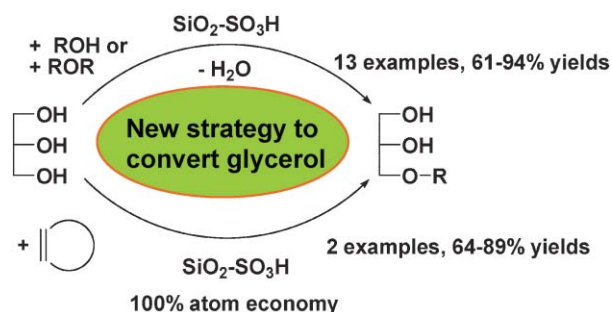
COMMUNICATIONS

164

Heterogeneously catalyzed etherification of glycerol: new pathways for transformation of glycerol to more valuable chemicals

Yanlong Gu, Ahmed Azzouzi, Yannick Pouilloux, François Jérôme* and Joël Barrault

Silica-supported sulfonic catalysts allow, for the first time, the selective synthesis of monoalkyl glyceryl ether directly from glycerol and alkyl alcohols, olefins or symmetrical ethers.

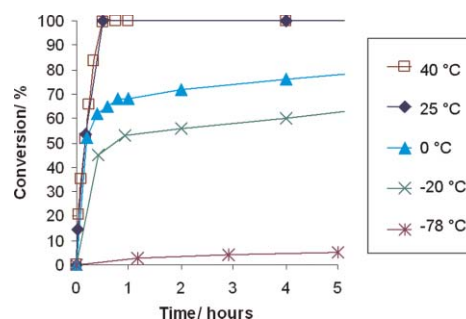


168

Aerobic oxidation of aldehydes under ambient conditions using supported gold nanoparticle catalysts

Charlotte Marsden, Esben Taarning, David Hansen, Lars Johansen, Søren K. Klitgaard, Kresten Egeblad and Claus Hviid Christensen*

A new, green protocol for producing simple esters by selectively oxidizing an aldehyde dissolved in a primary alcohol has been established.

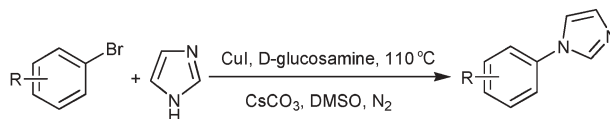


171

D-Glucosamine—a natural ligand for the N-arylation of imidazoles with aryl and heteroaryl bromides catalyzed by CuI

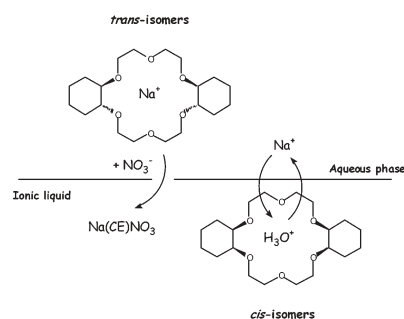
Dongping Cheng, Fengfeng Gan, Weixing Qian and Weiliang Bao*

D-Glucosamine, a natural ligand, can efficiently promote the N-arylation of imidazoles with aryl and heteroaryl halides using CuI as a catalyst.



COMMUNICATIONS

174

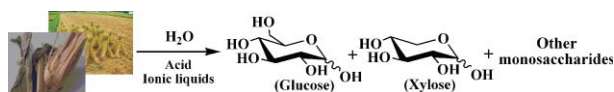
**Stereochemical effects on the mode of facilitated ion transfer into room-temperature ionic liquids**

Mark L. Dietz,* Sandrine Jakab, Kazuhiro Yamato and Richard A. Bartsch

Crown ether (CE) stereochemistry is shown to influence the mode of sodium ion partitioning between acidic nitrate media and a dialkylimidazolium-based room temperature ionic liquid containing various dicyclohexano-18-crown-6 (DCH18C6) isomers, in contrast to an analogous extraction system employing a conventional organic solvent.

PAPERS

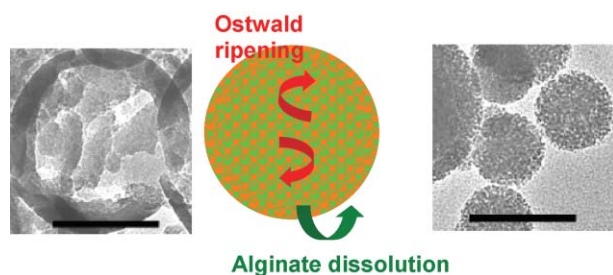
177

**Acid in ionic liquid: An efficient system for hydrolysis of lignocellulose**

Changzhi Li, Qian Wang and Zongbao K. Zhao*

An efficient system for hydrolysis of lignocellulosic materials in ionic liquids was developed with improved sugar yields at 100 °C under atmospheric pressure.

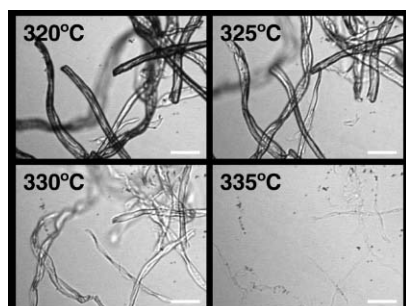
183

**A green route to silica nanoparticles with tunable size and structure**

Yun Yang and Thibaud Coradin*

The spray-drying of alginate and silicate mixtures provides a green route to hybrid nanoparticles of tunable size whose internal structure can be tailored by further ageing in water at variable temperatures.

191

**Crystalline-to-amorphous transformation of cellulose in hot and compressed water and its implications for hydrothermal conversion**

Shigeru Deguchi,* Kaoru Tsujii and Koki Horikoshi

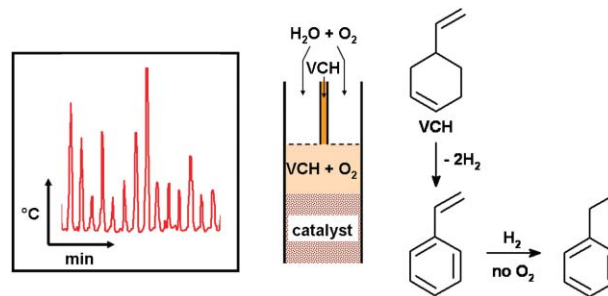
The transformation of crystalline cellulose to an amorphous state in hot and compressed water was studied with respect to various structural characteristics.

197

A dramatic switch in selectivity in the catalytic dehydrogenation of 4-vinylcyclohexene in high pressure steam; a cautionary lesson for continuous flow reactions

Morgan L. Thomas, Joan Fraga-Dubreuil, A. Stuart Coote and Martyn Poliakoff*

In the dehydrogenation of VCH in the presence of O₂, the occurrence of periodic temperature spikes gives rise to large variations in the observed product selectivity. This has important implications for other work involving continuous flow oxidations.

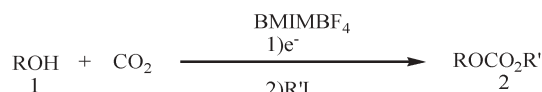


202

Electrochemical activation of CO₂ in ionic liquid (BMIMBF₄): synthesis of organic carbonates under mild conditions

Li Zhang, Dongfang Niu, Kai Zhang, Guirong Zhang, Yiwen Luo and Jiaying Lu*

A new electrochemical procedure for electrosynthesis of organic carbonates from CO₂ and alcohols has been established in CO₂-saturated room temperature ionic liquid BMIMBF₄ solution, followed by addition of an alkylating agent.

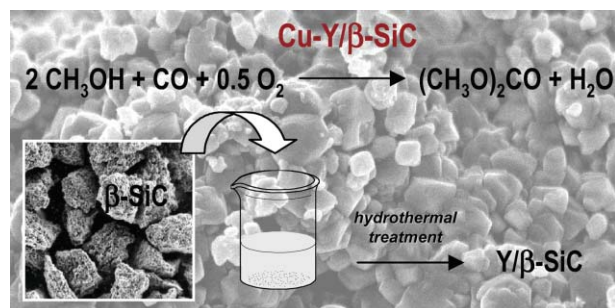


207

Cu–Y zeolite supported on silicon carbide for the vapour phase oxidative carbonylation of methanol to dimethyl carbonate

Guillaume Rebmann, Valérie Keller, Marc J. Ledoux and Nicolas Keller*

A β-SiC supported Cu–Y zeolite composite catalyst, prepared by performing the zeolite synthesis in the presence of SiC, combined the interest of using a thermoconductive material as support for an exothermic reaction and a Cu–Y zeolite catalyst for getting stable performances in the dimethyl carbonate synthesis by the vapor phase oxidative carbonylation of methanol.

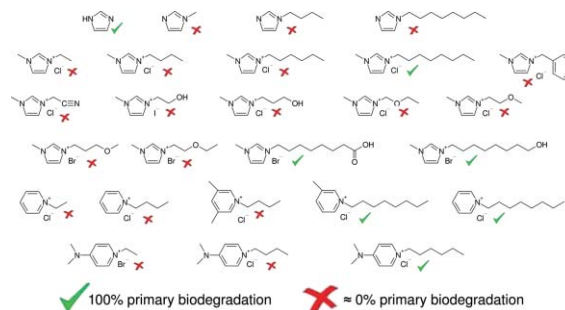


214

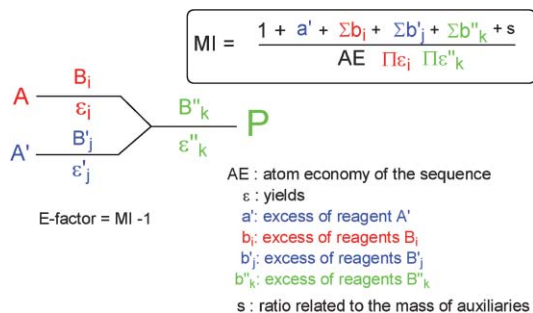
Primary biodegradation of ionic liquid cations, identification of degradation products of 1-methyl-3-octylimidazolium chloride and electrochemical wastewater treatment of poorly biodegradable compounds

Stefan Stolte,* Salha Abdulkarim, Jürgen Arning, Anne-Katrin Blomeyer-Nienstedt, Ulrike Bottin-Weber, Marianne Matzke, Johannes Ranke, Bernd Jastorff and Jorg Thöming

We investigated the primary biodegradation of different *N*-imidazoles, imidazolium, pyridinium and 4-(dimethylamino)pyridinium compounds substituted with various alkyl side chains and their analogues containing functional groups principally based on OECD guideline 301 D.



225

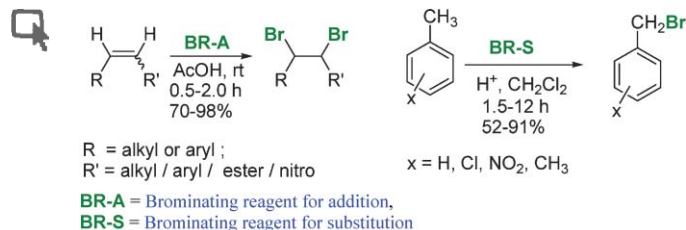


A new rationale of reaction metrics for green chemistry. Mathematical expression of the environmental impact factor of chemical processes

Jacques Augé

The E-factor of chemical processes has been calculated. The mathematical formula includes the overall atom economy, the yields, the excess of reagents and the mass of the auxiliaries.

232

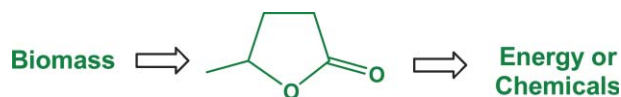


An alternative method for the regio- and stereoselective bromination of alkenes, alkynes, toluene derivatives and ketones using a bromide/bromate couple

Subbarayappa Adimurthy,* Sudip Ghosh, Paresh U. Patoliya, Gadde Ramachandraiah,* Manoj Agrawal, Mahesh R. Gandhi, Sumesh C. Upadhyay, Pushpito K. Ghosh* and Brindaban C. Ranu*

Mixtures of NaBr and NaBrO₃ have been used for stereoselective bromination of alkenes and alkynes, and regioselective bromine substitution at the α -carbon of ketones and the benzylic position of toluenes.

238

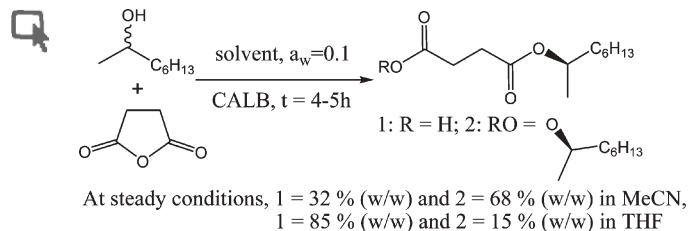


γ -Valerolactone—a sustainable liquid for energy and carbon-based chemicals

István T. Horváth,* Hasan Mehdi, Viktória Fábos, László Boda and László T. Mika

γ -Valerolactone exhibits the most important characteristics of an ideal sustainable liquid, which could be used for the production of both energy and carbon-based consumer products.

243



Lipase catalysed mono and di-acylation of secondary alcohols with succinic anhydride in organic media and ionic liquids

Rafał Bogel-Lukasik, Nuno M. T. Lourenço, Pedro Vidinha, Marco D. R. Gomes da Silva, Carlos A. M. Afonso, Manuel Nunes da Ponte and Susana Barreiros*

A study of the enzymatic acylation of (*R,S*)-2-octanol with succinic anhydride in a wide polarity range of ionic liquids and representative organic solvents demonstrates the occurrence of a critical balance for the sequential acylation, which is strongly dependent on the polarity of the solvent and on the solubility of succinic acid in it.

ADDITIONS AND CORRECTIONS

249

Copper catalyzed oxidative alkylation of sp^3 C–H bond adjacent to a nitrogen atom using molecular oxygen in water

Olivier Baslé and Chao-Jun Li

Dilute aqueous 1-butyl-3-methylimidazolium hexafluorophosphate: properties and solvatochromic probe behaviour

Maroof Ali, Abhra Sarkar, Mohammad Tariq, Anwar Ali and Siddharth Pandey

AUTHOR INDEX

- | | | | |
|--------------------------------------|----------------------------------|----------------------------|--------------------------|
| Abdulkarim, Salha, 214 | da Ponte, Manuel Nunes, 243 | Keller, Nicolas, 207 | Ranke, Johannes, 214 |
| Adimurthy, Subbarayappa, 232 | da Silva, Marco D. R. Gomes, 243 | Keller, Valérie, 207 | Ranu, Brindaban C., 232 |
| Afonso, Carlos A. M., 243 | Deguchi, Shigeru, 191 | Klitgaard, Søren K., 168 | Rebmann, Guillaume, 207 |
| Agrawal, Manoj, 232 | Dietz, Mark L., 174 | Ledoux, Marc J., 207 | Stolte, Stefan, 214 |
| Arning, Jürgen, 214 | Egeblad, Kresten, 168 | Li, Changzhi, 177 | Taarning, Esben, 168 |
| Augé, Jacques, 225 | Fábos, Viktória, 238 | Lourenço, Nuno M. T., 243 | Thomas, Morgan L., 197 |
| Azzouzi, Ahmed, 164 | Fraga-Dubreuil, Joan, 197 | Lu, Jiaying, 202 | Thöming, Jorg, 214 |
| Bao, Weiliang, 171 | Gan, Fengfeng, 171 | Luo, Yiwen, 202 | Tsujii, Kaoru, 191 |
| Barrault, Joël, 164 | Gandhi, Mahesh R., 232 | Lykakis, Ioannis N., 153 | Tuck, Kellie L., 153 |
| Barreiros, Susana, 243 | Ghosh, Pushpito K., 232 | Marsden, Charlotte, 168 | Upadhyay, Sumesh C., 232 |
| Bartsch, Richard A., 174 | Ghosh, Sudip, 232 | Matzke, Marianne, 214 | Vidinha, Pedro, 243 |
| Blomeyer-Nienstedt, Anne-Katrin, 214 | Gu, Yanlong, 164 | Mehdi, Hasan, 238 | Wang, Qian, 177 |
| Boda, László, 238 | Hansen, David, 168 | Mika, László T., 238 | Yamato, Kazuhiro, 174 |
| Bogel-Lukasik, Rafał, 243 | Horikoshi, Koki, 191 | Niu, Dongfang, 202 | Yang, Yun, 183 |
| Bottin-Weber, Ulrike, 214 | Horváth, István T., 238 | Patoliya, Paresh U., 232 | Zhang, Guirong, 202 |
| Cheng, Dongping, 171 | Jakab, Sandrine, 174 | Perchyonok, V. Tamara, 153 | Zhang, Kai, 202 |
| Christensen, Claus Hviid, 168 | Jastorff, Bernd, 214 | Poliakoff, Martyn, 197 | Zhang, Li, 202 |
| Coote, A. Stuart, 197 | Jérôme, François, 164 | Pouilloux, Yannick, 164 | Zhao, Zongbao K., 177 |
| Coradin, Thibaud, 183 | Johansen, Lars, 168 | Qian, Weixing, 171 | |
| | | Ramachandraiah, Gadde, 232 | |

FREE E-MAIL ALERTS AND RSS FEEDS

Contents lists in advance of publication are available on the web *via* www.rsc.org/greenchem - or take advantage of our free e-mail alerting service (www.rsc.org/ej_alert) to receive notification each time a new list becomes available.



Try our RSS feeds for up-to-the-minute news of the latest research. By setting up RSS feeds, preferably using feed reader software, you can be alerted to the latest Advance Articles published on the RSC web site. Visit www.rsc.org/publishing/technology/rss.asp for details.

ADVANCE ARTICLES AND ELECTRONIC JOURNAL

Free site-wide access to Advance Articles and the electronic form of this journal is provided with a full-rate institutional subscription. See www.rsc.org/ejs for more information.

* Indicates the author for correspondence: see article for details.

Electronic supplementary information (ESI) is available *via* the online article (see <http://www.rsc.org/esi> for general information about ESI).

A new journal from RSC Publishing Launching summer 2008

Energy & Environmental Science

A new journal linking all aspects of the chemical sciences relating to energy conversion and storage, alternative fuel technologies and environmental science.

As well as research articles, *Energy & Environmental Science* will also publish communications and reviews. It will be supported by an international Editorial Board, chaired by Professor Nathan Lewis of Caltech.

Contact the Editor, Philip Earis, at ees@rsc.org or visit the website for more details.



The current issue of *Energy & Environmental Science* will be freely available to all. Free access to all 2008 and 2009 content of the journal will be available following registration.

RSC Publishing

www.rsc.org/ees

Registered Charity Number 207890

Chemical Technology

Nanoparticle make up can be controlled by varying the foil's composition

Bimetallic particles from sputter deposition

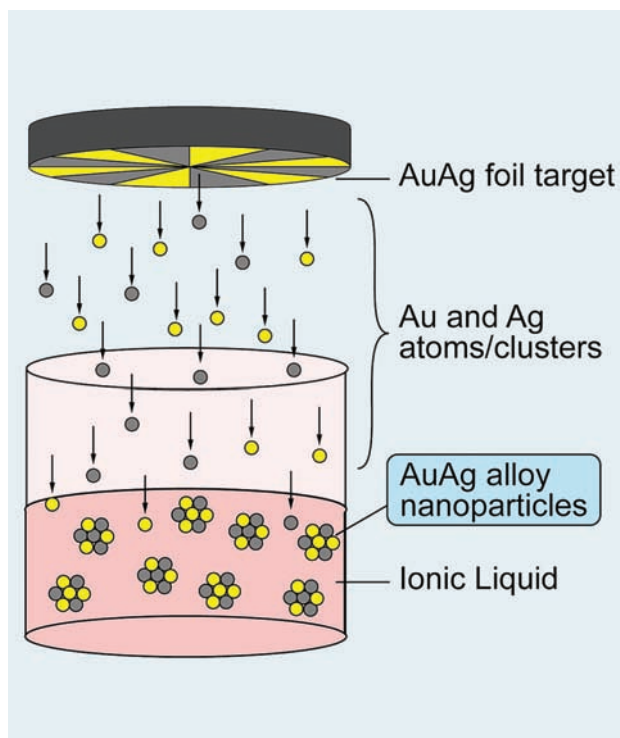
Gold and silver alloy particles have been made using a simple technique involving ionic liquids.

The team, led by Tsukasa Torimoto at Nagoya University and Susumu Kuwabata at Osaka University in Japan, have used a process called sputter deposition to form bimetallic particles. The particles, which have applications in biosensors and as catalysts, are formed in an ionic liquid from atoms sputtered from a metal foil.

Torimoto explained that the team investigated ionic liquids because of their very low vapour pressures. This means they can be used under the high vacuum conditions required for sputter deposition used here, without their physical and chemical properties changing.

The technique involves bombarding a gold and silver metal foil with high energy gaseous ions. Metal atoms are ejected from the surface of the foil into an ionic liquid, where they coalesce to form the bimetallic nanoparticles.

Up to now, explained Torimoto,



Ionic liquids can withstand the high vacuum conditions required

it has been difficult to obtain homogeneous alloy nanoparticles using conventional solution methods because of the differing chemical redox potentials of the metals. Using the sputtering technique the composition of the particles and their properties can be tuned by varying the composition ratios of the metal foil.

Frank Endres at Clausthal University of Technology in Germany said the team 'present a simple and therefore elegant process for the large-scale production of metal and alloy nanoparticles'. He suggested a further step could be to combine the sputter technique used by Torimoto with a plasmaelectrochemical deposition method developed by himself and colleagues in Germany. 'This might be a route to making ternary compound nanoparticles,' he explained.

Katherine Davies

Reference

K Okazaki et al, *Chem. Commun.*, 2008, 691 (DOI: 10.1039/b714761a)

In this issue

Make nanoparticles while the sun shines

Solar ablation less energy intensive than laser or chemical routes

Intelligent inks

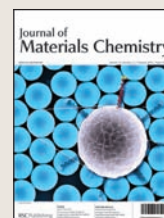
Colour change reveals faulty food packaging

Interview: Analyse this

Joe Caruso talks to May Copsey about warfare agents, proteomics and why elemental mass spectrometry is not just about the metal

Instant insight: Watching the burn

Craig Taatjes of Sandia National Labs, Livermore, US, and colleagues look inside the mysterious chemistry of combustion



The latest applications and technological aspects of research across the chemical sciences

Application highlights

Colour change reveals faulty packaging

Intelligent inks



An ink that changes its colour when exposed to oxygen could help shoppers decide if their packaged food is fresh.

Oxygen is the enemy of fresh food because it causes food to degrade and bacteria need it to grow. Hence, much of today's packaged food comes in a

protective atmosphere of gases such as nitrogen – with oxygen almost totally removed.

Andrew Mills and David Hazafy at University of Strathclyde, UK, have developed a blue ink that loses all its colour and becomes oxygen sensitive when activated with UV light. It only turns blue again after

The ink loses its colour when activated, then regains it when exposed to oxygen

Reference
A Mills and D Hazafy, *Analyst*, 2008, **133**, 213 (DOI: 10.1039/b713450a)

exposure to oxygen.

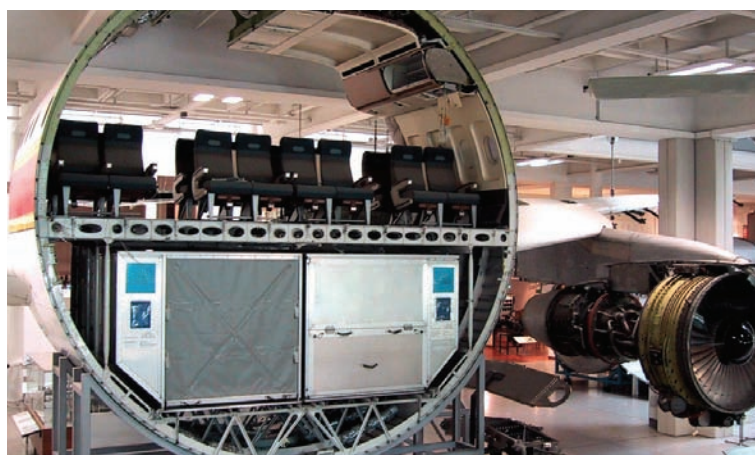
The major advantages of the oxygen ink over most of the traditional methods for detecting oxygen is that it is cheap and easy to use, especially as it relies on a colour change detectable by the human eye, said Mills. Solvent-based inks such as these are also easier to print on the common polymers used in food packaging, he added.

'An oxygen-sensitive ink, such as ours, could be used to show if the modified atmosphere remains intact, first at the packaging factory, then at the supermarket, ensuring faulty, damaged or tampered packages are not sold,' said Mills. The customers themselves will be able to pick up the food and tell instantly if it has been spoiled.

Sarah Corcoran

If you want to detect disease in an airline cabin, where do you put the sensors?

SARS on a plane



Fluid dynamics revealed the best place to find biological agents

It's fairly unlikely that you'll ever worry about snakes on a plane, but what if one of your co-passengers has SARS, or worse, is about to release some anthrax spores? US researchers are working to find the best way to detect such hazards.

Nearly two billion people travel on commercial airliners each year, and it is important to detect these

problems as quickly as possible by installing sensors. However, the number of sensors that can be installed is limited by cost, size and weight. The question then remains: Where do you put the sensors to get the fastest response?

Instead of using a full size replica of an airliner cabin, Sagnik Mazumdar and Qingyan Chen from

Purdue University, West Lafayette, created a virtual cabin and used computational fluid dynamics to study the effects of the seating arrangement and the number of occupants on the optimum position for these sensors.

'In 2003, one passenger passed on SARS to more than a dozen others,' said Mazumdar. 'It's this kind of tragedy that we hope to help avoid.'

Their research is one part of a larger coordinated research effort called ACER (airliner cabin environment research). 'It is essential to deploy sensors that can provide instantaneous information. New sensors that can provide instantaneous results, particularly for biological agents, is another important area for research,' said Mazumdar.

Stephen Davey

Reference
S Mazumdar and Q Chen, *J. Environ. Monit.*, 2008, **10**, 71 (DOI: 10.1039/b713187a)

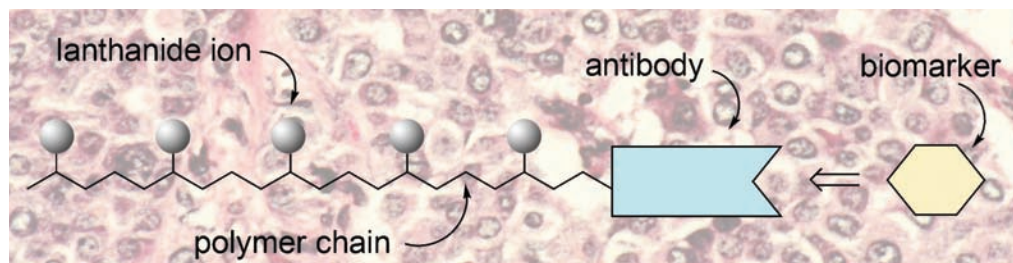
Simultaneous screening for many disease biomarkers is now on the horizon

Lanthanide ions hold key to disease screening

Canadian researchers have devised a way to assess biological samples for the presence of multiple small molecules, which has profound implications for rapidly identifying diseases.

Being able to distinguish diseased cells from healthy ones is vital in identifying diseases in humans. A rapidly advancing way of doing this is to determine the concentrations of small molecules (biomarkers) present in biological samples, as amounts of these chemicals differ between diseased and healthy cells. Vladimir Baranov and colleagues from the University of Toronto have now developed a sensitive method that, by using lanthanide ions, is able to determine the concentrations of many biomarkers at once. This, they say, will have important applications in clinical diagnostics.

Baranov and colleagues bound ^{151}Eu ions to a polymer chain chemically attached to an antibody, which itself binds to a natural



biomarker. Once the unreacted antibody derivative is washed away, the sample is exposed to inductively coupled plasma mass spectrometry. This atomises the entire sample and allows the elemental composition to be determined. In this case, the amount of ^{151}Eu correlates to the amount of biomarker present in the original sample. The number of ^{151}Eu ions within each molecule means that the method is more sensitive to the amount of biomarker than existing techniques, said Baranov.

The power of the team's method is that it can measure many biomarkers

Different biomarkers can be targeted by different lanthanide isotopes

Reference

O I Ornatsky *et al.*, *J. At. Anal. Spectrosc.*, 2008, DOI: 10.1039/b710510j

simultaneously, simply by using a different one of the 50-plus stable lanthanide isotopes for antibodies against different targets. Baranov's team are now working to apply their technique to the classification of leukaemia samples.

The importance of this research is emphasised by Les Ebdon, Vice-Chancellor of the University of Bedfordshire, UK, who said 'This exciting study ... promises to advance our abilities to understand and diagnose complex diseases such as leukaemia.'

David Barden

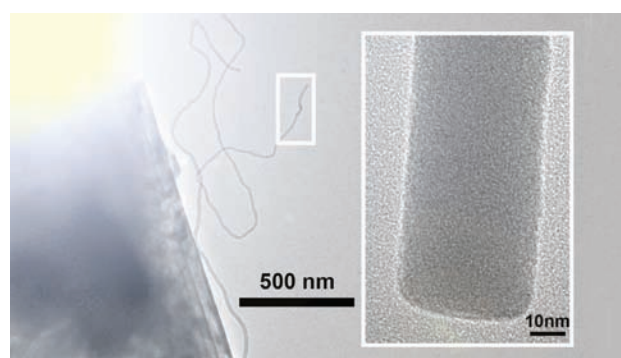
Solar ablation less energy intensive than laser or chemical routes

Make nanoparticles while the sun shines

Concentrated sunlight is all you need to make useful nanomaterials, according to Israeli researchers.

Jeffrey Gordon of Ben-Gurion University in the Negev desert, Reshef Tenne of the Weizmann Institute, Rehovot, and their collaborators collect solar radiation outdoors and transmit it to an indoor laboratory with optical fibres. Here it is focussed on molybdenum sulfide or quartz powders, transforming them into nanotubes and nanocages. This is the first time that silica nanofibres and nanospheres have been produced from pure quartz, they said.

Wolfgang Tremel, who works on inorganic nanoparticles at the University of Mainz in Germany explained 'A particular problem in the synthesis of fullerene-type nanoparticles and nanotubes is that high temperatures are needed to



interconnect the edges of fragments in such a way as to provide curvature to otherwise flat slabs.'

Gordon and Tenne believe that the solar route is far less energy intensive than laser ablation or high-temperature chemical reactors, simpler and less costly, with only an 'uncomplicated optical system' required to deliver the light to the reaction vessel.

Sunlight is transmitted to the reaction vessel by optical fibres

Reference

J M Gordon *et al.*, *J. Mater. Chem.*, 2008, **18**, 458 (DOI: 10.1039/b714108d)

There are plenty of refinements that can be made: 'We need to find optical and reactor configurations that ensure nanotube and nanoparticle generation in a more uniform and reproducible fashion,' said the researchers. And, they add, it opens up new mechanistic questions: 'Does photochemistry play a role or are the only important factors the temperature and flux gradients?'

Tremel warned that in its current state the technique will be unable to 'yield samples at the gram scale'. More importantly though, he said that it promises new sorts of fullerene-like nanoparticles. These conditions, he said, 'enable the formation and trapping of nanoparticles from metal oxide compounds which, like quartz, have significantly lower vapour pressures than metal chalcogenides'.

Colin Batchelor

Banned muscle strength hormone somatotropin detected months after use

Immunoassays put pay to foal play

French scientists have designed tests to catch cheats who use prohibited drugs to dope racehorses.

Somatotropin, a protein hormone, increases muscle strength. Recombinant equine somatotropin is banned in horseracing since it can enhance the performance of the horse, giving it an unfair advantage. Somatotropin can be used legitimately to help repair tendon or bone injuries in horses, or to improve the condition of horses that no longer race.

Ludovic Bailly-Chouriberry, who works at both the Laboratory of Horse Racing in Verrières-le-Buisson and the National Veterinary School in Nantes, and colleagues have developed a method to test for somatotropin based on detection of antibodies raised against the hormone in serum or plasma.

Other tests to screen for



somatotropin abuse, the researchers said, include the detection of insulin-like growth factor (IGF-1) whose production is also triggered by somatotropin. They hope that by detecting antibodies instead of IGF-1

Detecting antibodies enables a longer screening period

a longer period for screening will be possible.

They identified the antibodies using two techniques: a biosensor immunoassay (BIA) and an enzyme-linked immunosorbent assay (ELISA). The developed technologies meant it was possible to detect the antibodies 80 days after administering somatotropin with BIA and 200 days after with ELISA.

Bailly-Chouriberry said that this could also provide a cheap and important tool to indirectly detect insulin or recombinant erythropoietin (EPO) misuse through the detection of their antibodies, supposing it can be adapted.

Sarah Corcoran

Reference

L Bailly-Chouriberry *et al*, *Analyst*, 2008, **133**, 270 (DOI: 10.1039/b713712e)

A renewable alternative to crude-oil-based self-curing agents is now possible

Get set with the ene reaction

Researchers from the US have discovered that soy bean oil could be used as a renewable feedstock for gels and resins.

Materials with self-curing, thickening, and self-gelling properties are used in many industrial applications, as caulking agents, cements or coatings. However, many current products are ultimately derived from crude oil. Alongside current developments in the use of biofuels, there is also interest in alternative and renewable sources for such materials.

Now Atanu Biswas from the United States Department of Agriculture and co-workers have discovered that one such renewable raw material can be made to spontaneously form a gel. In the absence of solvent, and without the need for heating or catalyst, soy bean oil undergoes an ene reaction with DEAD (diethylazodicarboxylate).

'We have been interested in combining green chemistry

with the use of agricultural raw materials,' said Biswas. 'A particular interest of ours is vegetable oil, because it is relatively low-priced, abundant, and environmentally friendly,' he continued.

Biswas and colleagues hope that this work can be the beginning of a new platform for materials that need self-thickening, self-gelling and self-curing properties. 'Obviously for specific applications, some customization of end-use properties would be needed. Fortunately, there are many types of oils available that we can use to optimize given properties,' he



Soy bean oil spontaneously forms a gel

Reference

A Biswas *et al*, *Green Chem.*, 2008, DOI: 10.1039/b712385j

explained.

Surya Prakash from the University of Southern California, Los Angeles, US, said 'Biswas and colleagues have discovered a novel condensation of soybean oil leading to self-curing and thickening. This chemistry will have enormous promise in preparing gels, resins and adhesives using vegetable oil based bio-feedstocks.'

A future challenge will be to find an alternative to the aptly named DEAD, which is known to be toxic. However, Biswas is confident that this will be achievable. 'The key reaction for this new platform is the ene reaction. There are many reactants known to undergo ene reactions. For commercial applications, what is needed in the future is to screen these potential reactants, in view of reaction efficiency, toxicity, and economics, in order to target specific products,' he said.

Stephen Davey

Interview

Analyse this

Joe Caruso talks to May Copsey about warfare agents, proteomics and why elemental mass spectrometry is not just all about the metal



Joe Caruso

Joe Caruso is a professor of analytical chemistry at the University of Cincinnati. His research interests include metal profiling in clinical samples and studies of selenium phytoremediation. Formerly chairman of the Journal of Analytical Atomic Spectrometry editorial board, Joe is a member of the Chemical Society Reviews editorial board.

What inspired you to become a scientist?

I started out as a high school chemistry teacher but I realised that there was so much exciting chemistry out there and I wanted to teach it at a higher level. I became increasingly interested in the research. In particular, working with graduate students and postdocs is a great plus.

What influenced your decision to study analytical science?

I had a fantastic teacher at university who taught a course in qualitative analysis and he really inspired me. I also think analytical chemistry suits my personality. It is a very practical part of chemistry. For example, if you develop a new method to analyse for lead in somebody's blood, you see a clear application. It is this kind of outcome-based research that drives me.

Can you tell me about the techniques that you use?

Our main-stay is elemental mass spectrometry, known as ICP-MS. It's mainly a metal-based technique, but it does an excellent job at looking at non-metal elements such as bromine, iodine, phosphorus and sulfur. It can be used to analyse for a variety of compounds, such as brominated fire-retardants or phosphorus-based warfare agents. It has a wide range of uses, from small inorganic molecule analysis to proteomics.

What are you working on at the moment?

We are trying to obtain a better molecular understanding of phytoremediation, the use of plants to remove pollutants from soil or water. We study selenium because it is present at high levels in agricultural fields in the western US. There's relatively little difference between the amounts that are toxic and the amounts that are required for life. We look at selenium as it undergoes changes within the plant. You can actually modify certain metabolic changes genetically, taking chemical pathways in different directions and ultimately enhancing the bioremediation qualities of the plant.

We've also been looking at chemical warfare agent hydrolyzates. We aren't certified for handling the actual agents themselves so we study

these degradation products. These provide an interesting track to reveal if an agent was present or not. We started this project because our basis for detection is to look at phosphorus as an internal tag by mass spectrometry, rather than looking at the molecule or functional group.

Some of our work focuses on clinical applications of analytical mass spectrometry. We combine elemental mass spectrometry and molecular mass spectrometry to allow metabolite detection at very low levels. We are collaborating with a neuroscientist, Dr Joe Clarke, in the neurology department at Cincinnati. He's very interested in the metabolites associated with certain types of stroke. He believes there may be metabolic markers involving non-metals, such as phosphorus and sulfur, that appear at very low levels in patients with post-stroke complications. If detected early enough, an appropriate intervention might be taken, either through drug therapy or some kind of physical intervention.

What is the next big thing that you would like to tackle in your lab?

Our movement into clinical applications is going to expand. There are particular sets of proteins in the shell, or capsid, of viruses. There's very little known about the metalloprotein aspect of various capsid proteins and this is something we'd like to take a look at. We are interested in seeing how the capsid reacts to either adding metals or removing them.

Do you have any advice for a young researcher keen to develop a successful scientific career?

The important thing is to keep your mind open. Scientists should not limit themselves or their thinking from reaching out into new areas. Collaborations will be even more the way of the future, but this also is consistent with establishing yourself as an independent scientist.

What do you like doing when you're not doing chemistry?

I enjoy boating and my grandchildren. I like to travel with family or friends. I often combine a few days holiday with my scientific commitments.

Easier and more efficient than traditional LLE

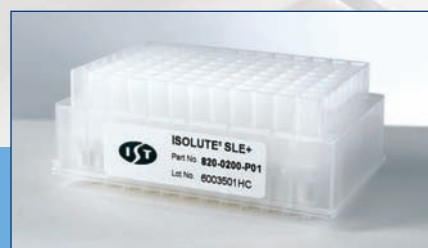
... SLE+ Supported Liquid Extraction Plates

Supported Liquid Extraction (SLE) provides an easier to automate alternative to liquid-liquid extraction (LLE), with no off-line steps (e.g. mixing or centrifuging) required. Problems including emulsion formation, and separation of liquid layers are eliminated.

ISOLUTE® SLE+ Supported Liquid Extraction Plates are optimized for simultaneous processing of 96 samples (extract up to 200 µL of plasma or urine per well), using a generic methodology for extraction of neutral, acidic and basic compounds.

ISOLUTE® SLE+ is available in the industry standard 2 mL fixed well 'SPE' plate format and is compatible with all commercially available automated liquid handling systems.

For more information or to request a free sample visit www.biotage.com.



NEW! ISOLUTE SLE+ Plates

Improve productivity and maximize analyte recovery with this new more efficient alternative to traditional liquid-liquid extraction.

- No emulsion formation
- Easy to automate
- Rapidly transfer methods from traditional LLE to ISOLUTE SLE+
- Excellent flow characteristics improve reproducibility


Biotage
www.biotage.com

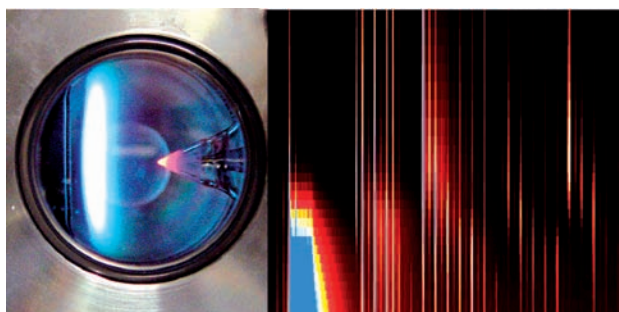
Instant insight

Watching the burn

Craig Taatjes of Sandia National Labs, Livermore, US, and colleagues look inside the mysterious chemistry of combustion using photoionization mass spectrometry combined with synchrotron radiation

Combustion is an ancient technology, but it remains the dominant means of releasing stored energy in the world today. When Nikolaus Otto invented the four-stroke engine in 1876 and when Rudolf Diesel patented his engine in 1898, scientists did not even have the basic knowledge that combustion was driven by chain-reaction chemistry, an insight that would yield Nikolay Semenov the Nobel Prize decades later. The science of combustion systems, with interacting fluid mechanics and complex chemistry, is a daunting multiscale and multiphase problem that continues to tax state-of-the-art computational and experimental methods. There is an intensifying emphasis on reducing pollutant levels, and new engine technologies are emerging that rely on chemical kinetics for ignition timing. These have made understanding the fundamentals of combustion a key to designing new practical devices and have brought detailed chemistry to the forefront of twenty-first-century combustion research.

Understanding the chemistry behind some of the most stubborn problems in combustion technology relies on knowledge of isomer-specific concentrations of products and intermediates. For example, the efficiency of advanced engines that rely on compression ignition of a premixed fuel-air charge depends on the particulars of alkylperoxy radical isomerizations. The problem of soot formation in hydrocarbon flames hinges on whether reactions of small hydrocarbon species in a flame form aromatic rings or not. Photoionization mass spectrometry is a powerful technique for probing chemical reactions and combustion processes, and the photon-energy



dependence of the ionization can distinguish isomers. Recently, photoionization by synchrotron radiation has been combined with simultaneous detection of multiple masses to investigate the chemistry of low-pressure flames. The brightness of the synchrotron source and the multiplexed mass spectrometry permits rapid acquisition of three-dimensional data: signal as a function of the mass, the ionization photon energy, and either reaction time or distance from the burner surface.

'Slices' taken out of such datasets by integrating over two of the dimensions would correspond to more traditional measurements, such as profiles of species as a function of distance from the burner or kinetic concentration against time. However, interpretation of the multidimensional data directly from an image yields great insight into global chemical mechanisms and can highlight previously unknown reactive pathways. For example, an image of the evolving mass spectrum of molecules sampled from a rich ethene flame as a function of the distance from the burner shows soot precursor chemistry at a glance. Moving away from the burner, the fuel is consumed and higher-molecular-weight hydrocarbons

A visual interpretation of multidimensional data can give a glimpse of chemical mechanisms – if you know what to look for

begin to be formed; species with three carbon atoms appear very close to the burner, four-carbon species slightly farther away, five-carbon species farther still, and so on. Comparison with an image of a similarly rich flame of the oxygenated fuel dimethyl ether shows immediately that the growth of these soot precursors is almost completely absent in the ether flame, consistent with the soot-reducing effects of oxygenates.

Additionally, possession of the entire three-dimensional data set allows the measurements to be correlated in different ways. As one example, the change in the photon-energy dependence of signal at a given mass can be related to a change in the isomeric populations. Correlating this with time then allows the separation of contributions from different stages of the reactions. Spectra derived from such correlations offer means to detect important ignition-chemistry intermediates.

The investigation of increasingly complex chemical systems not only requires the ability to simultaneously monitor many channels, but demands new strategies to manage and visualize the resulting data. Tunable photoionization and simultaneous multiple-mass detection can effectively depict flame and chemical kinetic processes; continuing development of spectroscopic and visualization technologies will deliver new insights into combustion.

Read more in Craig Taatjes *et al.*'s critical review "Imaging" combustion chemistry via multiplexed synchrotron-photoionization mass spectrometry' in issue 1, 2008 of PCCP.

Reference
Craig A Taatjes *et al.*, *Phys. Chem. Chem. Phys.*, 2008, **10**, 20 (DOI: 10.1039/b713460f)

Essential elements

Celebrating a decade of success

2008 is a big year for RSC Publishing as four titles from its successful journal portfolio celebrate their tenth year of publication. *CrystEngComm*, *Green Chemistry*, *Journal of Environmental Monitoring* (*JEM*), and *Physical Chemistry Chemical Physics* (*PCCP*) have all made huge advances in their first decade.

PCCP boasts the highest ISI immediacy index of any general physical chemistry journal and *CrystEngComm*, with an impact factor of 3.729, is the journal in which to publish crystal engineering research. *JEM* is packed full of cutting-edge work on environmental processes and impacts and *Green Chemistry*, the most highly cited journal in its field, has an impact factor of 4.192.



A number of celebratory activities are planned this year to mark the anniversaries, including receptions, sponsored

lectures, poster prizes and commissioned articles. Look out for specially selected reviews representing the many areas of *Green Chemistry*, and *JEM* sponsored lectures at Airmon 2008 (Albert Gilmudtinov) and DIOXIN 2008 (Kevin Jones). *PCCP* and *CrystEngComm* will also be maintaining a high profile at key conferences across their fields, including sponsoring ten poster prizes.

For further information on these and other anniversary events visit the website (www.rsc.org/journals) or speak to us at one of the many conferences RSC Publishing staff will be attending throughout 2008. Watch out for celebrations at the Spring ACS meeting in New Orleans in April...

And finally...



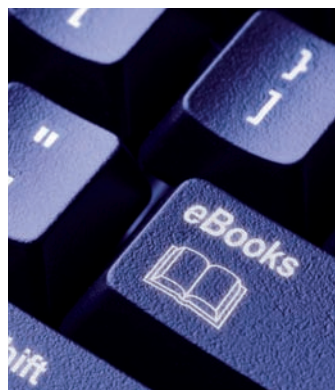
This month sees the publication of an exciting theme issue of *Molecular BioSystems* on the subject of metabolomic analysis of microorganisms. The issue is introduced by Hirotada Mori and Tadhg Begley of the *Molecular BioSystems* editorial board and features a good mix of review and primary research material.

The investigation of cellular metabolic pathway networks is a remarkably varied field, requiring a wide range of knowledge and theoretical and experimental tools taken from a diversity of scientific disciplines.

Approaches involving time-of-flight mass spectrometry, TOCSY NMR, informatics and computational strategies are described, along with the modelling and reconstruction of metabolic networks. A review of flux analysis, dynamic changes in metabolite profiles, new techniques to identify extracellular components and dynamic changes in gene regulation are all to be found in this issue. Enjoy! See www.molecularbiosystems.org

RSC Books 2008

2007 witnessed the launch of the RSC eBook Collection, an innovative online product for scientists across the globe. A further highlight was *Elegant Solutions* by Philip Ball being awarded the 2007 Dingle Prize for the best recent book to communicate the history of science, technology and/or medicine to a wide audience of non-specialists. As we begin 2008, RSC Publishing is confident that our exciting 2008 book list will achieve further success, reinforcing our position at the forefront of international chemistry research publishing.



Looking forward to the year ahead, RSC Books plans to continue providing a first

class online publishing service and is aiming to achieve simultaneous eBook and print publication. Our eBook project saw 44 new eBooks go live in 2007 with a further 52 forecast to go live during 2008. Expect to see groundbreaking titles from our exclusive RSC Nanoscience & Nanotechnology, RSC Biomolecular Sciences series and the new RSC Green Chemistry and RSC Energy Series which join the RSC eBook Collection during 2008.

For more information on our prestigious international best sellers visit www.rsc.org/books

Chemical Technology (ISSN:1744-1560) is published monthly by the Royal Society of Chemistry, Thomas Graham House, Science Park, Milton Road, Cambridge UK CB4 0WF. It is distributed free with *Chemical Communications*, *Journal of Materials Chemistry*, *The Analyst*, *Lab on a Chip*, *Journal of Atomic Absorption Spectrometry*, *Green Chemistry*, *CrystEngComm*, *Physical Chemistry Chemical Physics* and *Analytical Abstracts*.

Chemical Technology can also be purchased separately. 2008 annual subscription rate: £199; US \$396. All orders accompanied by payment should be sent to Sales and Customer Services, RSC (address above). Tel +44 (0) 1223 432360, Fax +44 (0) 1223 426017 Email: sales@rsc.org

Editor: Neil Withers

Associate editors: Nina Notman, Celia Clarke

Interviews editor: Joanne Thomson

Essential Elements: Daniel Bradnam, Rebecca Jeeves, and Valerie Simpson

Publishing assistant: Ruth Bircham

Publisher: Graham McCann

Apart from fair dealing for the purposes of research or private study for non-commercial purposes, or criticism or review, as permitted under the Copyright, Designs and Patents Act 1988 and the copyright and Related Rights Regulations 2003, this publication may only be reproduced, stored or transmitted, in any form or by any means, with the prior permission of the Publisher or in the case of reprographic reproduction in accordance with the terms of licences issued by the Copyright Licensing Agency in the UK. US copyright law is applicable to users in the USA.

The Royal Society of Chemistry takes reasonable care in the preparation of this publication but does not accept liability for the consequences of any errors or omissions.

Royal Society of Chemistry: Registered Charity No. 207890.

RSC Publishing

©The Royal Society of Chemistry 2008

Green chemistry, green solvents, and free radical reactions in aqueous media

DOI: 10.1039/b800137p

Since its birth over a decade ago, the field of green chemistry has seen rapid expansion, with numerous innovative scientific breakthroughs associated with the production and utilization of chemical products.¹ The concept and ideal of green chemistry now goes beyond chemistry and touches subjects ranging from energy to societal sustainability. The key notion of green chemistry is “efficiency”, including material efficiency, energy efficiency, man-power efficiency, and property efficiency (*e.g.*, desired function *vs.* toxicity). Any “wastes” aside from these efficiencies are to be addressed through innovative green chemistry means. “Atom-economy”² and minimization of auxiliary chemicals, such as protecting groups and solvents, form the pillar of material efficiency in chemical productions. By far, the largest amount of “auxiliary wastes” in most chemical productions are associated with solvent usage. In a classical chemical process, solvents are used extensively for dissolving reactants, extracting and washing products, separating mixtures, cleaning reaction apparatus, and dispersing products for practical applications. While the invention of various exotic organic solvents has resulted in some remarkable advances in chemistry, the legacy of such solvents has led to various environmental and health concerns. Consequently, as part of green chemistry efforts, a variety of cleaner solvents have been evaluated as replacements.³ However, an ideal and universal green solvent for all situations does not exist. Among the most widely explored greener solvents are ionic liquids,⁴ supercritical CO₂,⁵ and water.⁶ These solvents complement each other nicely both in properties and applications. *Importantly, the study of green solvents goes far beyond just solvent replacement.* The use of green solvents has led science to uncharted territories. For example, the study of ionic liquids made large-scale supported synthesis possible for the first time⁷ and the utilization of supercritical CO₂ has led

to breakthroughs in microelectronics and nanotechnologies.⁸ Although water is the most abundant, natural and non-toxic solvent on earth, it has been traditionally considered as a nuisance in most chemical productions. However, since Breslow’s⁹ report on the acceleration of Diels–Alder reactions in aqueous media, the re-examination of this solvent for chemical applications has exploded. The commercialization of aqueous-based hydroformylation and hydrogenation processes allow product separation and catalyst recycling readily.¹⁰ The development of aqueous organometallic reactions simplifies protection–deprotection of functional groups and allows the direct use of biomass-based feedstocks for synthetic purposes.¹¹ The innovative “on-water” concept,¹² water-tolerant Lewis acids,¹³ and aqueous organocatalyses¹⁴ led to new understandings of fundamental chemical reactivities.

Free-radicals represent a large class of chemical species such as atoms, molecules and reaction intermediates that possess unpaired electrons. Such chemical species can both be long lived and short lived. They played important roles in biological processes and regulations of the atmosphere.¹⁵ Chemically, most free radicals are highly reactive and form a fundamental class of chemical reactions.¹⁶ Such reactions generally follow a pattern of the three stages of initiation, propagation and termination. The termination only occurs when two radicals, both at very low concentrations, meet and annul each other. Sometimes, this makes the reaction disastrous (such as in ozone depletion or explosions). However, with proper design and control, radical reactions can also be very “economical”, for example in tandem reactions and atom-transfer synthesis.

Because most molecule-based radicals and reaction intermediates do not have charges, consequently radicals generally react *via* orbital–orbital interactions, which is analogous to the pericyclic reactions.¹⁷ As a first approximation,

the principles, phenomena and theories governing pericyclic reactions could be applicable to many free-radical reactions. The similarity between pericyclic reactions and radical reaction suggest that free-radical reactions can not only occur in water but may be even advantageously accelerated by water. In addition, the very strong O–H bond of water and the high energy required for homolytic cleavage of this bond suggests that water will be better than most organic solvents in preventing side-reactions. There are a variety of ways to initiate a radical reactions. Some classical radical initiators are less desirable and new ones have been developed.

The tutorial review by Tuck and co-workers¹⁸ in this issue on forming C–H bonds in aqueous media summarized recent developments on the subject of using radical chemistry to generate terminal products with the formation of C–H bonds. The review include several key sections: (i) a brief background on the subject; (ii) the fundamental ways to carbon-centered free radicals in aqueous media and selection criteria; (iii) the discussions of the advantages and the usages of three major classes (azo-based initiators, peroxides and boranes) radical initiators for aqueous free-radical reactions; (iv) the effect of substrate solubility and hydrogen-atom-transfer reactions in aqueous media; (v) discussions on various greener free-radical hydrogen donors for forming the final C–H bond as well as the concept of “on water” and “in water” related to radical reactions; and finally, (vi) several applications of the hydro-atom-transfer reactions in aqueous media including natural product syntheses, probing DNA structure, and deuterium isotopic labeling.

Green chemistry is about scientific innovations in creating new knowledge based on sustainability and resource efficiency, as well as to tackle wastes and hazards associated with the generation and utilization of chemical products. The arsenals created by green chemists

are ever increasing. The development of free radical reactions to form C–H bond in aqueous media is one more tool in the green chemistry toolbox.

Chao-Jun Li, McGill University, Canada

References

- 1 P. T. Anastas and J. C. Warner, *Green Chemistry Theory and Practice*, Oxford University Press, New York, 1998.
- 2 B. M. Trost, *Science*, 1991, **254**, 1471.
- 3 R. A. Sheldon, *Green Chem.*, 2005, **7**, 267.
- 4 *Acc. Chem. Res.*, 2007, **40**(11), special issue on ionic liquids, ed. Robin D. Rogers and Gregory A. Voth.
- 5 *Green Chemistry Using Liquid and Supercritical Carbon Dioxide*, ed. J. M. DeSimone and W. Tumas, Oxford University Press, New York, 2003;
- 6 C.-J. Li, *Chem. Rev.*, 2005, **105**, 3095; C.-J. Li and T.-H. Chan, *Comprehensive Organic Reactions in Aqueous Media*, Wiley & Sons, New York 2007; *Organic Reactions in Water*, ed. U. M. Lindstrom, Blackwell, 2007.
- 7 W. Miao and T. H. Chan, *Acc. Chem. Res.*, 2006, **39**, 897.
- 8 D. A. Britz, A. N. Khlobystov, J. W. Wang, A. S. O'Neil, M. Poliakoff, A. Ardavan and G. A. D. Briggs, *Chem. Commun.*, 2004, 176.
- 9 D. C. Rideout and R. Breslow, *J. Am. Chem. Soc.*, 1980, **102**, 7816.
- 10 *Aqueous-Phase Organometallic Catalysis*, ed. B. Cornils and W. A. Herrmann, Wiley-VCH, Weinheim, 2004.
- 11 C.-J. Li, *Tetrahedron*, 1996, **52**, 5643; C.-J. Li, in *Organic Synthesis in Water*, ed. U. M. Lindstrom, Blackwell, Oxford, 2007.
- 12 S. Narayan, J. Muldoon, M. G. Finn, V. V. Fokin, H. C. Kolb and K. B. Sharpless, *Angew. Chem., Int. Ed.*, 2005, **44**, 3275.
- 13 S. Kobayashi, M. Sugiura, H. Kitagawa and W. W.-L. Lam, *Chem. Rev.*, 2002, **102**, 2227.
- 14 N. Mase, Y. Nakai, N. Ohara, H. Yoda, K. Takabe, F. Tanaka and C. F. Barbas, III, *J. Am. Chem. Soc.*, 2006, **128**, 734.
- 15 B. Halliwell and J. Gutteridge, *Free Radicals in Biology and Medicine*, Oxford University Press, New York, 2007.
- 16 S. Z. Zard, *Radical Reactions in Organic Synthesis*, Oxford University Press, New York, 2004.
- 17 I. Fleming, *Frontier Orbitals and Organic Chemical Reactions*, John Wiley & Sons, Chichester, 1976.
- 18 V. T. Perchyonok, I. N. Lykakis and K. L. Tuck, Recent advances in C–H bond formation in aqueous media: a mechanistic perspective, *Green Chem.*, 2008, **10**(3), DOI: 10.1039/b709047a.

Recent advances in C–H bond formation in aqueous media: a mechanistic perspective

V. Tamara Perchyonok,^{*ab} Ioannis N. Lykakis^{*c} and Kellie L. Tuck^{*b}

Received 15th June 2007, Accepted 9th November 2007

First published as an Advance Article on the web 22nd November 2007

DOI: 10.1039/b709047a

Recent advances in free-radical chemistry have expanded the versatility and flexibility of carbon–hydrogen bond formation in aqueous media. This review highlights progress made in the last decade to “tame” reactive free-radical species in aqueous-phase reactions. Detailed are a broad range of synthetically useful transformations and their application in synthesis, DNA structural probing and isotope labelling. The review provides some practical hints useful for the design of high-yielding free-radical reactions in aqueous media.

1 Introduction

One of the challenges for today’s chemist is to move away from highly volatile, environmentally harmful, and/or biologically incompatible organic solvents.^{1–5} Research in this area has led to the use of ionic liquids, supercritical (and near supercritical) solvents, and fluorosolvents.² An obvious choice is to replace organic solvents with water, due to its cost and availability.^{3–6} Additional benefits are that water can aid in the removal of the environmentally unfriendly “heavy metal” by-products.^{4,7} With several key reviews highlighting the ‘greenness’ of water,^{1,2,4} there has been a push to develop chemical reactions in water (aqueous media). Free-radical reactions are an important class of synthetic reactions that have been traditionally performed in organic solvents. In recent years, the number of reports of free-radical reactions that use water has increased.^{1–9} Water is an ideal solvent for

free-radical reactions as it possesses no reactive functional groups and strong O–H bonds that make hydrogen abstraction unlikely.^{4,7,9}

^aCentre for Green Chemistry, Monash University, Clayton, Australia 3800

^bSchool of Chemistry, Monash University, Clayton, Australia 3800.

E-mail: tamara.perchyonok@sci.monash.edu.au;

kellie.tuck@sci.monash.edu.au

^cDepartment of Chemistry, University of Crete, Iraklion, Voutes, Crete, Greece 71003. E-mail: lykakis@chemistry.uoc.gr



V. Tamara Perchyonok

V. Tamara Perchyonok is a Research Fellow at the School of Chemistry and Centre of Green Chemistry at Monash University, Australia since September 2006. After DFG Postdoctoral Research fellowship (2000–2002) under the guidance of Prof. H. Zipse at LMU, Munich, she returned to Australia, as a Research Fellow at University of Melbourne (2002–2004). In 2004 she returned to Europe to undertake a Marie Curie Research Fellowship at the I.S.O.F., Consiglio Nazionale delle Ricerche, Bologna, Italy under the supervision of Dr C. Chatgililoglu. Her research interests covers aspects of free-radical chemistry and green chemistry.



Ioannis N. Lykakis

Ioannis N. Lykakis was born in 1975 in Greece. He completed MSc and PhD degrees in Organic Chemistry at the University of Crete. Dr Lykakis undertook a Marie Curie Research Fellowship at the I.S.O.F., Consiglio Nazionale delle Ricerche, Bologna, Italy (2005–2006) under the supervision of Dr C. Chatgililoglu followed by Post Doctoral Research Fellowship in Department of Chemistry at the University of Crete (2006–2007). Now he is a visiting



Kellie L. Tuck

Assistant Professor at the Chemistry Department of University of Crete. His research focuses on catalysis, free radical chemistry

and biomimetic models for mechanistic studies of biological processes.

Kellie Tuck received her BSc and PhD from the University of Adelaide, Australia in 1995 and 1999, respectively. After a post-doctoral position at the University of South Australia, she spent three years working with Professor Chris Abell at the University of Cambridge. She returned to Australia in 2004 to take up her current position as a lecturer in the School of Chemistry at Monash University.

Whilst there have been several excellent reviews on carbon–carbon (C–C) bond formation and reactions of carbon–hydrogen (C–H) bonds in water,^{4,6–9} this review addresses carbon–hydrogen bond formations in aqueous media via radical reactions (hydrogen-atom transfer (HAT), radical cyclization and deoxygenation) within the past decade. There is a specific focus on HAT reactions as they represent one of the major classes of the atom/group transfer reactions. In HAT reactions, a hydrogen atom is transferred from a chain carrier to the newly formed radical centre, through the general mechanism involving radical initiation, radical propagation and radical termination steps (Scheme 1). This reaction is important in biology, in the chemical industry and in the chemical laboratory.^{1,2,10–15}

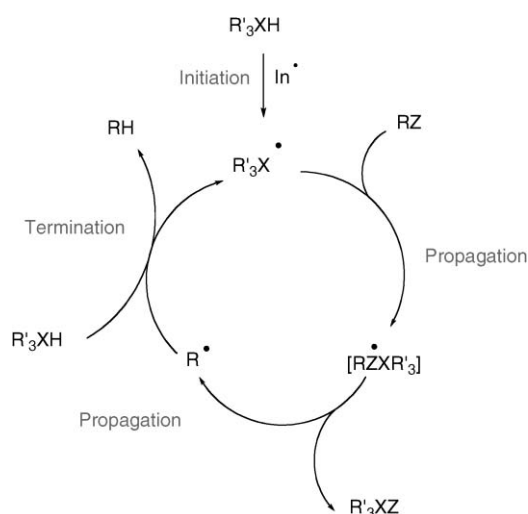
The review can be classified broadly into five main sections; the generation of carbon centered free radicals, radical initiators, solubility of substrate, the suitability of free-radical hydrogen donors and HAT reactions in aqueous media.

2 Generation of carbon-centered free radicals in aqueous media

In aqueous media carbon centered free radicals are typically generated by either chemical, photolysis or radiolysis methods. These methods are briefly discussed below and the criteria for the selection of a radical initiator and hydrogen donor are discussed in section 3 and 5 respectively.

Chemical methods used to generate carbon centered radicals include so called “building block” reactions of free-radical chemistry, such as HAT reactions,^{2,3} Barton–McCombie deoxygenation reactions,^{3,4} free-radical additions to double bonds,^{2,4} Fenton type reactions³ and thermal homolysis of organometallic compounds such as certain chromium species.¹⁶ Application of this method for generation of free radicals will be discussed further in section 3.

Photochemical methods for the formation of alkyl and other carbon centered radicals have been applied to the following “building block” reactions in the arsenal available to



Scheme 1 General diagram of the hydrogen-atom transfer (HAT) reaction.

free-radical chemists.^{17,18} Well suited for use in biological systems has also been used in synthetic applications in aqueous and organic solvents.^{3,4,5,6}

Radiolysis methods for the generation of carbon centered radicals in aqueous solution include irradiation of the reaction mixture to produce e_{aq}^- , H^\bullet or $\cdot OH$ radicals with various organic compounds. Although, this method is not currently used in synthesis, it is a very accurate and reliable probe for exploring mechanistic and kinetic properties of free radicals generated *in vivo*.^{19–25}

3 Radical initiators for aqueous free-radical reactions

There are three major classes of radical initiators; azo-based initiators, peroxides and boranes. In a free-radical reaction typically 5–10 mol% of the initiator is added, either in one portion or by slow addition to the reaction over a period of time. Water-soluble azo initiators have a number of advantages over organic peroxides. They are relatively inexpensive, do not produce undesirable decomposition products and/or toxic by-products and have a greater thermal stability. There are several commercially available azo radical initiators, see Fig. 1 for structures, that can be used for free-radical reactions in aqueous media. The most popular thermal radical initiator is 2',2'-azobisisobutyronitrile (AIBN) which has a half-life ($t_{1/2}$) in toluene of 1 h at 81 °C and 10 h at 65 °C.^{26–29} Whilst AIBN is a popular choice, other azo compounds can give superior results due to their varying half-life. The half-life of the radical is dependent on its substitution, consequently 2',2'-azobis(4-methoxy)-3,4-dimethylvaleronitrile (AMVN) has a half-life in toluene of 1 h at 56 °C and 10 h at 33 °C, 2',2'-azobis(2-methylpropionamide) dihydrochloride (APPH), a hydrophilic azo compound, has a $t_{1/2}$ of 10 h at 56 °C in organic solvents. The radical initiators AIBN, AMVN, V-501 and AAPH have been used in aqueous reactions.¹⁶ Peroxides are used when the reaction requires a more reactive initiating species.^{27,30} Initially an acyloxy radical is formed, followed by decarboxylation and a subsequent bimolecular reaction which affords the reactive carbon centered radical. Common peroxides that are used in organic media are *tert*-butyl perbenzoate ($PhC(O)OOBu-t$) and di-*tert*-butyl peroxide ($t-BuOOBu-t$), whose $t_{1/2}$ are 1 h at 125 and 147 °C, respectively.^{24,27}

Photochemically generated radical chain reactions are less familiar to the synthetic chemist than those described above.³ The above mentioned peroxides, *tert*-butyl perbenzoate and di-*tert*-butyl peroxide, have been used in the presence of light to initiate radical chain reactions at room temperature or lower. Azo compounds decompose under photochemical conditions and therefore are rarely used.³⁰

Triethyl borane (Et_3B), in the presence of a very small amount of oxygen, is an excellent initiator for radical chain reactions. For a long time it has been known that trialkylboranes (R_3B) will react spontaneously with molecular oxygen to give the corresponding alkyl radical (R^\bullet), but only in the last 10 years has this approach being successfully applied to the initiation of free-radical reactions.³⁰ These reactions can be run at temperatures as low as -78 °C, which allows for a high

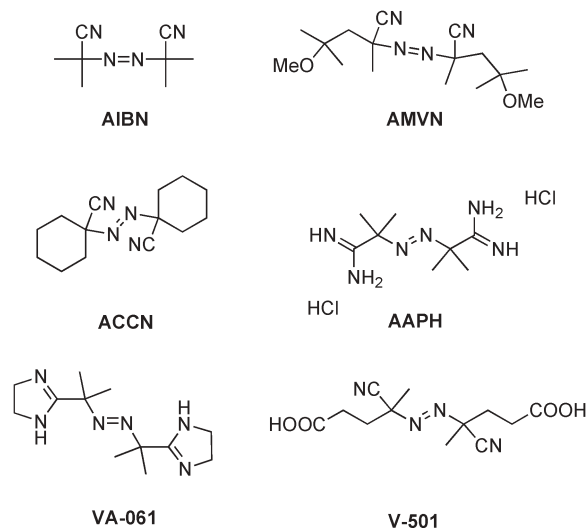


Fig. 1 Commercially available azo free-radical initiators.

degree of stereo-, regio- and enantioselectivity required in the synthesis of complex molecules.^{19,26,27,31–33}

It is advisable to add the initiators slowly during the course of the reaction with particular attention being paid to the half life of the decomposition of the initiator at the operating temperature of the reaction. The direct addition of the thermal initiator with a reaction temperature much higher than that of the 1 h half life generally does not lead to the optimal outcome of the free-radical reactions. At low temperatures, when the thermal initiation is not viable, Et₃B/O₂ is the best initiator to use initially.

4 Solubility of substrates and HAT reactions in aqueous media

Although a media effect in radical reactions was believed to be almost negligible, Oshima *et al.* reported recently that water increases the rate of radical reactions.³⁴ They have found that the atom transfer radical cyclization of allyl iodoacetate, promoted by triethylborane, is accelerated in water.³⁴ Moreover, they found that the yields of the cyclized products correspond to the solubility of the starting allyl iodoacetate derivative in water (Table 1).

Table 1 Cyclization of allyl iodoacetates with triethylborane

The reaction scheme shows the cyclization of an allyl iodoacetate derivative (1 mmol) with triethylborane (Et₃B, 0.1 mmol) in water (30 ml) to form a cyclic lactone product.

R	Solubility in water/mM	Yield (%)
H	10	67
CH ₃	4.4	77
C ₂ H ₅	1.4	72
n-C ₃ H ₇	0.4	18
n-C ₁₀ H ₂₁	0	0
CH ₂ OH	170	89

A similar solubility effect was observed in the radical addition of iodoacetamide to alkenes in water (Table 2).³⁴ Whereas alkenes with hydrophilic groups produced the lactone in high yields, water-insoluble 1-octene did not yield the desired lactone under the identical reaction conditions. The addition of organic co-solvent (EtOH–H₂O = 9 : 1) was required for the addition of iodoacetamide to 1-octene.³⁴

5 Free-radical hydrogen donors for C–H bond formation, “on water” and “in water”

Organotin hydrides, such as Bu₃SnH, Ph₃SnH and Me₃SnH, have been used as hydrogen donors in radical chain processes for the last 40 years.^{16,28,31,32,35,36} Since organostannanes are toxic, special handling during the disposal of tin residues is necessary and often problems with contamination after product purification are encountered. It is therefore not surprising that the so-called ‘tin problem’ has been addressed by introducing a variety of alternative hydride sources that can be used in conventional free-radical conditions as well as in aqueous media.³⁵ An increasing number of new reagents are being reported for use in aqueous media, these include silylated cyclohexadienes,^{35a} gallium hydride (HGaCl₂),³⁷ indium(II) chloride (InCl₂),³⁸ hypophosphorous acid (H₃PO₂)³ and 1-ethylpiperidine hypophosphite (EHPH)²⁶ (Fig. 2). The use of hypophosphorous acid as a H-donor is discussed in more detail in section 5.1.

Thiols are hydrogen donors in free-radical reactions due to the weak S–H bond (364 kJ mol^{−1} *cf.* 435 kJ mol^{−1} for O–H).³² Thiols are frequently employed in mechanistic studies as radical traps.¹⁶ An understanding of the kinetic rates of radical reactions is required for their development and

Table 2 Radical addition of various acetamide to alkenes in water

The reaction scheme shows the radical addition of iodoacetamide to an alkene (CH₂=CH–R) in water at 75°C for 16h, catalyzed by V-501, to form a lactone product.

R	Yield (%)
CH ₂ OH	88
(CH ₂) ₂ OH	91
(CH ₂) ₃ OH	85
(CH ₂) ₄ OH	95
(CH ₂) ₂ CO ₂ H	94
n-C ₆ H ₁₃	0

 Hypophosphorous acid	 Diethyl phosphine oxide	 N-ethylpiperidine Hypophosphite (EHPH)
TMS ₃ SiH	TMS ₃ SiH/RSH	
Tris(trimethylsilyl)silane	Tris(trimethylsilyl)silane/Thiol	

Fig. 2 Common hydrogen donors utilized in the radical hydrogen atom transfer reactions in water and aqueous media.

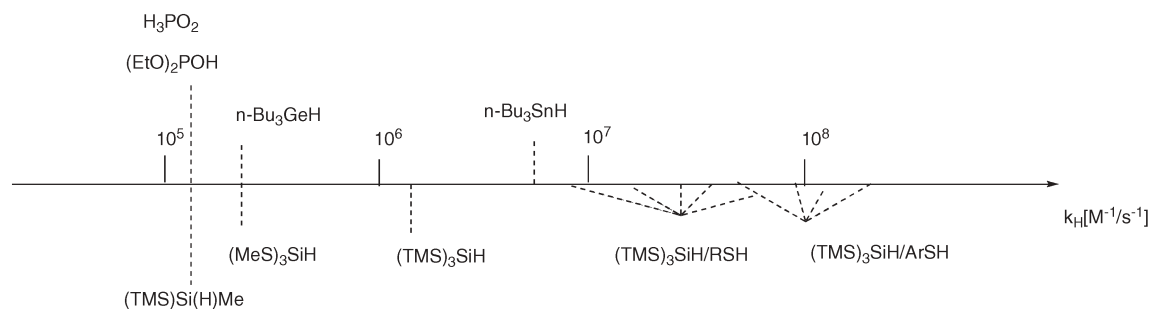


Fig. 3 Rate constants for hydrogen-atom transfer from hydrogen-donor systems and primary radicals at 80 °C.

alteration. To date a large volume of vital kinetic data has been collected, a kinetic timeline of the hydrogen donor abilities of various commonly used free-radical reducing agents is summarized in Fig. 3.^{28–30} Generally speaking for HAT reactions to be efficient the rate of the chain transfer step between the radicals and the starting materials must be higher than that of the chain termination steps between the radicals.³⁰

5.1 Hypophosphorous acid (H₃PO₂) and its derivatives as a free-radical hydrogen donor

5.1.1 Background and reaction rates. An understanding of the physical aspects and the reaction rates of P-centered radicals is required in order to benefit from the full potential offered by phosphorous-containing compounds. The radical reactions HAT, halogen atom abstractions, cyclizations and additions are reactions in the “tool box” of the widely applied free-radical chemistry.³⁹

It is interesting to note that hydrogen abstraction from hypophosphorous acid or its derivatives to form phosphonyl radicals is comparable to that of phenyl-substituted silanes ($1.2 \times 10^5 \text{ M}^{-1} \text{ s}^{-1}$).⁴⁰ Turro and Jockusch showed that phosphinoyl radicals ($\text{R}_2\text{P}(\text{O})\cdot$) are roughly ten times more prone to reduction by thiophenol than acylphosphinoyl ones ($(\text{RCO})_2\text{P}(\text{O})\cdot$).⁴¹ A considerable amount of work has linked the structure and reactivity of these radicals; phosphinoyl and phosphonyl radicals are non-planar and as a result have a variable degree of *s*-character,⁴² phosphonyl radicals are more bent than phosphinoyl ones and acylphosphinoyl radicals are further flattened (Fig. 4).⁴³ In general, the more bent the radical, the faster it will add to olefins. A trend that has been attributed to the relative accessibility of the localized spin to the trapping agent.

5.1.2 Use of P-centered radicals as efficient hydrogen donors. The use of the hypophosphorous acid and its derivatives as

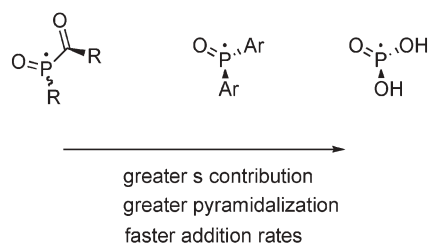
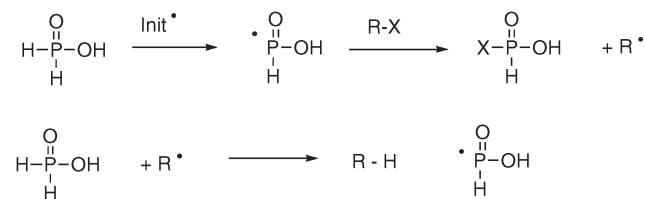


Fig. 4 Geometry of the P-centered radicals.

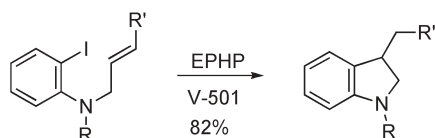
hydrogen donors comes from the crucial re-examination by Barton and Jaszberenyi of some old radical reductions involving hypophosphorous acid.⁴⁴ The use of water as a solvent for the clean and efficient reduction of organohalides has initiated and propagated the growth of the novel area of bioapplicable, biocompatible and “environmentally” friendly methodology in free-radical synthesis. For this reason, and because radical reactivities are complementary to other reactivities, the quest for alternative mediators/hydrogen donors is extremely active.¹² In the last decade, hypophosphorous acid and its derivatives have been used as mediators in several radical reactions in aqueous media.^{43–52} The mechanism of action of the P–H containing compounds is described in Scheme 2.⁵¹ Several classes of novel hydrogen donors was introduced by Jang *et al.*, these include sodium salts of hypophosphorous acid for the reduction of water-soluble organohalides and introduction of dibutylphosphine and diphenylphosphine oxides as novel, less hygroscopic reducing agents.^{44–46}

The groups of Murphy⁴⁷ and Stoodley⁴⁸ simultaneously reported that *N*-ethylpiperidine hypophosphite (EHP, Fig 2) initiates carbon–carbon bond formation either through a 5-*exo*-trig cyclization of an aryl radical obtained from an iodide⁴⁷ or through a 5-*exo*-dig cyclization of an alkyl α -keto radical obtained from a corresponding bromide⁴⁸ (Scheme 3). The final step of both transformation is the intra-molecular HAT reaction from EHP with the initiator V-501.

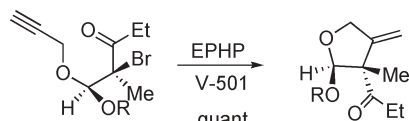
Kita and co-workers have built on previous results to report EHP-mediated cyclization of hydrophobic substrates in water.⁴⁹ The addition of a water-soluble initiator (VA-061, [2,2'-azobis(2-(2-imidazolin-2-yl)propane)], Fig 1) and the surfactant cetyltrimethylammonium bromide (CTAB) resulted in a yield increase from 25 to 98% (Scheme 4). The authors explain that this outstanding result is due to the micellar effect of by CTAB, contributing to the incorporation of the hypophosphoric acid in the micelles.⁵²



Scheme 2 General mechanism of the HAT reactions with hypophosphorous acid (H₃PO₂) as hydrogen donors.

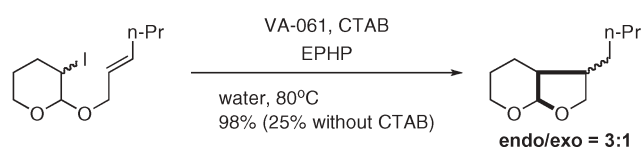
Murphy

Where R = Ms or Tos
R' = Me

Stoodley

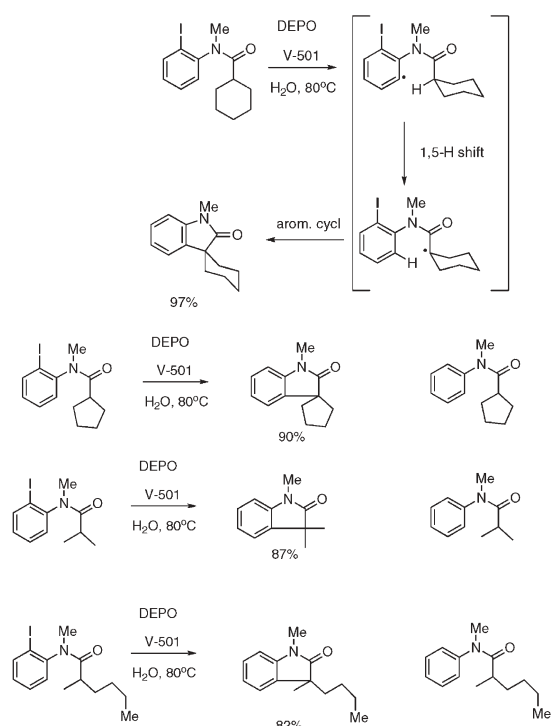
Where R = Me or Et

Scheme 3 EPHP-mediated radical cyclizations.



Scheme 4 EPHP-mediated radical cyclization in water of the hydrophobic substrate.

Recently, Murphy *et al.* used a water-soluble phosphine oxide to synthesize indolones in excellent yields in water in tandem radical reactions (aryl radical formation, HAT, cyclization and rearomatization) (Scheme 5).⁵¹ The reaction is mediated by diethyl phosphine oxide (DEPO) and the water-soluble radical initiator V-501. The advantages of these



Scheme 5 DEPO-mediated arylation of the amides in water.

reaction conditions are that reaction temperatures are significantly lower than is typically required for a similar reaction with tributyl tin hydride in benzene.³⁵ This permits significantly higher isolated yields than the corresponding reaction mediated by ethylpiperidine hypophosphite (EPHP).⁴⁹ DEPO is water soluble and more lipophilic than hypophosphorous acid and consequently it facilitates interaction between the water-soluble mediator, the initiator and the lipophilic substrates without requiring a phase transfer agent.⁵⁰ The pK_a of DEPO ($pK_a = 6$) ensures extraction of excess reagent into the basic layer during workup.

5.2 Radical deoxygenation in aqueous media, a special case of C–H bond formations

Tetraalkylammonium hypophosphites (TAHPs), recently reported by Cho and Jang,⁵⁰ are prepared by mixing various commercially available tetraalkylammonium hydroxide with aqueous H_3PO_2 . These mild and efficient reagents are used for the radical deoxygenation of alcohols and the formation of carbon–hydrogen bonds in water, without additives such as surfactants (Table 3).⁵⁰

Reaction of the model compound, cyclododecyl *S*-methyl dithiocarbonate, with several TAHPs (TAHP-1, TAHP-2, TAHP-3 and TAHP-4) in the presence of a water-soluble radical initiator, V-501, in water, can yield up to 94% of the deoxygenated product after 5 h (Table 4).

This methodology was applied to the synthesis of 2',3'-dideohydro-2',3'-dideoxynucleosides which have been shown to be potent anti-HIV agents.⁴⁹ The bis-xanthate of the *N*³-methyluridine derivative was subjected to the tandem radical cyclization followed by HAT reaction in water, giving the corresponding olefin in 82% yield (Scheme 6).⁵⁰ Similar results were also achieved in the case of adenosine derivative (76% yield).⁵⁰

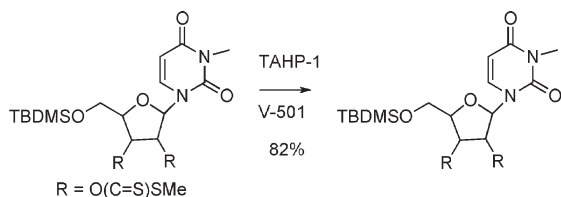
Table 3 Various tetraalkylammonium hypophosphites

M ⁺	M ⁺ (PO ₂ H ₂) [−]
(CH ₃) ₃ N ⁺ (CH ₂) ₁₅ CH ₃	TAHP-1
Bu ₄ N ⁺	TAHP-2
Bu ₃ N ⁺ CH ₃	TAHP-3
(CH ₃) ₄ N ⁺	TAHP-4

Table 4 Deoxygenation of *O*-cyclododecyl *S*-methyl dithiocarbonate with tetraalkylammonium hypophosphites in water

Entry	TAPH (equiv.)	V-501 (equiv.)	t/h	Yield (%)
1	TAPH-1 (3)	0.5	5	94
2	TAPH-1 (2)	0.5	8	84
3	TAPH-2 (3)	0.75	7	90
4	TAPH-3 (3)	0.75	8	62 (29) ^a
5	TAPH-4 (3)	0.75	8	45 (52) ^a

^a Recovered starting material.

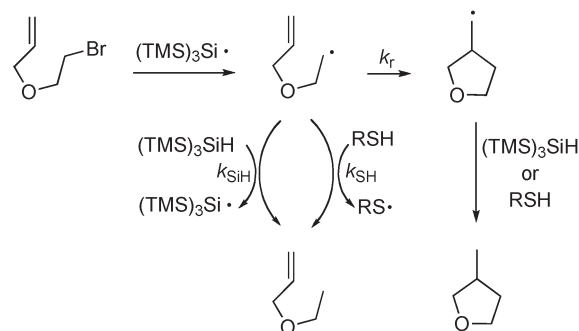


Scheme 6 Deoxygenation of N^3 -methyluridine derivative in water.⁵

Recently, Kita *et al.* found that the combination of water-soluble radical initiator (VA-061), water-soluble chain carrier (EHPH) and surfactant (CTAB), resulted in a radical cyclization that occurred in water with a variety of hydrophobic substrates (Table 5).⁵² Although the results were not as high yielding as in the case of $(\text{TMS})_3\text{SiH}$, it was shown for the first time that silane could be used as a silicon based hydrogen donor in aqueous media. This discovery highlighted that $(\text{TMS})_3\text{SiH}$ is an environmentally benign and powerful hydrogen donor “on water” and “in water”. By definition “on water” reactions are a group of organic reactions that take place as an emulsion in water and exhibit an unusual reaction rate acceleration compared to the same reaction in organic solvent or compared to the corresponding “dry media conditions”.⁵³ Reactions “in water” are usually defined as reactions that are miscible and are performed in water.

5.3 Tris(trimethylsilyl)silane ($(\text{TMS})_3\text{SiH}$) is an efficient radical hydrogen donor, “on water”

One of the drawbacks of radical reactions in aqueous media is the immiscibility of either reagents, reactants or initiators. However, recently this viewpoint has changed and immiscibility has started to be considered advantageous. Chemical reactions “on water” are now given greater attention, since the reactivity in the suspension obtained by vigorous stirring of immiscible reactants seems to benefit from the enhanced contact surface of the resulting tiny drops, as well as from the unique molecular properties developed at the interface between water and hydrophobic phase.⁵³ “Polarity reversal catalysis” is ideal for free-radical hydrogen transfer reactions “on water”.⁵⁴ The advantages of this methodology are based on the fact that the silane/thiol mixture not only enhances of the radical production and regeneration, but the system is also



Scheme 7 Radical chain reduction/cyclization of 3-(2-bromoethoxy)prop-1-ene by the $(\text{TMS})_3\text{SiH}$ /thiol (RSH) reducing system

flexible enough to accommodate the amphiphilic thiol (RSH) which increases the radical reactivity at the interface Scheme 7.

5.3.1 On “polarity reversal catalysis” and the benefits for silicon-based reducing agents in aqueous media. The reaction of thiyl radicals with silicon hydrides (Scheme 8) is a key step of the so called “polarity reversal catalysis” that has been utilized extensively in the radical chain reductions of alkyl halides as well as in the hydrosilylation of olefins using silane-thiol couple. The reaction is strongly endothermic and reversible. The rate constants k_{SH} and k_{SiH} were determined in cyclohexane at 60 °C, relative to $2k_t$ for the self termination of the thiyl radicals, using the kinetic analysis of the thiol-catalysed reduction of 1-bromooctane and 1-chlorooctane by silane, respectively.⁵⁵

Recently, Chatgililoglu and co-workers reported that by employing suitable thiol/silane mixture in the “polarity reverse” mediated HAT reaction the efficient synergy of radical production, regeneration and enhancement of the radical reactivity at the interface can be achieved.^{54,56,57} For the reduction of the organic halide (RX) by the combination $(\text{TMS})_3\text{SiH}/\text{HOCH}_2\text{CH}_2\text{SH}$ under radical conditions, the propagation steps suggested in the scheme are expected. That is, the alkyl radical abstracts hydrogen from the thiol and the



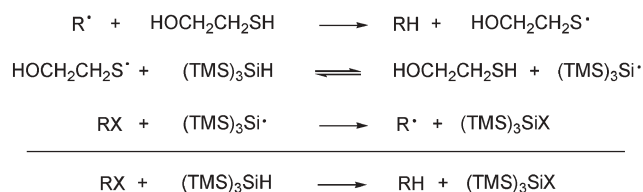
Scheme 8

Table 5 Radical cyclization reactions using various initiators, hydrogen donors and surfactants

Initiator	Yield (%) (<i>cis</i> : <i>trans</i>)	H-donor/V-061	Yield (<i>cis</i> : <i>trans</i>)	Additive	Yield (%) (<i>cis</i> : <i>trans</i>)
VA-061	98 (55 : 45)	None	0	None	64 (74 : 26)
AIBN	19 (57 : 43)	$(\text{TMS})_3\text{SiH}$	94 (67 : 33)	CTAB	98 (55 : 45)
Et_3B	50 (67 : 43)	EHPH	98 (55 : 45)	SDS	98 (51 : 49)
V-501	72 (51 : 49)	$\text{H}_3\text{PO}_2/\text{NaHCO}_3$	84 (78 : 22)	Triton X-100	98 (62 : 38)
VA-044	95 (50 : 50)	NaH_2PO_2	58 (78 : 22)	$\text{Et}_4\text{N}^+\text{Br}^-$	85 (65 : 35)

^a SDS = sodium dodecyl sulfate, Triton X-100 is a non-ionic surfactant.

mechanism:



Scheme 9 Proposed mechanism of polarity reversal catalysis using $(\text{TMS})_3\text{SiH}$ /thiol system.

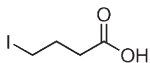
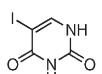
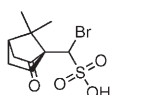
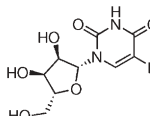
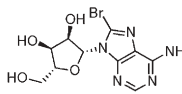
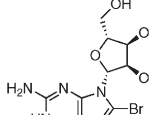
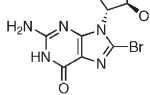
resulting thiyl radicals abstract hydrogen from the silane, so that the thiol is regenerated along with the chain carrying silyl radical for a given RX (Scheme 9).⁵⁶

Reduction of organohalides,⁵⁶ including bromonucleosides,⁵⁸ can be achieved in aqueous media using $(\text{TMS})_3\text{SiH}$. This procedure employs 2-mercaptoethanol as the catalyst and either ACCN as organic solvent-soluble initiator or AAPH as water-soluble radical initiator, the reduced compounds are obtained in yields of 75% to quantitative (Table 6). As $(\text{TMS})_3\text{SiH}$ does not react significantly with water, it is therefore a good reagent for radical based reductions in aqueous media.

5.4 Thiol/azo initiator system in fatty acid isomerization and peptide degradation in aqueous media

Chatgililoglu and co-workers have used the thiol/azo-initiator system for the isomerization of *cis* phospholipids to the corresponding *trans* compounds. Cascade reactions, as well as geometrical isomerization of the mono- and poly-unsaturated

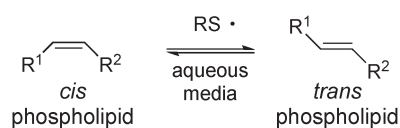
Table 6 Reduction of organic halides (10 mM) with $(\text{TMS})_3\text{SiH}$ (12 mM) and $\text{HOCH}_2\text{CH}_2\text{SH}$ (2.85 mM) in water

Substrate	Initiator (mM)	<i>T</i> /°C	Yield (%)
	APPH (3)	73	99
	ACCN (3)	100	100
	APPH (3)	73	90
	APPH (3)	73	—
	ACCN (3)	100	90
	ACCN (33)	100	95
	APPH (3)	73	—
	ACCN (3)	100	90
	APPH (3)	73	—
	ACCN (3)	100	94
	APPH (3)	73	—
	ACCN (3)	100	75
			

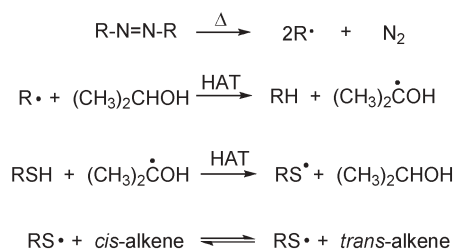
fatty acid double bonds can be achieved by using a combination of radical initiators and RSH as a hydrogen donor *in vitro* (Scheme 10). From the *in vitro* and *in vivo* studies it emerged that the thiyl radicals (RS^{\bullet}) are able to diffuse from the aqueous phase to the lipid phase and perform a reaction involving the membrane lipid double bonds thus forming *trans* fatty acids.^{59,60} In these studies a catalytic amount of thiols and various hydrophilic and hydrophobic azo-initiators, such as AAPH, AIBN and AMVN, were used at 37, 71 and 54 °C respectively, in aqueous media.⁶¹ Thiyl radicals addition to the *cis* and *trans* double bond of phospholipids in aqueous media is accompanied by isomerization, according to the mechanism proposed in Scheme 10. This addition is reversible and gives the *trans* geometric isomer in up to an 80% relative yield. In all cases, HAT reactions take place at the initial pathways, between alcohol and alkyl radical intermediate (R^{\bullet}) forming the corresponding α -hydroxy carbon radical ($\text{C}^{\bullet}\text{-OH}$), which can abstract a H-atom from the thiol to generate the corresponding RS^{\bullet} (Scheme 10).

Sulfides have been shown to catalyze the lipid isomerization processes⁶¹ with a series of hydrophobic and hydrophilic sulfides ($\text{HOCH}_2\text{CH}_2\text{SCH}_3$, $\text{HOCH}_2\text{CH}_2\text{CH}_2\text{SCH}_3$, *S*-methyl cysteine and *S*-methyl homocysteine) were used with AAPH as the initiator or under γ -radiation conditions. It was suggested that under γ -radiolysis the H^{\bullet} atoms react with sulfides to form a sulfuranyl species (Scheme 11) which in turn collapses to give directly or indirectly the MeS^{\bullet} radical (or HS^{\bullet} in the case of thiols). On the other hand the alkyl radicals R^{\bullet} or the $\text{C}^{\bullet}\text{-OH}$ generated from the azo-initiator can abstract a hydrogen atom from positions that are activated by the neighboring groups forming the corresponding tertiary radical. These radical are expected to generate MeS^{\bullet} radicals *via* β -elimination (Scheme 11). Similarly, thiols such as $\text{HOCH}_2\text{CH}_2\text{SH}$ and cysteine should form sulfhydryl radicals HS^{\bullet} (or $\text{S}^{\bullet-}$) radical, which are able to isomerize efficiently lipid double bonds in aqueous media.^{62,63}

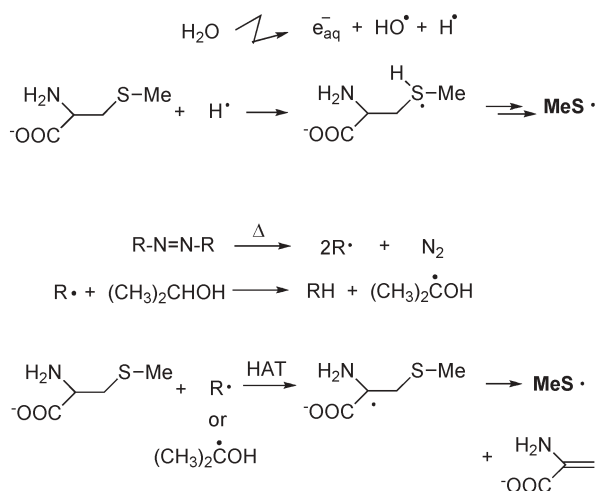
The reaction of hydrogen atoms with peptides containing methionine (Met) residues such as Met-enkephalins,⁶⁴ RNase A⁶⁵⁻⁶⁷ and amyloid β -peptides,⁶⁸ have been investigated. In these studies H^{\bullet} atoms are generated by radiolytic conditions from the reaction of aqueous electrons with dihydrogen



Radical Pathways:



Scheme 10 Thiol/azo-initiator system catalyzes lipid double bond isomerization in aqueous media.



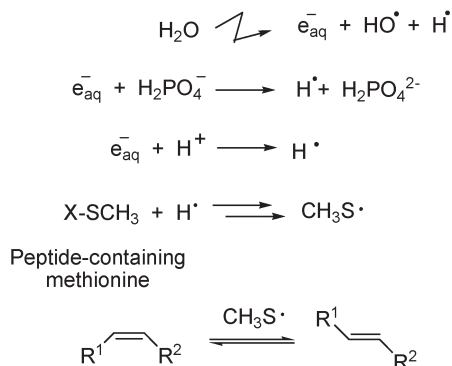
Scheme 11 Sulfide/azo-initiator system used in lipid double bond isomerization in aqueous media.

phosphate anion (H_2PO_4^-), as shown in Scheme 12. For Met-enkephalin it was calculated that 30–40% of H^\bullet should react with the Met residue.⁶⁴ The formation of diffusible thiol radicals such as $\text{CH}_3\text{S}^\bullet$, derived from the reaction of the H^\bullet with the Met moiety, was monitored with *trans* lipids as markers. Using this peptide-liposome model, it was proposed that $\text{CH}_3\text{S}^\bullet$ is able to migrate from the aqueous layer to the membrane compartment thereby cause the geometrical isomerization of lipid double bonds.

6 Several applications of the HAT reactions in aqueous media

6.1 Free-radical synthesis of natural products in water, is it a reality

Hypophosphite hydrides can add to unsaturated compounds and thus lead to the formation of the corresponding phosphinates. Fukuyama designed a highly selective and elegant synthesis of indoles by reacting hypophosphite salts with unsaturated thioanilides.⁶⁹ Initial regioselective addition of the P-centered radical onto the C=S bond generated a new stabilized carbon radical that could cyclize onto the olefin in the ortho position, thus giving rise to the indolic skeleton.



Scheme 12 Hydrogen atom reaction with peptides containing Met-residues in aqueous media.

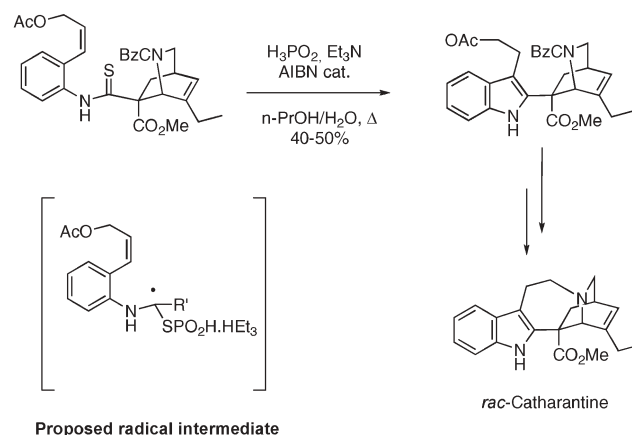
Aromatization of the compound generated the desired 2,3-substituted indole. The authors have employed this reaction as a key step towards the total synthesis of (\pm)-catharantine, a presumed biological precursor of anti-tumor alkaloids vinblastine and vincristine (Scheme 13).⁶⁹

6.2 Generation of radicals for probing DNA structures

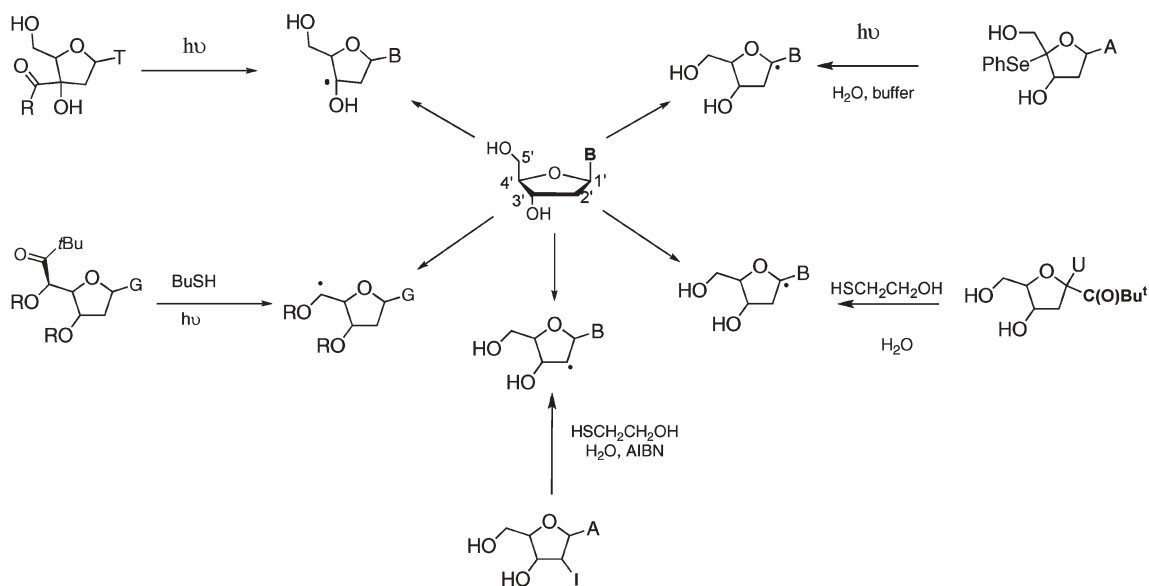
The various conformations of DNA, the A, B and Z forms, the protein-induced DNA kink, and the G-quartet form are thought to play important biological roles in processes such as DNA replication, gene expression and regulation, and the repair of DNA damage.¹⁰ Investigation of local DNA conformational changes associated with biological events is essential in understanding the function of DNA. The susceptibility of damage to the sugar unit of DNA is mainly determined by formation of free radicals through hydrogen atom abstraction from one of the five available positions. The radicals *in vivo* can repair itself by hydrogen atom abstraction from glutathione, or can lead to modification of the sugar unit (DNA-damage), however they can lead to the strand breakage. The ability of a chemist to generate the desired radicals using “nature like conditions” is essential to understanding radical mediated DNA damage. To date there are several ways of generating C1',⁷⁰ C2',⁷¹ C3',⁷² C4',⁷³ and C5'^{74,75} radicals under “aqueous conditions” which are summarized in Scheme 14.

6.3 Deuterium isotopic labeling in aqueous media

Recent progress in the fields of NMR spectroscopy and mass spectrometry has allowed stable isotope labeling to become an important technique in metabolic research for determining the biological behavior of small molecules. The development of synthetic methods for the preparation of compounds labeled with non-radioactive isotopes such as deuterium has therefore gained importance. Common methods for the incorporation of deuterium into organic molecules include ionic reactions using deuterides such as NaBD_4 and LiAlD_4 , triethylsilane/boron trifluoride system ($\text{Et}_3\text{SiD}\cdot\text{BF}_3$) and radical methods involving *n*- Bu_3SnD .^{76,77} Unfortunately, radical reactions using tin deuterides have serious drawbacks when used in the synthesis of biologically active compounds, because of the inherent



Scheme 13 Formation of indole from thioanilide.



Scheme 14 Various methods of generation C1', C2', C3', C4' and C5' radicals from suitable radical precursors.

toxicity of organotin derivatives and the difficulty of removal of residual tin compounds. Recently radical cyclizations have employed non-toxic and easily removed phosphinic acid (H_3PO_2) in aqueous solvents.⁷⁸ Oshima *et al.* introduced a broad range of phosphorous based deuterating agents to achieve radical deuteration, these include deuterated hypophosphorous acid potassium salts, deuterated phosphinic acid/DBU mixture and a deuterated phosphinic acid/DCI/ K_2CO_3 combination.⁷⁸ Deuteration of hydrophobic substrates is possible, although the incorporation of deuterium was not optimal (<20%), however less hydrophobic substrates gave deuteration with total incorporation (Scheme 15).⁷⁷ It is noteworthy to mention that in this radical reaction a quaternary center is created bearing a deuterium in high yield. Various hydrogen/deuterium exchanges were conducted in

either D_2O or D_2O /dioxane mixture and complete deuterium incorporation could be achieved by the reactions in D_2O without the addition of an organic co-solvent and/or organic base.

7 Conclusions

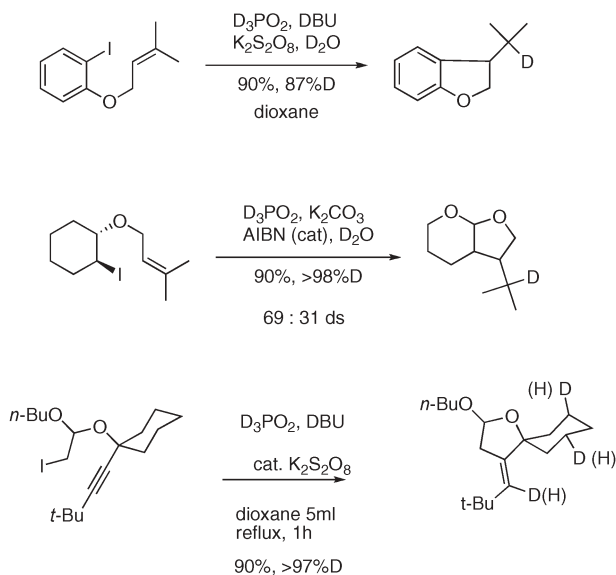
This review highlights several methods for carbon–hydrogen transfer reactions in aqueous media with various reducing agents. The simplicity of water, its abundance and wide availability, will undoubtedly lead the development of novel and exciting methodologies. The development of environmentally benign applications based on radical hydrogen atom transfer reactions is just around the corner.

Acknowledgements

V. T. P. would like to acknowledge the help, support and critical reading of the manuscript by Prof. Steven J. Langford.

References

- D. J. Adams, P. J. Dyson and S. J. Taverner, *Chemistry in Alternative Reaction Media*, Wiley-Interscience, Cambridge, 2004;
- W. M. Nelson, *Green Solvents for Chemistry, Perspectives and Practice*, Oxford University Press, New York, 2003.
- W. Wei, C. C. K. Keh and C.-J. Li, *Clean Technol. Environ. Policy*, 2005, **7**, 62–69.
- D. Leca, L. Fensterbank, E. Lacote and M. Malacria, *Chem. Soc. Rev.*, 2005, **34**, 858–865, and references cited therein.
- U. M. Lindstrom, *Chem. Rev.* 2002., 2002, **102**, 2751–2772, and references cited therein.
- D. Font, C. Jimeno, M. Pericas and A. Miquel, *Org. Lett.*, 2006, **8**, 4653–4655.
- L. Chen and C.-J. Li, *Adv. Synth. Catal.*, 2006, **348**, 1459–1484.
- C.-J. Li, *Chem. Rev.*, 2005, **105**, 3095–3166, and references cited therein.
- C. I. Herrerías, X. Yao, Z. Li and C.-J. Li, *Chem. Rev.*, 2007, **107**, 2546–2562, and references cited therein.
- C.-J. Li, *Chem. Rev.*, 1993, **93**, 2023–2035, and references cited therein.



Scheme 15 D_3PO_2 -Mediated radical reaction in aqueous medium.

- 10 Y. Xu and H. Sugiyama, *Angew. Chem., Int. Ed.*, 2006, **45**, 1354–1362.
- 11 J. F. J. Coelho, M. Carreira, A. V. Popov, P. M. O. F. Goncalves and M. H. Gil, *Eur. Polym. J.*, 2006, **42**, 2313–2319.
- 12 M. K. Chaudhuri and S. Hussain, *J. Mol. Catal. A: Chem.*, 2007, **269**, 214–217.
- 13 A. P. Brogan and T. J. Dickerson, *Angew. Chem., Int. Ed.*, 2006, **45**, 8100–8102.
- 14 H. Sugimoto, M. Tarumizu, H. Miyake and H. Tsukube, *Eur. J. Inorg. Chem.*, 2006, **22**, 4494–4497.
- 15 Y. Gu, C. Ogawa, J. Kobayashi, Y. Mori and S. Kobayashi, *Angew. Chem., Int. Ed.*, 2006, **45**, 7217–7220.
- 16 For an excellent general reference book in free-radical chemistry see: B. Giese, *Radicals in Organic Synthesis: Formation of Carbon–Carbon Bonds*, Pergamon Press, 1986, and references cited therein.
- 17 S. Itsuno, Y. Arakawa and N. Haraguchi, *Nippon Gomu Kyokaishi*, 2006, **79**, 448–454.
- 18 Y. Gu, C. Ogawa and S. Kobayashi, *Chem. Lett.*, 2006, **35**, 1176–1177.
- 19 For an excellent review on applications of photolysis in free-radical chemistry, see: (a) *CRC Handbook of Organic Photochemistry and Photobiology*, ed. W. Horspool and F. Lenci, CRC Press, USA, 2nd edn, 2004, and references cited therein; (b) For the original paper on the use of photolysis deoxygenation reaction, see: D. H. R. Barton and C. Tachdjian, *Tetrahedron*, 1992, **48**, 7109–7120.
- 20 P. Neta, J. Grodkowski and A. B. Ross, *J. Phys. Chem. Ref. Data*, 1996, **25**, 709–1050, and references cited therein.
- 21 G. V. Buxton, C. L. Greenstock, W. P. Helman and A. B. Ross, *J. Phys. Chem. Ref. Data*, 1988, **17**, 513–886.
- 22 D. Veltwisch, E. Janata and K.-D. Asmus, *J. Chem. Soc., Perkin Trans. 2*, 1980, 146–156.
- 23 D. Brault and P. Neta, *J. Phys. Chem.*, 1984, **88**, 2857–2862.
- 24 L. J. Mittal and J. P. Mittal, *Radiat. Phys. Chem.*, 1986, **28**, 363–371.
- 25 D. G. Kelley, A. Marchaj, A. Bakac and J. H. Espenson, *J. Am. Chem. Soc.*, 1991, **113**, 7583–7587.
- 26 D. Dakternieks, V. T. Perchyonok and C. H. Schiesser, *Tetrahedron: Asymmetry*, 2003, **14**, 3057–3068.
- 27 (a) C. Walling, *Tetrahedron*, 1985, **19**, 3887–3900; (b) Y. Kita and M. Matsugi, in *Radical in Organic Synthesis*, ed. P. Renaud and M. P. Sibi, Wiley-VCH, Weinheim, 2001, vol. 1, pp. 1–10.
- 28 K. Itami and J. Yoshida, *Chem. Rec.*, 2002, **2**, 213–224.
- 29 C. Chatgililoglu, *Helv. Chim. Acta*, 2006, **89**, 2387–2398, and references cited therein.
- 30 C. Chatgililoglu, in *Organosilanes in Radical Chemistry*, John Wiley & Sons, Ltd, West Sussex, UK, 2004, and references cited therein.
- 31 J. Zimmerman and M. Sibi, *Top. Curr. Chem.*, 2006, **263**, 107–162.
- 32 L. Zeng, D. Dakternieks, A. Duthie, T. Perchyonok and C. Schiesser, *Tetrahedron: Asymmetry*, 2004, **15**, 2547–2554.
- 33 L. Zeng, V. T. Perchyonok and C. H. Schiesser, *Tetrahedron: Asymmetry*, 2004, **15**, 995–999.
- 34 H. Yorimitsu, T. Nakamura, H. Shinokubo, K. Oshima, K. Omoto and H. Fujimoto, *J. Am. Chem. Soc.*, 2000, **122**, 11041–11047.
- 35 (a) On the broad applications and utility of tin based reducing agents, see: P. A. Baguley and J. C. Walton, *Angew. Chem., Int. Ed.*, 1998, **37**, 3072–3082; A. Studer and S. Amrein, *Synthesis*, 2002, 835–849; (b) for pioneering work on removal of tin reagents, see: J. Light and R. Breslow, *Tetrahedron Lett.*, 1990, **31**, 2957–2958; D. L. Clive and W. Yang, *J. Org. Chem.*, 1995, **60**, 2607–2609; (c) on the use of fluoros tin hydrides to facilitate separation of organotin by-products, see: D. P. Curran, S. Hadida, S. Y. Kim and Z. Luo, *J. Am. Chem. Soc.*, 1999, **121**, 6607–6615; (d) on the use of polymer bound tin hydrides, see selected references: J. Junggebauer and W. P. Neumann, *Tetrahedron*, 1997, **53**, 1301–1310; D. Laporte, H. Deleuze, B. Mailard and K. Mulholland, *Synth. Commun.*, 2001, **31**, 3207–3218, and references cited therein.
- 36 M. Tullberg, K. Luthman and M. Grotli, *J. Comb. Chem.*, 2006, **8**, 915–922.
- 37 S. Mikami, K. Fujita, T. Nakamura, H. Yorimitsu, H. Shinokubo, S. Matsubara and K. Oshima, *Org. Lett.*, 2001, **3**, 1853–1855.
- 38 K. Takami, S. Mikami, H. Yorimitsu, H. Shinokubo and K. Oshima, *Tetrahedron*, 2003, **59**, 6627–6635.
- 39 (a) T. Sumiyoshi and W. Schnabel, *Makromol. Chem.*, 1985, **186**, 1811–1823; (b) T. Sumiyoshi, W. Schnabel, A. Henne and P. Lechtken, *Polymer*, 1985, **26**, 141–146.
- 40 C. Chatgililoglu, V. I. Timokhin and M. Ballestri, *J. Org. Chem.*, 1998, **63**, 1327–1329.
- 41 S. Jockusch and N. J. Turro, *J. Am. Chem. Soc.*, 1998, **120**, 11773–11777.
- 42 (a) M. Geoffroy and E. A. C. Lucken, *Mol. Phys.*, 1971, **22**, 257; (b) C. M. L. Kerr, K. Webster and F. Williams, *J. Phys. Chem.*, 1975, **79**, 2650–2662.
- 43 G. W. Sluggett, P. F. McGarry, I. V. Koptuyug and N. J. Turro, *J. Am. Chem. Soc.*, 1996, **118**, 7367–7372.
- 44 D. H. R. Barton, J. A. Ferreira and J. C. Jaszberenyi, *Preparative Carbohydride Chemistry*, 1997, pp. 151–157.
- 45 D. O. Jang, *Tetrahedron Lett.*, 1996, **37**, 5367–5368.
- 46 D. O. Jang, D. H. Cho and J. Kim, *Synth. Commun.*, 1998, **28**, 3559–3565.
- 47 C. Gonzales Martin, J. A. Murphy and C. R. Smith, *Tetrahedron Lett.*, 2000, **41**, 1833–1836.
- 48 R. McCague, R. G. Pritchard, R. J. Stoodley and D. S. Williamson, *Chem. Commun.*, 1998, 2691–2692.
- 49 H. Nambu, G. Anilkumar, M. Matsugi and Y. Kita, *Tetrahedron*, 2003, **59**, 77–85.
- 50 D. H. Cho and D. O. Jang, *Tetrahedron Lett.*, 2005, **46**, 1799–1802.
- 51 T. A. Khan, R. Tripoli, J. J. Crawford, C. G. Martin and J. A. Murphy, *Org. Lett.*, 2003, **5**, 2971–2974.
- 52 Y. Kita, H. Nambu, N. G. Ramesh, G. Anilkumar and M. Matsugi, *Org. Lett.*, 2001, **3**, 1157–1160.
- 53 S. Narayan, J. Muldoon, M. G. Finn, V. V. Fokin, H. C. Kold and K. B. Sharpless, *Angew. Chem., Int. Ed.*, 2005, **44**, 3275–3279.
- 54 C. Chatgililoglu, M. Guerra and Q. G. Mulazzani, *J. Am. Chem. Soc.*, 2003, **125**, 3839–3848.
- 55 F. Villar, O. Andrey and P. Renaud, *Tetrahedron Lett.*, 1999, **40**, 3375–3378.
- 56 Al Postigo, C. Ferreri, M. L. Navacchia and C. Chatgililoglu, *Synlett*, 2005, **18**, 2854–2856.
- 57 L. B. Jimenez, S. Encinas, M. A. Miranda, M. L. Navacchia and C. Chatgililoglu, *Photochem. Photobiol. Sci.*, 2004, **3**, 1042–1046.
- 58 C. Chatgililoglu, M. L. Navacchia and Al Postigo, *Tetrahedron Lett.*, 2006, **47**, 711–714.
- 59 C. Chatgililoglu and C. Ferreri, *Acc. Chem. Res.*, 2005, **38**, 441–448.
- 60 C. Ferreri and C. Chatgililoglu, *ChemBioChem*, 2005, **6**, 1722–1734.
- 61 (a) C. Chatgililoglu, C. Ferreri, M. Ballestri, Q. G. Mulazzani and L. Landi, *J. Am. Chem. Soc.*, 2000, **122**, 4593–4601; (b) C. Ferreri, C. Costantino, L. Perrotta, L. Landi, Q. G. Mulazzani and C. Chatgililoglu, *J. Am. Chem. Soc.*, 2001, **123**, 4459–4468; (c) C. Ferreri, A. Samadi, F. Sassatelli, L. Landi and C. Chatgililoglu, *J. Am. Chem. Soc.*, 2004, **126**, 1063–1072.
- 62 C. Chatgililoglu, C. Ferreri, I. N. Lykakis and P. Wardman, *Bioorg. Med. Chem.*, 2006, **14**, 6144–6148.
- 63 I. N. Lykakis, C. Ferreri and C. Chatgililoglu, *Angew. Chem., Int. Ed.*, 2007, **46**, 1914–1916.
- 64 O. Mozziconacci, K. Bobrowski, C. Ferreri and C. Chatgililoglu, *Chem.–Eur. J.*, 2007, **13**, 2029–2033.
- 65 C. Ferreri, I. Manco, M. R. Faraone-Mennella, A. Torreggiani, M. Tamba and C. Chatgililoglu, *ChemBioChem*, 2004, **5**, 1710–1712.
- 66 C. Ferreri, I. Manco, M. R. Faraone-Mennella, A. Torreggiani, M. Tamba, S. Manara and C. Chatgililoglu, *ChemBioChem*, 2006, **7**, 1738–1744.
- 67 A. Torreggiani, M. Tamba, I. Manco, M. R. Faraone-Mennella, C. Ferreri and C. Chatgililoglu, *Biopolymers*, 2006, **81**, 39–50.
- 68 V. Kadlick, C. Sicard-Roselli, C. Houee-Levin, M. Kodicek, C. Ferreri and C. Chatgililoglu, *Angew. Chem., Int. Ed.*, 2006, **45**, 2595–2598.
- 69 M. T. Reding and T. Fukuyama, *Org. Lett.*, 1999, **1**, 973–976.
- 70 (a) T. Gimisis, G. Ialongo, M. Zamboni and C. Chatgililoglu, *Tetrahedron Lett.*, 1995, **36**, 6781–6784; (b) T. Gimisis, G. Ialongo and C. Chatgililoglu, *Tetrahedron*, 1998, **54**, 573–592.
- 71 C. Chatgililoglu, M. Duca, C. Ferreri, M. Guerra, M. Ioele, Q. G. Mulazzani, H. Strittmatter and B. Giese, *Chem.–Eur. J.*, 2004, **10**, 1249–1255.

- 72 K. Steffi, A. Bryant-Friedrich and B. Giese, *J. Org. Chem.*, 1999, **64**, 1559–1564.
- 73 (a) B. Giese, P. Erdmann, T. Schaefer and U. Schwitter, *Synthesis*, 1994, 1310–1312; (b) B. Giese, A. Dussy, C. Elie, P. Erdmann and U. Schwitter, *Angew. Chem., Int. Ed. Engl.*, 1994, **33**, 1941–1944; (c) B. Giese, A. Dussy, E. Meggers and M. Petretta, *J. Am. Chem. Soc.*, 1997, **119**, 11130–11142.
- 74 A. Manetto, D. Georganakis, L. Leondiadis, T. Gimisis, P. Mayer, T. Carell and C. Chatgililoglu, *J. Org. Chem.*, 2007, **72**, 3659–3666.
- 75 M. Russo, L. B. Jimenez, Q. G. Mulazzani, M. D'Angelantonio, M. Guerra, M. A. Miranda and C. Chatgililoglu, *Chem.–Eur. J.*, 2006, **12**, 7684–7693.
- 76 M. Orfanopoulos and I. Smonou, *Synth. Commun.*, 1988, **18**, 833–839.
- 77 I. N. Lykakis and M. Orfanopoulos, *Tetrahedron Lett.*, 2005, **46**, 7835–7839.
- 78 H. Yorimitsu, H. Shinokubo and K. Oshima, *Bull. Chem. Soc., Jpn.*, 2001, **74**, 225–235.

Textbooks from the RSC

The RSC publishes a wide selection of textbooks for chemical science students. From the bestselling *Crime Scene to Court*, 2nd edition to groundbreaking books such as *Nanochemistry: A Chemical Approach to Nanomaterials*, to primers on individual topics from our successful *Tutorial Chemistry Texts series*, we can cater for all of your study needs.

Find out more at www.rsc.org/books

Lecturers can request inspection copies – please contact sales@rsc.org for further information.



Registered Charity No. 207890

RSC Publishing

www.rsc.org/books

Heterogeneously catalyzed etherification of glycerol: new pathways for transformation of glycerol to more valuable chemicals†

Yanlong Gu, Ahmed Azzouzi, Yannick Pouilloux, François Jérôme* and Joël Barrault

Received 12th October 2007, Accepted 28th November 2007

First published as an Advance Article on the web 10th December 2007

DOI: 10.1039/b715802e

Direct etherification of glycerol with alkyl alcohols, olefins and dibenzyl ethers was successfully catalyzed by acid functionalized silica, allowing the first catalytic access to valuable monoalkyl glyceryl ethers.

Over the last ten years, glycerol has gained a lot of attention because of the tremendous industrial development of vegetable oils especially for the production of biodiesel. Indeed, glycerol is the main co-product of the vegetable oil industry and the rapid expansion of biodiesel demand is creating a significant glut of the glycerol market, unavoidably accompanied by an alteration of the cost and availability of this natural polyol. In order to further advance the production and utilization of biodiesel, new and innovative catalytic processes based on the use of glycerol were recently developed. Some of these works can be found in recent comprehensive reviews.¹ However, up to now, all these studies are mainly dedicated to the transformation of glycerol to low value added chemicals such as surfactants,^{1b} fuel additives,² acrolein,³ carbonate,⁴ etc... This tendency comes from the fact that the use of glycerol as a building block for advanced organic synthesis raises major drawbacks such as (i) the presence of three hydroxyl groups with similar pK_a (~ 13.5) which requires the assistance of protective agents,⁵ (ii) its high hydrophilicity which makes its interaction with organic substrates highly difficult and (iii) its high viscosity raising some substrate diffusion problems. For these reasons, although numerous elaborate organic substrates exhibit a glycerol moiety as organic skeleton, for instance amphiphilic polymers,⁶ antifungal agents⁷ and various pharmaceutical ingredients,⁸ glycerol has never been used as a starting material for their synthesis. Indeed, in order to get satisfactory synthetic yields, highly reactive and toxic reagents such as epichlorohydrin, 3-chloro-1,2-propanediol or glycidol are always preferred to the cheap and non-toxic glycerol. However, regarding the availability, the environmental and the economical viability of the process, the use of glycerol would be much more preferable.

In this context, heterogeneous catalysis is expected to play a pivotal role by offering to organic chemists useful tools for the successful use of glycerol in advanced organic synthesis. In this respect, we report here that acid organomodified silica materials are much more efficient than other solid catalysts in performing various organic transformations from glycerol with high yield. In particular, we show here that Brønsted sulfonic catalysts

immobilized over siliceous solid support are a very active solid catalyst for the metal and salt free (i) etherification of glycerol with alkyl alcohols, (ii) nucleophilic addition of glycerol to olefins and (iii) cleavage of ether bonds with glycerol. This study affords, in a one step process and without addition of any organic solvent, a diverse array of glycerol-based organic structures in moderate to excellent yields. It is noteworthy that this study opens, for the first time, environmentally friendly and easy routes for the transformation of glycerol to higher value added chemicals. Indeed, monoether glyceryl ethers (MAGEs) resulting from these transformations are highly valuable chemicals since they exhibit a wide spectrum of biological activities such as anti-inflammatory,⁹ antibacterial, antifungal,¹⁰ immunological stimulation,¹¹ and anti-tumor properties.¹² They are also important precursors for the preparation of 1,3-dioxolan-2-ones¹³ and bis(sodium sulfonate ester) type cleavable surfactants.¹⁴

We initially investigated the catalytic etherification of glycerol with alkyl alcohols. To the best of our knowledge, this pathway has been discussed very little and only a few pioneer efforts for drug derivatization are reported.¹⁵ Alkyl chlorides are generally used for selective etherification of alcohols including glycerol.¹⁶ However, this process requires a stoichiometric amount of base or the use of $\text{Cu}(\text{acac})_2$ ¹⁷ as catalyst which unfortunately leads to an extensive production of salts which has to be treated and disposed of. With the aim of searching for new catalytic pathways, we discovered that silica supported sulfonic moieties ($\text{SiO}_2\text{-SO}_3\text{H}$ **1**)¹⁸ were able to catalyze the direct etherification of glycerol with 1-phenyl-1-propanol. Indeed, when an equimolar mixture of glycerol and 1-phenyl-1-propanol was heated at 80 °C in the presence of 1.7 mol% of sulfonic catalyst grafted over silica, resulting MAGEs were obtained, after 4.5 h of reaction, in 73% yield with an exclusive selectivity (Table 1, entry 2). Further increase of the reaction time with the aim of increasing the MAGEs yield was found to be ineffective due to the side formation of double-etherified product at higher conversion (entry 3). Fortunately, the selectivity and the yield to the desired MAGEs were significantly improved when 4.2 equiv. of glycerol were used (entry 4). Temperature also affected the reaction quite notably, and optimal yield was achieved at 80 °C (entries 4, 5). It is interesting to note that, in all cases, the desired α -monoalkyl glyceryl ether (**1c**) was always obtained with more than 88% regioselectivity.

Remarkably, very low amounts of $\text{SiO}_2\text{-SO}_3\text{H}$ **1** catalyst can be employed without affecting the reaction yield. Indeed, in the presence of only 0.8 mol% of immobilized sulfonic catalyst, MAGEs were obtained with 95% yield after 7.5 h of reaction (Fig. 1). Conversely, an increase of the catalyst amount from 1.7 to 2.6 mol % of grafted $\text{-SO}_3\text{H}$ caused a surprising drop of the

Laboratoire de Catalyse en Chimie Organique, Université de Poitiers-CNRS, 40 Avenue du recteur Pineau, Poitiers Cedex, 86022, France.
E-mail: francois.jerome@univ-poitiers.fr

† Electronic supplementary information (ESI) available: Further experimental details. See DOI: 10.1039/b715802e

Table 1 Screening of catalysts^a

Entry	Catalyst	GC yield (%)	
		1c	1d
1	Naked SiO ₂	0	0
2 ^b	SiO ₂ -SO ₃ H 1	73 ^c (1c/1d = 90/10)	<1
3 ^{b,d}	SiO ₂ -SO ₃ H 1	76 ^c (1c/1d = 88/12)	12
4	SiO ₂ -SO ₃ H 1	96 ^c (1c/1d = 90/10)	<1
5 ^e	SiO ₂ -SO ₃ H 1	73 ^c (1c/1d = 90/10)	<1
6	PTSA	64 ^c (1c/1d = 86/14)	<1
7	CH ₃ SO ₃ H	60 ^c (1c/1d = 83/17)	<1
8	Carbon-SO ₃ H	12 ^c (1c/1d = 89/11)	<1
9	Amberlyst-16	12 ^c (1c/1d = 88/12)	<1
10	Zeolite HFAU ^f	18 (1c/1d = 54/46)	<1
11 ^g	SiO ₂ -SO ₃ H 1	96 ^c (1c/1d = 88/12)	<1

^a 1b/1a molar ratio = 4.2. ^b 1b/1a molar ratio = 1. ^c The remainder is unreacted starting material. ^d 7 h. ^e 60 °C. ^f Zeolite CBV-720 with total framework Si/Al ratio of 16, 10 wt%. ^g Reused in the fifth run.

reaction yield from 95 to 69%. Further inspection revealed that, in this case, more than 20% of carbon mass balance was lost probably due to a polymerisation of reactants.

The efficiency of SiO₂-SO₃H **1** was then compared to other known solid catalysts in order to highlight the large contribution of silica-based materials for the use of glycerol in organic synthesis. Surprisingly, with homogenous catalysts, such as *p*-toluenesulfonic acid (PTSA) and methanesulfonic acid (CH₃SO₃H), the reaction rate was lower than in the case of SiO₂-SO₃H **1** since the desired MAGEs were produced with only 64% and 60% yield respectively (entries 6, 7) after 4.5 h of reaction. The same results were obtained when SiO₂-SO₃H was compared to other known acid solid catalysts such as acidic carbon (carbon-SO₃H, H⁺ exchange capacity = 0.3 mmol g⁻¹), Amberlyst-16 (H⁺ exchange capacity = 5.0 mmol g⁻¹), and zeolite CBV-720 (with total framework Si/Al ratio of 16).¹⁸ Indeed, with these solid catalysts, no reaction yield

beyond 20% was observed (entries 8–10) after 4.5 h of reaction. It should be noted that, in all cases, except with CBV-720 zeolite for which an important loss (*ca.* 60%) of carbon mass balance was observed probably due to a polymerization of products, the reaction mixture was clean as only starting materials and products were detected by GC during the reaction.

Recyclability of the SiO₂-SO₃H solid catalyst was also investigated. After each cycle, the used catalyst was filtered, washed with ethanol and reused for the next catalytic run. The activity of SiO₂-SO₃H **1** was unaffected even after five catalytic runs (Table 1, entry 11) (see also ESI†). This higher performance of the silica based catalyst compared to other catalytic systems might be ascribed to its strong affinity for glycerol. Indeed, these materials are known to be highly polar¹⁹ and probably stronger interact with glycerol than other solid catalysts leading thus to higher reaction rate.

Having found suitable conditions for the catalytic dehydrative etherification of glycerol over SiO₂-SO₃H **1** solid catalyst, we then proceeded to screen a wide range of different alcohols and the results are shown in Table 2. Many benzyl alcohols including 1-phenyl-1-ethanol, 1-tolyl-1-ethanol, 1-(4-chlorophenyl)-1-ethanol, 1-phenyl-1-pentanol, benzhydrol and benzyl alcohol were successfully converted to their corresponding MAGEs in 85% to 96% yields (entries 1–5). Interestingly, the present catalytic process tolerated the use of functionalized alkyl alcohols such as α -vinylbenzyl alcohol, 1-phenyl-1-pentyn-3-ol and 1-phenyl-2-propyn-1-ol. Indeed, yields ranging between 70 and 83% were obtained in all cases and no polymerization or cleavage of the double and triple bond was observed (entries 6–8). Amphiphilic MAGEs resulting from the etherification of glycerol with a long alkyl chain are useful surfactants for industry because of their high

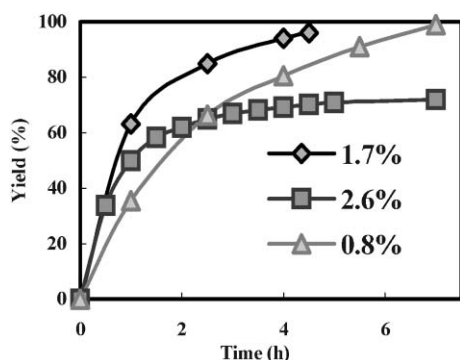
**Fig. 1** Effect of catalyst amount.

Table 2 Etherification between glycerol and alkyl alcohols over $\text{SiO}_2\text{-SO}_3\text{H}$ 1

Entry	Alcohols	Time/h	Isolated yield (%)	2a/2b
1		2.5	85	93/7
2 ^a		2.0	94	94/6
3		8.0	89	93/7
4 ^b		2.0	96	94/6
5		19	76	84/16
6		48	83	88/12
7 ^c		7	70	90/10
8		4	82	92/8
9		5	83	89/11
10		48	0	—
11 ^d		39	61	79/21 ^e

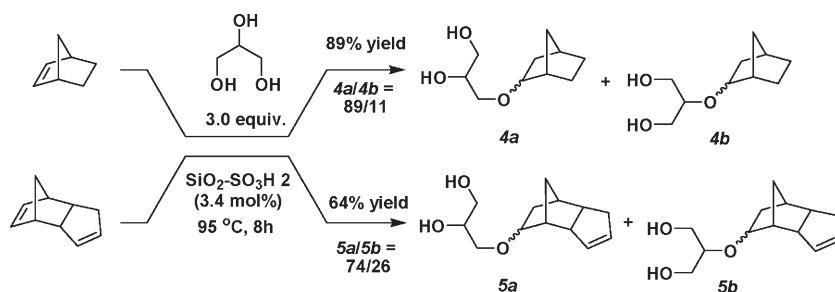
^a 1.4 mol% catalyst, 65 °C. ^b 70 °C. ^c 60 °C. ^d 2.5 mol% catalyst, 85 °C, GC yield, *trans/cis* = 2.0. ^e Calculated based on GC (for *cis*-product) and ¹H NMR (for *trans*-product).

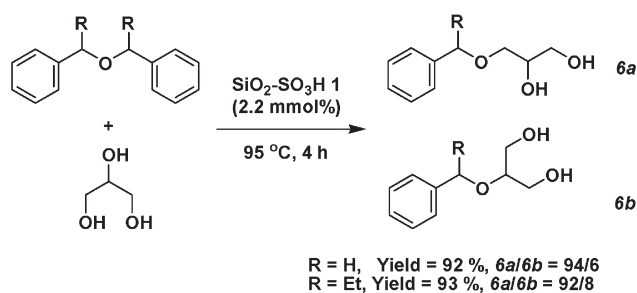
stability.¹⁶ For this reason, we then examined the reactivity of aliphatic alcohols with glycerol. The present catalytic process was found only efficient starting from *exo*-norborneol for which 83% yield was obtained (entry 9). All attempts to catalytically etherify glycerol with dodecanol were unsuccessful and no reaction was observed even at higher temperature or with longer reaction time (entry 10). Fortunately, starting from long chain allylic alcohols such as *trans*-2-octene-1-ol, amphiphilic MAGEs were obtained with more than 61% yield offering new and green access to robust glycerol-based surfactants (entry 11).

In seeking further improvements using glycerol as the glyceryl donor, we then moved on to the direct nucleophilic addition of glycerol to olefins. In the literature, catalytic addition of glycerol to isobutene has been already reported. However, this process requires a large excess of isobutene and a lack of selectivity was observed since tri-etherified products were mainly obtained.²⁰ Recently, Zhang and Corma reported an efficient procedure for the etherification of alcohols with olefins. This reaction was catalyzed by gold catalyst in the presence of copper as co-catalyst.²¹ Selective and metal free nucleophilic addition of glycerol to olefins would be, if realized, conceptually interesting and industrially relevant because of the 100% of atom economy of this reaction. Results of this study are reported in Scheme 1. Under optimized conditions, $\text{SiO}_2\text{-SO}_3\text{H}$ 2¹⁸ allowed successful conversions of norbornylene and dicyclopentadiene to the corresponding mono-ethers of glycerol in 89% and 64% yields, respectively. Interestingly, in the case of dicyclopentadiene, the nucleophilic addition of glycerol exclusively occurred to the 5,6-double bond. To the best of our knowledge, the present catalytic process is the first example of a salt and metal free route for the direct and selective nucleophilic addition of polyols to olefins.

In order to further demonstrate the large contribution of $\text{SiO}_2\text{-SO}_3\text{H}$ solid catalysts for the use of glycerol as a safe organic building block, dibenzyl ethers were then used to react with glycerol. In the presence of 2.2 mol% of sulfonic catalyst immobilized on silica ($\text{SiO}_2\text{-SO}_3\text{H}$ 2), dibenzyl ether and di(α -phenyl)propyl ether were readily reacted with glycerol at 95 °C to afford the corresponding ethers with more than 90% yield within 4 h (Scheme 2). The regioselectivity of this reaction was still very high since α -regioisomers (**6a**) were produced with more than 92% selectivity.

In conclusion, glycerol has been proven as a green, cheap and sustainable glyceryl donor for the synthesis of various derivatives instead of traditional expensive and toxic epichlorohydrin, 3-chloro-1,2-propanediol and glycidol. In this study, we have shown that $\text{SiO}_2\text{-SO}_3\text{H}$ catalysts are able to couple glycerol with

**Scheme 1** Synthesis of MAGEs from glycerol and olefins.



Scheme 2 Synthesis of MAGEs from glycerol and dibenzyl ethers.

various organic substrates under environmentally friendly conditions. Indeed, with benzyl, propargyl and allyl alcohols, olefins and dibenzyl ethers, glycerol was converted to the corresponding MAGEs in moderate to excellent yields. This method not only contributes to conversions of glycerol to more value added chemicals but also opens, for the first time, a salt and metal free catalytic alternative to the stoichiometric synthesis of MAGEs.

The authors thank the French Ministry of Research and CNRS for their financial support and the post-doctoral grant for YG.

Notes and references

- (a) M. Pagliaro, R. Ciriminna, H. Kimura, M. Rossi and C. D. Pina, *Angew. Chem., Int. Ed.*, 2007, **46**, 4434; (b) A. Corma, S. Iborra and A. Velty, *Chem. Rev.*, 2007, **107**, 2411; (c) N. Armaroli and V. Balzani, *Angew. Chem., Int. Ed.*, 2007, **46**, 52; (d) J. N. Chheda, G. W. Huber and J. A. Dumesic, *Angew. Chem., Int. Ed.*, 2007, 7164; (e) R. R. Soares, D. A. Simmonetti and J. A. Dumesic, *Angew. Chem., Int. Ed.*, 2006, 3982.
- K. Klepáčová, D. Mravec, A. Kaszonyi and M. Bajus, *Appl. Catal. A*, 2007, **328**, 1.
- (a) L. Ott, M. Bicker and H. Vogel, *Green Chem.*, 2006, **8**, 214; (b) S.-H. Chai, H.-P. Wang, Y. Liang and B.-Q. Xu, *Green Chem.*, 2007, **9**, 1130.
- C. Vieville, J. W. Yoo, S. Petet and Z. Mouloungui, *Catal. Lett.*, 1998, **56**, 245.
- C. C. Yu, Y.-S. Lee, B. S. Cheon and S. H. Lee, *Bull. Korean Chem. Soc.*, 2003, **24**, 1229.
- (a) M.-C. Jones, P. Tewari, C. Blei, K. Hales, D. J. Pochan and J.-C. Leroux, *J. Am. Chem. Soc.*, 2006, **128**, 14599; (b) A. Sunder, M. Krämer, R. Hanselmann, R. Müllhaupt and H. Frey, *Angew. Chem., Int. Ed.*, 1999, **38**, 3552.
- C. Len, D. Postel, G. Ronco, P. Villa, C. Goubert, E. Jeurfault, B. Mathon and H. Simon, *J. Agric. Food Chem.*, 1997, **45**, 3.
- S. Brandange, H. Leijonmarck and T. Minassie, *Acta Chem. Scand.*, 1997, **51**, 953.
- W. Chalmers, A. C. Wood, A. J. Shaw and J. J. Majnarich, *US Pat.*, 32946391966.
- (a) M. P. Haynes, H. R. Buckley, M. L. Higgins and R. A. Pieringer, *Antimicrob. Agents Chemother.*, 1994, **38**, 1523; (b) B. Boeryd, B. Hallgren and G. Ställberg, *Br. J. Exp. Pathol.*, 1971, **52**, 221.
- A. Brohult, J. Brohult, S. Brohult and I. Joelsson, *Acta Obstet. Gynecol. Scand.*, 1986, **65**, 779.
- (a) R. Mori and Y. Kabata, *Jpn. Kokai Tokkyo Koho*, JP 63077833, 1988; (b) N. Weber, in *Progress in Biochemical Pharmacology*, ed. P. Braquet, H. K. Mangold and B. B. Vargaftig, Karger, Basel, 1988, vol. 22, pp. 48–57.
- (a) M. Horibe, K. Suzuki, E. Ogura and N. Yamamoto, *Jpn. Kokai Tokkyo Koho*, JP 2000239271, 2000; (b) M. Okutsu and T. Kitsuki, *Jpn. Kokai Tokkyo Koho*, JP 2004168674, 2004.
- D. Ono, S. Yamamura, M. Magamura and T. Takeda, *J. Surfactants Detergents*, 1998, **1**, 201.
- (a) M. Hovorka, I. Stibor, R. Scigel and I. Smiskova, *Synlett*, 1995, 251; (b) T. C. McMorris, J. Yu, R. Lira, R. Dawe, J. R. MacDonald, S. J. Waters, L. A. Estes and M. J. Kelner, *J. Org. Chem.*, 2001, **66**, 6158.
- S. Queste, P. Bauduin, D. Touraud, W. Kunz and J.-M. Aubry, *Green Chem.*, 2006, **8**, 822.
- O. Sirkecioglu, B. Karliga and N. Talinli, *Tetrahedron Lett.*, 2003, **44**, 8483.
- Two SiO₂-SO₃H catalysts were used: SiO₂-SO₃H **1** (H⁺ exchange capacity: 0.32 mmol g⁻¹) and SiO₂-SO₃H **2** (H⁺ exchange capacity: 0.57 mmol g⁻¹). All solid catalysts, except commercially available ones (Amberlyst-16 and zeolite HFAU), were prepared and titrated according to our previous methods: (a) A. Karam, Y. Gu, F. Jérôme, J.-P. Douliez and J. Barrault, *Chem. Commun.*, 2007, 2222; (b) Y. Gu, A. Karam, F. Jérôme and J. Barrault, *Org. Lett.*, 2007, **9**(16), 3145.
- D. J. Macquarrie, D. B. Jackson, J. E. G. Mdoe and J. H. Clark, *New J. Chem.*, 1999, **23**, 539.
- K. Klepáčová, D. Mravec and M. Bajus, *Appl. Catal. A*, 2005, **294**, 141.
- X. Zhang and A. Corma, *Chem. Commun.*, 2007, 3080–3082.

Aerobic oxidation of aldehydes under ambient conditions using supported gold nanoparticle catalysts†

Charlotte Marsden, Esben Taarning, David Hansen, Lars Johansen, Søren K. Klitgaard, Kresten Egeblad and Claus Hviid Christensen*

Received 8th August 2007, Accepted 14th November 2007

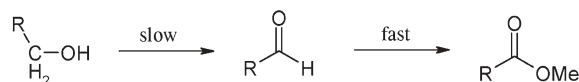
First published as an Advance Article on the web 26th November 2007

DOI: 10.1039/b712171g

A new, green protocol for producing simple esters by selectively oxidizing an aldehyde dissolved in a primary alcohol has been established, utilising air as the oxidant and supported gold nanoparticles as catalyst. The oxidative esterifications proceed with excellent selectivities at ambient conditions; the reactions can be performed in an open flask and at room temperature. Benzaldehyde is even oxidised at a reasonable rate below $-70\text{ }^{\circ}\text{C}$. Acrolein is oxidised to methyl acrylate in high yield using the same protocol.

Over the past decade, the utilisation of gold catalysis has increased rapidly.¹ For a long time, gold was thought to be relatively inactive as a catalyst, but finally in 1973 it was shown to be active for the hydrogenation of olefins.² Later, the hydrochlorination of acetylene and the aerobic oxidation of carbon monoxide was reported by Hutchings³ and Haruta *et al.*,⁴ respectively. Since that time, gold has been identified as the most active catalyst in a variety of reactions. Oxidations with molecular oxygen, in particular, have attracted increasing attention over recent years, since they represent “green” oxidation methods.⁵ The oxidation of alcohol and aldehyde moieties using gold nanoparticles has previously been studied in some detail.^{6–8}

Herein, we show that supported gold nanoparticles can be used to catalyse the oxidation of benzaldehyde dissolved in different alcohols to directly produce various benzoate esters. The oxidising agent is air, a cheap and abundant resource. The experiments are conducted at room temperature, thus requiring no external heating, yielding an economic and practical route. The experiments take place in a flask open to air. It has been shown that if an alcohol is oxidised in the presence of a stoichiometric amount of aqueous base, carboxylates are achieved.⁹ Base can in fact be negated from the starting reaction mixture, but then elevated temperatures are required to drive the reaction to full conversion. If the reactions are carried out in water, carboxylic acids result.^{10,11} If performed in methanol, primary alcohols are converted into methyl esters.^{12,13} For the latter process, only a catalytic amount of base is required. It has recently been established that the oxidation of alcohols to their corresponding methyl esters proceeds *via* an aldehyde intermediate. The rate determining step is believed to be dehydrogenation of the alcohol to form this aldehyde intermediate.¹⁴ The second step—oxidation to form the methyl

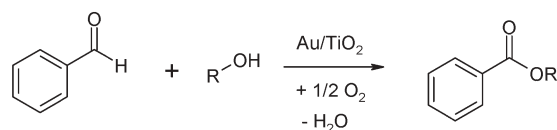


Scheme 1

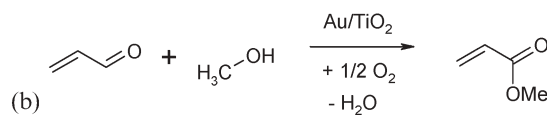
ester—proceeds relatively rapidly, indicated by the lack of accumulation of the aldehyde. This points to the possibility for aldehyde oxidations at much milder conditions than those used for alcohols. The reaction pathway can be seen in Scheme 1. Previous work on the oxidation of aldehydes to carboxylic acids has been conducted by Rossi *et al.*¹⁵

The catalytic reactions were carried out in an open glass flask, fitted with a condenser. All chemicals were used without further purification. NaOMe was used as a 30% solution in MeOH. In a typical experiment, gold supported on titanium dioxide (1% Au/TiO₂ supplied by Mintek) was suspended in the solvent alcohol. The aldehyde and base were added under stirring. Small aliquots were taken at selected times, the samples were filtered directly through a 13 mm syringe filter and analysed by GC and GC-MS. The GC column used was Agilent Technologies Inc. HP-5. For the acrolein reactions, a CP-PoraPLOT Q-HT column was used. The reaction equation for benzaldehyde is shown in Scheme 2a, and that for acrolein in Scheme 2b, which is considered later as an application of the method presented.

Fig. 1 shows the formation of methyl benzoate at varying temperatures. It can be seen that at decreasing temperatures the rate of formation of methyl benzoate decreases. The temperature is the limiting factor below $25\text{ }^{\circ}\text{C}$. Above this temperature it can be seen that there is no difference in the rates of reactions, implying that a factor other than temperature is now the rate determining factor. This could be the availability of atmospheric oxygen; we



R = CH₃, CH₂CH₃, (CH₂)₂CH₃, (CH₂)₃CH₃, CH₂(C₆H₅)
(a)



(b)

Scheme 2

Center for Sustainable and Green Chemistry, Department of Chemistry, Technical University of Denmark, Kemitorvet building 207, DK-2800, Kgs. Lyngby, Denmark. E-mail: chc@kemi.dtu.dk; Tel: +45 4525 2402
† The Center for Sustainable and Green Chemistry is sponsored by the Danish National Research Foundation.

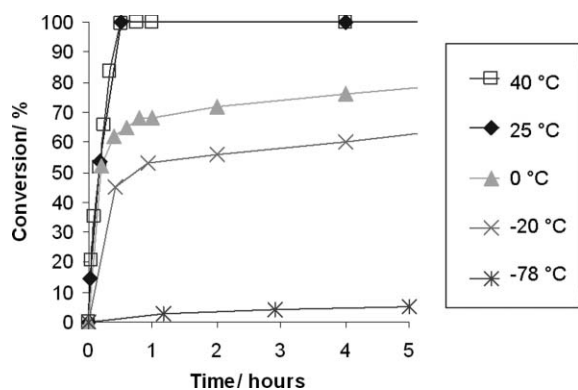


Fig. 1 Rate of formation of methyl benzoate at selected temperatures. Reaction conditions: Benzaldehyde : methanol 1 : 30, 0.2 mol% 1 wt% Au/TiO₂ from Mintek, 10 mol% 30% NaOMe soln. in MeOH.

would expect approximately the same amount of oxygen to be dissolved in the solution at 25 °C as at 40 °C, thus accounting for the similar reaction rates.¹⁶

Methyl benzoate can be formed from benzaldehyde at temperatures as low as -78 °C, proving this to be a facile and extremely fast reaction at room temperature. The remarkable catalytic activity of gold nanoparticles for aerobic oxidation of benzaldehyde at -78 °C was verified in an independent series of experiments. At these reaction conditions, *ca.* 2.7 mmol benzaldehyde was oxidized per mmol gold per hour.

Fig. 2a depicts the effect on the reaction rate of varying the amount of base present. Sodium hydroxide can also be utilised as

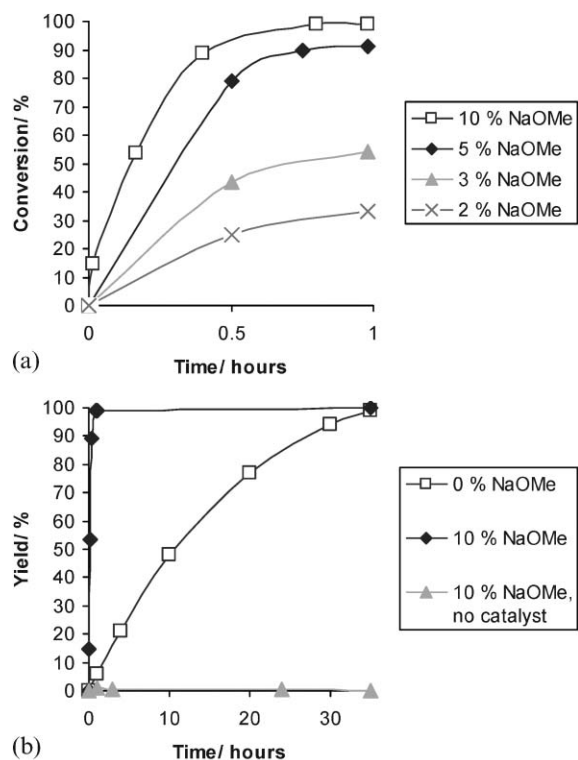


Fig. 2 a. Rate of formation of methyl benzoate with various amounts of base present. b. Conversion of benzaldehyde to methyl benzoate with no base present. Reaction conditions: Benzaldehyde : methanol 1 : 30, 0.2 mol% 1 wt% Au/TiO₂ from Mintek, *T* = 25 °C.

the base, but sodium methoxide was selected for practical purposes. A higher percentage of base yields a substantially faster reaction. With lower quantities of base the reaction takes longer to go to completion. Fig. 2b shows the results for formation of methyl benzoate in the absence of base. Formation of methyl benzoate with 10% base present is shown alongside for comparison. The fact that product formation occurs in excellent yield and selectivity even without base indicates that the protocol can be easily modified to the conditions required in special cases. Temperature, base presence and amount, and the use of oxygen or air as the oxidant can be varied, and full conversion with good to excellent yields are obtained; hence this can be viewed as a versatile and practical process. Furthermore, the reaction was run without catalyst (Fig. 2b), highlighting the necessity of the supported nanoparticles.

The protocol for methyl ester formation was investigated to study more generally ester formation. A range of simple alkyl alcohols and benzyl alcohol were utilised in place of methanol (Fig. 3). Formation of the methyl ester is by far the most rapid. On utilisation of longer chained alcohols, the rate of reaction decreases. This can be observed in the decreasing reaction rates of the alkyl alcohols, progressing from methanol to 1-butanol. When benzaldehyde is reacted with benzyl alcohol, the reaction rate is slower than that observed for methanol, but more rapid than for the alkyl alcohols. However in all cases, the reaction conditions can be tuned to produce the desired ester in high yield. Moreover, analogous experiments with hexanal and 2-methyl pentanal showed that it is also possible to achieve the corresponding methyl ester from these substrates in yields above 90%. However, full conversion is only reached after about 10 h showing that these aliphatic substrates are oxidized more slowly than benzaldehyde.

Further experimentation on the protocol set out above was executed using acrolein as the aldehyde starting material. Acrolein can be obtained from glycerol by dehydration at high temperatures,¹⁷ and subsequently oxidised in methanol to furnish the methyl ester, methyl acrylate. Glycerol, as a by-product from biodiesel formation, is a very cheap and abundant feedstock.¹⁸ Acrylate esters constitute an important group of feedstocks, for example, they are used to make water-based paints, solvent-based coatings and acrylic coatings. Our methodology enables such

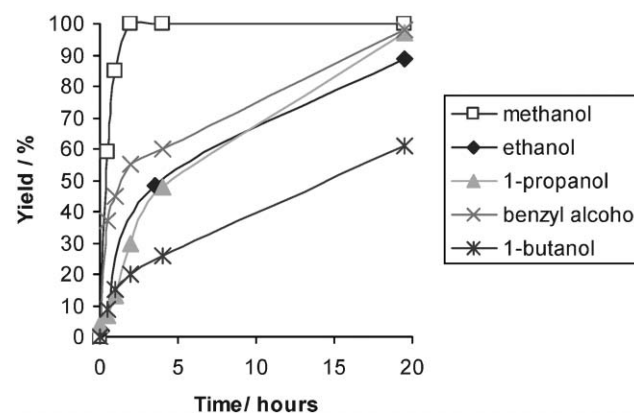


Fig. 3 Gold catalysed oxidation of benzaldehyde in alcohol solvent. Reaction conditions: Benzaldehyde : methanol 1 : 30, 0.2 mol% 1 wt% Au/TiO₂ from Mintek, *T* = 25 °C, 20 mol% 30% NaOMe soln. in MeOH.

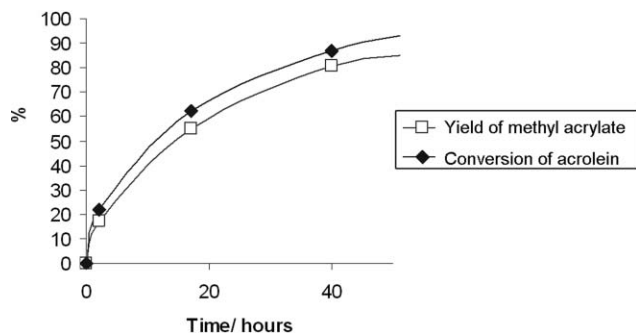


Fig. 4 Gold catalysed oxidation of acrolein in methanol. *Reaction conditions:* Acrolein : methanol 1 : 80, 0.9 mol% 1 wt% Au/ZnO from Mintek, $T = 25\text{ }^{\circ}\text{C}$. Yield of methyl acrylate is shown.

acrylate esters to be synthesised, at room temperature, using air as the oxidant, thus providing a “green” route to methyl acrylate.

Methyl acrylate was synthesised from acrolein by the present aerobic oxidation protocol with 87% selectivity at 97% conversion (Fig. 4 and Scheme 2b). This result is achieved with no optimisation, thus providing a good yield of methyl acrylate at this stage.

In conclusion, we have described a practically, and potentially economically, very attractive route to furnish esters from aldehydes. The simplest available oxidant, air, is used and the oxidative esterifications run to full conversion with good to excellent selectivities. The oxidation reactions even take place at $-78\text{ }^{\circ}\text{C}$, demonstrating the highly catalytic ability of gold nanoparticles. The methodology can be tuned to allow for varying temperatures and amounts of base, depending on the required

reaction conditions. In addition, we have synthesised methyl acrylate from acrolein using the same advantageous process, and the scope for synthesising other acrylate esters by the same method stands as a strong possibility.

Notes and references

- 1 A. Stephen, K. Hashmi and G. J. Hutchings, *Angew. Chem., Int. Ed.*, 2006, **45**, 7896.
- 2 G. C. Bond, P. A. Sermon, G. Webb, D. A. Buchanan and P. B. Wells, *J. Chem. Soc., Chem. Commun.*, 1973, 444.
- 3 G. J. Hutchings, *J. Catal.*, 1985, **96**, 292.
- 4 M. Haruta, S. Tsubota, T. Kobayashi and S. Ijima, *J. Catal.*, 1989, **115**, 301.
- 5 T. Mallat and A. Baiker, *Chem. Rev.*, 2004, **104**, 3037.
- 6 S. Biella, L. Prati and M. Rossi, *J. Catal.*, 2002, **206**, 242.
- 7 A. Abad, C. Almela, A. Corma and H. Garcia, *Tetrahedron*, 2006, **62**, 6666.
- 8 P. Haider and A. Baiker, *J. Catal.*, 2007, **248**, 175.
- 9 L. Prati and M. Rossi, *J. Catal.*, 1998, **176**, 552.
- 10 C. H. Christensen, B. Jørgensen, J. Rass-Hansen, K. Egeblad, R. Madsen, S. K. Klitgaard, S. M. Hansen, M. R. Hansen, H. C. Andersen and A. Riisager, *Angew. Chem., Int. Ed.*, 2006, **45**, 4648.
- 11 A. Corma and M. E. Domínez, *Chem. Commun.*, 2005, 4042.
- 12 T. Hayashi, T. Inagaki, N. Itayama and H. Baba, *Catal. Today*, 2006, **117**, 210.
- 13 I. S. Nielsen, E. Taarning, K. Egeblad, R. Madsen and C. H. Christensen, *Catal. Lett.*, 2007, **116**, 35.
- 14 B. Jørgensen, S. Egholm, M. L. Thomsen and C. H. Christensen, *J. Catal.*, 2007, **251**, 332.
- 15 S. Biella, L. Prati and M. Rossi, *J. Mol. Catal. A: Chem.*, 2003, **197**, 207.
- 16 J. Tokunaga, *J. Chem. Eng. Data*, 1975, **20**, 41.
- 17 A. Neher, T. Haas, D. Arntz, H. Klenk and W. Girke, *US Pat.*, 5 387 720, 1995.
- 18 M. Pagliaro, R. Cirimna, H. Kimura, M. Rossi and C. D. Pina, *Angew. Chem., Int. Ed.*, 2007, **119**, 4516.

D-Glucosamine—a natural ligand for the *N*-arylation of imidazoles with aryl and heteroaryl bromides catalyzed by CuI[†]

Dongping Cheng,^{ab} Fengfeng Gan,^a Weixing Qian^a and Weiliang Bao^{*a}

Received 5th September 2007, Accepted 19th November 2007

First published as an Advance Article on the web 30th November 2007

DOI: 10.1039/b713658g

D-Glucosamine, a natural ligand, can efficiently promote the *N*-arylation of imidazoles with aryl and heteroaryl halides using CuI as a catalyst.

Copper-catalyzed *N*-arylation is an important transformation in organic synthesis and the resulting arylated products have widely spread applications in pharmaceutical and agrochemical industries. Traditional copper-catalyzed Ullmann coupling protocols often require the use of stoichiometric amounts of copper reagents, which leads to the problems of waste disposal on scale.¹ It also necessitates the high reaction temperature and has low toleration of functional groups. Therefore, for a long time, the transformation has not exhibited its promising advantage. Although some significant achievements in palladium-catalyzed *N*-arylation have been made,² its practical application for industry is problematic mainly due to the toxicity and high cost of the palladium catalyst and the specific ligands. In recent years, the economic attractiveness of copper has led to a resurgence of interest in Ullmann-type reactions and great progress³ has been made in the context of some special ligands such as aliphatic diamines,⁴ 1,10-phenanthroline and its derivatives,⁵ ethylene glycol,⁶ diethylsalicylamide,⁷ amino acids,⁸ oxime-type,⁹ Schiff base¹⁰ and phosphine-containing ligands.¹¹ However, except for amino acids, almost all of the ligands are nonnatural and not eco-friendly. For example, some ligands, such as aliphatic diamines and 1,10-phenanthroline, are toxic or corrosive; other ligands, such as diethylsalicylamide, oxime-type and Schiff bases usually need tedious procedures to synthesize. Based on the concerns of green chemistry, hazardous materials may not be the preferred choices in manufacture and application of chemical products. Environmentally benign and easy to obtain ligands are still in demand.

Within the *N*-arylation of imidazole, the copper-catalyzed Ullmann coupling reaction is the most efficient method. Most coupling of imidazoles uses aryl iodides as the electrophilic coupling partner and only a few examples with aryl bromides are reported.¹² Since ethylene glycol, diamine and their derivatives, usually unnatural, are good ligands for the Ullmann reaction in published papers, with the interest of green chemistry,¹³ we intend to find a natural compound which contains an hydroxyl and amino group as a green ligand for the *N*-arylation coupling

reaction. D-Glucosamine is a main raw material in the synthesis of antibiotics and anticarcinogens and is also used in pharmaceuticals due to its important physiological functions.¹⁴ Herein, we wish to report D-glucosamine promoted *N*-arylation of imidazole with aryl and heteroaryl bromides using CuI as a catalyst.

At first, bromobenzene **1a** and imidazole **2** were selected as the model substrates (Table 1, Scheme 1). Catalyzed by CuI, different natural ligands, several bases and solvents were examined to set up standard reaction conditions. When the reaction was performed in DMSO in the presence of 2.1 equivalents of Cs₂CO₃ at 110 °C for 24 h with D-glucose as a ligand, the desired product **3a** was obtained in 60% yield (Table 1, entry 1). Then, other multi-hydroxyl natural compounds such as D-mannitol, D-fructose and D-glucosamine were investigated. From the results in Table 1, it is obvious that D-glucosamine is the most efficient ligand examined (Table 1, entries 1–4) and gave the coupling product in 84% yield. With D-glucosamine as a ligand, the change of the base to K₃PO₄ and K₂CO₃ resulted in decreased yields (Table 1, entries 5–6). Besides DMSO, a number of other solvents such as DMF, NMP, 1,4-dioxane and [Bmim]BF₄ were further surveyed. It was found that use of an ionic liquid as the solvent suppressed the coupling reaction entirely. DMF, NMP and 1,4-dioxane were not good choices here and the yields were comparatively lower. Compared with the catalytic effect of CuI, the other copper(I) sources, such as CuBr, CuCl, or Cu₂O showed slightly lower catalytic activities (Table 1, entries 11–13). Interestingly, the *N*-arylation product was

Table 1 *N*-arylation of imidazole under different conditions^a

Entry	Ligand	Base	Solvent	Catalyst	Yield (%) ^b
1	D-Glucose	Cs ₂ CO ₃	DMSO	CuI	60
2	D-Mannitol	Cs ₂ CO ₃	DMSO	CuI	59
3	D-Fructose	Cs ₂ CO ₃	DMSO	CuI	65
4	D-Glucosamine	Cs ₂ CO ₃	DMSO	CuI	84
5	D-Glucosamine	K ₃ PO ₄	DMSO	CuI	70
6	D-Glucosamine	K ₂ CO ₃	DMSO	CuI	65
7	D-Glucosamine	Cs ₂ CO ₃	DMF	CuI	30
8	D-Glucosamine	Cs ₂ CO ₃	NMP	CuI	70
9	D-Glucosamine	Cs ₂ CO ₃	Dioxane	CuI	25
10	D-Glucosamine	Cs ₂ CO ₃	[Bmim]BF ₄	CuI	0
11	D-Glucosamine	Cs ₂ CO ₃	DMSO	Cu ₂ O	70 ^c
12	D-Glucosamine	Cs ₂ CO ₃	DMSO	CuBr	65
13	D-Glucosamine	Cs ₂ CO ₃	DMSO	CuCl	58
14	None	Cs ₂ CO ₃	DMSO	CuI	20
15	D-Glucosamine	Cs ₂ CO ₃	DMSO	CuI	81 ^d

^a Reaction conditions: Bromobenzene (1.2 mmol), imidazole (1.0 mmol), CuI (0.2 mmol), ligand (0.4 mmol) and base (2.1 mmol) in solvent (1.0 ml) under N₂. ^b Isolated yields. ^c Cu₂O (0.1 mmol). ^d 5 equivalents of H₂O were added.

^a Department of Chemistry, Zhejiang University, Xi Xi Campus, Hangzhou, 310028, Zhejiang, P. R. China.

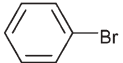
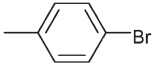
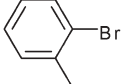
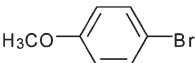
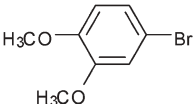

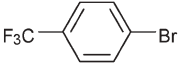
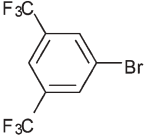
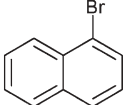
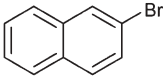
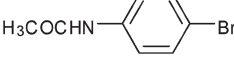
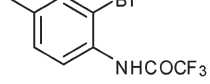
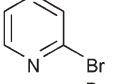
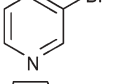
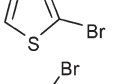
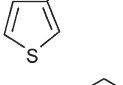
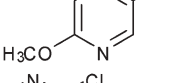
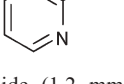
E-mail: wlbao@css.zju.edu.cn; Fax: +86 571-88273814;

Tel: +86 571-88273814

^b College of Pharmaceutical Science, Zhejiang University of Technology, Hangzhou, 310014, Zhejiang, P. R. China

[†] Electronic supplementary information (ESI) available: Experimental details and characterisation data. See DOI: 10.1039/b713658g

Table 2 *N*-arylation of imidazole^a

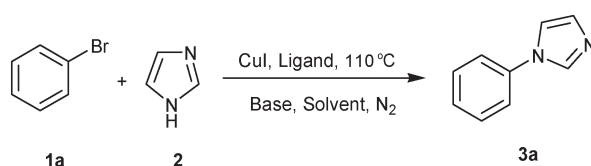
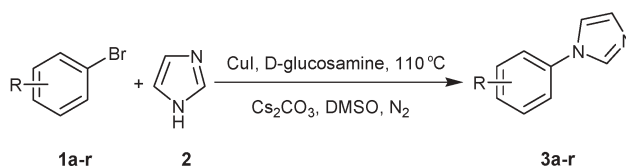
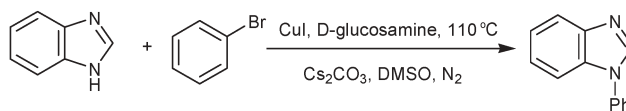
Entry	Arylating agent	Product	Time	Yield (%) ^b
1		3a	24 h	84
2		3b	24 h	80
3		3c	24 h 48 h	35 55
4		3d	24 h	73
5		3e	24 h	79
6		3f	22 h	90
7		3g	24 h	72
8		3h	20 h	91
9		3i	24 h	68
10		3j	22 h	86
11		3k	24 h	72
12		3l	10 h	90 ^c
13		3m	24 h	78
14		3n	24 h	70
15		3o	22 h	82
16		3p	20 h	83
17		3q	24 h	71
18		3r	18 h	95

^a Arylhalide (1.2 mmol), imidazole (1.0 mmol), CuI (0.2 mmol), D-glucosamine (0.4 mmol) and Cs₂CO₃ (2.1 mmol) in DMSO (1.0 ml) under N₂. ^b Isolated yields. ^c Performed at 60 °C.

obtained in 20% yield in the absence of the ligand, which might indicate that maybe imidazole promotes the coupling reaction itself. It should be noted that the process is fairly insensitive to water, which is demonstrated by the observation that only a small decrease in reaction yield occurred when 5 equivalents of water (relative to bromobenzene) were added to the reaction mixture (Table 1, entry 15). Therefore, no special precautions to exclude small amounts of moisture from this reaction are required.

With the optimized procedure in hand, the scope of this coupling reaction was further explored with different aryl and heteroaryl bromides as the substrates and the results are summarized in Table 2, Scheme 2. From the results, no significant electronic effects were observed for *para*- and *meta*-substituted aryl bromides; the rates and yields of the reactions were comparable. 2-Methylbromobenzene typically required longer reaction time and gave an acceptable yield (Table 2, entry 3). It indicated that the yield of the coupling reaction is strongly affected by the steric hindrance of the methyl in 2-methylbromobenzene. To our delight, 2-bromo-4-methyltrifluoroacetanilide can be efficiently used as the substrate and excellent yield was obtained in shorter time (Table 2, entry 12). This may be ascribed to the existence of an accelerating effect caused by an *ortho*-amide group, which was in accordance with the result of Ma *et al.*¹⁵ Moreover, heterocyclic aryl bromides, such as different types of substituted bromopyridines and bromothiophenes were compatible with the present procedure and good to excellent results were obtained. Especially, 2-chloropyrimidine, can also be used as an appropriate substrate and affords the corresponding product smoothly (Table 2, entry 18). The coupling of benzimidazole with bromobenzene also gave the corresponding product in 60% yield (Scheme 3).

In summary, we have disclosed that D-glucosamine, a natural ligand, can efficiently promote the *N*-arylation of imidazoles with aryl and heteroaryl halides using CuI as a catalyst. It provides a green ligand for selection of copper-catalyzed *N*-arylation for practical use.

**Scheme 1****Scheme 2****Scheme 3**

Acknowledgements

This work was financially supported by the Natural Science Foundation of China (No. 20572095).

Notes and references

- (a) F. Ullmann, *Ber. Dtsch. Chem. Ges.*, 1903, **36**, 2382; (b) J. Lindley, *Tetrahedron*, 1984, **40**, 1433; (c) J. Hassan, M. Sévignon, C. Gozzi, E. Schulz and M. Lemaire, *Chem. Rev.*, 2002, **102**, 1359.
- For reviews see: (a) J. F. Hartwig, *Angew. Chem., Int. Ed.*, 1998, **37**, 2046; (b) J. P. Wolfe, S. Wagaw, J.-F. Marcoux and S. L. Buchwald, *Acc. Chem. Res.*, 1998, **31**, 805; (c) J. F. Hartwig, *Acc. Chem. Res.*, 1998, **31**, 852; (d) B. H. Yang and S. L. Buchwald, *J. Organomet. Chem.*, 1999, **576**, 125.
- For review see: (a) K. Kunz, U. Scholz and D. Ganzer, *Synlett*, 2003, 2428; (b) S. V. Ley and A. W. Thomas, *Angew. Chem., Int. Ed.*, 2003, **42**, 5400; (c) I. P. Beletskaya and A. V. Cheprakov, *Coord. Chem. Rev.*, 2004, **248**, 2337.
- (a) A. Klapars, J. C. Antilla, X. Huang and S. L. Buchwald, *J. Am. Chem. Soc.*, 2001, **123**, 7727; (b) J. C. Antilla, A. Klapars and S. L. Buchwald, *J. Am. Chem. Soc.*, 2002, **124**, 11684; (c) J. C. Antilla, J. M. Baskin and S. L. Buchwald, *J. Org. Chem.*, 2004, **69**, 5578.
- (a) R. K. Gujadhur, C. G. Bates and D. Venkataraman, *Org. Lett.*, 2001, **3**, 4315; (b) D. V. Allen and D. Venkataraman, *J. Org. Chem.*, 2003, **68**, 4590.
- F. Y. Kwong, A. Klapars and S. L. Buchwald, *Org. Lett.*, 2002, **4**, 581.
- F. Y. Kwong and S. L. Buchwald, *Org. Lett.*, 2003, **5**, 793.
- (a) D. Ma, Y. Zhang, J. Yao, S. Wu and F. Tao, *J. Am. Chem. Soc.*, 1998, **120**, 12459; (b) D. Ma and C. Xia, *Org. Lett.*, 2001, **3**, 2583; (c) D. Ma, Q. Cai and H. Zhang, *Org. Lett.*, 2003, **5**, 2453; (d) D. Ma and Q. Cai, *Org. Lett.*, 2003, **5**, 3799; (e) D. Ma and Q. Cai, *Synlett*, 2004, 128; (f) H. Zhang, Q. Cai and D. Ma, *J. Org. Chem.*, 2005, **70**, 5164.
- H.-J. Cristau, P. P. Cellier, J.-F. Spindler and M. Taillefer, *Eur. J. Org. Chem.*, 2004, 695.
- H.-J. Cristau, P. P. Cellier, J.-F. Spindler and M. Taillefer, *Chem.–Eur. J.*, 2004, **10**, 5607.
- (a) A. A. Kelkar, N. M. Patil and R. V. Chaudhari, *Tetrahedron Lett.*, 2002, **43**, 7143; (b) A. S. Gajare, K. Toyota, M. Yoshifuji and F. Ozawab, *Chem. Commun.*, 2004, 1994; (c) H. Rao, H. Fu, Y. Jiang and Y. Zhao, *J. Org. Chem.*, 2005, **70**, 8107; (d) H. Rao, Y. Jin, H. Fu, Y. Jiang and Y. Zhao, *Chem.–Eur. J.*, 2006, **12**, 3636.
- (a) H. J. Cristau, P. P. Cellier, J. F. Spindler and M. Taillefer, *Chem.–Eur. J.*, 2004, **10**, 5607; (b) D. Ma and Q. Cai, *Synlett*, 2004, 128; (c) H. Zhang, Q. Cai and D. Ma, *J. Org. Chem.*, 2005, **70**, 5164; (d) E. Alcalde, I. Dinarès, S. Rodríguez and C. Garcia de Miguel, *Eur. J. Org. Chem.*, 2005, 1637; (e) M. Kull, L. Bekedam, G. M. Visser, A. van den Hoogenband, J. W. Terpstra, P. C. J. Kamer, P. W. N. M. van Leeuwen and G. P. F. van Strijdonck, *Tetrahedron Lett.*, 2005, **46**, 2405; (f) L. Liu, M. Frohn, N. Xi, C. Donminguez, R. Hungate and P. J. Reider, *J. Org. Chem.*, 2005, **70**, 10135; (g) T. Jerphagnon, G. P. M. van Klink, J. G. de Vries and G. van Koten, *Org. Lett.*, 2005, **7**, 5241; (h) L. Xu, D. Zhu, R. Wang and B. Wan, *Tetrahedron*, 2005, **61**, 6553; (i) Z. Zhang, J. Mao, D. Zhu, F. Wu, H. Chen and B. Wan, *Tetrahedron*, 2006, **62**, 4435; (j) R. Hosseinzadeh, M. Tajbakhsh and M. Alikarami, *Tetrahedron Lett.*, 2006, **47**, 5203; (k) M. L. Kantam, G. T. Venkanna, C. Sridhar and K. B. Kumar, *Tetrahedron Lett.*, 2006, **47**, 3897; (l) R. Hosseinzadeh, M. Tajbakhsh and M. Alikarami, *Synlett*, 2006, 2124; (m) X. Guo, H. Rao, H. Fu, Y. Jiang and Y. Zhao, *Adv. Synth. Catal.*, 2006, **348**, 2197; (n) Y. Xie, S. Pi, D. Yin and J. Li, *J. Org. Chem.*, 2006, **71**, 8324; (o) R. A. Altman and S. L. Buchwald, *Org. Lett.*, 2006, **8**, 2779; (p) R. A. Altman, E. D. Koval and S. L. Buchwald, *J. Org. Chem.*, 2007, **72**, 6190; (q) L. Zhu, L. Cheng, Y. Zhang, R. Xie and J. You, *J. Org. Chem.*, 2007, **72**, 2737; (r) A. Kiyomori, J. K. Marcoux and S. L. Buchwald, *Tetrahedron Lett.*, 1999, **40**, 2657.
- (a) X. Lv and W. Bao, *J. Org. Chem.*, 2007, **72**, 3863; (b) W. Bao and Z. Wang, *Green Chem.*, 2006, **8**, 1028; (c) Z. Wang, H. Mo and W. Bao, *Synlett*, 2007, 91; (d) D. Chang and W. Bao, *Synlett*, 2006, 1786; (e) X. Lv, Z. Wang and W. Bao, *Tetrahedron*, 2006, **62**, 4756; (f) Z. Wang, W. Bao and Y. Jiang, *Chem. Commun.*, 2005, 2849; (g) W. Bao, Z. Wang and Y. Li, *J. Org. Chem.*, 2003, **68**, 591.
- (a) G. R. Gale, *Can. J. Microbiol.*, 1964, **10**, 887; (b) E. Tubaro, *Boll. Chim. Farm.*, 1966, **105**, 97; (c) A. Takatsuki and G. Tamura, *J. Antibiot.*, 1971, **24**, 232.
- (a) B. Zou, Q. Yuan and D. Ma, *Angew. Chem., Int. Ed.*, 2007, **46**, 2598; (b) D. W. Ma, *J. Am. Chem. Soc.*, 2006, **128**, 16050; (c) D. W. Ma, *J. Org. Chem.*, 2007, **72**, 4844; (d) Q. Cai, B. Zou and D. Ma, *Angew. Chem., Int. Ed.*, 2006, **45**, 1276.

Stereochemical effects on the mode of facilitated ion transfer into room-temperature ionic liquids

Mark L. Dietz,^{*a} Sandrine Jakab,^{ab} Kazuhiro Yamato^c and Richard A. Bartsch^c

Received 7th September 2007, Accepted 22nd November 2007

First published as an Advance Article on the web 5th December 2007

DOI: 10.1039/b713750h

Crown ether stereochemistry is shown to influence the mode of sodium ion partitioning between acidic nitrate media and a dialkylimidazolium-based room temperature ionic liquid containing various dicyclohexano-18-crown-6 (DCH18C6) isomers, in contrast to an analogous extraction system employing a conventional organic solvent.

Progress toward the design of viable ionic liquid (IL)-based systems for metal ion separations requires an improved understanding of the fundamental aspects of the processes involved in the transfer of a metal ion from an aqueous phase into an IL in the presence of various types of complexants and extractants.¹ To this end, we have been carrying out a systematic examination of the influence of various parameters, among them the composition of the aqueous phase, the nature of the metal ion, the properties of the extractant, and the constituents of the solvent, on the mode of metal ion partitioning into ionic liquids.^{2–9} In contrast to liquid–liquid systems involving metal ion extraction into conventional organic solvents, ion partitioning into ionic liquids is frequently a complex, multi-pathway process. In the transfer of alkali and alkaline earth cations from nitric acid solution into dialkylimidazolium bis[(trifluoromethyl)sulfonyl]imides (abbreviated hereafter as $C_n\text{mim}^+\text{Tf}_2\text{N}^-$, with $n = 5–10$) in the presence of a crown ether (CE), for example, exchange of the cationic metal-CE complex for the cationic component of the IL appears to be the preferred process for short ($n < 8$)-chain (and thus, relatively hydrophilic) ionic liquids.^{5,7,8} As the alkyl chain-length increases, however, other pathways emerge. In the extraction of strontium ions by dicyclohexano-18-crown-6 (DCH186), a gradual shift in the predominant mode of partitioning from ion-exchange involving the cationic portion of the IL to conventional neutral nitrate complex extraction as the hydrophobicity of the IL cation increases (from $n = 5$ to $n = 10$ in $C_n\text{mim}^+\text{Tf}_2\text{N}^-$) has been reported.⁵ In contrast, sodium ion partitioning in the same systems involves a shift from ion-exchange involving the IL cation to “crown ether-mediated” ion-exchange, in which exchange of the sodium ion for a hydronium ion in a DCH18C6- H_3O^+ adduct is observed.⁷ For practical reasons, in particular the need to minimize loss of the IL to the aqueous phase during a separation process⁹ and the desirability of achieving satisfactory metal ion extraction from aqueous phases containing high acid (or nitrate)

concentrations and facile recovery in aqueous phases containing little or no acid (or nitrate),^{10–13} only the extraction of a neutral nitrate complex is regarded as a satisfactory route for partitioning.¹³ Therefore, effective means for suppressing other pathways for ion transfer are clearly desirable, indeed essential, if ILs are to realize their potential as “green” replacements for conventional organic solvents.⁵

In the course of ongoing efforts to prepare various stereoisomers of DCH18C6 and its dialkyl-substituted derivatives and to characterize their complexation and extraction behavior,^{14–20} we have observed a marked difference in the dependence of sodium ion partitioning into $C_{10}\text{mim}^+\text{Tf}_2\text{N}^-$ on the aqueous nitric acid concentration between the *cis*²¹ and *trans*^{18–20} forms of DCH18C6 (Fig. 1).† As will now be shown, this difference is consistent with the suppression of crown ether-mediated ion-exchange in the case of the *trans* isomers.

Fig. 2A depicts the nitric acid dependencies of D_{Na} observed for the five stereoisomers of DCH18C6 in a conventional organic solvent, 1-octanol. In interpreting these dependencies, it is important to keep in mind that electroneutrality must be maintained during the partitioning process. In conventional solvent systems, this can be accomplished in only one way. That is, an extracted cation must be accompanied by sufficient aqueous phase anions (e.g., nitrate) to yield a neutral complex (here, $\text{NaNO}_3\cdot\text{DCH18C6}$). Consistent with this, increasing acidity (i.e., nitrate concentration) for the *cis* isomers is typically accompanied by an increase in sodium ion partitioning (as reflected in the value of the sodium distribution ratio, D_{Na} , defined as $[\text{Na}]_{\text{org}}/[\text{Na}]_{\text{aq}}$ at equilibrium). (At sufficiently high acidities ($>ca. 3 \text{ M HNO}_3$), a decrease in sodium extraction is observed for the two all-*cis* isomers (*cis-syn-cis* and *cis-anti-cis*). This is a result of increasing acid extraction by the crown ether and the decreased effectiveness of the acid-complexed form ($\text{CE}\cdot n\text{HNO}_3$, with $n = 1$ or 2) as a metal ion extractant.¹⁶) Similarly, for the *trans* isomers, sodium

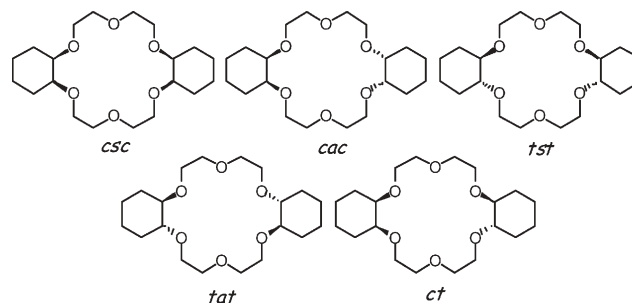


Fig. 1 Structures of the *cis-syn-cis* (*csc*), *cis-anti-cis* (*cac*), *trans-syn-trans* (*tst*), *trans-anti-trans* (*tat*), and *cis-trans* (*ct*) isomers of DCH18C6.

^aArgonne National Laboratory, Chemistry Division, Bldg. 200, 9700 S. Cass Avenue, Argonne, IL, 60439, USA. E-mail: mdietz@anl.gov; Fax: +1-630-252-7501; Tel: +1-630-252-3647

^bEcole Nationale Supérieure de Chimie de Paris, Paris, France

^cDepartment of Chemistry and Biochemistry, Texas Tech University, Lubbock, TX, 79409-1061, USA

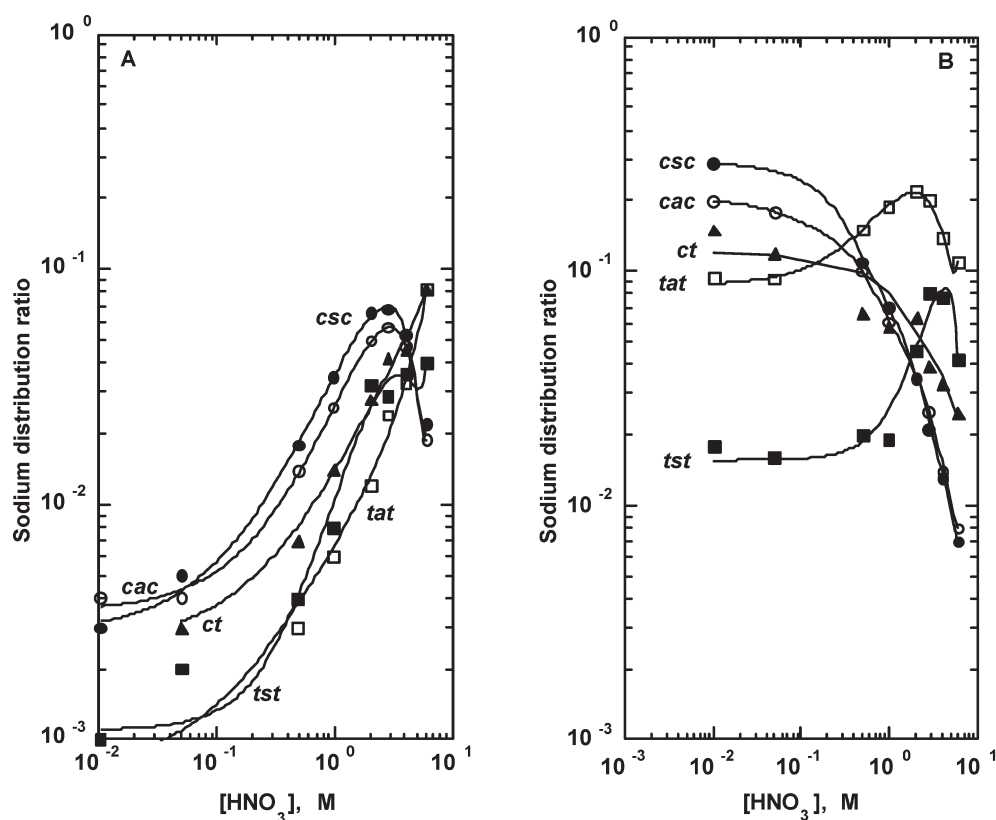


Fig. 2 Nitric acid dependency of the extraction of the sodium ion into (A) 1-octanol or (B) $C_{10}mim^+Tf_2N^-$ in the presence of the various isomers of DCH18C6 (0.05 M; $T = 23\text{ }^\circ\text{C}$).

extraction initially increases as the aqueous nitric acid concentration is raised, but in this case, continues to do so even at high acid concentrations. This behavior is fully consistent with the known lower affinity of the *trans* isomers for nitric acid.²³

Fig. 2B presents the corresponding dependencies observed when 1-octanol is replaced with $C_{10}mim^+Tf_2N^-$ as the organic diluent. For the *cis* isomers, rising nitric acid concentration is eventually accompanied by steeply falling values of the sodium distribution ratio. As noted previously,⁷ such a dependency is indicative of crown ether-mediated exchange of a sodium ion for a hydronium ion in a DCH18C6- H_3O^+ adduct. In contrast, for the *trans* isomers, rising aqueous acidity is accompanied by increasing sodium extraction, consistent with partitioning of a neutral sodium nitrate-crown ether complex, over much of the range considered (*i.e.*, at $[HNO_3] > ca. 0.5\text{ M}$). Only at high acidities (*ca.* 3–4 M), does D_{Na} begin to decline. Infrared spectra of the IL phases containing the *trans* isomers exhibit no bands characteristic of a DCH18C6- H_3O^+ adduct, even after contact with 10 M nitric acid. Therefore, this decrease does not result from crown ether-mediated ion-exchange, but rather is a possible consequence of either activity effects or the formation of a neutral acid-extractant adduct, $CE \cdot HNO_3$, as is the case in 1-octanol. Taken together, the results demonstrate that a change from a *cis* to a *trans* isomer of DCH18C6 alters the predominant mode of sodium ion partitioning into $C_{10}mim^+Tf_2N^-$ from ion-exchange to neutral complex extraction. It is suggested that this is due to the greater ability of the *cis* isomers to form hydronium ion-crown ether adducts.

The results described here are significant for both practical and fundamental reasons. The results are of fundamental importance

because they demonstrate that extractant stereochemistry represents yet another parameter that determines the “balance of pathways” in metal ion partitioning in IL-based extraction systems. From a more practical perspective, the results are of significance in that they represent one of the few reported examples of an extractant-IL system (*i.e.*, the *trans* isomers of DCH18C6- $C_{10}mim^+Tf_2N^-$) for which the preferred mode of ion partitioning (*i.e.*, neutral complex extraction) into the IL is the same as that observed in a conventional organic solvent. More importantly, they demonstrate that an undesirable pathway for metal ion partitioning (*i.e.*, extractant-mediated ion-exchange) can be suppressed and a partitioning process rendered “greener” simply by changing the isomeric form of the extractant. To our knowledge, such a change in the predominant mode of ion partitioning with extractant stereochemistry is without precedent. We expect these results to have significant utility in the design of improved approaches to metal ion separations employing ionic liquids. Work addressing such opportunities is now underway in this laboratory.

This work was performed under the auspices of the United States Department of Energy, Office of Basic Energy Sciences, Division of Chemical Sciences, Geosciences, and Biosciences, under contract number DE-AC02-06CH11357.

The submitted manuscript has been created by UChicago Argonne, LLC, Operator of Argonne National Laboratory (“Argonne”). Argonne, a U.S. Department of Energy, Office of Science laboratory, is operated under Contract No. DE-AC02-06CH11357. The U.S. Government retains for itself, and others acting on its behalf, a paid-up, non-exclusive, irrevocable

worldwide license in said article to reproduce, prepare derivative works, distribute copies to the public, and perform publicly and display publicly, by or on behalf of the Government.

Notes and references

† The ionic liquid, 1-decyl-3-methylimidazolium bis[(trifluoromethyl)sulfonyl] imide ($C_{10}mim^+Tf_2N^-$), was prepared according to published methods.²² The *cis-syn-cis* (*csc*) and *cis-anti-cis* (*cac*) isomers of DCH18C6 were purchased from Acros Organics (Pittsburgh, PA, USA) and used as received. The corresponding *trans-syn-trans* (*tst*), *trans-anti-trans* (*tat*), and *cis-trans* (*ct*) isomers were prepared as described in prior reports.^{18,19} 1-Octanol was obtained from Aldrich Chemical Co. (Milwaukee, WI, USA) and used without further purification. All sodium distribution ratios were determined radiometrically using a commercial Na-22 radiotracer (Isotope Product Laboratories, Valencia, CA, USA), assayed *via* gamma spectroscopy using standard procedures.

- M. L. Dietz, J. A. Dzielawa, M. P. Jensen, J. V. Beitz and M. Borkowski, in *Ionic Liquids IIIB: Fundamentals, Progress, Challenges, and Opportunities*, ed. R. D. Rogers and K. R. Seddon, American Chemical Society, Washington, DC., 2005, vol. 902, pp. 2–18.
- M. L. Dietz and J. A. Dzielawa, *Chem. Commun.*, 2001, 2124–2125.
- M. P. Jensen, J. A. Dzielawa, P. Rickert and M. L. Dietz, *J. Am. Chem. Soc.*, 2002, **124**, 10664–10665.
- M. L. Dietz, M. P. Jensen, J. V. Beitz and J. A. Dzielawa, in *Hydrometallurgy 2003-Fifth international Conference in Honor of Professor Ian Ritchie-Vol. 1: Leaching and Solution Purification*, ed. C. A. Young, A. M. Alfantazi, C. G. Anderson, D. B. Dreisinger, B. Harris and A. James, TMS (The Minerals, Metals & Materials Society), Vancouver, BC, 2003, pp. 929–939.
- M. L. Dietz, J. A. Dzielawa, I. Laszak, B. A. Young and M. P. Jensen, *Green Chem.*, 2003, **5**, 682–685.
- D. C. Stepinski, M. P. Jensen, J. A. Dzielawa and M. L. Dietz, *Green Chem.*, 2005, **7**, 151–158.
- M. L. Dietz and D. C. Stepinski, *Green Chem.*, 2005, **7**, 747–750.
- H. Heitzman, B. A. Young, D. J. Rausch, P. Rickert, D. C. Stepinski and M. L. Dietz, *Talanta*, 2006, **69**, 527–531.
- P. G. Rickert, D. C. Stepinski, D. J. Rausch, R. M. Bergeron, S. Jakab and M. L. Dietz, *Talanta*, 2007, **72**, 315–320.
- E. P. Horwitz, M. L. Dietz and D. E. Fisher, *Anal. Chem.*, 1991, **63**, 522–525.
- M. L. Dietz and E. P. Horwitz, *LC-GC*, 1993, **11**, 424–436.
- M. L. Dietz, E. P. Horwitz and R. D. Rogers, *Solvent Extr. Ion Exch.*, 1995, **13**, 1–17.
- D. C. Stepinski, B. A. Young, M. P. Jensen, P. G. Rickert, J. A. Dzielawa, A. A. Dilger, D. J. Rausch and M. L. Dietz, in *Separations for the Nuclear Fuel Cycle in the 21st Century*, ed. G. J. Lumetta, K. L. Nash, S. B. Clark and J. I. Friese, American Chemical Society, Washington, DC., 2006, vol. 933, pp. 233–247.
- E. P. Horwitz, M. L. Dietz and D. E. Fisher, *Solvent Extr. Ion Exch.*, 1990, **8**, 557–572.
- M. L. Dietz, A. H. Bond, B. P. Hay, R. Chiarizia, V. J. Huber and A. W. Herlinger, *Chem. Commun.*, 1999, 1177–1178.
- M. L. Dietz, A. H. Bond, M. Clapper and J. W. Finch, *Radiochim. Acta*, 1999, **85**, 119–129.
- V. J. Huber and M. L. Dietz, *Tetrahedron Lett.*, 2001, **42**, 2945–2948.
- K. Yamato, R. A. Bartsch, M. L. Dietz and R. D. Rogers, *Tetrahedron Lett.*, 2002, **43**, 2153–2156.
- K. Yamato, F. A. Fernandez, H. F. Vogel, R. A. Bartsch and M. L. Dietz, *Tetrahedron Lett.*, 2002, **43**, 5229–5232.
- K. Yamato, R. A. Bartsch, G. A. Broker, R. D. Rogers and M. L. Dietz, *Tetrahedron Lett.*, 2002, **43**, 5805–5808.
- R. M. Izatt, B. L. Haymore, J. S. Bradshaw and J. J. Christensen, *Inorg. Chem.*, 1975, **14**, 3132–3133.
- P. Bonhôte, A.-P. Dias, N. Papageorgiou, K. Kalyanasundaram and M. Grätzel, *Inorg. Chem.*, 1996, **35**, 1168–1178.
- H. F. Vogel, R. A. Bartsch and M. L. Dietz, unpublished results, Argonne National Laboratory, 2002.

Acid in ionic liquid: An efficient system for hydrolysis of lignocellulose

Changzhi Li,^{ab} Qian Wang^a and Zongbao K. Zhao^{*a}

Received 27th July 2007, Accepted 3rd December 2007

First published as an Advance Article on the web 17th December 2007

DOI: 10.1039/b711512a

Acid in ionic liquid was demonstrated as an efficient system for hydrolysis of lignocellulosic materials with improved total reducing sugars (TRS) yield under mild conditions. TRS yields were up to 66%, 74%, 81% and 68% for hydrolysis of corn stalk, rice straw, pine wood and bagasse, respectively, in C₄mimCl in the presence of 7 wt% hydrogen chloride at 100 °C under atmospheric pressure within 60 min. Different combinations between ionic liquids, such as C₆mimCl, C₄mimBr, AmimCl, C₄mimHSO₄, and SbmimHSO₄, and acids, including sulfuric acid, nitric acid, phosphoric acid, as well as maleic acid, afforded similar results albeit longer reaction time was generally required comparing with the combination of C₄mimCl and hydrochloric acid. FT-IR spectra and elemental analysis of the recovered residues indicated that modification of lignin occurred during sulfuric acid catalyzed hydrolysis. In addition, kinetic modeling based on experimental data suggested that the hydrolysis likely followed a consecutive first-order reaction sequence, where k_1 and k_2 , the rate constants for TRS formation and TRS degradation, were determined as 0.068 min⁻¹ and 0.007 min⁻¹, respectively. This novel system may be valuable to facilitate cost-efficient conversion of biomass into biofuels and biobased products.

Introduction

Lignocellulosic materials are renewable biomass that assume the potential to serve as a sustainable feedstock, *in lieu of* diminishing crude oil and coal, for future biofuels and chemicals (*e.g.* alcohols, organic acids, *etc.*).¹ Extensive research and development programs have been initiated worldwide to convert lignocellulosic biomass, such as agricultural residues, forestry wastes and energy crops, into valuable products, through a sugar platform which includes two processes: hydrolysis of the lignocellulosic materials to monosaccharides (Fig. 1) and transforming the sugars into bio-based products (usually through fermentation).

Unfortunately, nature provides us lignocellulosic materials with physiochemical, structural and compositional features that confer a notorious resistance to hydrolysis.² This “biomass recalcitrance” property holds back a cost effective technology to convert lignocellulosic materials to sugars. Up to now, hydrolysis of lignocellulose to monosaccharides is usually catalyzed either by enzymes or by acid catalysts under heterogeneous conditions,³ and none of the known methods are yet cost-effective for large-scale applications. For example,

enzymatic hydrolysis suffers a low rate and enzymes are too expensive; the traditional diluted acid hydrolysis process requires harsh conditions, *e.g.*, high pressure, and elevated temperature (usually at above 200 °C). Furthermore, pretreatment, a rather energy intensive and/or waste-generating process, is usually required in the above methods.⁴ Concentrated acids such as sulfuric acid and hydrochloric acid have also been used to treat lignocellulosic materials. Although they are powerful agents for cellulose hydrolysis, concentrated acids are toxic, hazardous and require corrosion-resistant reactors. In addition, the concentrated acid must be recovered after hydrolysis to make the process economically feasible.⁵ Therefore, hydrolysis of lignocellulose *via* a green and energy efficient approach remains a challenge.

Pioneer studies by Rogers *et al.* showed that ionic liquid (IL) 1-butyl-3-methylimidazolium chloride (C₄mimCl) is a powerful solvent for cellulose, up to 25 wt% of cellulose can be dissolved in C₄mimCl to form a homogeneous solution.⁶ It has since attracted much attention⁷ and subsequent chemical derivation,⁸ hydrolysis⁹ and hydrogenolysis¹⁰ of cellulose in ILs were reported. In addition, non-degradation dissolution of ball-milled plant cell walls was also documented.¹¹ We therefore envisioned that IL might be a superior solvent to dissolve lignocellulosic materials, which may overcome the physical and biochemical barriers for the hydrolysis reaction. In this paper we would like to report our results on acid catalyzed hydrolysis of lignocellulose in ILs. Ours provides a simple method for the hydrolysis of the polysaccharides

^aDalian Institute of Chemical Physics, CAS, Dalian 116023, P. R. China. E-mail: zhaozb@dicp.ac.cn; Fax: +86 411-84379211; Tel: +86 411-84379211

^bGraduate School of the Chinese Academy of Sciences, Beijing 100039, P. R. China

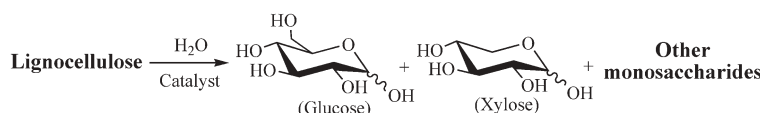


Fig. 1 Schematic illustration of lignocellulosic materials hydrolysis.

(usually referred to as cellulose and hemicellulose) to monosaccharides for further biorefinery.

Results and discussion

Comparison the hydrolysis results between previous studies and the present work

Table 1 summarizes the hydrolysis results catalyzed with hydrochloric acid using C_4mimCl as the reaction medium, as well as some representative results achieved in conventional enzymatic or acid hydrolysis processes. In C_4mimCl , a TRS yield of 66% for corn stalk was obtained within 30 min, at 100 °C in the presence of 7 wt% hydrogen chloride (entry 1). Ion chromatography analysis of the hydrolysate revealed that the distribution of monosaccharides was as follows, glucose 48%, xylose 32%, arabinose 15%, and galactose 3%. In the comparative trial (entry 6), hydrolysis carried out in water under otherwise identical conditions afforded substantially fewer reducing sugars; even when the reaction time reached 48 h, the TRS yield was only 52% (entry 7). These parallel experiments demonstrated clearly that hydrochloric acid/ C_4mimCl was a superior reaction system for hydrolysis of corn stalk. In order to understand the catalytic capability of this system, an experiment with reduced acid loading (2 wt%) was carried out, which gave a TRS yield of 64% albeit it took longer reaction time (entry 2). Further trials on other raw materials also afforded satisfying results under the same

Table 1 The results of lignocellulosic materials hydrolysis reactions promoted by conventional catalytic methods and in a hydrochloric acid/ C_4mimCl system^a

Entry	Material	Time/min	Temperature/°C	TRS yield (%)
1	Corn stalk	30	100	66
2	Corn stalk ^b	330	100	64
3	Rice straw	45	100	74
4	Pine wood	50	100	81
5	Bagasse	60	100	66
6	Corn stalk ^c	30	100	4
7	Corn stalk ^c	2880	100	52
8	Rice straw ^d	2880	50	68
9	Rice straw ^e	2880	50	11
10	Pine wood ^f	4320	40	80
11	Pine wood ^g	1	230	60
12	Pine wood ^h	60	30	85

^a Unless otherwise specified, reaction conditions were: 0.04 g hydrochloric acid, 4.0 g C_4mimCl , 0.03 g H_2O , 0.2 g lignocellulosic material, 100 °C. 0.04 g of hydrochloric acid equals to 0.014 g of HCl; hence, HCl/corn stalk mass ratio was 7%. ^b Corn stalk used for substrate was 0.66 g, HCl/corn stalk mass ratio was 2%. ^c Water used for the solvent and substrate was 4.0 g. ^d Ref. 12. Pretreatment: rice straw concentration 10%; sulfuric acid concentration 0.80 wt%; temperature 160 °C; time 10 min. Hydrolysis condition: suspended pretreated sample at 50 g L⁻¹ in 60 mL of 0.05 M sodium acetate buffer (pH 5.0), with stirring at 50 °C for 48 h, *Cellulase 100L* (1 FPU mL⁻¹) was used for catalyst. ^e Ref. 12. Rice straw was untreated sample, other conditions were the same as entry 8. ^f Ref. 5. Pretreatment: steam (19 bar, 210 °C) + SO₂, 30 min. Hydrolysis condition: enzymes (produced from 6% of the pretreated material) and the major part of the pretreated material reacting at 40 °C for 72 h. ^g Ref. 5. Pretreatment: steam (12 bar, 188 °C) + SO₂, 30 min. Hydrolysis condition: using 0.2% of dilute HCl as catalyst, reacting at 230 °C, for 1 min, the pressure was higher than 20 bar. ^h Ref. 5. 4.2 ton hydrochloric acid (41 wt%) per ton raw material is used, reacting at 30 °C for 60 min.

conditions used for entry 1. As illustrated in entries 3–5, a significantly improved TRS yield (66%–81%) were achieved within 60 min for rice straw, pine wood and sugarcane bagasse.

Further, the results obtained in hydrochloric acid/ C_4mimCl system are compared with those achieved in conventional enzymatic or acid hydrolysis processes. Vlasenko *et al.* reported that a TRS yield of 68% was achieved for hydrolysis of the pretreated rice straw with *Cellulase 100L* for 48 h (entry 8),¹² while the yield was significantly lower for the crude material (11%) (entry 9). Nevertheless, those results were not as good as what was achieved in our study (entry 3). Von Sivers and Zacchi⁵ compared three hydrolysis processes, namely the enzymatic, dilute acid and concentrated acid processes for the production of sugars from pine wood. Both the enzymatic and the dilute acid processes used pine wood samples that were subjected to extensive pretreatments, yet to attain a relative higher TRS yield, the enzymatic process required significantly longer reaction time (48 h) (entry 10), and the dilute acid process was carried out in a rather harsh condition, *i.e.* 230 °C, >20 bar (entry 11). The concentrated acid process utilized 4.2 ton of concentrated hydrochloric acid per ton of pine wood, affording a TRS yield of 85% (entry 12). It was thus clear that an expensive reactor and extensive post-treatment would have to be incorporated. In sharp comparison, hydrolysis in ILs demonstrated that 81% TRS yield was obtained in 50 min without any pretreatment in the presence of a catalytic amount of hydrogen chloride (7 wt%) at 100 °C under atmospheric pressure (entry 4).

Collectively, hydrochloric acid/ C_4mimCl was an efficient system for hydrolysis of lignocellulosic biomass. The excellent behaviour of this system might be attributed to the following features. First, lignocellulosic materials dissolved in C_4mimCl promoted the dispersion of most of the cellulose and hemicellulose molecules; accordingly, the substrates are more exposed to H⁺ in the homogeneous solution, which should be advantageous compared to conventional enzymatic or dilute acid hydrolysis under heterogeneous conditions. Therefore, the physical barrier for hydrolysis has been overcome through formation of a solution. In addition, the dissociated Cl⁻ and the electron rich aromatic π system of $[C_4mim]^+$ in C_4mimCl may also weaken the glycosidic linkage contained in the substrates.⁶

Corn stalk hydrolysis promoted by hydrochloric acid in different ILs

Excellent results in C_4mimCl impelled us to carry out the hydrolysis reaction of corn stalk in other ILs. As shown in Table 2, hydrolysis in C_4mimBr , AmimCl and C_6mimCl also afforded reasonable good TRS yields, albeit optimal reaction time was longer compared to that in C_4mimCl . Specifically, reaction in C_6mimCl required 1200 min to obtain a TRS yield of 49%.

We also tried to use strong acidic ILs, namely $C_4mimHSO_4$ and SbmimHSO₄, as dual catalyst-solvent for the hydrolysis of corn stalk. It was found that the material dissolved quickly, and a solution with lower viscosity formed, indicating that depolymerisation of the polysaccharides occurred readily in a short time. To our surprise, TRS yields of 23% and 15% were

Table 2 The comparative results of hydrolysis reaction of corn stalk in different ILs^a

Entry	Ionic liquid	Time/min	TRS yield (%)
1	C ₄ mimBr	60	47
2	AmimCl	90	65
3	C ₆ mimCl	1200	49
4	C ₄ mimHSO ₄ ^b	5	23
5	SbmimHSO ₄ ^b	2	15
6	C ₄ mimCl ^c	45	71
7	C ₄ mimCl ^d	35	68

^a Unless otherwise specified, reaction conditions were: 0.04 g hydrochloric acid, 4.0 g IL, 0.03 g H₂O, 0.2 g corn stalk, 100 °C. ^b Hydrochloric acid was omitted. ^c 0.1 g of C₄mimHSO₄, in lieu of 0.04 g hydrochloric acid, was employed. ^d 0.1 g of SbmimHSO₄, in lieu of 0.04 g hydrochloric acid, was employed.

obtained in 5 min when C₄mimHSO₄ and SbmimHSO₄, respectively, were employed (entries 4 and 5); and a longer reaction time gave even lower TRS yields (data not shown). We speculated that strong acidic ILs may not only promote the depolymerisation reaction, but also speed up sugar degradation substantially. To confirm our speculation, catalytic amounts of HSO₄⁻ functionalized ILs were used as catalysts for the hydrolysis of corn stalk in C₄mimCl. As expected, TRS yields of 58% and 61% were achieved for C₄mimHSO₄ and SbmimHSO₄, respectively (entries 6 and 7). Hence, acidic ILs *per se* could act as good catalysts for the hydrolysis of lignocellulosic biomass. It should be noted that ILs with a poor capability of dissolving cellulose, *e.g.*, C₄mimPF₆ and C₄mimBF₄,⁶ were found infertile in our study.

Comparison of the activity of different acids in C₄mimCl

To further explore the generality of lignocellulose hydrolysis in ILs, other acids, including sulfuric acid, nitric acid and phosphoric acid, as well as an organic acid (maleic acid) were tested, and the results are summarized in Table 3. In the standard reaction setting with 0.04 g hydrochloric acid loading, H⁺ concentration was estimated to be 0.10 mol L⁻¹, and the TRS yield was 66% after 0.5 h (entry 1). However, when sulfuric acid was added to a final H⁺ concentration of 0.20 mol L⁻¹, the yield of TRS was only 37% after 6 h (entry 2). To improve this reaction, we had a few trials by increasing sulfuric acid loading. It was not until the corresponding H⁺ equivalent concentration reached 0.50 mol L⁻¹, that a high TRS yield (62%) was attained in 0.67 h (entry 3). It is also observed that nitric acid was inferior to hydrochloric acid.

Table 3 The results of various acids hydrolysis of corn stalk in ionic liquid C₄mimCl^a

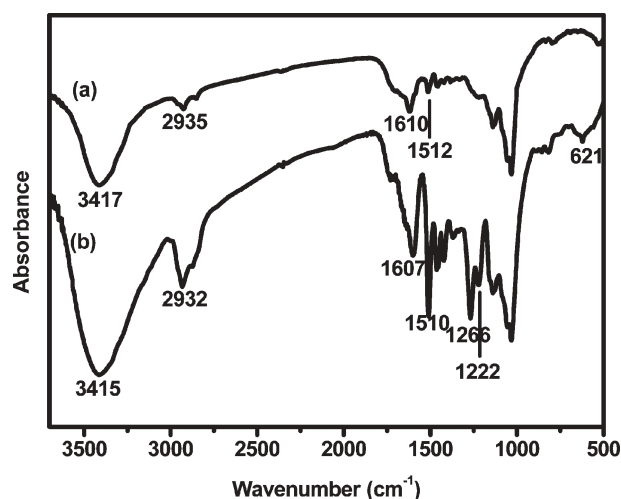
Entry	Catalyst	[H ⁺]/mol L ⁻¹	Time/h	TRS yield (%)
1	Hydrochloric acid ^b	0.10	0.5	66
2	Sulfuric acid ^b	0.20	6.0	37
3	Sulfuric acid	0.50	0.67	62
4	Nitric acid	0.25	0.67	73
5	Phosphoric acid	0.65	34	44
6	Maleic acid ^c	0.43	23	59

^a Unless otherwise noted, the reaction conditions are: Corn stalk (40 mesh, 0.2 g) in the presence of acid catalyst (0.1 g) and H₂O (0.03 g) in C₄mimCl (4.0 g) at 100 °C, atmospheric pressure. ^b The amount of acid catalyst was 0.04 g. ^c Water (0.04 g) was added.

When nitric acid was supplemented to a H⁺ equivalent concentration of 0.10 mol L⁻¹, the TRS yield was only 31% in 0.67 h (data not shown), whereas the TRS yield reached 73% upon the H⁺ equivalent concentration up to 0.25 mol L⁻¹ (entry 4). For phosphoric acid, the hydrolysis reaction went extremely slow, and the yield of TRS was 44% after 34 h despite that it was employed to a H⁺ equivalent concentration of 0.65 mol L⁻¹ (entry 5). Note that acid promoted hydrolysis of cellulose is predominantly limited to mineral acids, it was interesting to find out that maleic acid also effectively accelerated the hydrolysis reaction in C₄mimCl. Under an identical reaction condition, maleic acid was superior to phosphoric acid, affording a TRS yield of 59% in 23 h (entry 6). Collectively, the catalytic activity on hydrolysis of lignocellulose in C₄mimCl for these acids roughly followed the sequence: hydrochloric acid > nitric acid > sulfuric acid > maleic acid > phosphoric acid.

Although there is no solid data available to predict acid strength in ILs, we were still puzzling over the fact that more sulfuric acid than hydrochloric acid was routinely required to obtain a similar TRS yield. It thus occurred to us that the lignin may have done the trick, as it is known that lignin can be sulfonated under various conditions.^{13,14} To test such a speculation, the solid residue was recovered, and submitted for FT-IR and elemental analysis.

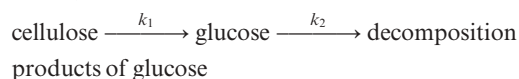
Fig. 2 shows the FT-IR spectra of the solid samples recovered from hydrolysis of corn stalk in C₄mimCl catalyzed by hydrochloric acid (a) and sulfuric acid (b), respectively. The absorbance at around 3415 cm⁻¹ is associated with the hydroxyl group stretching vibrational bands of lignin; around 2932 cm⁻¹ are methyl, methylene or methyne stretching vibrational bands; the absorbances at 1607 cm⁻¹ and 1510 cm⁻¹ are the characteristic bands of aromatic rings, they are typical stretching vibrational bands of the C–C, C=C conjugate system. These bands indicate clearly that both of the two solid samples shared the basic framework of lignin.¹³ It is also clear that spectrum (b) has additional bands. The bands at 1269 cm⁻¹ and 1222 cm⁻¹ are assigned to an S=O stretching vibration; and the absorbance at 621 cm⁻¹ is associated with an

**Fig. 2** The FT-IR spectra of (a) sample catalyzed with hydrochloric acid, (b) sample catalyzed with sulfuric acid.

S–O stretching vibration. These distinct bands suggest the presence of a sulfonic group. Furthermore, elemental analysis revealed that the residue sample had a sulfur content of $0.274 \pm 0.006\%$. Collectively, these data suggest that modification of lignin (esterification, sulfonation, *etc.*) occurs during the sulfuric acid catalyzed hydrolysis, resulting in more sulfuric acid requirement. It will be thus interesting to look into lignin modification in ILs. As mentioned above, more nitric acid requirement might also be due to modification of lignin.

Kinetic model

Various kinetic studies on the acid-catalyzed hydrolysis using a range of cellulosic materials have been reported in the literature.¹⁵ The first systematic kinetic study on biomass hydrolysis to glucose was performed in 1945 by Saeman,¹⁶ who studied the hydrolysis reaction of Douglas fir in batch reactors. In this study, the hydrolysis reaction is modeled by the following two consecutive first-order reactions:



where k_1 is the rate constant for cellulose hydrolysis and k_2 is the rate constant for glucose degradation. This model has been applied to most of the kinetic studies and found to give reasonable levels of agreement with experimental data.

We have monitored the time course of TRS formation from corn stalk in $C_4\text{mimCl}$ for 95 min. As shown in Fig. 3, in the beginning, TRS formation increased remarkably with an increase of reaction time, the yield of TRS reached 86 mg within 30 min, thereafter, the increased reaction time gave decreased TRS yield, indicating that TRS decomposed. Regression analysis of the experimental data by non-linear least squares curve fitting using software Origin 7.0 indicated that the kinetics likely followed a consecutive first-order reaction sequence ($R^2 = 0.98456$), where k_1 and k_2 , the rate constants for TRS formation and TRS degradation, were determined as 0.068 min^{-1} and 0.007 min^{-1} , respectively.

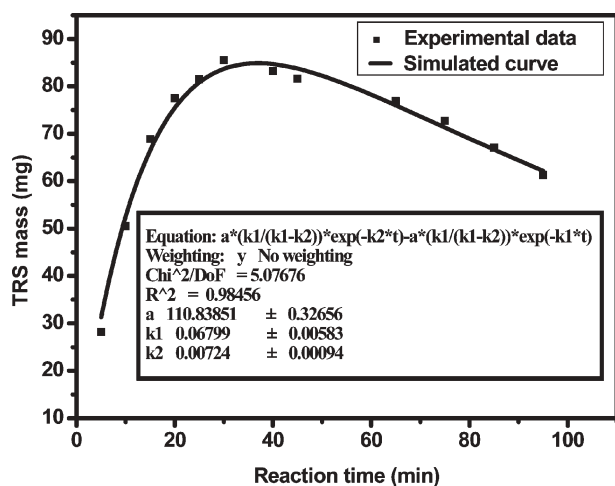


Fig. 3 Experimental data and the simulated curve for corn stalk hydrolysis. Reaction conditions: corn stalk (0.20 g), H_2O (0.03 g) and 0.04 g of hydrochloric acid in $C_4\text{mimCl}$ (4.0 g), 100°C .

Obviously, the rate constant for TRS formation is higher than the rate constant for TRS degradation; therefore, corn stalk hydrolysis proceeded significantly faster than TRS degradation.

The kinetic model revealed much information regarding lignocellulose hydrolysis in ILs. Note that the k_2 value is about 10% that of k_1 ; it is very important to find an optimal time window to maximize the TRS yield. The model also implied that it is pivotal to control acid loading in this system, as increased acid concentration could speed up both the lignocellulose hydrolysis and the TRS degradation process. It is expected that maximal TRS yield may be reached in a few minutes with excess acid loading, which would significantly complicate the sample handling and analysis. Indeed, when 0.10 g hydrochloric acid was employed for the hydrolysis of corn stalk in $C_4\text{mimCl}$, the TRS yield was determined as 52% at 5 min, and 65% at 10 min. Therefore, it seemed that the limitation was technically how to effectively mix, monitor and quench the reaction, so that TRS released under the harsher conditions would be devoid of extensive degradation.

Conclusions

In this paper, we have demonstrated that acid in ionic liquids is an effective combination for hydrolysis of lignocellulosic materials. High TRS yields are realized under mild conditions with reduced acid loading, usually 2–50 wt%. This system overcomes the intrinsic bottleneck of biomass hydrolysis by dispersing the cellulose and hemicellulose into selected ILs, and thus makes glycosidic linkage more H^+ -accessible. Overall, the method described herein may be valuable to facilitate cost-efficient conversion of biomass into biofuels and biobased products.

Experimental

Materials

Corn stalk, rice straw, pine wood and sugarcane bagasse were all local materials (Liaoning province, Northeast of China). These materials were cut into small pieces, milled to pass 40 mesh, and dried under vacuum at 90°C for 3 days before use. 1-Methylimidazole (99%) was obtained from J&K Chemical Ltd. (Beijing, China). 1-Chlorobutane (98%) and 1-chlorohexane (99%) were purchased from ABCR GmbH & Co. (Karlsruhe, Germany) and were freshly distilled before use. Hydrochloric acid (36 wt%), sulfuric acid (98 wt%), nitric acid (65–68 wt%), maleic acid (99%), phosphoric acid (85 wt%), allyl chloride (CP) and other chemicals were all supplied by local suppliers. Unless otherwise specified, acids were direct used in their corresponding received concentration or purity.

Preparation of the ionic liquids

$C_4\text{mimCl}$ used for all the studies was prepared according to the method described in our previous work.¹⁷ A mixture of 1-Methylimidazole (41 g, 0.50 mol) and 1-chlorobutane (61 g, 0.65 mol) was refluxed at 80°C for 96 h. After cooling, the reaction mixture formed two phases. The lower layer was separated and was washed with ethyl acetate ($3 \times 30 \text{ mL}$),

dried in vacuum at 70 °C for 5 h to give a yellowish liquid (80.2 g, 92%).

1-Butyl-3-methylimidazolium bromide (C₄mimBr) and 1-hexyl-3-methylimidazolium chloride (C₆mimCl) were synthesized following the similar procedures except for the reaction temperature of C₄mimBr was 50 °C. The yields of C₄mimBr and C₆mimCl were 93% and 88%, respectively.

1-Allyl-3-methylimidazolium chloride (AmimCl),¹⁸ 1-butyl-3-methylimidazolium bisulfate (C₄mimHSO₄), 1-(4-sulfobutyl)-3-methylimidazolium bisulfate (SbmimHSO₄),¹⁹ 1-butyl-3-methylimidazolium tetrafluoroborate (C₄mimBF₄)²⁰ and 1-butyl-3-methylimidazolium hexafluorophosphate (C₄mimPF₆)²¹ were prepared according to the procedures described elsewhere.

Typical procedures for lignocellulose hydrolysis in ionic liquids

Lignocellulosic material (0.2 g) was added in one portion to ionic liquid (4.0 g) that was preheated to 100 °C. The mixture was stirred under atmospheric pressure, followed by addition of H₂O (0.03 g) and an appropriate amount of acid (usually 2–7 wt% that of lignocellulosic sample). The reaction was then vigorously stirred. At different time intervals, samples were withdrawn, weighed (recorded as M₁), and quenched immediately with cold water. The aqueous solutions were neutralized with 0.05 mol L⁻¹ NaOH, centrifuged at 10 000 rpm for 5 min, the volume measured (recorded as V₁) and subjected to sugar analysis.

Sugar analysis

A mixture contained 0.5 mL of 3,5-dinitrosalicylic acid (DNS) reagent²² and 0.5 mL of reaction sample was heated for 5 min in a boiling water bath, then cooled to room temperature, and mixed with 4 mL of deionized water. The color intensity of the mixture was measured in a JASCO V-530 Model spectrophotometer at 540 nm with a slit width of 0.06 mm. The concentration of TRS was calculated based on a standard curve obtained with glucose. The mass of TRS and the yield of TRS were calculated as follows,

$$M_T = \text{TRS concentration (mg mL}^{-1}\text{)} \times V_1 \times (M_0/M_1)$$

$$\text{TRS yield} = M_T \times 0.9/(200 \times A) \times 100\%$$

in which, M_T is the mass of TRS, V₁ is the volume of the sample, M₀ is the total mass of the reaction solution, M₁ is the mass of sample, and A is the weight percentage of the polysaccharides contained in lignocellulosic materials. For corn stalk, rice straw, pine wood and sugarcane bagasse, A are 58%,²³ 59%,²⁴ 62%⁵ and 74%,²⁵ respectively.

A representative corn stalk hydrolytic mixture (entry 1, Table 1) has also been analyzed on an ICS-2500 IC system equipped with an analytical column (CarboPac PA10, 250 mm × 4 mm) and an ED50 pulsed electrochemical detector.

FT-IR and elemental analysis

After the acid catalyzed hydrolysis reaction was completed, the mixture was diluted with cold water, neutralized with

0.05 mol L⁻¹ NaOH, and centrifuged at 10 000 rpm for 10 min. The pellet was collected, re-suspended in deionized water, and centrifuged. The purification sequence was repeated 5 times. The recovered solid material was dried at 108 °C to a constant weight, and submitted for FT-IR and elemental analysis. All the FT-IR spectra were collected on an FTIR spectrometer (Nicolet Nexus 470) with a resolution of 4 cm⁻¹ and 64 scans in the region of 4000–400 cm⁻¹. IR spectra of the hydrolysis residue samples were recorded as KBr pellets. Elemental analysis was done on a Vario MICRO elemental analyzer.

Acknowledgements

This work was supported by the National Basic Research Program of China (973 Program) (No. 2004CB719703) and CAS “100 Talents” program.

References

- 1 A. J. Ragauskas, C. K. Williams, B. H. Davison, G. Britovsek, J. Cairney, C. A. Eckert, W. J. Frederick Jr., J. P. Hallett, D. J. Leak, C. L. Liotta, J. R. Mielenz, R. Murphy, R. Templer and T. Tschaplinski, *Science*, 2006, **311**, 484.
- 2 M. E. Himmel, S.-Y. Ding, D. K. Johnson, W. S. Adney, M. R. Nimlos, J. W. Brady and T. D. Foust, *Science*, 2007, **315**, 804.
- 3 G. Stephanopoulos, *Science*, 2007, **315**, 801.
- 4 N. Mosier, C. Wyman, B. Dale, R. Elander, Y. Y. Lee, M. Holtzapple and M. Ladisch, *Bioresour. Technol.*, 2005, **96**, 673.
- 5 M. von Sivers and G. Zacchi, *Bioresour. Technol.*, 1995, **51**, 43.
- 6 R. P. Swatloski, S. K. Spear, J. D. Holbrey and R. D. Rogers, *J. Am. Chem. Soc.*, 2002, **124**, 4974; R. C. Remsing, R. P. Swatloski, R. D. Rogers and G. Moyna, *Chem. Commun.*, 2006, 1271.
- 7 D. A. Fort, R. C. Remsing, R. P. Swatloski, P. Moyna, G. Moyna and R. D. Rogers, *Green Chem.*, 2007, **9**, 63; V. M. Egorov, S. V. Smirnova, A. A. Formanovsky, I. V. Pletnev and Y. A. Zolotov, *Anal. Bioanal. Chem.*, 2007, **387**, 2263; B. Dereskei and A. Dereskei-Kovacs, *Mol. Simulat.*, 2006, **32**, 109; S. D. Zhu, Y. Wu, Q. Chen, Z. Yu, C. Wang, S. Jin, Y. Ding and G. Wu, *Green Chem.*, 2006, **8**, 325.
- 8 See for example: J. Wu, H. Zhang, J. He, Q. He and M. Guo, *Biomacromolecules*, 2004, **5**, 266; S. Barthel and T. Heinze, *Green Chem.*, 2006, **8**, 301; A. P. Abbott, T. J. Bell, S. Handa and B. Stoddart, *Green Chem.*, 2005, **7**, 705; M. B. Turner, S. K. Spear, J. D. Holbrey and R. D. Rogers, *Biomacromolecules*, 2004, **5**, 1379; T. Heinze, K. Schwikal and S. Barthel, *Macromol. Biosci.*, 2005, **5**, 520.
- 9 C. Li and Z. K. Zhao, *Adv. Synth. Catal.*, 2007, **349**, 1847.
- 10 N. Yan, C. Zhao, C. Luo, P. J. Dyson, H. Liu and Y. Kou, *J. Am. Chem. Soc.*, 2006, **128**, 8714.
- 11 F. Lu and J. Ralph, *Plant J.*, 2003, **35**, 535.
- 12 E. Y. Vlasenko, H. Ding, J. M. Labavitch and S. P. Shoemaker, *Bioresour. Technol.*, 1997, **59**, 109.
- 13 M. Dawy, A. A. Shabaka and A. M. A. Nada, *Polym. Degrad. Stabil.*, 1998, **62**, 455.
- 14 T. Foyle, L. Jennings and P. Mulcahy, *Bioresour. Technol.*, 2007, **98**, 3026.
- 15 H. E. Grethlein, *J. Appl. Chem. Biotechnol.*, 1978, **28**, 296; R. D. Fagan, H. E. Grethlein, A. O. Converse and A. Porteous, *Environ. Sci. Technol.*, 1971, **5**, 545; D. R. Thompson and H. E. Grethlein, *Ind. Eng. Chem. Prod. Res. Dev.*, 1979, **18**, 166; J. P. Franzidis, A. Porteous and J. Anderson, *Conserv. Recycl.*, 1982, **5**, 215; M. Green, S. Kimchie, A. I. Malester, B. Rugg and G. Shelef, *Biol. Wastes*, 1988, **26**, 285; I. A. Malester, M. Green and G. Shelef, *Ind. Eng. Chem. Res.*, 1992, **31**, 1998; M. M. Bhandari, D. G. Macdonald and N. N. Bakshi, *Biotechnol. Bioeng.*, 1984, **26**, 320; D. K. Sidiras and E. G. Koukios, *Biomass*, 1989, **19**, 289.
- 16 J. F. Saeman, *Ind. Eng. Chem.*, 1945, **37**, 43.

- 17 D. H. Yin, C. Li, B. Li, L. Tao and D. Yin, *Adv. Synth. Catal.*, 2005, **347**, 137.
- 18 H. Zhang, J. Wu, J. Zhang and J. He, *Macromolecules*, 2005, **38**, 8272.
- 19 W. Keim, *WO Pat.*, 00/16 902, 2000.
- 20 P. A. Z. Suarez, J. E. L. Dullius, S. Einloft, R. F. De Souza and J. Dupont, *Polyhedron*, 1996, **15**, 1217.
- 21 J. G. Huddleston, H. D. Willauer, R. P. Swatloski, A. E. Visser and R. D. Rogers, *Chem. Commun.*, 1998, **16**, 1765.
- 22 G. L. Miller, *Anal. Chem.*, 1959, **31**, 426.
- 23 C. Liu and C. E. Wyman, *Bioresour. Technol.*, 2005, **96**, 1978.
- 24 S. Jin and H. Chen, *Process Biochem.*, 2007, **42**, 188.
- 25 C. Matin, H. B. Klinke and A. B. Thomsen, *Enzyme Microb. Technol.*, 2007, **40**, 426.



STOP!

searching...

Save valuable time searching for that elusive piece of vital chemical information.

Let us do it for you at the Library and Information Centre of the RSC.

We are your chemical information support, providing:

- Chemical enquiry helpdesk
- Remote access chemical information resources
- Speedy response
- Expert chemical information specialist staff

Tap into the foremost source of chemical knowledge in Europe and send your enquiries to

library@rsc.org

RSCPublishing

www.rsc.org/library

12120515

A green route to silica nanoparticles with tunable size and structure†

Yun Yang and Thibaud Coradin*

Received 3rd September 2007, Accepted 29th November 2007

First published as an Advance Article on the web 14th December 2007

DOI: 10.1039/b713438j

A green and simple route to silica nanoparticles with tunable size, structure and stability is presented. Hybrid nanoparticles containing alginate, a polysaccharide, and silicates are obtained using the well-established spray drying technology. Subsequent exposure to water leads to the release of alginate and the particle structural re-organization *via* Ostwald ripening. Through adjustment of ripening time, of initial composition and concentration of bio-organic/inorganic precursors, silica nanoparticles with morphologies varying from plain spheres to hollow shells can be synthesized. The synthetic procedure is straightforward, inexpensive and environment-friendly, and may be suitable for large-scale production.

Introduction

Over the past few years, fabrication of hollow silica spheres has been extensively studied due to their wide applications in catalysis,¹ encapsulation of biologicals,² drug release systems,³ and magnetic nanomaterials⁴ benefiting from their large specific surface area, good biocompatibility and stability. Template-assisted synthesis is the most popular approach to obtaining such hollow structures. This approach usually involves the preparation of the template, its coating using silica precursors to form an outer shell and its removal to obtain hollow structures. The templates mainly include soft-templates such as organic surfactants⁵ and hard-templates consisting of polymeric spheres,⁶ inorganic oxides,⁷ semiconductor⁸ and calcium carbonate⁹ nanoparticles, and droplets in emulsion systems¹⁰. However, the template removal step often involves the use of organic solvents (droplet and polystyrene spheres), strong acids (metal and inorganic nanoparticle) or calcination (micelles) generating toxic gas, all of which are environmentally unfriendly. It is therefore desirable to develop alternative procedures to obtain hollow silica spheres following Green Chemistry principles.

Recently, two template-free technologies, involving Ostwald ripening¹¹ and the Kirkendall effect,¹² have been used to prepare spherical particles with hollow structures. Since the first report of the formation of hollow nanoparticles based on the Kirkendall effect by Yin *et al.*, hollow nanoparticles, mainly formed by crystalline materials, such as ZnO, CuS and CoO, have been generated by this approach.¹³ Unlike the Kirkendall effect, Ostwald ripening is a route suitable for both crystalline and amorphous structures.¹⁴ Concerning the use of Ostwald ripening to create hollow spheres, the key point is to produce initial spherical particles for which the external surface layer is less soluble than the interior material. During the ripening process, interior core species remain

supersaturated and out of equilibrium with the surrounding solution, in contrast with the external layer, so that shell thickness increases at the expense of the inner core, resulting in a hollow structure. Based on this route, numerous hollow particles have been synthesized.¹⁴ However, to the best of our knowledge, there has been no similar report for hollow silica nanoparticles.

Herein, we demonstrate a green, facile and versatile synthesis of hollow silica nanoparticles with tunable size and structure based on the Ostwald ripening process. In our procedure, hybrid silica nanospheres containing sodium alginate and sodium silicate are first prepared using a home-made spray drier, as described in the Experimental section. These hybrid nanoparticles are then placed in water and the structure, size, hollowing time and stability of recovered silica nanospheres can be controlled by simply adjusting the precursor solution composition and the water temperature. Most importantly, the whole synthetic process just involves two agents which are biocompatible and often used in drug delivery and bioencapsulation,^{2,15,16} so that our process is simple, environmentally friendly and promising for nanoscaled bio-material design. Furthermore, spray drying, which is a well-developed technique widely used in industries for the preparation of particles,¹⁷ favours large-scale synthesis, a major factor for forthcoming applications.

Experimental

Synthesis of hybrid nanoparticles

Alginate/silicate hybrid particles synthesis is derived from our previous reports.¹⁸ Typically, appropriate amount of sodium silicate (10% NaOH, 27% SiO₂ from Riedel-de Haen) and alginate (from *Macrocystis pyrifera*, low viscosity, from Sigma) are independently dissolved in 250 mL of distilled water. 15 mL of each solution are mixed in a 50 mL flask under stirring. Resulting solutions are sonicated for 5 min before introduction in the spray-dryer.

Our home-made spray drying system is illustrated in Fig. 1. In a typical drying process, a high-pressure inlet gas jet (Fig. 1 (1), air, 10 psi) is injected in an atomizer head. Under pump

Chimie de la Matière Condensée de Paris, Université Pierre et Marie Curie, CNRS UMR 7574, 4 place Jussieu, F-75252 Paris cedex 05, France

† Electronic supplementary information (ESI) available: TEM images of fragmented silica nanoparticles as well as HR TEM of nanoparticles obtained after thermal treatment. See DOI: 10.1039/b713438j

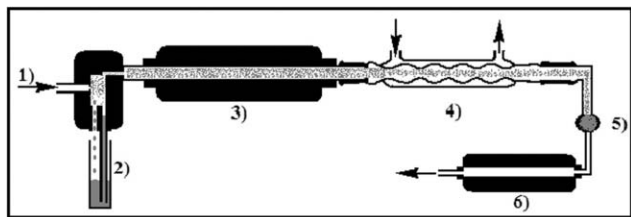


Fig. 1 Description of the spray-drying process: (1) air injection at constant pressure and flow rate; (2) starting solution container; (3) furnace at 200 °C; (4) condenser; (5) particle membrane filter paper; (6) pump.

(Fig. 1 (6)) and high-pressure air flow, the solution is inhaled and broken into droplets. Larger droplets are backscattered into the initial solution container (Fig. 1 (2)), while the smaller ones enter the furnace (Fig. 1 (3)) where solvent evaporate quickly and non-volatile species form spherical particles. After cooling (Fig. 1 (4)), aerosol is recovered on a filter paper (Fig. 1 (5)).

Synthesis of hollow silica spheres

10 mg of as-prepared hybrid nanoparticles are added to 10 mL of distilled water, and the suspension is left at room temperature or placed into an oven at 95 °C for 2 h–20 days. After ageing, the resulting products are harvested by centrifugation (11 000 rpm) and washed several times with de-ionized water. The samples were characterized using scanning electron microscopy (SEM) and transmission electron microscopy (TEM).

Results and discussion

Nanoparticle size tuning by adjusting silicate content

The size of particles obtained by a spray-drying technology usually depends on many parameters including concentration, composition, chemical and physical properties of non-volatile substances, and also on some technical factors (size of nozzle, spray flow rate, atomization pressure).¹⁷ Herein, the effects of alginate and silicate content on particle size are studied when parameters of the spray drying system are kept constant.

Fig. 2 shows the SEM images and the corresponding size distribution (based on later TEM images) of silica spheres obtained by mixing 15 mL of alginate solution (0.05 wt%) with 15 mL of silicate solutions at various concentrations and further exposed to water for 4 days. It clearly shows that the resulting nanoparticle size increases with the silicate content. In Fig. 2a1–3, for a 0.02 M silicate concentration, it was difficult to obtain clear observation of the particles *via* SEM due to limited resolution of our microscope. With silicate concentration increasing to 0.05 M, the mean diameter is 160 nm (Fig. 2b3), and the sphere-like shape can be demonstrated definitely, as shown in Fig. 2b1–2. A moderate size increase is then observed for a 0.1 M silicate concentration but a 0.25 M silicate addition induces a major change in particle dimension to *ca.* 250 nm. Moreover, when a 0.5 M silicate solution was added, a number of particles with diameters over 1 μm were observed in addition to the nanoparticle population (Fig. 2e1–3).

When the silicate content is kept constant (0.1 M), SEM images and histograms of size distribution in Fig. 3 indicate that the amount of alginate also can lead to size change, but to a much lesser extent. 0.01 wt% (Fig. 2f1–3), 0.05 wt% (Fig. 2c1–3) and 0.25 wt% (Fig. 2g1–3) alginate solutions produce nanoparticles with 176 nm, 180 nm and 186 nm mean diameter, respectively. This suggests that alginate does not have the same function as surfactants, which can reduce surface tension of droplets.¹⁹

It is worth noting that dynamic light scattering (DLS) studies of nanoparticle suspensions in water indicate main particle diameters in the 150 nm–200 nm range for all samples, suggesting only limited particle agglomeration (not shown).

Thus, it appears that particle size is mainly determined by silicate concentration. However, it is worth noting at this stage that the alginate content seems to play a role in the particle stability as the hybrid nanospheres prepared with the highest polymer concentration were rapidly dissociated after only a few hours in water at room temperature. Therefore, it could be expected that the polysaccharide/silicate ratio may influence the nanoparticle internal structure.

Nanoparticle structure control by modifying silicate content

First investigations of nanospheres using TEM reveal that the silicate content also has a major impact on the structural evolution of the nanoparticle structure, as shown in Fig. 3. For the lowest silicate concentration (0.02 M), most particles are hollow, as indicated by Fig. 3a, in which some basket-like spheres are also observed. With the concentration of silicate increasing to 0.05 M, particles present an inner-core structure partially separated from the outer shell (Fig. 3b). When a 0.1 M silicate solution is used, fragmented particles are formed, together with nanospheres with loose cores, as seen in Fig. 3c. By further increasing silicate concentration, fragmented silica spheres, shown in Fig. 3d, are also obtained, few of which have small internal voids. Here, the largest concentration tested is 0.5 M, just generating fragmented silica spheres as revealed in Fig. 3e. For the last two samples, we hypothesized that the fragmentation results from the release of alginate from the hybrid nanoparticles. This could be demonstrated by a control experiment where as-synthesized particles were dispersed in ethanol, a poor solvent for alginate. In these conditions, no fragmented structure could be observed after a 6 day ageing period. The release of alginate in water was also supported by EDX measurements, showing a decrease of the C:Si ratio with time (not shown).

The samples obtained by changing the alginate content were also studied by TEM and the results are shown in Fig. 3. For the lowest concentration of alginate (0.01 wt%), samples exhibit a fragmented structure similar to those obtained for a 0.05 wt% concentration (compare Fig. 3f with Fig. 3c). However, when the alginate concentration is increased to 0.25 wt%, very poor mechanical stability does not allow a good preservation of original particles during centrifugation. After 6 days of ageing, many fragments from broken particles occupy the images, as seen in Fig. 3g. Back to SEM results in Fig. 2g, after 2 h in water the presence of plain spheres is very obvious, which means that most of the alginate is still trapped

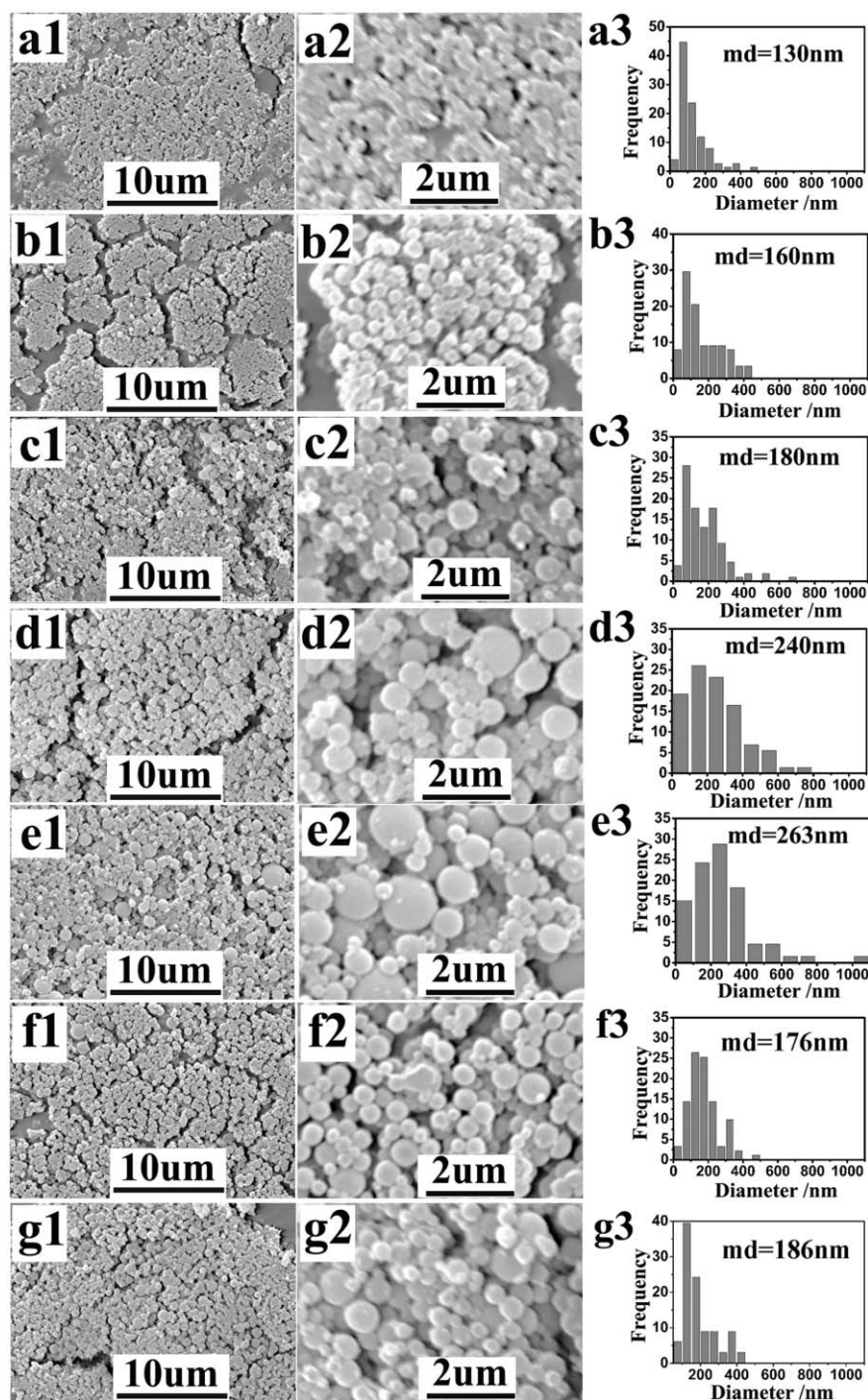


Fig. 2 SEM images and size distribution histograms of particles synthesized using alginate concentration = 0.05 wt% with silicate concentration = (a1–3) 0.02 M, (b1–3) 0.05 M, (c1–3) 0.1 M, (d1–3) 0.25 M, (e1–3) 0.5 M and using silicate concentration = 0.1 M with alginate concentration = (f1–3) 0.01 wt%, (g1–3) 0.25 wt%. All characterizations are carried out after 4 days of ageing at room temperature. md = mean diameter.

in the hybrid system after this delay. For a longer ageing period, alginate is fully removed from hybrid nanoparticles. Because alginate is initially present in large amounts, silicates are dispersed in the polymer network. Such a poor connectivity limits silicate condensation so that the resulting silica network is easily destroyed by centrifugal force. However, Fig. 3g also reveals that some of the particles still exhibit intact morphologies as hollow structures, whereas most fragments are pieces

of shells, suggesting that particles have hollow architectures before the centrifugation procedure.

Nanoparticle structural evolution with ageing time

In order to get more information about structural evolution of the nanoparticle, time-dependent experiments were carried out using samples prepared with a 0.1 M silicate concentration and

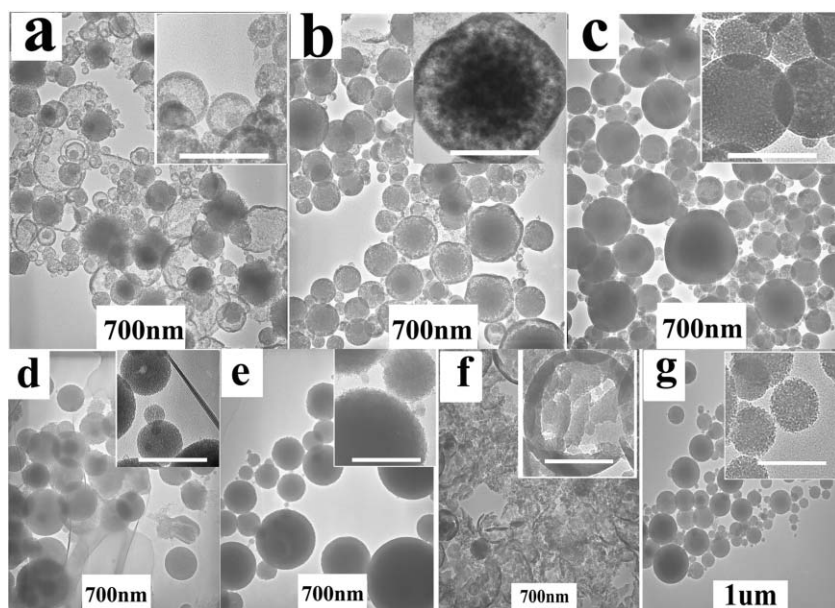


Fig. 3 TEM images of particles synthesized using alginate concentration = 0.05 wt% with silicate concentration = (a) 0.02 M, (b) 0.05 M, (c) 0.1 M, (d) 0.25 M, (e) 0.5 M and using silicate concentration = 0.1 M with alginate concentration = (f) 0.01 wt%, (g) 0.25 wt%. All characterizations are carried out after 4 days of ageing at room temperature. All scale bars in inserted images are 200 nm.

a 0.05 wt% alginate solution (Fig. 4). As shown in Fig. 4a, after 1 h in water the particles show a dense structure and no fragmentation is apparent. After 1 d in water, the release of the biomolecule is indicated by an obvious fragmented structure (Fig. 4b). With an increase of ageing time up to 6 days, as shown in Fig. 4c, some particles have partly separated core and shell, and for small-size particles hollow structures are observed. The particles obtained after a 13 d ripening time are shown in Fig. 4d, where cores and shells separate in most particles, similarly to the samples described in Fig. 3b

Effect of temperature on nanoparticle structural evolution

Although the process described above allows a structural control of the nanoparticles, formation of hollow structures takes very long time for most samples. Heat, which can generally accelerate molecular motion and shorten reaction time, is widely used in the preparation of nanoparticles, such as CdS, TiO₂ and CuO.¹⁴ In the following section, it is shown that heat, together with other conditions (modification of

alginate and silicate content) (Table 1), can be used to tailor particle structure.

When compared with results shown in Fig. 4, obtained for samples aged at room temperature, Fig. 5a–c clearly demonstrate the effect of heat on the structural evolution of nanoparticles obtained with the same silicate (0.1 M) and alginate (0.05 wt%) concentrations. When the reaction time is 2 h at 95 °C, voids between core and shell can be observed clearly, as indicated by lighter parts in particles (Fig. 5a). In contrast, for particles prepared in the same conditions and aged at room temperature, a 2 h ripening cannot even produce porous structure, as illustrated in Fig. 4a. A hollowing effect is observed for particles recovered after longer reaction times. As reported in Fig. 5b, the voids within the nanospheres are further enlarged when the ripening time is extended to 2 days. Samples with a 6 day ripening time, in which only little solid cores are left, are shown in Fig. 5c. It should be noted that inner solid cores are not separated completely from the shell and connections still exist, which may result from silicate species in a midway migration path to the shell.

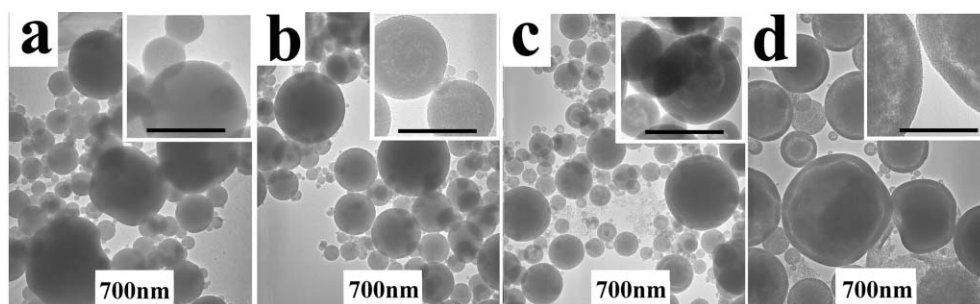


Fig. 4 TEM images for samples aged for (a) 2 h, (b) 1 d, (c) 6 d and (d) 13 d. Original samples were prepared with 0.1 M silicate concentration and a 0.05 wt% alginate solution. All scale bars in inserted images are 200 nm.

Table 1 Synthetic parameters for hollow spheres obtained after thermal treatment

Sample	[Alginate] (wt%)	[SiO ₂]/mol L ⁻¹	Temperature/°C	Ageing time
a	0.05	0.1	95	2 h
b	0.05	0.1	95	2 d
c	0.05	0.1	95	13 d
d	0.05	0.02	37	2 d
e	0.05	0.5	95	27 d
f	0.01	0.1	95	13 d
g	0.25	0.1	37	6 d

Lowering the initial concentration to 0.02 M while keeping the alginate concentration constant, we tried to hollow as-created products at 95 °C. However, in contrast to the room temperature procedure (Fig. 3a), these samples were unstable under heat, and degrade into much smaller nanoparticles (see Electronic Supplementary Information†). This fragmentation was confirmed by centrifugation experiments that did not allow the recovery of any material. Such a degradation can be attributed to the low silicate content, leading to poor mechanical stability of the hybrid nanoparticles, and to the high dispersion state of silica within the polymer network, as already mentioned. To overcome this problem, the temperature was set at 37 °C and the ageing time limited to 2 days. In this case, no obvious dissolution takes place, and the TEM characterizations reveals that most particles are hollow (Fig. 5d). In contrast, for particles obtained with 0.5 M silicate, an ageing period up to 27 days was necessary to get hollow structures at 95 °C (Fig. 5e).

As previously mentioned, modification of the alginate concentration can also be used to tailor particle size and structure. For a 0.01 wt% concentration, samples left in water for 13 days at 95 °C lead to dense particles where no clear fragmentation is observed (Fig. 5f), thus differing from nanoparticles obtained after room temperature treatment (Fig. 3f). In contrast, when the alginate concentration reaches

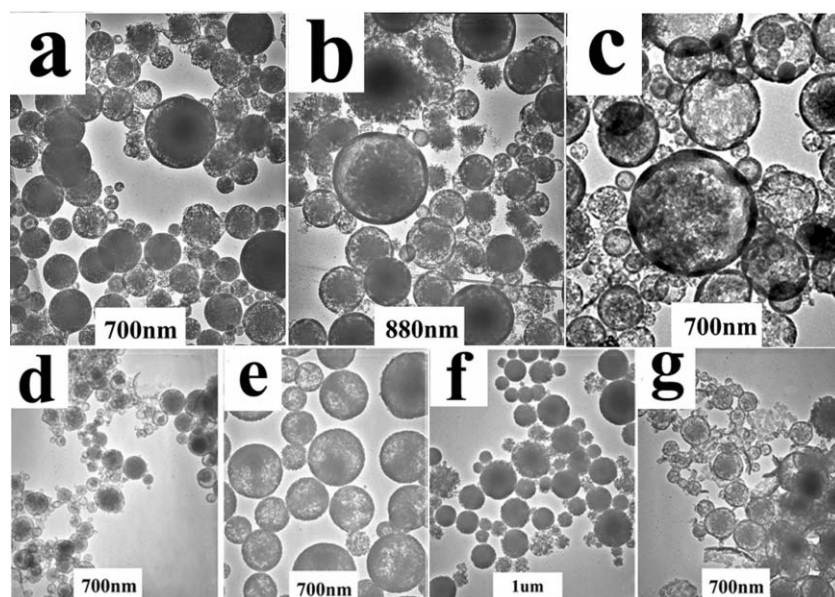
0.25 wt%, particles are broken into nano-scaled fragments, as already observed for a low silicate concentration. Here again, in order to protect particles against centrifugation and heat-induced fragmentation, a lower temperature treatment was used (37 °C). Moreover, intact particles could be recovered by several sedimentation/water re-dispersion steps. These samples mainly consist of hollow structures but some fragments of broken particles are also observed (Fig. 5g).

Overall, these observations confirm the importance of the silica content on the mechanical and thermal stability of the nanoparticles and also imply that their degradation rate can be tailored by adjusting the alginate/silicate ratio.

Structure evolution mechanism

In order to figure out the possible structure evolution mechanism based on TEM observations, the discussion first needs to take into account the process of spray drying. In a typical spray-drying process (Fig. 1), a solution containing non-volatile species is atomized by high-pressure gas flow, and subsequently small liquid drops are heated to form solid spherical nanoparticles after solvent evaporation.¹⁷

The size of the recovered particles and the polydispersity of the samples, are known to depend on the concentration and solubility of non-volatile species in the initial solution.¹⁷ In particular, high concentrations of poorly soluble species lead to larger particles with significant polydispersity. In the present case, it appears that hybrid nanoparticle size is mainly determined by silicate concentration. This reflects the higher density of silica when compared with alginate, which leads to an expected increase of nanoparticle volume with silicate content. Additionally, comparison of size distributions for all samples also indicates that polydispersity increases with silicate concentration but does not depend significantly on alginate content. This may be attributed to the fact that, whereas the polymer is expected to be chemically inert during the spray-drying process, silicate species are undertaking a

**Fig. 5** TEM images of particles aged at 37 °C or 95 °C. See Table 1 for preparation conditions.

condensation reaction leading to silica formation. As condensation proceeds, the water solubility of the formed silicate species decreases, which may explain the observed increase in sample polydispersity.

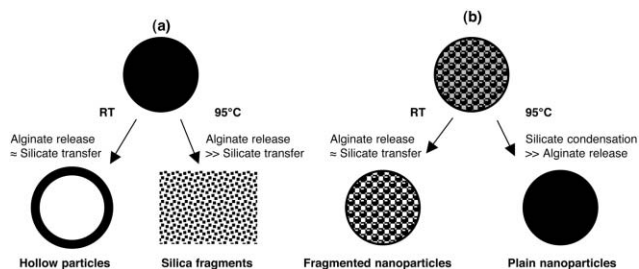
Considering the nanoparticle's internal structure, it is well-known that the drying is an external-to-interior process where the surface layer of liquid drops is first heated so that, in most cases, the external shell of as-created particles is different from their interior.¹⁷ In the case of spray-dried alginate/silicate solutions, silicate species in atomized droplets first condense on their outer layer due to more efficient heating of this area, so that the silica network constituting the shell is expected to possess a higher condensation degree and better stability against dissolution than the core material, opening up the possibility of using Ostwald ripening for the preparation of hollow structures.¹⁴ In addition, the presence of alginate leads to a dispersion of silicate species, limiting their condensation and therefore enhancing their solubility.

When hybrid nanoparticles are exposed to water, the release of alginate can occur freely, driven by dissolution and diffusion, because there is no attractive interaction between the polymer and silicates. This release of alginate also liberates silica species that now have the possibility to diffuse and condense further. Then, the ensuing evolution upon ageing is a typical Ostwald ripening process, in which the thickness of the less soluble shell increases at the cost of more-soluble inner core. With prolongation of time, the inner core becomes smaller until finally a hollow structure is formed.¹⁴

In our system, three main mass transfers take place. Alginate is released from the nanoparticles to the surrounding water, driven by concentration difference. Silicates, initially trapped in the alginate network, can also migrate from the inner core to the shell by Ostwald ripening. Additionally, water diffuses from the surrounding medium to the particle interior. Among the three mass transfers, water invasion and subsequent alginate release are expected to take place simultaneously as the water-soluble biopolymer can dissolve and diffuse very quickly. In contrast, compared with alginate and water transfers, the silicate migration requires (i) alginate dissolution and (ii) silicate transfer that is controlled by transfer distance and transfer mass and should therefore take a relatively longer time.

Considering the influence of polymer dissolution, for a high initial alginate/silica ratio, the silica structure within the particle core can be visualized as individual blocks dispersed in the alginate matrix rather than as a continuous network (Scheme 1(a)). In traditional Ostwald ripening definition, such small-sized blocks possess high solubility,¹¹ which can also accelerate the hollowing rate and subsequently reduce the time to form hollow structure (Fig. 3g). In contrast, a low alginate/silica ratio leads to large blocks of condensed silica incorporating small amounts of polymer (Scheme 1(b)). Alginate dissolution should therefore create voids and induce the fragmentation of the silica network, as illustrated on Fig. 3f.

As far as silicate transfer is concerned, small particles need less time to form hollow shells because they correspond to shorter transfer distances. Furthermore, fewer species within the inner core can also reduce the time taken to produce a hollow structure, *i.e.*, looser cores need less time than denser



Scheme 1 Schematic illustration of the structural evolution of hybrid alginate (grey)/silica (dark) nanoparticles with (a) low silica content and (b) low alginate content at room temperature (RT) and 95 °C.

cores to re-organize. In Fig. 3, those particles that have been obtained using the lowest concentration of silicates have the smallest size, which leads to the shortest mass transfer distance. Therefore, within a short period of time, formation of hollow particles is achieved. Some basketball-like particles could be seen, and Zeng *et al.* suggested they were typical results of asymmetrical ripening.¹⁴ With the concentration of silicate increasing, mass transfer distance and transferred mass increases, requiring a longer time to form hollow structures. Thus, images shown in Fig. 3 represent different stages of the hollowing process: the final stage for most particles in Fig. 3a (especially for small particles), midway in Fig. 3b and 3c, and possibly the starting period in Fig. 3d and 3e. Accordingly, Fig. 4 illustrates the size-dependence of the structural evolution process where the smallest particles show a hollow structure (final stage), whereas a distinct separation between core and shell materials is observed for the largest ones (midway stage).

Additional studies performed on the effect of temperature also confirm our proposed mechanism. It is expected that heat increases both dissolution and diffusion phenomena. In parallel, temperature should enhance silicate condensation kinetics. The first effect is illustrated by the difference between room temperature and 95 °C experiments, as shown in Figs. 4 and 5. For similar intermediate alginate and silica content, voids between core and shell materials are already observed after 2 h at high temperature (Fig. 5a), whereas similar structures are only obtained after 13 d at room temperature (Fig. 4d). Interestingly, at a low silica content, the Ostwald ripening process is slow at room temperature whereas the heat-induced alginate release kinetics at 95 °C appear too fast to allow silicate diffusion and shell formation, so that unstable, fragmented particles are obtained (Scheme 1a). This problem is overcome by lowering the temperature to 37 °C, indicating that optimum temperature should be found for each nanoparticle composition. The influence of temperature on silica condensation can be clearly seen at low alginate concentration. In this case, particles left at 95 °C over 13 days are almost unmodified as silicate condensation may proceed upon alginate removal (Fig. 5f), whereas fragmented structures are obtained at room temperature (Fig. 3f) (Scheme 1b).

These data deserve to be discussed in the frame of future applications. Alginate/silica nanoparticles obtained using a similar spray-drying approach are currently studied as drug delivery systems.¹⁸ It was demonstrated that these

nanoparticles could be taken-up by living cells and could release model fluorophores intra-cellularly. After cellular incorporation, nanoparticles were found degraded in the cell cytoplasm, leaving silica fragments that are very similar to those observed in this study. Since these experiments were performed at 37 °C, our previous assumption that nanoparticle degradation was due to a specific cellular activity may need to be reconsidered. At the same time, *in vitro* release experiments indicated a rapid fluorophore delivery that was attributed to the thin silica shell observed for these nanoparticles. On the basis of the results obtained here, it should now be possible to control in a more systematic manner both the *in vivo* and *in vitro* behaviour of these hybrid nanocarriers.

Finally, it is worth comparing the spray-drying approach described here with some other methods developed to control nanostructure formation. Owing to its simplicity, the aerosol technique appears suitable for elaboration of hybrid nanoparticles. If several attempts have been made to control the internal architecture of spray-dried powders, the precise control of as-synthesized particle size and poly-dispersity is difficult to achieve, relying on both initial solution content and equipment performance.¹⁷ This indeed contrasts with the traditional routes to silica nanopowders, usually involving the so-called Stöber process.²⁰ However, these methods use silicon alkoxides, and not soluble silicates, as precursors as well as organic solvents, which are not compatible with Green Chemistry requirements. Moreover, it is not possible, *via* this method, to introduce large amounts of organics within the silica network. Another limitation of the spray-drying approach lies in the fact that, since the spherical shape of obtained nanoparticles originates from the drying of sprayed droplets, the control of the particle shape is not straightforward. Very often, such control involves the combination of a surface-regulating agent or an anisotropic template and a precise control of reaction conditions, especially temperature.²¹ Alternatively, soft chemistry methods have been described where the desired shape is obtained by controlling the chemical transformation occurring upon ageing in solution which might involve the Ostwald ripening process.²² Noticeably, most of these approaches have been developed for crystalline nanostructures (metal, metal chalcogenide, ...) and may be more difficult to achieve for amorphous materials, such as silica. Nevertheless, the present work shows that, for lack of size and shape control, it is possible to tailor the internal architecture of silica nanoparticles by controlling the ageing conditions of spray-dried hybrid nanoparticles.

Conclusions

The procedure described here involves two biocompatible agents (alginate and silicate), uses only aqueous media and generates no by-products as both precursors are non-volatile and are fully recovered in the resulting powder. In addition, this process demonstrates a large flexibility in terms of size, structure and stability of the final products, which can be simply controlled by adjusting the composition of the initial mixture and the ageing temperature. All these arguments, together with the use of the technically well-established spray

drying technology, make this method highly promising for further applications.

Acknowledgements

Y. Y. thanks the Université Paris VI for its postdoctoral funding. The help of C. Boissière (CMCP) in setting-up spray-drying experiments is kindly acknowledged. This work was performed in the frame of the FAME European network of excellence.

References

- (a) F. Caruso, *Chem. Eur. J.*, 2000, **6**, 413; (b) F. Caruso, *Adv. Mater.*, 2001, **13**, 11; (c) X. Song and L. Gao, *J. Phys. Chem. C*, 2007, **111**, 8180; (d) P. M. Arnal, M. Comotti and F. Schüth, *Angew. Chem., Int. Ed.*, 2006, **45**, 8224.
- (a) T. Coradin, N. Nassif and J. Livage, *Appl. Microbiol. Biotechnol.*, 2003, **61**, 429; (b) R. K. Sharma, S. Das and A. Maitra, *J. Colloid Interface Sci.*, 2005, **284**, 358.
- (a) J. Chen, H. Ding, J. Wang and L. Shao, *Biomaterials*, 2004, **25**, 723; (b) Y. Zhu, J. Shi, W. Shen, X. Dong, J. Feng, M. Ruan and Y. Li, *Angew. Chem., Int. Ed.*, 2005, **44**, 5083.
- P. Tartaj, T. Gonzalez-Carretero and C. J. Serna, *Adv. Mater.*, 2001, **13**, 1620.
- (a) J.-S. Jan, S. Lee, C. S. Carr and D. F. Shantz, *Chem. Mater.*, 2005, **17**, 4310; (b) N. E. Botterhuis, Q. Sun, P. C. M. M. Magusin, R. A. van Santen and N. A. J. M. Sommerdijk, *Chem. Eur. J.*, 2006, **12**, 1448; (c) Y.-Q. Yeh, B.-C. Chen, H.-P. Lin and C.-Y. Tang, *Langmuir*, 2006, **22**, 6; (d) A. Khanal, Y. Inoue, M. Yada and K. Nakashima, *J. Am. Chem. Soc.*, 2007, **129**, 1534; (e) H.-P. Hentze, S. R. Raghavan, C. A. McKelvey and E. W. Kaler, *Langmuir*, 2003, **19**, 1069; (f) X. Wu, Y. Tian, Y. Cui, L. Wei, Q. Wang and Y. Chen, *J. Phys. Chem. C*, 2007, **111**, 9704.
- (a) R. A. Caruso, A. Susa and F. Caruso, *Chem. Mater.*, 2001, **13**, 400; (b) I. Tissot, J. P. Reymond, F. Lefebvre and E. Bourgeat-Lami, *Chem. Mater.*, 2002, **14**, 1325; (c) Z. Niu, Z. Yang, Z. Hu, Y. Y. Lu and C. C. Han, *Adv. Funct. Mater.*, 2003, **13**, 949; (d) M. Chen, L. Wu, S. Zhou and B. Yu, *Adv. Mater.*, 2006, **18**, 801; (e) X. Sun, J. Liu and Y. Li, *Chem. Eur. J.*, 2006, **12**, 2039; (f) K. J. C. van Bommel, J. H. Jung and S. Shinkai, *Adv. Mater.*, 2001, **13**, 1472; (g) A. Cabanas, E. Encisco, M. C. Carbajo, M. J. Torralvo, C. Pando and J. A. R. Renuncio, *Chem. Mater.*, 2005, **17**, 6137.
- (a) N. Ren, B. Wang, Y. Yang, Y. Zhang, W. Yang, Y. Yue, Z. Gao and Y. Tang, *Chem. Mater.*, 2005, **17**, 2582; (b) G. Liu and G. J. Hong, *Solid State Chem.*, 2005, **178**, 1647; (c) D. K. Yi, S. S. Lee, G. C. Papaefthymiou and J. K. Ying, *Chem. Mater.*, 2006, **18**, 614; (d) F. J. Suarez, M. Sevilla, S. Alvarez, T. Valdes-Solis and A. B. Fuertes, *Chem. Mater.*, 2007, **19**, 3096; (e) P. M. Arnal, C. Weidenthaler and F. Schüth, *Chem. Mater.*, 2006, **18**, 2733.
- (a) F. Teng, Z. Tian, G. Xiong and Z. Xu, *Catal. Today*, 2004, **93–95**, 65; (b) M. Darbandi, R. Thomann and T. Nann, *Chem. Mater.*, 2007, **19**, 1700.
- J. Chen, J. Wang, R. Liu, L. Shao and L. Wen, *Inorg. Chem. Commun.*, 2004, 7447.
- (a) P. J. Bruinsma, A. Y. Kim, J. Liu and S. Baskaran, *Chem. Mater.*, 1997, **9**, 2507; (b) W. Li, X. Sha, W. Dong and Z. Wang, *Chem. Commun.*, 2002, 2434; (c) Q. Sun, P. J. Kooyman, J. G. Grossmann, P. H. H. Bomans, P. M. Frederik, P. C. M. M. Magusin, T. P. M. Beelen, R. A. van Santen and N. A. J. M. Sommerdijk, *Adv. Mater.*, 2003, **15**, 1097; (d) M. Fujiwara, K. Shiokawa, Y. Tanaka and Y. Nakahara, *Chem. Mater.*, 2004, **16**, 5420; (e) S. M. Yang, S. H. Hong, J. H. Moon, J. M. Lim and S. H. Kim, *Langmuir*, 2005, **21**, 10416; (f) J. Wang, Q. Xiao, H. Zhou, P. Sun, Z. Yuan, B. Li, D. Ding, A. Shi and T. Chen, *Adv. Mater.*, 2006, **18**, 3284; (g) M. Fujiwara, K. Shiokawa, I. Sakakura and Y. Nakahara, *Nano Lett.*, 2006, **6**, 2925; (h) H. Zhang, J. Wu, L. Zhou, D. Zhang and L. Qi, *Langmuir*, 2007, **23**, 1107.

- 11 (a) W. Ostwald, *Z. Phys. Chem.*, 1897, **22**, 289; (b) W. Ostwald, *Z. Phys. Chem.*, 1900, **34**, 495.
- 12 A. D. Smigelskas and E. O. Kirkendall, *Trans. Am. Inst. Min., Metall. Pet. Eng.*, 1947, **171**, 130.
- 13 (a) Y. Yin, R. M. Rioux, C. K. Erdonmez, S. Hughes, G. A. Somorjai and A. P. Alivisatos, *Science*, 2004, **304**, 711; (b) Y. Wang, L. Cai and Y. Xia, *Adv. Mater.*, 2005, **17**, 473; (c) Y. Yin, C. Erdonmez, S. Aloni and A. P. Alivisatos, *J. Am. Chem. Soc.*, 2006, **128**, 12671; (d) Y. Yin, C. K. Erdonmez, A. Cobot, S. Hughes and A. P. Alivisatos, *Adv. Funct. Mater.*, 2006, **16**, 1389; (e) A. H. Latham, M. J. Wilson, P. Schiffer and M. E. Williams, *J. Am. Chem. Soc.*, 2006, **128**, 12632; (f) J. Gao, G. Liang, B. Zhang, Y. Kuang, X. Zhang and B. Xu, *J. Am. Chem. Soc.*, 2007, **129**, 1428; (g) A. E. Henkes, Y. Vasquez and R. E. Schaak, *J. Am. Chem. Soc.*, 2007, **129**, 1896.
- 14 (a) Y. Chang, J. J. Teo and H. C. Zeng, *Langmuir*, 2005, **21**, 1074; (b) B. Liu and H. C. Zeng, *Small*, 2005, **1**, 566; (c) J. Yu, H. Guo, S. A. Davis and S. Mann, *Adv. Funct. Mater.*, 2006, **16**, 2035; (d) Y. Zheng, Y. Cheng, Y. Wang, L. Zhou, F. Bao and C. Jia, *J. Phys. Chem. B*, 2006, **110**, 8284; (e) B. Li, Y. Xie, M. Jing, G. Rong, Y. Tang and G. Zhang, *Langmuir*, 2006, **22**, 9380; (f) H. C. Zeng, *J. Mater. Chem.*, 2006, **16**, 649; (g) K. K. Yao and H. C. Zeng, *J. Phys. Chem. B*, 2006, **110**, 14736; (h) W. Wang, Y. Zhu and L. Yang, *Adv. Funct. Mater.*, 2007, **17**, 59.
- 15 (a) K. I. Draget, G. Skjak-Braek and O. Smidsrod, *Int. J. Biol. Macromol.*, 1997, **21**, 47; (b) W. R. Gombotz and S. F. Wee, *Adv. Drug Delivery Rev.*, 1998, **31**, 267; (c) G. Lambert, E. Fattal and P. Couvreur, *Adv. Drug. Delivery Rev.*, 2001, **47**, 99; (d) G. Orive, S. Ponce, R. M. Hernandez, A. R. Gascon, M. Igartua and J. L. Pedraz, *Biomaterials*, 2002, **23**, 3825.
- 16 (a) H. P. van Dokkum, J. H. J. Hulskotte, K. J. M. Kramer and J. Wilmot, *Environ. Sci. Technol.*, 2004, **38**, 515; (b) T. Coradin and J. Livage, *Acc. Chem. Res.*, 2007, **40**, 819; (c) N. Nassif, O. Bouvet, M. N. Rager, C. Roux, T. Coradin and J. Livage, *Nat. Mater.*, 2002, **1**, 42; (d) I. Roy, T. Y. Ohulchansky, D. J. Bharali, H. E. Pudavar, R. A. Misretta, N. Kaur and P. N. Prasad, *Proc. Natl Acad. Sci. U. S. A.*, 2005, **102**, 279.
- 17 (a) Y. Lu, H. Fan, A. Stump, T. L. Ward, T. Rieker and C. J. Brinker, *Nature*, 1999, **398**, 223; (b) J. P. Hecht and C. J. King, *Ind. Eng. Chem. Res.*, 2000, **39**, 1756; (c) S. Lyonard, J. R. Bartlett, E. Sizgek, K. S. Finnie, Th. Zemb and J. L. Woolfrey, *Langmuir*, 2002, **18**, 10386; (d) C. Palencia, J. Nava, E. Herman, G. C. Rodriguez-Jimenes and M. A. Garcia-Alvarado, *Drying Technol.*, 2002, **20**, 569; (e) J. Elvesson, A. Millqvist-Fureby, G. Alderborn and U. Elorsson, *J. Pharm. Sci.*, 2003, **92**, 900; (f) A. S. Mujumdar, *Handbook of industrial drying*, CRC Press, 3rd edn., 2006, p. 215; (g) D. Sen, O. Spalla, L. Belloni, T. Charpentier and A. Thill, *Langmuir*, 2006, **22**, 3798; (h) K. Hadinoto, P. Phanapavudhikul, Z. Kewu and R. B. Tan, *Ind. Eng. Chem. Res.*, 2006, **45**, 3697.
- 18 (a) M. Boissière, P. J. Meadows, R. Brayner, C. Hélyary, J. Livage and T. Coradin, *J. Mater. Chem.*, 2006, **16**, 1178; (b) M. Boissière, J. Allouche, C. Chanéac, R. Brayner, J.-M. Devoisselle, J. Livage and T. Coradin, *Int. J. Pharm.*, 2007, **344**, 128.
- 19 (a) A. S. Barnard and L. A. Curtiss, *Nano Lett.*, 2005, **5**, 1261; (b) C. O. Rangel-Yagui, A. Pessoa Jr and L. C. Tavares, *Pharm. Pharmaceut. Sci.*, 2005, **8**, 147; (c) A. Kara and T. S. Rahman, *Surf. Sci. Rep.*, 2005, **56**, 159; (d) C. Artelt, H.-J. Schmid and W. Peukert, *Chem. Eng. Sci.*, 2006, **61**, 18.
- 20 W. Stober, A. Fink and E. Bohn, *J. Colloid Interface Sci.*, 1968, **26**, 62.
- 21 (a) F. Kim, S. Connor, H. Song, T. Kuykendall and P. Yang, *Angew. Chem., Int. Ed.*, 2004, **43**, 3673; (b) X.-S. Fang, C.-H. Ye, L.-D. Zhang, Y.-H. Wang and Y.-C. Wu, *Adv. Funct. Mater.*, 2005, **15**, 63; (c) J. T. McCann, D. Li and Y. Xia, *J. Mater. Chem.*, 2005, **15**, 735.
- 22 (a) B. Mayers and Y. Xia, *J. Mater. Chem.*, 2002, **12**, 1875; (b) U. Jeong, P. H. Camargo, Y. H. Lee and Y. Xia, *J. Mater. Chem.*, 2006, **16**, 3893; (c) X. S. Fang and L. D. Zhang, *J. Mater. Sci. Technol.*, 2006, **22**, 1; (d) M. N. Nadagouda and R. S. Varma, *Green Chem.*, 2006, **8**, 516.

Crystalline-to-amorphous transformation of cellulose in hot and compressed water and its implications for hydrothermal conversion†

Shigeru Deguchi,*^a Kaoru Tsujii^b and Koki Horikoshi^a

Received 5th September 2007, Accepted 28th November 2007

First published as an Advance Article on the web 14th December 2007

DOI: 10.1039/b713655b

The behaviour of cellulose was studied in water at high temperatures and high pressures by *in situ* high-resolution optical microscopy. It was found that crystalline cellulose underwent transformation to an amorphous state in hot and compressed water, which was followed by complete dissolution. The finding shows that the chemical stability of cellulose in hot and compressed water is determined by the unique properties of cellulose that arise from extensive networks of hydrogen bonds among the cellulose chains in the crystal. The implications of the observation for hydrothermal conversion of cellulose are discussed.

Introduction

Interest in glucose production from biomass has never been higher due to the escalating demand for bioethanol as an alternative fuel.^{1,2} In the production of bioethanol, glucose is first obtained from chemical or enzymatic hydrolysis of polysaccharides, after which it is fermented to produce ethanol. Starch is the major source of glucose at present,^{1,2} but the glucose production from cellulose, which is the most abundant biomass and 1.5×10^{12} tons are produced annually,³ is indispensable for large-scale use of bioethanol.¹

Starch is a polysaccharide made of glucose connected mainly *via* α -1-4 glycosidic linkages. It is semi-crystalline at room temperature, but undergoes crystalline-to-amorphous transformation when heated in water to 60–70 °C (known as gelatinisation),⁴ which accounts for the various changes of starchy foods when they are cooked. The starch chains become swollen upon gelatinisation and can be attacked readily by hydrolytic enzymes, resulting in better digestibility of cooked starchy foods. Gelatinisation is an indispensable step for processing starch in the food industry, and is also the preliminary process necessary to render starch suitable for enzyme-catalyzed biomass conversion.⁵

Cellulose is also a polysaccharide made of glucose, but the glucose units are connected *via* β -1-4 glycosidic linkages. The difference in connectivity results in a profound difference in properties of the polysaccharides, and cellulose shows various unique characteristics such as resistance to chemical or enzymatic hydrolysis, insolubility in common solvents

including water, and structural rigidity. These characteristics arise from extensive hydrogen bonding networks that are formed between the cellulose chains in the crystals.⁶ However, unlike starch, the crystalline structure of cellulose is so robust that it cannot be broken up no matter how long it is cooked in boiling water, and this is the major reason that hampers efficient conversion of cellulosic biomass.

Interestingly, some sorts of change of the crystalline structure had been suggested when cellulose was treated in water at significantly higher temperatures under pressures. Transformation of a crystalline structure was first reported after annealing crystalline cellulose by saturated steam above 260 °C for 30 min.^{7,8} More recently, very high hydrolysis rate was achieved by processing cellulose in water near and above its critical point ($T_c = 374$ °C, $P_c = 22.1$ MPa).^{9–14} In supercritical water, conversion of cellulose was extremely rapid, achieving 99.0% conversion within 0.01 s even without using any catalysts,¹² and the process attracted considerable interest as an environmentally benign process for cellulose conversion.⁹ A change in crystalline structure was considered responsible for the anomalous reaction behaviour.^{12,14} However, behaviour of crystalline cellulose in hot and compressed water remains unclear because of experimental difficulties associated with studying cellulose under such extreme conditions.

We developed an optical microscope equipped with a high-temperature and high-pressure sample chamber,^{15,16} and studied the chemical stability of polystyrene and silica,¹⁷ and the Brownian motion of colloids,¹⁶ all in water at high temperatures and high pressures up to a supercritical state. By performing *in situ* polarized microscopic observation, the first direct experimental evidence was obtained showing that crystalline cellulose underwent transformation into an amorphous form when heated in water at 320 °C and 25 MPa.¹⁸ This paper reports a detailed study on the behaviour of cellulose in water at high temperatures and pressures, which is carried out by using *in situ* high-resolution optical microscopy. The results are discussed with respect to the hydrolysis behaviour of cellulose in hot and compressed water.

^aExtremobiosphere Research Center, Japan Agency for Marine–Earth Science and Technology (JAMSTEC), 2-15 Natsushima-cho, Yokosuka, 237-0061, Japan. E-mail: shigeru.deguchi@jamstec.go.jp; Fax: +81 46-867-9715; Tel: +81 46-867-9679

^bNanotechnology Research Center, Research Institute for Electronic Science, Hokkaido University, N21, W10, Kita-ku, Sapporo, 001-0021, Japan

† Electronic supplementary information (ESI) available: Movies showing behaviour of starch and crystalline cellulose (SF) in water at high temperatures and high pressures. See DOI: 10.1039/b713655b

Results

Observation of cellulose in hot and compressed water

Fig. 1 shows a series of optical microscopic images of cellulose in water at high temperatures and high pressures, which were taken while heating the sample at $15\text{ }^{\circ}\text{C min}^{-1}$. Crystalline cellulose (CF) remained unchanged up to $310\text{ }^{\circ}\text{C}$ (Fig. 1A), above which the fibres became transparent gradually with temperature (Fig. 1B and C). Twisting and bending of the fibres were also observed. CF eventually dissolved in water at around $340\text{ }^{\circ}\text{C}$ (Fig. 1D). No precipitate appeared when the specimen was cooled to room temperature, suggesting that cellulose was hydrolyzed rapidly in hot and compressed water after it was transformed to an amorphous state.^{12,14}

The observation was quantified by a computer-based image analysis, in which the change of relative brightness of the images was measured as a function of temperature (Fig. 1E).¹⁸ The analysis parallels a turbidity measurement. The relative brightness was almost constant up to $310\text{ }^{\circ}\text{C}$, and started to increase gradually with temperature, mainly due to increasing transparency of the cellulose fibres. It then increased sharply

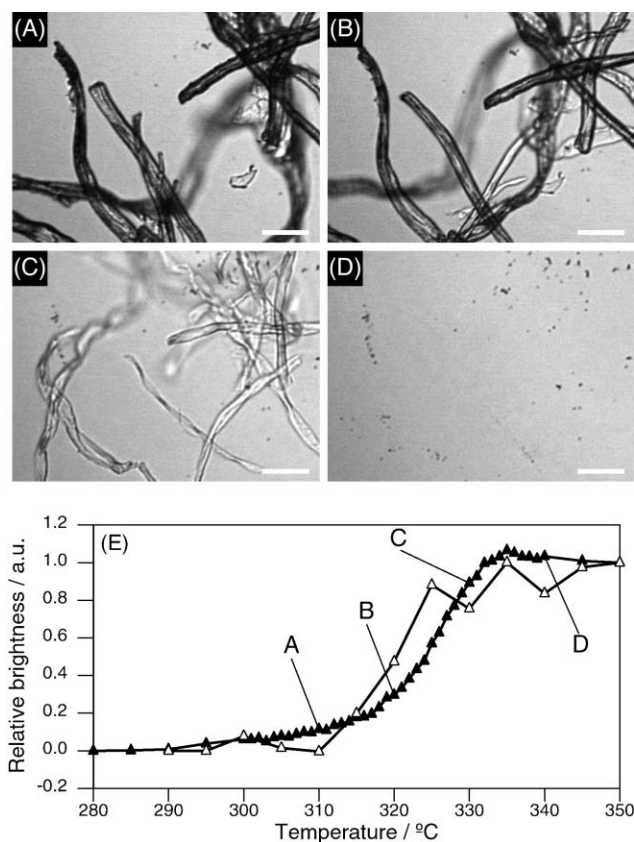


Fig. 1 A series of *in situ* optical microscopic images showing crystalline cellulose (CF) in water at a constant pressure of 25 MPa and different temperatures. (A) $310\text{ }^{\circ}\text{C}$, (B) $320\text{ }^{\circ}\text{C}$, (C) $330\text{ }^{\circ}\text{C}$, and (D) $340\text{ }^{\circ}\text{C}$. Images were taken while heating the specimen at a heating rate of $15\text{ }^{\circ}\text{C min}^{-1}$. Scale bar represents $100\text{ }\mu\text{m}$. The bottom figure shows change of relative brightness of the images (filled triangles). The letters in the figure indicate the corresponding micrographs. Shown together are the results obtained by *in situ* polarized optical microscopy (open triangles), which are taken from ref. 18.

within a narrow temperature range between 320 and $330\text{ }^{\circ}\text{C}$, which was ascribed to both increasing transparency and dissolution of the cellulose fibres. It became constant again above $330\text{--}340\text{ }^{\circ}\text{C}$ due to the complete dissolution.

In the previous study, we used polarized optical microscopy and found that the dissolution was preceded by crystalline-to-amorphous transformation of cellulose.¹⁸ Transformation was evidenced by the loss of birefringence, and the same image analysis procedure was used to quantify the observation.¹⁸ The results obtained by polarized microscopy are shown together in Fig. 1E. The results obtained with or without polarizers agree well. This means that increase of the transparency of crystalline cellulose with temperature between $320\text{--}330\text{ }^{\circ}\text{C}$ corresponds to crystalline-to-amorphous transformation. In other words, constant brightness up to $320\text{ }^{\circ}\text{C}$ demonstrates the crystalline structure of cellulose is retained up to this high temperature.

Comparison with starch

Unsurpassed stability of crystalline cellulose in hot and compressed water was also revealed by comparing the behaviour of cellulose and starch. Fig. 2 shows a sequence of microscopic images showing starch granules when heated in water up to $200\text{ }^{\circ}\text{C}$ at 25 MPa. The starch granules are swollen dramatically between 80 and $90\text{ }^{\circ}\text{C}$, which is one of the characteristic features of a crystalline-to-amorphous transformation of starch.⁴ Upon further heating, the texture of the swollen starch granules became fainter with temperature, and was lost completely at around $200\text{ }^{\circ}\text{C}$. Like cellulose, no precipitate appeared upon cooling the specimen to room temperature, suggesting that the swollen starch chains were hydrolyzed in hot and compressed water at around $200\text{ }^{\circ}\text{C}$.

The observation suggests that the α -1-4-glycosidic linkage, which connects glucose residues to form the starch chain, is too labile in water at such high temperature. It is likely that the β -1-4-glycosidic linkage that makes up the cellulose chain should have similar susceptibility to hydrolysis in hot and compressed water. Thus, the fact that cellulose remains unaffected at significantly higher temperatures is ascribed to

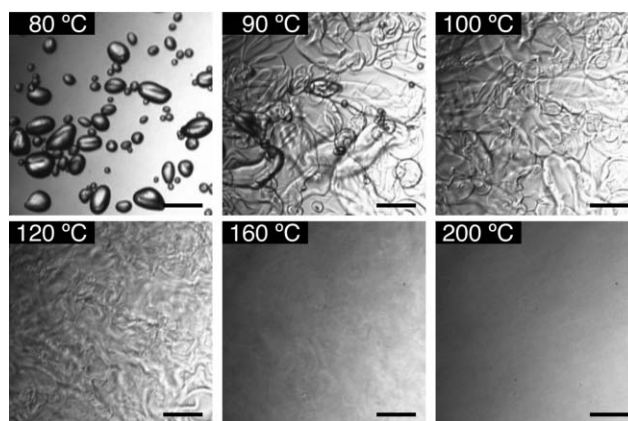


Fig. 2 A series of *in situ* optical microscopic images showing starch granules in water at a constant pressure of 25 MPa and different temperatures. Each bar represents $100\text{ }\mu\text{m}$. A movie showing the process is available as ESI.†

Table 1 Characteristics of cellulose samples

	MW ^a	DP ^b	Crystallinity ^c (%)	Crystalline form ^c	Ref.
CF	3.8×10^4	2.3×10^2	73.4	Cellulose-I	18
SF	3.6×10^4	2.2×10^2	58.2	Cellulose-I	21
SF-II	4.2×10^4	2.6×10^2	44.5	Cellulose-II	21

^a Measured by viscometry in copper ethylenediamine according to TAPPI standard T 230 su-66. ^b Degree of polymerization. ^c Measured by X-ray diffraction.

a protective role of the crystals, in which extensive networks of hydrogen bonds among the cellulose chains are formed.⁶ Upon transformation to an amorphous state, the network is broken up and the cellulose chains become accessible to high-temperature water, leading to rapid hydrolysis.

Observation of cellulose having different structural characteristics

Considering the crucial role of the crystalline structure for the stability of cellulose in hot and compressed water, structural characteristics such as crystallinity should affect the behaviour of cellulose. We compared the behaviour of three cellulose samples of different structural characteristics. The characteristics of the samples are summarized in Table 1. SF shares the same crystalline form (cellulose-I) with CF, but differs in crystallinity. SF-II is a highly porous material consisting of very thin fibres (20–50 nm thick) of crystalline cellulose, while the granules of SF have smooth surfaces (Fig. 3).^{19–21} Consequently, the specific surface area of porous cellulose ($\sim 200 \text{ m}^2 \text{ g}^{-1}$)²⁰ is one or two orders of magnitude larger than that for typical crystalline cellulose ($\sim 1\text{--}10 \text{ m}^2 \text{ g}^{-1}$).²² Thus, comparison of SF-II with the others would help to understand possible surface effects, such as hydrolysis on the surface or diffusion of water molecules into the cellulose crystals, on the behaviour of cellulose in hot and compressed water. The crystalline form of SF-II (cellulose-II) also differs from others

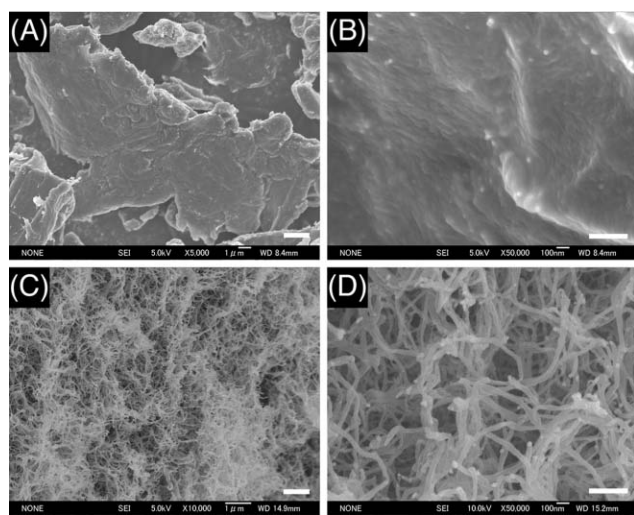


Fig. 3 SEM images comparing morphology of crystalline cellulose (SF) (A and B) and regenerated porous cellulose (SF-II) (C and D). Scale bar, (A) 2 μm , (B) and (D) 300 nm, (C) 1 μm .

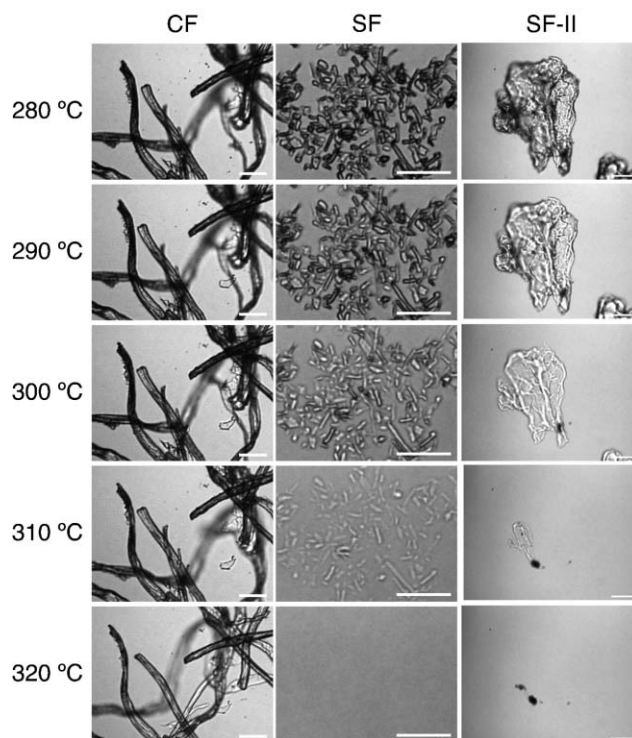


Fig. 4 Effect of crystallinity, crystalline structure, and morphology on the dissolution behaviour of cellulose in water at high temperatures and at a constant pressure of 25 MPa. The top images demonstrate CF, SF, and SF-II in water at a constant pressure of 25 MPa and at different temperatures. Each bar represents 100 μm . Images for SF-II are taken from ref. 21.

(cellulose-I). As cellulose-II is thermodynamically more stable than cellulose-I,³ the difference may have an impact on the crystalline-to-amorphous transformation of cellulose.

Both SF and SF-II showed similar behaviour to CF in hot and compressed water (Fig. 4). Above certain temperatures, SF and SF-II became transparent with temperature, and eventually dissolved completely, indicating that these samples also underwent crystalline-to-amorphous transformation in hot and compressed water and were hydrolyzed. However, compared with CF, the complete dissolution was observed at lower temperatures (Fig. 5). Complete dissolution of SF was observed at around 320 $^{\circ}\text{C}$, a temperature which was approximately 20 $^{\circ}\text{C}$ lower than the temperature at which the complete dissolution of CF was observed (Fig. 1). The result indicates that the crystallinity is an important factor that determines crystalline-to-amorphous transformation of cellulose in hot and compressed water.

It was rather unexpected that the nanofibrous form of cellulose (SF-II) exhibited stability comparable to the others (SF and CF), despite the huge difference in the specific surface area. The observation clearly shows that the surface effect does not affect the behaviour of cellulose in hot and compressed water, and corroborate the previous conclusion that the crystalline structure of cellulose is essential in the stability in hot and compressed water. The difference in the crystalline form between SF-II and others may also contribute to the stability of the nanofibres.

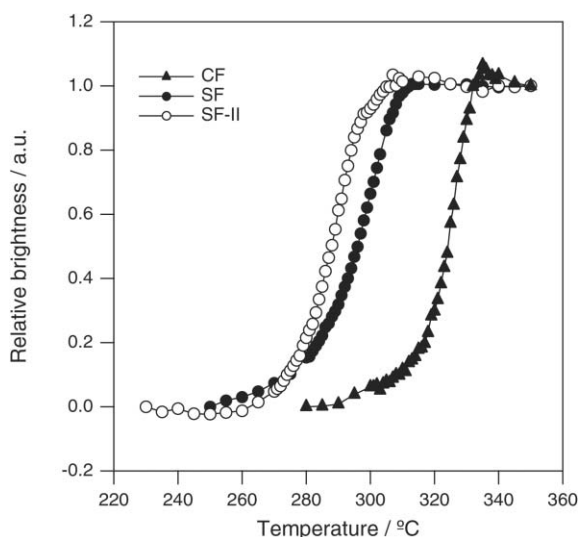


Fig. 5 Effect of crystallinity, crystalline structure, and morphology on temperature dependent change of relative brightness.

It is interesting to note that the fine crystals of SF moved around on the surface of the lower optical window of the cell due to convective flow (ESI†). Random reorientation of the crystals due to thermal fluctuations was also evident. However, the movements ceased completely at around 260–270 °C, which was followed by a crystalline-to-amorphous transformation. The observation suggests that the transformation is preceded by a change of surface properties of cellulose crystals, which makes the crystals stick on the diamond surface.

Discussion

Hydrolysis of cellulose in hot and compressed water

In the first study on the transformation of cellulose crystals after annealing by saturated steam, the transformation was observed only when the temperature of the steam was above 260 °C.⁷ In another study in which crystalline cellulose was hydrolyzed in a batch reactor, it was reported that cellulose was decomposed quickly between 240 and 270 °C, but not at lower temperatures.²³ However, the significance of such temperature dependence was not realized at all.

This study provides the first experimental clue to explain such temperature dependent change of the reaction behaviour of cellulose. It is now clear that cellulose is transformed from a crystalline state to an amorphous state under such conditions, and this is the underlying process that is responsible for anomalous temperature dependent changes of properties.

Crystalline-to-amorphous transformation of starch has been studied extensively, and it is well known that dramatic swelling of starch granules, as is seen in Fig. 2, follows the transformation.⁴ Similar swelling was also observed for cellulose when its dissolution process in iron–sodium tartrate (FeTNa) and LiCl/dimethylacetamide was studied by phase contrast optical microscopy.²⁴ However, such swelling was not observed at all in this work. The lack of swelling could be ascribed to rapid hydrolysis of amorphous cellulose formed after the transformation, because decomposition of cellulose is

very rapid in water at 320 °C and 25 MPa (99.3% conversion in 9.9 s).¹²

The same authors also showed that cellulose oligomers were indeed produced and solubilised in hot and compressed water during hydrolysis of cellulose. When cellulose was heated in water at 320 °C and 25 MPa for 1.6 or 2.5 s, cellulose precipitated in the solution that was clear and transparent just after the reaction.¹² However, no such precipitation was observed at longer heating times (above 3.8 s). The results indicate that such cellulose oligomers are hydrolyzed promptly in hot and compressed water. In our observation, cellulose was kept at temperatures above 300 °C for significantly longer time (no less than 10 min). Thus, no precipitate appeared when the specimen was cooled to room temperature.

Cellulose conversion in subcritical and supercritical water

The hydrolysis behaviour of cellulose was studied extensively in water at even higher temperatures and higher pressures up to a supercritical state.^{9–14} Detailed kinetic analysis revealed an abrupt increase of the hydrolysis rate in subcritical water, and break-up of the crystalline structure was inferred to be responsible for the increase.^{12,14} However, the change of the crystalline structure was expected at 350 °C¹² or 370 °C,¹⁴ the temperature of which was significantly higher than the temperatures where crystalline-to-amorphous transformation was observed in this study. Such discrepancy was also reported when hydrolysis of cellulose was performed in a diamond anvil cell (DAC) while observing the reaction mixture.¹²

The apparent discrepancy could be ascribed to dissolution kinetics. The end products of hydrolysis of cellulose in subcritical and supercritical water are not glucose and water soluble oligomers alone, but various decomposition products are also obtained.¹² Indeed, after hydrolysis of cellulose in water at 320 °C and 25 MPa for 9.9 s, more than half of cellulose was converted to organic acids.¹² Thus, in order to suppress overdecomposition and maximize the glucose yield, the hydrolysis experiments were done by using a very short reaction time, typically less than a second.¹³ It seems highly unlikely that crystalline-to-amorphous transformation of cellulose is completed within such a short period of time. To complete the transformation under such conditions, and thus accelerate the hydrolysis, a significantly higher temperature has to be employed for the reaction. The influence of the structural characteristics on the reaction behaviour is not evident either under such conditions.¹¹

Thermal properties of cellulose

Crystalline-to-amorphous transformation is not simple thermal melting of cellulose crystals, but water plays an important role because no such transformation is observed in ethanol.¹⁸ However, at temperatures where the transformation is observed, high thermal energy prevents clustering of the water molecules, leading to properties that are remarkably different from those of ambient water.²⁵ For example, the dielectric constant, which is 78 at 25 °C and 0.1 MPa, decreases to 21 at 300 °C and 25 MPa. The value is comparable to that of 1-propanol, and it seems unlikely that such nonpolar water interacts favourably with cellulose.

On the other hand, changes in solid properties of crystalline cellulose are known at temperatures above 200 °C. For example, a glass transition temperature (T_g) of cellulose is estimated to be 250 °C.²⁶ The drastic change in the hydrogen-bond structure of crystalline cellulose was reported recently at around 220 °C.²⁷ Considering the similarity between these changes and crystalline-to-amorphous transformation in terms of the temperature range, it seems safe to conclude that transformation of crystalline cellulose to an amorphous state in hot and compressed water should be a consequence of synergetic effect between the unique properties of hot and compressed water and thermal properties of crystalline cellulose.

Native cellulose-I consists of two allomorphs, triclinic cellulose-I α and monoclinic cellulose-I β , and the proportion of I α /I β depends very much on the source. Celluloses from primitive organisms such as bacterial cellulose are cellulose-I α dominant, while celluloses from the higher plants are rich in cellulose-I β .²⁸ It was recently reported that cellulose-I α is more unstable than cellulose-I β at high temperatures.²⁹ This suggests that thermal properties of cellulose depend on its native source. The native source also affects the crystallite widths.²⁸ Crystallites of cotton cellulose (5.0–7.0 nm) are larger than those of wood cellulose (3.5–4.0 nm). These source dependent structural differences might also have affected the difference in the stability between CF (derived from cotton) and SF (derived from wood) in hot and compressed water.

Conclusion

In situ optical microscopy revealed that crystalline cellulose underwent transformation to an amorphous state in hot and compressed water, and the transformation was affected by the structural characteristics. The surface effect was found negligible. The finding suggests that studying the behaviour of cellulose is essential in understanding hydrothermal conversion of cellulose, and has immediate implications for designing the hydrothermal treatment of cellulose, in which an efficient conversion is hampered by the robust crystalline structure.³⁰

The benefits of visual information are often overlooked in chemistry, but our results demonstrate clearly that optical microscopy is a powerful tool for investigating a system of which little is known.^{16,31} It is also clear that the observations have to be supplemented by other analytical techniques. In this case, differential scanning calorimetry (DSC), differential thermal analysis (DTA), or X-ray diffraction (XRD) would certainly allow a quantitative and thus much more rigorous assessment of crystalline-to-amorphous transformation of cellulose. The present study would be of help in preparing such experiments.

Experimental

Materials

Celluloses used in this work were CF1 fibrous cellulose powder (derived from cotton, Whatman, Brentford, UK) and Funacel SF for thin-layer chromatography (derived from wood, Funakoshi, Tokyo, Japan). Regenerated porous crystalline

cellulose¹⁹ was prepared by using SF. The preparation and physicochemical characteristics of the porous crystalline cellulose are described elsewhere.²¹ The three different cellulose samples are denoted as CF, SF and SF-II, respectively. Potato starch was purchased from Wako Pure Chemical Industries, Ltd. (Osaka, Japan).

In situ high-resolution optical microscopy

Observation was made on an optical microscope equipped with a high-temperature and high-pressure cell.¹⁵ The small cell can be set up on a conventional inverted optical microscope, and the system allows *in situ* microscopic observation of specimens in water at temperatures and pressures up to 400 °C and 35 MPa with an optical resolution of 2 μm .¹⁵

Polysaccharides were dispersed in pure water, and introduced into the cell. The specimen in the cell was pressurized to 25 MPa at room temperature, and heated to 400 °C while keeping the pressure constant at 25 MPa. A typical temperature profile during heating is shown in Fig. 6. The instrument is able to heat the sample to 350 °C within 25 min. At temperatures above 50 °C, the heating rate was nearly constant at around 15 °C min^{-1} . Imaging was done by using a colour chilled CCD camera (C5810, Hamamatsu Photonics K. K., Hamamatsu, Japan) onto a VCR (GV-D300, SONY, Tokyo, Japan) while heating the specimen. The VCR is interfaced to a personal computer, and the recorded images can be transferred digitally via IEEE 1394a to the computer for image analysis or video editing.

Due to the flow type design of the cell, it is not possible to recover the specimen after observation, and end products of the specimen after observation were not analyzed in this study.

Image analysis

The observation was quantified by calculating the brightness of the images.¹⁸ The analysis parallels turbidity measurements. The values were normalized so that the brightness at the lowest

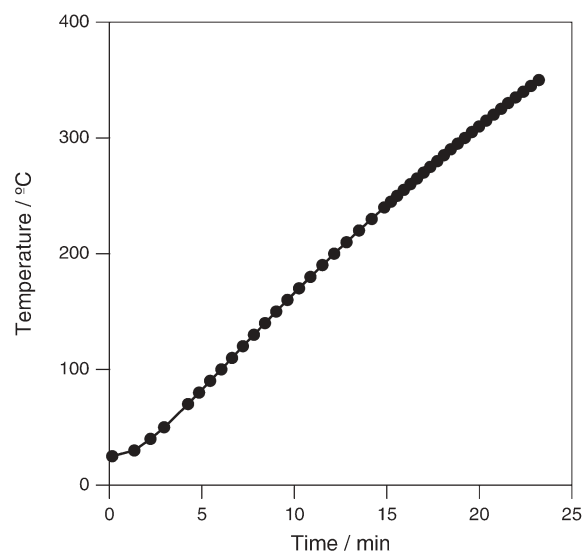


Fig. 6 Typical temperature profile during observation.

measurement temperature became 0 and the brightness at the highest measurement temperature became 1. The image analysis was performed using ImageJ.³²

Scanning electron microscopy

The morphology of SF and SF-II was examined by scanning electron microscopy (SEM). The lyophilized samples were coated with osmium,³³ and examined on a JSM-6700F (JEOL, Tokyo, Japan).

Acknowledgements

We thank Katsuyuki Uematsu, JAMSTEC, for technical assistance in the SEM observation, and Sada-atsu Mukai, Kyushu University, for comments on the manuscript. Financial support from the Ministry of Education, Culture, Sports, Science and Technology (Grant-in-Aid for Young Scientists (B) No. 15750109) is acknowledged.

References

- 1 A. E. Farrell, R. J. Plevin, B. T. Turner, A. D. Jones, M. O'Hare and D. M. Kammen, *Science*, 2006, **311**, 506–508.
- 2 J. Hill, E. Nelson, D. Tilman, S. Polasky and D. Tiffany, *Proc. Natl. Acad. Sci. USA*, 2006, **103**, 11206–11210.
- 3 D. Klemm, B. Heublein, H.-P. Fink and A. Bohn, *Angew. Chem., Int. Ed.*, 2005, **44**, 3558–3393.
- 4 W. A. Atwell, L. F. Hood, D. R. Lineback, E. Varriano-Marston and H. F. Zobel, *Cereal Foods World*, 1988, **33**, 306–311.
- 5 R. Bigelis, in *Enzymes in Food Processing*, ed. T. Nagodawithana and G. Reed, Academic Press, San Diego, 3rd edn, 1993, pp. 123–125.
- 6 P. Langan, Y. Nishiyama and H. Chanzy, *Biomacromolecules*, 2001, **2**, 410–416; Y. Nishiyama, P. Langan and H. Chanzy, *J. Am. Chem. Soc.*, 2002, **124**, 9074–9082; Y. Nishiyama, J. Sugiyama, H. Chanzy and P. Langan, *J. Am. Chem. Soc.*, 2003, **125**, 14300–14306.
- 7 F. Horii, H. Yamamoto, R. Kitamaru, M. Tanahashi and T. Higuchi, *Macromolecules*, 1987, **20**, 2946–2949.
- 8 H. Yamamoto, F. Horii and H. Odani, *Macromolecules*, 1989, **22**, 4130–4132.
- 9 T. Adschiri, S. Hirose, R. Malaluan and K. Arai, *J. Chem. Eng. Jpn.*, 1993, **26**, 676–680.
- 10 M. Sasaki, B. Kabyemela, R. Malaluan, S. Hirose, N. Takeda, T. Adschiri and K. Arai, *J. Supercrit. Fluids*, 1998, **13**, 261–268.
- 11 S. Saka and T. Ueno, *Cellulose*, 1999, **6**, 177–191.
- 12 M. Sasaki, Z. Fang, Y. Fukushima, T. Adschiri and K. Arai, *Ind. Eng. Chem. Res.*, 2000, **39**, 2883–2890.
- 13 K. Ehara and S. Saka, *Cellulose*, 2002, **9**, 301–311.
- 14 M. Sasaki, T. Adschiri and K. Arai, *AIChE J.*, 2004, **50**, 192–202.
- 15 S. Deguchi and K. Tsujii, *Rev. Sci. Instrum.*, 2002, **73**, 3938–3941.
- 16 S. Mukai, S. Deguchi and K. Tsujii, *Colloids Surf., A*, 2006, **282–283**, 483–488.
- 17 S. Deguchi, S. K. Ghosh, R. G. Alargova and K. Tsujii, *J. Phys. Chem. B*, 2006, **110**, 18358–18362.
- 18 S. Deguchi, K. Tsujii and K. Horikoshi, *Chem. Commun.*, 2006, 3293–3295.
- 19 S. Kuga, *J. Colloid Interface Sci.*, 1980, **77**, 413–417.
- 20 H. Jin, Y. Nishiyama, M. Wada and S. Kuga, *Colloids Surf., A*, 2004, **240**, 63–67.
- 21 S. Deguchi, M. Tsudome, Y. Shen, S. Konishi, K. Tsujii, S. Ito and K. Horikoshi, *Soft Matter*, 2007, **3**, 1170–1175.
- 22 S. Ardizzone, F. S. Dioguardi, T. Mussini, P. R. Mussini, S. Rondinini, B. Vercelli and A. Vertova, *Cellulose*, 1999, **6**, 57–69.
- 23 T. Minowa, F. Zhen and T. Ogi, *J. Supercrit. Fluids*, 1998, **13**, 253–259.
- 24 E.-W. Unger, H.-P. Fink and B. Philipp, *Das Papier*, 1995, **49**, 297–307.
- 25 S. Deguchi and K. Tsujii, *Soft Matter*, 2007, **3**, 797–803.
- 26 K. Kamide and M. Saito, *Polym. J.*, 1985, **17**, 919–928; Y. Nishio, S. K. Roy and R. S. J. Manley, *Polymer*, 1987, **28**, 1385–1390.
- 27 A. Watanabe, S. Morita and Y. Ozaki, *Biomacromolecules*, 2006, **7**, 3164–3170.
- 28 A. C. O'sullivan, *Cellulose*, 1997, **4**, 173–207.
- 29 A. Watanabe, S. Morita and Y. Ozaki, *Biomacromolecules*, 2007, **8**, 2969–2975.
- 30 A. Fukuoka and P. L. Dhepe, *Angew. Chem., Int. Ed.*, 2006, **45**, 5161–5163.
- 31 K. Arai and T. Adschiri, *Fluid Phase Equilib.*, 1999, **158–160**, 673–684.
- 32 W. S. Rasband, *ImageJ*, U. S. National Institutes of Health, Bethesda, Maryland, USA, 1997–2007.
- 33 A. Tanaka, *J. Electron Microsc.*, 1994, **43**, 177–182.

A dramatic switch in selectivity in the catalytic dehydrogenation of 4-vinylcyclohexene in high pressure steam; a cautionary lesson for continuous flow reactions

Morgan L. Thomas,^a Joan Fraga-Dubreuil,^{†a} A. Stuart Coote^b and Martyn Poliakoff^{**a}

Received 9th May 2007, Accepted 23rd October 2007

First published as an Advance Article on the web 21st November 2007

DOI: 10.1039/b706711a

We report an investigation of the continuous oxidative dehydrogenation of 4-vinylcyclohexene (VCH) in high pressure steam. Oxidative dehydrogenation reactions such as this are often limited by unselective or total oxidation. We find that these side-reactions not only occur in this case, but can also have a major influence on the selectivity; a small increase in flow rate results in a complete switch in selectivity of the reaction. Our results suggest that styrene (ST) is formed as the initial product but that unless the H₂ is sequestered, ST may then be hydrogenated to yield ethylbenzene (EB).

The observation of periodic temperature spikes near the surface of the catalyst bed indicate cycles of propagating flames occur in a relatively small volume of the reactor, leading to total oxidation of some VCH and removal of O₂, which would otherwise sequester the H₂. These flames give rise to the large variations in the observed product selectivity. We suggest that these observations may not be restricted to this reaction system and reactor configuration, and may occur in other situations where small-scale continuous flow oxidation reactors are used.

1. Introduction

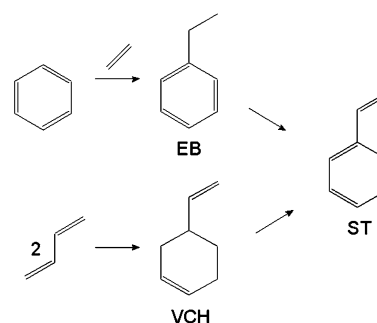
The current interest in near-critical and supercritical fluids as reaction media is leading to an increasing use of continuous flow reactors.¹ Such reactors have safety advantages over sealed autoclaves,² even on a laboratory scale. Furthermore, continuous reactors have a relatively straightforward path for scale up, which at least in principle, should be less expensive than for high pressure batch processes. However, the use of high pressure continuous reactors on the small scale can lead to a whole series of uncertainties, for example, in residence time or reaction temperature, which do not occur in a well-stirred autoclave. These uncertainties are exacerbated in supercritical fluids, where the large pressure and temperature dependence of fluid density and phase equilibria can have major effects.³ Particularly dramatic effects can be observed when fixed catalyst beds are used for highly exothermic reactions in continuous mode; for example, we recently reported how the catalytic dehydrogenation of 4-vinylcyclohexene (VCH) can “light off” in supercritical CO₂ with a temperature rise of only 2 °C (*i.e.* going from zero to nearly 100% conversion of VCH).⁴

In this paper, we report an effect in the oxidative dehydrogenation of VCH in high pressure steam, in which a modest increase in flow rate results in a complete switch in selectivity of the reaction. Our observation has twin

implications for green chemistry. It underlines that considerable care is needed in interpreting the results of experiments in continuous reactors and re-emphasises the role that reactor design can play in determining the observed chemistry.

The oxidative dehydrogenation of VCH is of importance as one step in an alternative route for the manufacture of styrene (ST). Currently, ST is manufactured largely from benzene *via* ethylbenzene (EB), Scheme 1. VCH is involved in a route which starts with the dimerisation of butadiene.^{5–7} This route is potentially attractive because it eliminates the need for an aromatic feedstock.

The selective dehydrogenation of VCH with heterogeneous catalysts has been investigated by several authors. Alimardanov and Abdullayev reported⁵ the formation of ST *via* EB using Cu–Mg–O and zeolite catalysts in the vapour phase, route a–b–c in Scheme 2. However, other reports suggest a mechanism involving direct dehydrogenation *i.e.* the

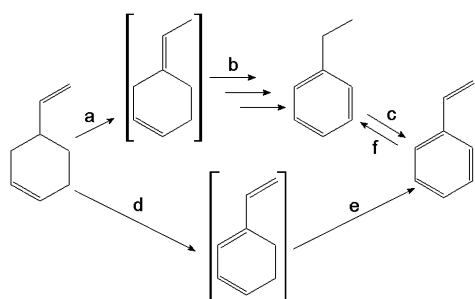


Scheme 1 Current route to styrene (ST) from benzene *via* ethylbenzene (EB) and the proposed route from butadiene *via* 4-vinylcyclohexene (VCH).

^aSchool of Chemistry, University Park, Nottingham, UK NG7 2RD.
E-mail: martyn.poliakoff@nottingham.ac.uk; Fax: +44 (0)115 951 3058;
Tel: +44 (0)115 951 3520

^bINVISTA Performance Technologies, Wilton, Cleveland, UK TS10 4XX

[†] Present address: INVISTA Performance Technologies, Wilton, Cleveland, UK TS10 4XX



Scheme 2 Possible reaction pathways for the dehydrogenation of VCH.

exocyclic double bond is retained, route d–e in Scheme 2. Notably, Neumann *et al.* reported the reaction in the presence of a polyoxometalate,⁶ and Choi *et al.* have studied this transformation using a promoted ZrO₂ catalyst.⁷ In earlier work, Castellan and Tausznik reported dehydrogenation and isomerisation as parallel pathways in their work using Pd catalysts supported on alumina.⁸ To our knowledge, there has been no suggestion that the ST formed in these reactions can be hydrogenated to EB as a further reaction step, *i.e.* step f in Scheme 2. Previous work conducted in our group concerning the dehydrogenation of VCH in supercritical CO₂ investigated the mechanistic pathway of the isomerisation and dehydrogenation (a–b) in the absence of oxygen. ST was not observed in any of these experiments.⁴

Recently, we have been investigating the homogeneously catalysed aerobic oxidation of methyl aromatics in supercritical H₂O (scH₂O) as a route to terephthalic acid and other aromatic acids.^{9–11} This route has potential advantages in terms of energy recovery compared to existing processes, and in replacement of the traditional solvent, acetic acid, and its associated waste and by-products.¹⁰ Thus, the oxidative dehydrogenation of VCH offers an interesting opportunity to extend our scH₂O approach to another organic transformation of industrial relevance, and in particular, to investigate the use of heterogeneous catalysts under these conditions.

2. Results and discussion

All of our reactions were carried out continuously in the reactor shown in Fig. 1. The concentration of VCH, ST and EB in the product stream were analysed quantitatively by GC (see Experimental). Qualitative off-line micro-GC analysis was also performed to identify the gaseous products.

Our first experiments indicated that the reaction was unsuccessful, with negligible dehydrogenation detected, in the

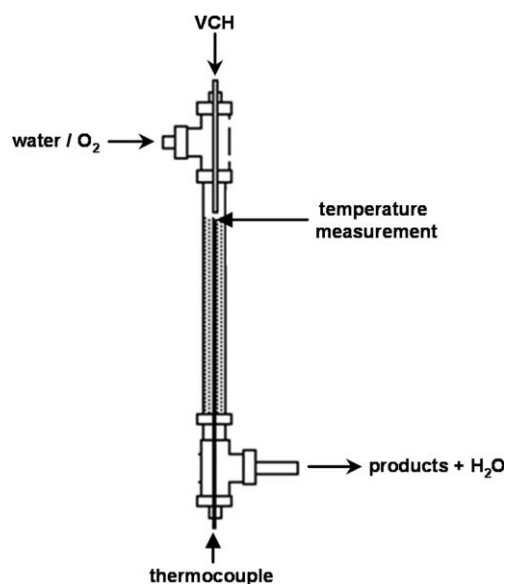


Fig. 1 Schematic view of the fixed bed reactor used in this work; a full diagram of the equipment is given in Fig. 5 in the Experimental section. The position of the thermocouple in the reactor and the point of temperature detection are marked. Details of the exact dimensions of the reactor are provided in the Experimental section.

reactor system under scH₂O conditions ($T_c = 374$ °C, $p_c = 221$ bar, $\rho_c = 0.32$ g cm⁻³). However, significant catalytic activity was observed when the reaction was performed in the vapour phase at 90 bar, Table 1.

Although there was no clear trend in the conversion of VCH, the selectivity for ST was greatest at lower temperatures. This selectivity compares well with other results in the literature.^{7,12} Aside from the main products, ST and EB, we also observed small amounts of toluene and benzene, with yields of *ca.* 1%. These by-products have been reported previously for the reactions of VCH at high temperature.¹³

The conversion of VCH was much greater than the yield of ST and EB, presumably because of the production of carbon oxides as a result of unselective oxidation. CO₂ was detected in the effluent gases using gas chromatography. Such uncontrolled oxidation is undesirable, but is common in many high temperature oxidation processes. In this case, oxidation would be a major barrier to industrial implementation.

By contrast, the reaction showed a remarkable dependence on flow rate, Table 2 and Fig. 2. The ratio of the feeds was kept constant, whilst the total flow rate was increased. There is a complete switch in selectivity with only a modest change in flow rate. At 3 ml min⁻¹ EB is the major product, while at

Table 1 Variation in product selectivity with temperature for the continuous catalytic dehydrogenation of VCH in high pressure steam^a

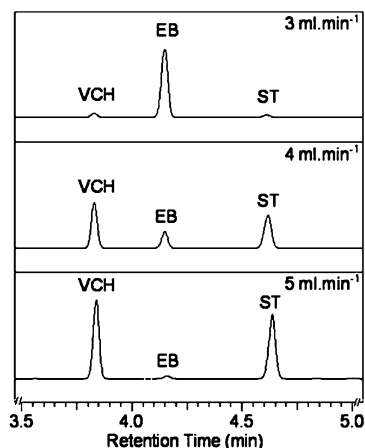
Temperature/°C	VCH conversion (%)	EB yield ^b (%)	ST yield ^b (%)	EB selectivity ^b (%)	ST selectivity ^b (%)
360	67	1	43	3	95
410	73	3	25	11	84
460	51	4	24	12	78

^a Flow rate 6 ml min⁻¹, pressure 90 bar, 2% (vol.) VCH feed, 2.5 mol O₂ : 1.0 mol VCH, catalyst 2.8 g of 1% Pd/Al₂O₃, VCH = 4-vinylcyclohexene, EB = ethylbenzene, ST = styrene. ^b Yields and selectivities based on products observed by gas chromatography, CO_x not included.

Table 2 Variation in product selectivity with flow rate for the continuous catalytic dehydrogenation of VCH in high pressure steam^a

Total flow/ml min ⁻¹	VCH conversion (%)	EB yield ^b (%)	ST yield ^b (%)	EB selectivity ^b (%)	ST selectivity ^b (%)	Unaccounted material ^c (%)
3	93	46	3	86	6	40
4	62	8	33	18	76	18
5	60	2	41	3	93	15

^a Temperature 420 °C, see Table 1 for further notes. ^b See Table 1. ^c Unaccounted material based on difference between conversion and yields of EB, ST, toluene (1–2%) and benzene (1–2%).

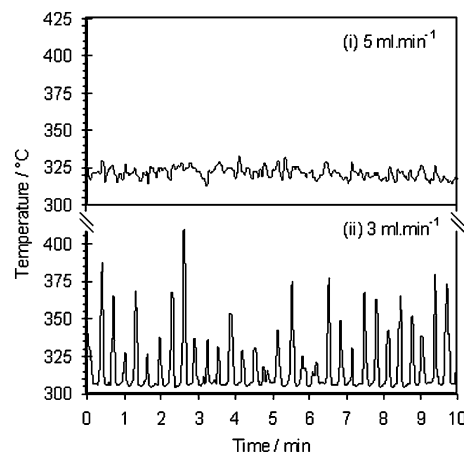
**Fig. 2** Chromatograms showing the complete switch in product selectivity with flow rate, see Table 2 for quantitative details.

5 ml min⁻¹, it is ST. The implication is that EB is formed at longer residence time, suggesting that H₂ present in the reaction mixture can react with ST.

The amount of unaccounted material in these experiments was generally quite high, especially at the lowest flow rates, *ca.* 40%. In the absence of O₂, there was no reaction of the VCH, and close to 100% mass accountability. Similarly the amount of unaccounted material became progressively worse as the proportion of O₂ was increased, Table 3.

A strong clue as to why the selectivity switches so dramatically, was found when a thermocouple was placed in the top layer of the catalyst bed, see Fig. 1. The temperature recorded (305 °C) was more than 100 °C lower than half way down the catalyst bed, 420 °C. At a flow rate of 5 ml min⁻¹, there were small, apparently random fluctuations in the temperature recorded by the thermocouple, Fig. 3(i). However, at 3 ml min⁻¹, there were very strong and regularly spaced temperature excursions up to 100 °C, Fig. 3(ii).

It is important to stress that the temperature oscillations were only noticed when a thermocouple was placed right at the top of the catalyst bed. Monitoring the temperature lower down or at the reactor outlet did not indicate any significant differences between the different flow rates. There were no

**Fig. 3** Temperature recording in upper region of catalyst bed at (i) lower flow rate (3 ml min⁻¹, large variations in temperature) and (ii) higher flow rate (5 ml min⁻¹, small variations in temperature). Data were recorded after 40 min at reaction conditions in both cases.

temperature oscillations in the absence of O₂. It seems reasonable to assume that these temperature excursions are the result of exothermic reactions involving O₂ and VCH, namely unselective oxidation. The period of the oscillations (at 3 ml min⁻¹ total flow, *ca.* 20 s) was not associated with any obvious periodic event originating within the reactor equipment, for example the pump stroke rate.

Similar oscillations in temperature, dependent on space velocity and the ratio of O₂ to substrate, have been reported in the oxidative dehydrogenation of ethane,¹⁴ and periodic blue flames have also been observed in such reactions.¹⁵ Other examples include periodic temperature spiking in the reaction of isobutene with O₂.^{16,17}

Based on these previous reports, we suggest that the temperature oscillations observed in the upper region of our catalyst bed can be attributed to the presence of a series of flames, as shown in Fig. 4. We envisage these flames igniting at the catalyst bed surface, propagating upwards (counter-flow) towards the fuel source (the organic feed pipe), and extinguishing when all of the available oxygen has been consumed. When the O₂ is replenished, ignition can occur again, resulting in the periodic oscillations in temperature that we observe.

Table 3 Effect of increasing the O₂ : organic ratio on the continuous catalytic dehydrogenation of VCH in high pressure steam^a

mol O ₂ : mol VCH	VCH conversion (%)	EB yield ^b (%)	ST yield ^b (%)	EB selectivity ^b (%)	ST selectivity ^b (%)	Unaccounted material ^c (%)
1.25 : 1.00	69	46	10	76	16	12
2.50 : 1.00	93	46	3	86	6	40
3.00 : 1.00	99	27	1	87	3	68

^a Temperature 420 °C, see Table 1 for further notes. ^b See Table 1. ^c See Table 2.

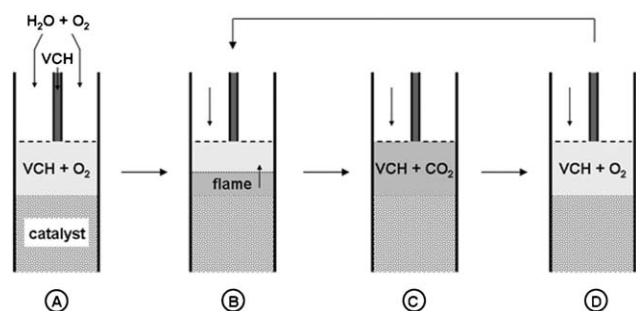


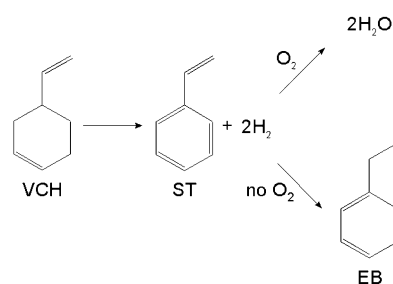
Fig. 4 Steps in the production of periodic flames in our reactor: (A) – the initial state; (B) – the flammable mixture of VCH and oxygen ignites at the surface of the catalyst, with a subsequent counter-flow flame propagation towards the fuel source; (C) – extinction of the flame at the point of mixing of VCH and O_2 ; (D) – the continuing streams of H_2O , O_2 and VCH replenish the supply of fuel and oxidant to restart the ignition cycle.

It seems clear that these temperature oscillations must have a substantial effect on the dehydrogenation of VCH. At a total flow rate of 3 ml min^{-1} , EB is the major product, while ST is formed at the higher flow, 5 ml min^{-1} . We suggest that, at the higher flow rate, the flame cannot propagate in the counter-flow direction at a sufficient rate, and hence, the ignition is suppressed.

The molar ratio of O_2 : VCH in our experiments is considerably lower than the stoichiometric requirement for total oxidation of all of the VCH. With 2.5 moles of O_2 per mole VCH, total oxidation would consume only *ca.* 23 mol% of the VCH, an amount somewhat lower than that of the unaccounted material at lower flow rates, Table 2. The remainder of the lost VCH may be attributable to pyrolysis of VCH and/or the retro-Diels Alder reaction.

Thus, the temperature oscillations suggest that total oxidation occurs at the lower flow rate, where large temperature spikes are observed, and where EB is the major product. The removal of O_2 from the system by total oxidation would prevent the reaction of H_2 and O_2 , so that the H_2 could then react with ST to yield EB, Scheme 3. At the higher flow rate, where ST is observed as the major product, the temperature oscillations are only a few degrees Celsius in magnitude, suggesting that total oxidation does not occur. In that case, O_2 is available as the VCH passes through the catalyst bed and the H_2 produced by the dehydrogenation of VCH can be consumed, with ST being isolated as the final product.

This explanation is supported by the experiments summarised in Table 4, which show (a) that ST reacts with H_2 to form EB over the same catalyst bed as used to dehydrogenate VCH; the dependence of the yield of ST on flow rate is



Scheme 3 Proposed pathways for VCH dehydrogenation in the presence and absence of O_2 .

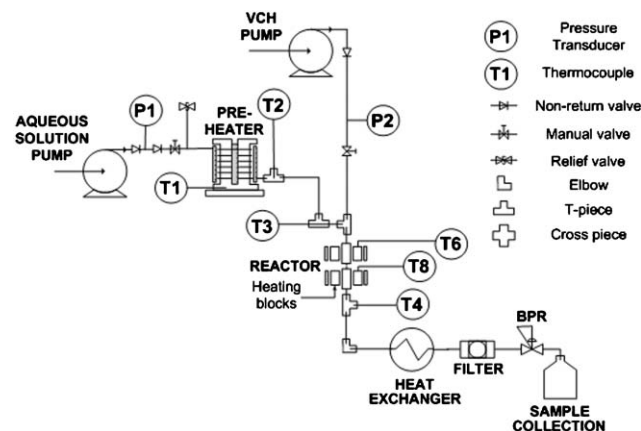


Fig. 5 Schematic diagram of the experimental set-up for the investigation of heterogeneously catalysed oxidative dehydrogenation in high temperature water, primarily comprising HPLC pumps, a preheater and reactor heaters, a heat exchanger (cooler) and a back pressure regulator (BPR).

presumably the effect of residence time and (b) that EB cannot be dehydrogenated in the presence of O_2 over this catalyst to give significant quantities of ST. The unaccounted material in the EB oxidation reactions is in the range 30–35%, and can be attributed to total oxidation.

3. Experimental

We have previously described a typical experimental set-up for small scale continuous flow high temperature water reactions,⁹ a schematic is shown in Fig. 5. The reactor was constructed from a 19 cm length of $\frac{1}{4}$ " o.d. Hastelloy C276 with an inner diameter of 0.180" (0.457 cm). The reactor thermocouple was positioned 5 mm vertically below the exit of the organic substrate feed pipe. The catalyst was retained in the reactor using a 5 micron filter disk. Gilson 306 HPLC pumps were

Table 4 Investigation of the further reactions of EB and ST during the continuous catalytic dehydrogenation of VCH in high pressure steam^a

Reaction	Temperature/ $^{\circ}C$	Total flow/ ml min^{-1}	Product	Product yield (%)
ST + H_2	410	3	EB	53
ST + H_2	410	5	EB	4
EB + O_2	360	5	ST	3
EB + O_2	460	5	ST	5

^a Pressure 90 bar, 2% (vol.) organic feed, 2.5 mol O_2 (or H_2): mol substrate, 2.8 g 1% Pd/ Al_2O_3 /VCH = 4-vinylcyclohexene, EB = ethylbenzene, ST = styrene.

used for all feeds; all flow rates refer to the pumping rates of the appropriate pump at room temperature. The system was brought to reaction temperature using a flow of pure water, and the pressure was maintained with a TESCO back pressure regulator (BPR).

O₂ was generated *in situ* by decomposition of a dilute aqueous solution of 100 vol. H₂O₂ (Fisher) in the preheater, as described previously.^{11,18} For the hydrogenation experiments, an analogous method with a dilute solution of formic acid (Aldrich) was used as reported previously.¹⁹ 1% Pd/Al₂O₃ (Aldrich), 4-vinylcyclohexene (99%, Aldrich), ethylbenzene (99% Lancaster) and styrene (99%, Merck) were used as supplied. De-ionised water was obtained from an Elga PURELAB unit.

Samples were collected periodically over the course of a reaction, and were extracted into ether prior to quantitative analysis with a Perkin–Elmer Autosystem GC, with a flame ionisation detector (FID) and a 30 m Alltech column (non-polar EC-1, 0.32 mm inner diameter, 1.00 µm film). The isomers resulting from isomerisation, dehydrogenation and hydrogenation of VCH have similar boiling points; separation of chromatographic peaks was achieved using an isothermal method (oven temperature held at 100 °C for 5 min). Confirmation of chromatographic data was obtained using ¹H NMR spectroscopy (Bruker DPX300, CDCl₃, 300 MHz). Qualitative gas analysis was performed using a Varian CP-4900 gas chromatograph with a 20 m MolSieve 5A column (O₂, H₂) and a 25 cm HayeSep column (CO₂).

4. Conclusions

Although chemically interesting, this reaction is unlikely to provide a competitive commercial route to styrene. Whilst high selectivities to styrene were observed (95% of liquid products), a large degree of total oxidation to CO₂ was observed. Its significance in the context of green chemistry is as a demonstration of the sensitivity of the outcome of the reaction to a small change in reaction conditions. With greater interest in scaling up supercritical and high pressure reactions, larger numbers of laboratories are using continuous reactors. Our experiments suggest that (a) any reaction carried out on such a reactor should be investigated under a wide range of conditions, (b) complete diagrams of the continuous reactor should be given and (c) care should be taken in extrapolating the results of a particular experiment to other reaction conditions. This work also demonstrates the importance of careful selection of equipment, concentrations and flow rates for continuous reactions.

Acknowledgements

We thank Dr L.M. Dudd, Dr P.A. Hamley, Dr J.R. Hyde and Dr C. Yan, for advice and helpful suggestions. We are grateful to INVISTA Performance Technologies, the Chemistry Innovation Knowledge Transfer Network and the EPSRC for support. We thank Mr M. Guyler, Mr R. Wilson and Mr P.A. Fields for their assistance.

References

- J. R. Hyde, P. Licence, D. Carter and M. Poliakoff, *Appl. Catal., A*, 2001, **222**(1–2), 119–131.
- T. Kletz, *Process Plants: A Handbook for Inherently Safer Design*, Taylor & Francis, Philadelphia, 2001.
- (a) M. A. McHugh and V. J. Krukonic, *Supercritical Fluid Extraction: Principles and Practice*, Butterworths, Boston, 1986; (b) *Chemical Synthesis Using Supercritical Fluids*, ed. P. G. Jessop and W. Leitner, Wiley-VCH, Weinheim, 1999.
- J. R. Hyde, B. Walsh and M. Poliakoff, *Angew. Chem., Int. Ed.*, 2005, **44**, 1–5.
- K. M. Alimardanov and A. F. Abdullayev, *Petrol. Chem.*, 1995, **35**(6), 508–520.
- (a) R. Neumann and I. Dror, *Appl. Catal., A*, 1998, **172**(1), 67–72; (b) M. De bruyn and R. Neumann, *Adv. Synth. Catal.*, 2007, **349**, 1624–1628.
- Y. S. Choi, Y. K. Park, J. S. Chang, S. E. Park and A. K. Cheetham, *Catal. Lett.*, 2000, **69**(1–2), 93–101.
- A. Castellan and G. R. Tauszik, *J. Catal.*, 1977, **50**(1), 172–175.
- P. A. Hamley, T. Ilkenhans, J. M. Webster, E. Garcia-Verdugo, E. Venardou, M. J. Clarke, R. Auerbach, W. B. Thomas, K. Whiston and M. Poliakoff, *Green Chem.*, 2002, **4**(3), 235–238.
- E. Garcia-Verdugo, E. Venardou, W. B. Thomas, K. Whiston, W. Partenheimer, P. A. Hamley and M. Poliakoff, *Adv. Synth. Catal.*, 2004, **346**(2–3), 307–316.
- E. Garcia-Verdugo, J. Fraga-Dubreuil, P. A. Hamley, W. B. Thomas, K. Whiston and M. Poliakoff, *Green Chem.*, 2005, **7**(5), 294–300.
- D. A. Hucul, *US Pat.*, 5336822, 1994.
- E. Gil-Av, J. Shabtai and F. Steckel, *J. Chem. Eng. Data*, 1960, **5**, 98–105.
- V. R. Chaudhary and A. M. Rajput, *J. Chem. Soc., Faraday Trans.*, 1995, **91**(5), 843–846.
- A. L. Y. Tonkovich, J. L. Zilka, D. M. Jimenez, G. L. Roberts and J. L. Cox, *Chem. Eng. Sci.*, 1996, **51**(5), 789–806.
- V. Caprio, A. Insola and P. G. Lignola, *Combust. Flame*, 1981, **43**, 23–33.
- B. R. Johnson and S. K. Scott, *J. Chem. Soc., Faraday Trans.*, 1990, **86**(22), 3701–3705.
- B. D. Phenix, J. L. DiNaro, J. W. Tester, J. B. Howard and K. A. Smith, *Ind. Eng. Chem. Res.*, 2002, **41**, 624.
- E. Garcia-Verdugo, Z. M. Liu, E. Ramirez, J. Garcia-Serna, J. Fraga-Dubreuil, J. R. Hyde, P. A. Hamley and M. Poliakoff, *Green Chem.*, 2006, **8**(4), 359–364.

Electrochemical activation of CO₂ in ionic liquid (BMIMBF₄): synthesis of organic carbonates under mild conditions

Li Zhang, Dongfang Niu, Kai Zhang, Guirong Zhang, Yiwen Luo and Jiaying Lu*

Received 6th August 2007, Accepted 30th October 2007

First published as an Advance Article on the web 22nd November 2007

DOI: 10.1039/b711981j

A new electrochemical procedure for electrosynthesis of organic carbonates from CO₂ and alcohols has been established in CO₂-saturated room temperature ionic liquid BMIMBF₄ solution, followed by addition of an alkylating agent. The synthesis was carried out under mild ($P_{\text{CO}_2} = 1.0$ atm, $T = 55$ °C) and safe conditions. The use of volatile and toxic solvents and catalysts as well as of any additional supporting electrolytes has been avoided. The influence of temperature, cathode material, working potential, alcohol concentration and the charge passed on the reaction using methanol (**1a**) as the model compound was examined. The ionic liquid used for the reaction was recyclable. The obtained results showed that the primary and secondary alcohols were converted in good yields, whereas tertiary alcohol and phenol were unreactive.

Introduction

Dialkyl carbonates are an important class of compounds whose versatility allows their application in several fields of the chemical and pharmaceutical industry.^{1–5} Recently, the utilization of organic carbonates and the methods for their synthesis have been extensively reviewed.⁶ The most important routes to these esters involve the direct and indirect use of phosgene, a very toxic and corrosive reagent.⁷ Other available methods use carbon monoxide, drastic conditions and/or metal catalysts, whose potential environmental impact should not be underestimated.^{8–10}

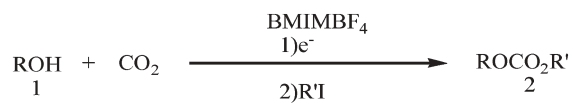
Compared with other methods, the synthesis of organic carbonates starting from CO₂ and alcohols is one of the promising projects in the development of an environmentally benign process based on the utilization of a naturally abundant carbon resource. CO₂ is an attractive C1 building block in organic synthesis because it is abundant, cheap, nontoxic and nonflammable. The direct synthesis of organic carbonates from CO₂ and alcohols has always been performed under high pressure¹¹ or in the presence of catalysts such as organometallic complexes,^{12,13} inorganic bases,¹⁴ modified ZrO₂^{15–17} or electrogenerated base.¹ However, its conversion is very low because of thermodynamic limitations.¹⁸

Room temperature ionic liquid (RTILs) are salts that are liquids at or near room temperature. They exhibit many desirable properties such as negligible volatility, thermal and chemical stability, ability to dissolve a wide range of organic or inorganic compounds.¹⁹ Many reactions have been reported to occur in ionic liquids with good to excellent performance.²⁰ Recently, chemical fixation of CO₂ with epoxides in RTILs to form cyclic carbonates has been described.²¹ In addition, 5-methylene-1,3-oxazolidin-2-ones were isolated *via* reaction

of propargyl alcohols, aliphatic primary amines, and CO₂ in ionic liquids under relatively mild conditions.²²

In addition to the above reported properties, RTILs, which show a high ionic conductivity and a wide electrochemical potential window, have been frequently used as electrolytes for studies related to organic electrosynthesis and to the evaluation of the redox behavior of electroactive substrates,²³ as well as metal deposition, batteries, photovoltaic devices, fuel cells, and solar cells.^{24,25} Concerning electrochemically promoted CO₂ fixation, the synthesis of cyclic carbonates from epoxides in ionic liquids has been reported by Deng *et al.*²⁶ The synthesis of organic carbamates from amines and CO₂ in ionic liquid have been reported by Feroci *et al.*²⁷ In our previous work, we reported the electrocarboxylation of activated olefins with CO₂ in ionic liquid and achieved good results.²⁸

With our continuous research on the fixation of CO₂ in ionic liquid, here, we report an efficient and environmentally benign method for synthesis of organic carbonate from CO₂ and alcohols in a RTIL solution (Scheme 1). The aim of this investigation was to set up an alternative methodology for the synthesis of organic carbonates *via* electrochemical reduction of CO₂. The synthesis was carried out in an ionic liquid, 1-butyl-3-methylimidazolium tetrafluoroborate (BMIMBF₄) by cathodic activation of CO₂, under mild conditions ($P_{\text{CO}_2} = 1.0$ atm, $T = 55$ °C). The use of volatile and toxic solvents and catalysts as well as of any additional supporting electrolytes has been avoided. The influence of temperature, cathode material, working potential, alcohol concentration and the charge passed on the reaction using methanol (**1a**) as the model



R = (a) CH₃, (b) C₂H₅, (c) *n*-C₄H₉, (d) *sec*-C₄H₉, (e) *tert*-C₄H₉, (f) PhCH₂, (g) Ph(CH₂)₂, (h) Ph
R' = (a) CH₃, (b-h) C₂H₅

Scheme 1

Shanghai Key Laboratory of Green Chemistry and Chemical Process, Department of Chemistry, East China Normal University, Shanghai, China 200062. E-mail: jxlu@chem.ecnu.edu.cn; Fax: +86 21 6223 2414; Tel: +86 21 6223 3491

compound was investigated. Results for some representative alcohols have been subjected to the process, to establish the generality and limits of this new procedure.

Results and discussion

Cyclic voltammetry of CO₂ in BMIMBF₄

The reduction of CO₂ in BMIMBF₄ was examined by cyclic voltammetry. Fig. 1 shows cyclic voltammograms (CVs) recorded on Ti, Cu, Ni and Ag electrodes for the reduction of CO₂ at 25 °C under atmospheric pressure. In cyclic voltammetry, no redox peaks appeared in the sweeping region in the absence of CO₂ using Ti electrode as the model electrode (Fig. 1, curve a). After BMIMBF₄ was saturated with CO₂, single irreversible peaks were all observed on four electrodes (Fig. 1, curves b–e). The inset chart is the reduction of CO₂ on Ag electrode because its peak current is low enough not to be observed clearly.

The data obtained on Ti, Cu, Ni and Ag electrodes are listed in Table 1. The peak potentials (E_p) and peak currents (I_p) of CO₂ reduction are different from one another regarding the material used. The nature of the electrode material may strongly influence the reduction of CO₂.²⁹ The CVs observed on four electrodes in BMIMBF₄ have been ascribed to one-electron irreversible reduction of CO₂, which generated an anion radical of CO₂ (CO₂^{•-}).^{30,31} It is noteworthy that the E_p of CO₂ reduction in BMIMBF₄ is more positive than that in organic solvents. Direct electrochemical reduction of CO₂ required a very negative potential in aprotic medium (beyond -2.2 V vs. SCE).³² And in our previous research, the peak potential on Cu electrode in acetonitrile (MeCN), dimethyl formamide (DMF) and dimethyl sulfoxide (DMSO) containing 0.1 mol L⁻¹ tetraethylammonium bromide (TEABr) as supporting electrolyte was -2.19, -2.30 and -2.28 V vs. Ag/AgI, respectively.³³ This positive shift of potential can be considered to be due to a strong ion-pairing between CO₂^{•-} and BMIM⁺ cation in the solution.³⁴ It also shows that CO₂ reduction is comparatively easier than that in organic solvents. The results of cyclic voltammetry provided the basis for electrosynthesis in CO₂ saturated-BMIMBF₄ solution. Further

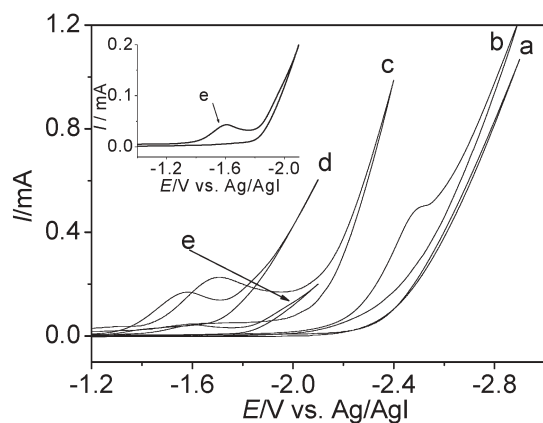


Fig. 1 Cyclic voltammograms of CO₂ in BMIMBF₄ recorded at $\nu = 0.1 \text{ V s}^{-1}$ on four electrodes ($\Phi = 2 \text{ mm}$). (a) Under N₂ on Ti, (b)–(e) BMIMBF₄ saturated with CO₂ (b) Ti, (c) Cu, (d) Ni, (e) Ag; $T = 25 \text{ }^\circ\text{C}$.

Table 1 Peak potentials and currents for CO₂ reduction in BMIMBF₄ on four electrodes^a

Electrodes	Ti	Cu	Ni	Ag
$E_p/\text{V vs. Ag/AgI}$	~ -2.50	-1.71	-1.58	-1.61
I_p/mA	~ 0.4873	0.1902	0.1587	0.0376

^a In the presence of saturated CO₂ at 25 °C under atmosphere pressure.

electrosynthesis experiments were examined in CO₂ saturated-BMIMBF₄ solution.

Influence of reaction conditions

The reactivity of alcohols *versus* electrochemically activated CO₂ in BMIMBF₄ was analyzed according to the following procedure. A solution of BMIMBF₄ with continuous bubbling of CO₂, was electrolyzed under potentiostatic control in an undivided cell until 1.0 F mol⁻¹ of the charge of alcohol was passed. At the end of electrolysis, alcohols **1a–h** were added, which were stirred for 1.0 h. Last, a 3-fold molar excess CH₃I or C₂H₅I as the alkylating agent was added and the reaction mixture was stirred at 55 °C for 5 h. Workup of the cathodic solution (see Experimental Section) provided the corresponding carbonates **2a–h**. The yields of **2a–h** are based on the starting alcohols. The results using methanol (**1a**) as the model compound obtained in several experiments are reported in Table 2. The selectivity of the products was 100% in all our experiments. No other byproducts were detected by GC and GC-MS for all the experiments. Accordingly, the influence of temperature, cathode material, working potential, alcohol concentration and the charge passed on the yield was investigated.

(a) Influence of temperature

The influence of temperature on the formation of dimethyl carbonate **2a** (DMC) was investigated in the range 25 °C to

Table 2 Electrosynthesis of dimethyl carbonate (**2a**) from **1a** and CO₂ in BMIMBF₄ under various conditions^a

Entry	$T/^\circ\text{C}$	Cathode	$E/\text{V vs. Ag/AgI}$	$c/\text{mol L}^{-1}$	2a Yield (%)
1	25	Cu	-1.8	0.124	33
2	35	Cu	-1.8	0.124	35
3	45	Cu	-1.8	0.124	60
4	55	Cu	-1.8	0.124	73
5	65	Cu	-1.8	0.124	70
6	75	Cu	-1.8	0.124	52
7	55	Ag	-1.8	0.124	74
8	55	Stainless steel	-1.8	0.124	67
9	55	Ti	-2.5	0.124	58
10	55	Ni	-1.8	0.124	18
11	55	Cu	-1.6	0.124	57
12	55	Cu	-2.0	0.124	67
13	55	Cu	-2.2	0.124	38
14	55	Cu	-2.3	0.124	17
15	55	Cu	-1.8	0.049	57
16	55	Cu	-1.8	0.161	59
17	55	Cu	-1.8	0.198	41
18	55	Cu	-1.8	0.124	—
19 ^b	55	Cu	—	0.124	—

^a In the presence of saturated CO₂ in BMIMBF₄ under atmosphere pressure; charge passed, 1.0 F mol⁻¹; CH₃I as the alkylating agent.

^b Reacted without current.

75 °C. The results are reported in Table 2 (entries 1–6). It is worth noting that BMIMBF₄ ionic liquid is suitable for the reaction even at room temperature. A temperature of 55 °C is optimum for the electrolysis and the highest yield (73%) was achieved (Table 2, entry 4).

The temperature can influence the viscosity of the ionic liquid and the solubility of CO₂ in the ionic liquid. Lower temperature is favorable to increase the solubility of CO₂; simultaneously to increase the viscosity.³⁵ The higher viscosity decreases the transport and diffusion ability of CO₂ in the solution, which also causes voltammetric and preparative electrolysis currents to be low, requiring long electrolysis time. At higher temperature, the viscosity of ionic liquid decreases, and CO₂ diffuses faster towards the electrode surface, leading to the increase of peak currents, while the solubility of CO₂ decreases. Combining the two factors, a temperature of 55 °C is the most favorable for the reaction.

(b) Influence of cathode material

The use of magnesium (Mg) as anode, and copper (Cu), silver (Ag), stainless steel, titanium (Ti) and nickel (Ni) electrodes as cathode material was tested for electrosynthesis. The electrolysis was carried out at a potential *ca.* –0.2 V beyond the CO₂ reduction peaks on different cathodes as obtained by cyclic voltammograms. This means that the applied potentials are –1.8 V for Cu, Ag, Ni or stainless steel electrodes and –2.5 V for Ti electrode. These values are enough to ensure electroreduction of CO₂. The influence of cathode material was found to be greater under the same conditions. The yield of DMC decreased in the order Cu ≈ Ag > Stainless steel > Ti > Ni (Table 2, entries 4, 7–10). It showed Cu and Ag cathodes were better than the others and 73 and 74% of DMC were obtained, respectively. In the case of stainless steel and Ti cathode the yield of DMC was 67 and 58%. The employment of Ni decreased the yield to 18%. The nature of the cathode material may influence the reduction of CO₂ which is consistent with the results of cyclic voltammetry. Because the Cu material compared with Ag material is cheaper and easily obtained, Cu electrode is chosen as the cathode material for further investigation.

(c) Influence of working potential

As shown in Table 2 (entries 4, 11–14), appreciable differences in the yield of DMC were found at the end of the electrosynthesis at different working potentials. As shown in Table 1 and Fig. 1, the potential of CO₂ reduction peak was –1.71 V *vs.* Ag/AgI on Cu electrode. Around –1.71 V, the values of –1.6, –1.8, –2.0, –2.2 and –2.3 V were chosen as potentials for the electrosynthesis. The best yield was achieved at –1.8 V. A more positive potential will not be effective for CO₂ reduction. At more negative potential, the BMIMBF₄ itself will polarize and is a disadvantage for CO₂ reduction.

(d) Influence of alcohol concentration

The concentration of alcohol (**1a**) was evaluated from 0.049 mol L^{–1} to 0.198 mol L^{–1}. As shown in Table 2 (entries 4, 15–17), the alcohol concentration influenced

dramatically the yield of DMC. It had a peak value at 0.124 mol L^{–1}. At lower concentration the contact opportunity of **1a** and CO₂ decreased, which resulted in lower yield. Too much **1a** may retard the interaction between CO₂^{•–} and BMIMBF₄, which resulted in a decrease of the yield.

(e) Influence of the charge passed

The yield of DMC strongly depended on the charge passed (*Q*) supplied to the electrodes during the reduction of CO₂ to CO₂^{•–}. As shown in Fig. 2, it had a peak value at 1.0 F mol^{–1}, namely, the best yield was achieved when the amount of electrogenerated CO₂^{•–} was equal to that of alcohol (**1a**). Before that point, the yield of **2a** increased rapidly because the concentration of CO₂^{•–} in BMIMBF₄ increased with increasing the charge consumption. After that point, superabundant CO₂^{•–} will favour the reaction where CO₂^{•–} reacted itself,³¹ resulting in a decrease of the yield.

Therefore, the optimized condition for the electrosynthesis of **2a** from CO₂ and **1a** in BMIMBF₄ required 0.124 mol L^{–1} of **1a** using Cu as cathode electrode with a potential of –1.8 V *vs.* Ag/AgI at 55 °C under 1 atm with a charge consumption of 1.0 F mol^{–1}.

Recycle of ionic liquid

In order to investigate the possibility of recycling the BMIMBF₄ ionic liquid, the recycle experiments were conducted. In this study, the ionic liquid can be easily separated from DMC **2a** and **1a** by simple distillation after the first run and then used directly in the next run. This procedure was repeated for 5 cycles. The yield results are shown in Fig. 3. After the ionic liquid had been used 5 times, the yield of **2a** was decreased after the second time, then maintained at a level of about 50%. This indicates that the ionic liquid for electrosynthesis is recyclable.

Other alcohols

To test the effectiveness and generality of this methodology, we extended the investigation to alcohols **1b–h**, carrying out the reactions under optimized conditions. The results of analyses are reported in Table 3 and some conclusions can be drawn. Carbonates (**2a–d**, **f–g**) were obtained in good yields (33–73%) from the primary alcohol and secondary aliphatic

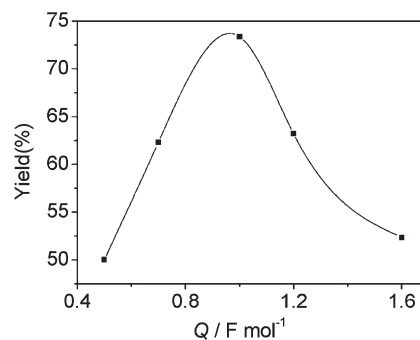


Fig. 2 Influence of the charge passed on the yield of **2a**. Reaction conditions: **1a**, 0.124 mol L^{–1}; *E* = –1.8 V *vs.* Ag/AgI; *P*_{CO₂} = 1 atm; *T* = 55 °C; Cu as cathode and Mg as anode; CH₃I as the alkylating agent.

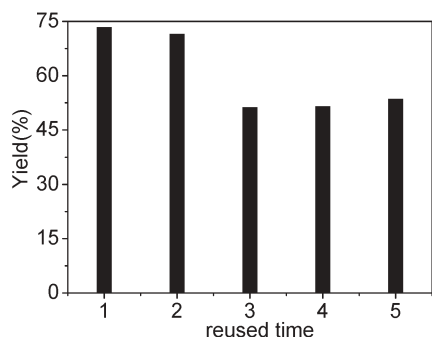


Fig. 3 Reuse of BMIMBF₄ in electro-synthesis. Reaction conditions as in Table 1, entry 4.

Table 3 Synthesis of carbonates (**2b–h**) via reaction of alcohol (**1b–h**) with electrochemically activated CO₂ in BMIMBF₄^a

Entry	Alcohols	Products	Yield (%)
1	1b	2b	67
2	1c	2c	52
3	1d	2d	57
4	1e	2e	—
5	1f	2f	37
6	1g	2g	33
7	1h	2h	—

^a Reaction condition: **1b–h**, 0.124 mol L⁻¹; $E = -1.8$ V vs. Ag/AgI; $Q = 1.0$ F mol⁻¹; $T = 55$ °C; $P_{\text{CO}_2} = 1$ atm; Cu as cathode and Mg as anode; C₂H₅I as the alkylating agent.

alcohol (Table 2, entry 4 and Table 3, entries 1–3, 5–6). The yield decreased according to the increase of chain. Tertiary alcohol and phenol (**1e**, **h**) can not convert to the corresponding carbonates (Table 3, entries 4, 7).

Mechanism of electro-synthesis of organic carbonates in BMIMBF₄

Though the reaction mechanism for the electro-synthesis is not clear at this stage, it can be conjectured primarily, based on the experimental results. According the procedure of electro-synthesis, the alcohol is added into the solution after electrolysis. CO₂^{•-} (which is formed by CO₂ reduction and stable through the formation of CO₂^{•-}-BMIM⁺ ion-pairing) reacted with alcohol to form the carbonates after addition of the alkylating agent.

To ascertain the role of CO₂^{•-} and of neutral CO₂, an alternative procedure was set up, the electrolysis was carried out under N₂ at the optimal conditions. At the end of the electrolysis, **1a** was added to the solution, which was stirred under CO₂ for 1 h. Last, CH₃I was added. As shown in Table 2 (entry 18 vs. entry 4), no **2a** was formed. And, it can be seen that no reaction could be observed if a voltage was not applied (Table 2, entry 19). Consequently, the reaction of CO₂^{•-} in BMIMBF₄ versus alcohol is unrelated to the presence of neutral CO₂.

Conclusion

In conclusion, a novel electrochemical procedure for electro-synthesis of organic carbonates from CO₂ and alcohols

without additional supporting electrolytes and catalysts has been established in CO₂-saturated BMIMBF₄ solution, followed by addition of an alkylating agent. The synthesis was carried out under mild ($P_{\text{CO}_2} = 1.0$ atm, $T = 55$ °C) and safe conditions and carbonates were isolated in good yield. Cyclic voltammetry of CO₂ in BMIMBF₄ on Ti, Cu, Ni and Ag electrodes show that ionic liquid, BMIMBF₄, can act as a medium for CO₂ reduction and CO₂ reduction is comparatively easier than that in organic solvents. The influence of temperature, cathode material, working potential, alcohol concentration and the charge passed on the product yield using methanol (**1a**) as the model compound was investigated and the optimized condition for electro-synthesis was obtained. The ionic liquid used for the reaction was recyclable. The obtained results showed that primary and secondary alcohols were converted in good yields, whereas tertiary alcohol and phenol were unreactive. The mechanism was discussed primarily on the results. Further investigations using different classes of RTILs to establish the scope and the generality of this procedure are in progress.

Experimental

The ionic liquid, 1-butyl-3-methylimidazolium tetrafluoroborate (BMIMBF₄) was synthesized according to the procedures in the literature.³⁶ The ionic liquid was dried under vacuum at 80 °C for 24 h prior to use. Voltammetric measurements were carried out using CHI650C electrochemical station (Shanghai Chenhua Instruments Company). Silver (Ag), copper (Cu), titanium (Ti), and nickel (Ni) were used as working electrodes. The counter electrode was Pt wire. The reference electrode was Ag/AgI electrode. The experimental medium was BMIMBF₄ (10 ml) solution. All experiments were performed under atmospheric pressure.

The potentiostatic electrolyses were performed in BMIMBF₄ (10 ml) under a slow stream of CO₂ in an undivided glass cell equipped with a Cu cathode (8.0 cm²), a magnesium sacrificial anode and Ag/AgI reference electrode, until 1.0 F mol⁻¹ of charge was passed under atmospheric pressure. At the end of the electrolyses, alcohols **1a–h** were added, which were stirred for 1.0 h. Lastly, a 3-fold molar excess of CH₃I or C₂H₅I as the alkylating agent was added and the reaction mixture was stirred at 55 °C for 5 h. The workup of the solutions provided the corresponding carbonates. The reaction mixture was distilled to obtain product **2a–b**. For product **2c–h**, the reaction mixture was extracted with diethyl ether (3 × 20 ml) after the solvent was removed under reduced pressure, and combined organic layers were dried over anhydrous MgSO₄ for 12 h. Products **2a–e** were determined by GC-MS, **2f–g** were purified by column chromatography affording pure carbonates and determined by GC-MS, IR and NMR. The yields of **2a–h** were based on the starting alcohols.

Dimethyl carbonate (**2a**): MS (*m/z*, %): 90 (M⁺, 8), 75 (1), 60 (9), 59 (77), 45 (100), 33 (8), 31 (47), 29 (36), 28 (8), 15 (37).

Diethyl carbonate (**2b**): MS (*m/z*, %): 91 (M⁺, 59), 75 (3), 63 (18), 59 (3), 45 (67), 30 (2), 31 (29), 29 (46), 28 (100), 27 (11).

n-Butylethyl carbonate (**2c**): MS (*m/z*, %): 119 (M⁺, 5), 91 (71), 73 (37), 63 (100), 57 (64), 56 (88), 41 (59), 29 (72), 28 (59), 31 (35).

sec-Butylethyl carbonate (**2d**): MS (*m/z*, %): 131 (M^+ , 1), 91 (12), 73 (25), 59 (32), 57 (43), 56 (18), 45 (100), 41 (23), 29 (32), 28 (44).

Benzylethyl carbonate (**2f**): $^1\text{H NMR}$ (CDCl_3): δ (ppm) 7.39–7.25 (m, 5H), 5.16 (s, 2H), 4.24–4.20 (q, 2H, $J = 7.0$ Hz), 1.32–1.27 (q, 3H, $J = 7.0$ Hz). IR (KBr): 1743 cm^{-1} ($\nu_{\text{C=O}}$); MS (*m/z*, %): 180 (M^+ , 44), 135 (13), 107 (53), 91 (100), 79 (63), 77 (24), 65 (16), 51 (9), 39 (6), 29 (8).

Phenethylethyl carbonate (**2g**): $^1\text{H NMR}$ (CDCl_3): δ (ppm) 7.35–7.25 (m, 5H), 4.38–4.34 (t, 2H, $J = 8.0$ Hz), 4.22–4.18 (q, 2H, $J = 7.0$ Hz), 3.02–2.99 (t, 2H, $J = 7.0$ Hz), 1.33–1.30 (t, 3H, $J = 8.0$ Hz); IR (KBr): 1744 cm^{-1} ($\nu_{\text{C=O}}$); MS (*m/z*, %): 194 (M^+ , 1), 106 (33), 105 (100), 92 (21), 91 (6), 79 (10), 78 (13), 65 (14), 64 (8), 51 (13).

Acknowledgements

This work is financially supported by the Natural Science Foundation of China (20573037), Natural Science Foundation of Shanghai (05JC14070) and Shanghai Leading Academic Discipline Project (B409).

References

- M. A. Casadei, S. Cesa and L. Rossi, *Eur. J. Org. Chem.*, 2000, 2445.
- B. M. Bhanage, S. Fujita, Y. Ikushima and M. Arai, *Appl. Catal., A*, 2001, **219**, 259.
- Y. Ono, *Appl. Catal., A*, 1997, **155**, 133.
- D. D. Kanne, US Pat., 5004480, 1991.
- Y. Ono, *Catal. Today*, 1997, **35**, 15.
- A.-A. G. Shaikh and S. Sivaram, *Chem. Rev.*, 1996, **96**, 951.
- J. P. Parrish, R. N. Salvatore and K. W. Jung, *Tetrahedron*, 2000, **56**, 8207.
- T. Sakakura, Y. Saito, M. Okano, J.-C. Choi and T. Sako, *J. Org. Chem.*, 1998, **63**, 7095.
- J. Sun, B. Yang, H. Lin, X. Wang and D. Wang, *J. Organomet. Chem.*, 2005, **690**, 1300.
- T. Tatsumi, Y. Watanabe and K. A. Koyano, *Chem. Commun.*, 1996, 2281.
- S. Fujita, B. M. Bhanage, Y. Ikushima and M. Arai, *Green Chem.*, 2001, **3**, 87.
- N. S. Isaacs, B. O'Sullivan and C. Verhaelen, *Tetrahedron*, 1999, **55**, 11949.
- T. Zhao, Y. Han and Y. Sun, *Fuel Process. Technol.*, 2000, **62**, 187.
- B. M. Bhanage, S. Fujita, Y. Ikushima, K. Torii and M. Arai, *Green Chem.*, 2003, **5**, 71.
- K. Tomishige, T. Sakaihorii, Y. Ikeda and K. Fijimoto, *Catal. Lett.*, 2000, **58**, 225.
- Y. Ikeda, T. Sakaihorii, K. Tomishige and K. Fijimoto, *Catal. Lett.*, 2000, **66**, 59.
- K. Tomishige, Y. Ikeda, T. Sakaihorii and K. Fijimoto, *J. Catal.*, 2000, **192**, 355.
- C. Song, *Catal. Today*, 2006, **115**, 2.
- M. C. Buzzeo, R. G. Evans and R. G. Compton, *Chem. Phys. Chem.*, 2004, **5**, 1106.
- R. Sheldon, *Chem. Commun.*, 2001, 2399.
- J. Sun, S. Fujita and M. Arai, *J. Organomet. Chem.*, 2005, **690**, 3490.
- Y. Gu, Q. Zhang, Z. Duan, J. Zhang, S. Zhang and Y. Deng, *J. Org. Chem.*, 2005, **70**, 7376.
- B. K. Sweeny and D. G. Peters, *Electrochem. Commun.*, 2001, **3**, 712.
- M. C. Kroon, W. Buijs, C. J. Peters and G.-J. Witkamp, *Green Chem.*, 2006, **8**, 241.
- A. I. Bhatt, A. M. Bond, D. R. MacFarlane, J. Zhang, J. L. Scott, C. R. Strauss, P. I. Iotov and S. V. Kalcheva, *Green Chem.*, 2006, **8**, 161.
- H. Yang, Y. Gu, Y. Deng and F. Shi, *Chem. Commun.*, 2002, 274.
- M. Feroci, M. Orsini, L. Rossi, G. Sotgiu and A. Inesi, *J. Org. Chem.*, 2007, **72**, 200.
- H. Wang, G. Zh, Y. Liu, Y. Luo and J. Lu, *Electrochem. Commun.*, 2007, **9**, 2235.
- M. Jitaru, D. A. Lowy, M. Toma, B. B. Toma and L. Oniciu, *J. Appl. Electrochem.*, 1997, **27**, 875.
- H. Kamekawa, H. Senboku and M. Tokuda, *Tetrahedron Lett.*, 1998, **39**, 1591.
- C. Amatore and J.-M. Savéant, *J. Am. Chem. Soc.*, 1981, **103**, 5021.
- B. R. Eggins and J. McNeill, *J. Electroanal. Chem.*, 1983, **148**, 17.
- L. Zhang, Y. Luo, D. Niu, L. Xiao and J. Lu, *Chem. J. Chinese Univ.*, 2007, **28**, 1660 (in Chinese).
- M. M. Islam, B. N. Ferdousi, T. Okajima and T. Ohsaka, *Electrochem. Commun.*, 2005, **7**, 789.
- O. O. Okoturo and T. J. VanderNoot, *J. Electroanal. Chem.*, 2004, **568**, 167.
- P. Bonhôte, A.-P. Dias, N. Papageorgiou, K. Kalyanasundaram and M. Grätzel, *Inorg. Chem.*, 1996, **35**, 1168.

Cu–Y zeolite supported on silicon carbide for the vapour phase oxidative carbonylation of methanol to dimethyl carbonate

Guillaume Rebmann, Valérie Keller, Marc J. Ledoux and Nicolas Keller*

Received 17th August 2007, Accepted 9th November 2007

First published as an Advance Article on the web 26th November 2007

DOI: 10.1039/b712705g

A medium surface area β -SiC supported Cu–Y zeolite composite catalyst was prepared by performing the zeolite synthesis in the presence of the β -SiC grains. The composite material was used as a catalyst for the vapour phase oxidative carbonylation of methanol to dimethyl carbonate, with improved space time yields of dimethyl carbonate and limited influence of the temperature. The composite catalyst combined the interest of using a thermoconductive material as support for an exothermic reaction and of using a Cu–Y zeolite catalyst for getting stable performances in the dimethyl carbonate synthesis.

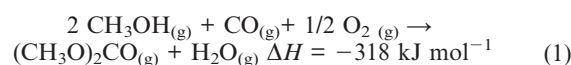
1. Introduction

Over the last few decades, an environmental consideration, the impact of chemicals over humans, has been pointed out as a major public concern. The increasing public health and environmental protection pressure resulted in ever stricter legislation requirements related to both use and production of chemicals, carried out as bills or regulations by national or supranational executives. This led industrials to be involved in developing clean and eco-friendly synthesis processes meeting such environmental restrictions within a sustainable chemistry approach.

The production and chemical use of dimethyl carbonate (DMC) are directly affected by this policy frame. The 2500 recent reference citations listed by the *Chemical Abstracts* database highlight the growing interest in this area over a few years:¹ the search for better performing catalysts and processes in order to meet the ever increasing standards in the eco-technology field has created an incentive and is driving research in this area. This increasing focus is mainly due to the biodegradability and the low toxicity of DMC, it being about 1000 times less toxic than phosgene.² The DMC applications cover wide fields,^{1–3} including uses as a fuel additive due to a high oxygen content which significantly improves the fuel oxygenation, as a phosgene alternative in phosgene-free aromatic polycarbonate and isocyanate syntheses due to a great reactivity towards phenol or primary amine nucleophilic molecules, as a methylation agent in substitution of dimethyl sulfate and methyl iodide, and as a solvent in the lithium ion battery and in replacement of ketones and ester acetates due to a strong solvation force.

The old phosgenation process, consisting in reacting methanol and phosgene,⁴ has been totally banned for years, and world production remains mainly achieved by the Enichem and UBE processes, based on liquid phase methanol

oxycarbonylation in the presence of a copper(I) chloride catalyst⁵ and gas phase methyl nitrite carbonylation,⁶ respectively. In 1997, the world production of DMC amounted to 170 t d⁻¹, and achieving an oxygen content of 1 wt.% in fuel would require from each *major supplier* a DMC production of at least 1360 t d⁻¹, which greatly exceeds the world production.² The liquid phase Enichem process suffers from the highly corrosive nature of the copper chloride active phase in a liquid slurry reactor, rapid deactivation and recurrent catalysts/products separation problems. This example put forward the need for better DMC production processes and suggested that transfer to vapour phase processes should be preferred. Amongst different routes, including direct synthesis from CO₂ and the transesterification of ethylene carbonate and urea, performing the methanol oxycarbonylation in the vapour phase rather than in the liquid phase is a promising alternative (eqn. 1).^{7–14}



High surface area activated charcoal is nowadays the most used support material for dispersing active Cu^{II} chloride-based catalysts, such as CuCl₂, CuCl₂–PdCl₂ or CuCl₂ promoted by acetates or hydroxides. Although a high methanol conversion rate can be obtained, such systems suffer from a strong deactivation due to loss of chloride involved in the reaction mechanism for forming DMC. Works by King¹⁵ and Root *et al.*¹⁶ proved that chloride was not necessary to catalyse the reaction. By replacing chloride by a negatively charged zeolite framework, King first showed that Cu-exchanged Y zeolite catalysts, prepared by a solid-state ion exchange method, displayed good productivity and selectivity for DMC synthesis with a strongly enhanced stability compared with the usual activated charcoal supported chloride-based catalysts. This opened a route for preparing stable catalysts for the DMC synthesis. Interesting works on Cu-impregnated Y zeolite catalysts at elevated pressure in a microreactor, and at normal pressure in a parallel 16 channel flow microreactor, were recently published by Richter *et al.*¹⁷

Laboratoire des Matériaux, Surfaces et Procédés pour la Catalyse, European Laboratory for Catalysis and Surface Sciences (ELCASS), CNRS, Louis Pasteur University, 25 rue Becquerel, 67087 Strasbourg, France. E-mail: nkeller@chimie.u-strasbg.fr; Fax: +33 (0) 3 90 24 27 61; Tel: +33 (0) 3 90 24 28 11

However, the use of Cu–Y zeolite remains limited by a low conversion level, which requires us to increase the reaction temperature for reaching competitive conversions, leading unfortunately to side-reactions and to a decrease in the DMC selectivity by favouring dimethyl ether (DME) and CO₂ production notably. In addition to that, the macroscopic shaping of zeolites, necessary to avoid detrimental pressure drops and moving-bed phenomena in fixed-bed reactors, suffers from diffusion limitations and requires the use of unwanted binders, which limits the reactant access.¹⁸ Thermoconductive silicon carbide (SiC) under its β form has been reported to be an interesting alternative to conventional support materials such as activated charcoal, silica or alumina, for endo- and exothermic reactions especially, for which its high thermal conductivity is of high interest,^{19,20} as detailed in a recent review.²¹ Recently β -SiC was successfully used as support for ZSM-5 and BEA zeolites in methanol-to-olefins processes and Friedel–Crafts reactions, respectively.^{22,23}

This article reports on the use of thermoconductive β -SiC for supporting a Cu–Y zeolite, in order to combine the advantage of using a thermoconductive support for an exothermic reaction, in the interests of using a Cu–Y zeolite for producing DMC.

2. Experimental

2.1. Catalyst preparation

β -SiC in a granular form (0.4–1 μm) was prepared by the Shape Memory Synthesis (SMS) method developed by Pham-Huu and Ledoux,²⁴ consisting of a gas–solid reaction between a pre-shaped carbon source and SiO vapours. It had a specific surface area of 8.6 m² g⁻¹ free of any microporosity. Details on the synthesis and the material characterization can be found elsewhere.²¹ One could put forward the view that the surface of the β -SiC obtained by the SMS method was partly composed of an SiO_xC_y–SiO₂ mixed phase.^{20,21}

The β -SiC supported Y zeolite was prepared by extending the hydrothermal synthesis method described by Ginter for synthesizing the Linde Y type zeolite.²⁵ The preparation of the gel used for synthesizing the Y zeolite consisted of three steps, using sodium aluminate (50–56 wt.% Al₂O₃, 40–45 wt.% Na₂O) as the aluminium source and a sodium silicate solution (27 wt.% SiO₂, 14 wt.% NaOH) as the silicon source. 1.02 g of sodium hydroxide was first dissolved with 0.53 g of sodium aluminate in 5 g of distilled water, before adding 5.68 g of sodium silicate after complete dissolution. The seed gel obtained was placed under stirring during 10 min, and subsequently aged for 24 h to get sub-micronic growth germs of NaY zeolite. In parallel, a second gel was prepared by dissolving 0.035 g of sodium hydroxide with 3.37 g of sodium aluminate into 32.74 g of distilled water, before 35.61 g of sodium silicate was added after complete dissolution. The resulting mixture was placed under strong stirring till the appearance of a smooth dense gel. The final gel was obtained by adding the second gel to 4.13 g of the seed gel, under strong stirring for 20 min, for homogenizing the growth germs within the final gel. Finally, 5 g of β -SiC, previously calcined at 900 °C for 2 h to increase its surface content of silica by use of

this superficial oxidation,^{20,26} was incorporated. The molar composition of the gel was as follows: 4.62 Na₂O, 10 SiO₂, 180 H₂O, Al₂O₃. The zeolite crystallization was performed in a Teflon-lined stainless steel autoclave under pressure at 90 °C for 22 h. Afterwards, the solid obtained consisted of a mixture of bulk NaY crystals and the NaY/SiC composite. Following separation by size exclusion filtration, both materials were washed with distilled water until the washing water reached pH <9. The bulk zeolite was dried at 110 °C for 24 h, whereas the NaY/SiC composite was first ultra-sonicated to remove the zeolite crystals that could be trapped within the support porous network, and further dried at 110 °C for 24 h. The whole synthesis was performed twice for increasing the amount of zeolite anchored on the β -SiC support, by replacing the bare β -SiC grains by NaY/SiC grains.

The NH₄ form of synthesized materials was obtained by cationic exchange for 12 h using a 1 M ammonium chloride aqueous solution under reflux at 90 °C, before final calcination at 550 °C for 12 h to get their corresponding acidic forms, denoted HY and HY/SiC. The Cu exchange was performed by vapour phase exchange, based on the reaction at 650 °C for 16 h between the solid and gaseous CuCl fed with He, previously obtained by vaporizing solid CuCl as the Cu^I solid source at the same temperature. This exchange mode was the direct transposition to the vapour phase of the high temperature anhydrous reaction exchange described by King.¹⁵ It displayed advantages such as the absence of any direct contact between the host zeolite and the Cu solid source, the passing through the whole solid of the gaseous Cu source after vaporization, a progressive and controllable vaporization inside the reactor resulting from a low vaporization temperature compared with the theoretical one, and the low fusion temperature of CuCl compared with those of impurities such as Cu₂O or CuO, resulting in a pure CuCl_g/He flow.

2.2. Vapour phase methanol oxidative carbonylation

The gas phase oxycarbonylation of methanol was performed at a total pressure of 12 bar in a fixed bed reactor (10 mm id). CO, O₂ and He were fed into the reactor by mass flow controllers, whereas gaseous methanol was injected through a liquid flow mass controller coupled to a controlled evaporator mixer. 1.5 g (2.5 mL) of material was used as the catalyst. The reactor temperature was regulated by an external thermocouple, whereas that of the catalytic bed was measured by a thermocouple located inside the catalytic bed. The reactional feed was composed of gaseous methanol (17.5 mL min⁻¹, 20%vol.), CO (52.5 mL min⁻¹, 60%vol.), O₂ (3.5 mL min⁻¹, 4%vol.) and balanced helium (16%vol.), with a methanol mass flow of 1.41 g h⁻¹, corresponding to O₂/CO/methanol molar ratios of 1:5:15 and a gas hourly space velocity of 1800 h⁻¹. The products were analysed on-line by a Varian 3300 gas chromatograph with a CP-PoraPlot U column for DMC, DME, methyl formate (MF), dimethoxymethane (DMM) and methyl acetate (MA) hydrocarbons and a Carbosieve SII packed column for the CO, O₂ and CO₂ gases, coupled to FID and TCD detectors respectively.

The methanol conversion was derived from Peng *et al.*:²⁷

$$C_{\text{CH}_3\text{OH}} = \frac{2\text{DME} + 2\text{MF} + 3\text{DMM} + 3\text{MA} + 2\text{DMC}}{2\text{DME} + 2\text{MF} + 3\text{DMM} + 3\text{MA} + 2\text{DMC} + \text{CH}_3\text{OH}}$$

Selectivities to DMC, calculated on the basis of the products issued from CO and methanol, have been defined as follows:^{14,27}

$$S_{\text{DMC}/\text{CO}} = \frac{\text{DMC}}{\text{CO}_2 + \text{DMC}}$$

$$S_{\text{DMC}/\text{MeOH}} = \frac{2\text{DMC}}{2\text{DME} + 2\text{MF} + 3\text{DMM} + 3\text{MA} + 2\text{DMC}}$$

Selectivities to other products (relative to methanol, *e.g.* $S_{\text{DME}/\text{MeOH}}$) were defined following a similar calculation way. The DMC yield was set as: $Y_{\text{DMC}} = C_{\text{MeOH}} \times S_{\text{DMC}/\text{MeOH}} \times 100\%$.

The hourly weight yield to DMC (STY, space time yield) was set as the weight amount of DMC formed per catalyst litre per hour, *i.e.*, the catalyst productivity towards DMC.²⁸

3. Results and discussion

3.1. β -SiC supported Y zeolite composite synthesis

The XRD pattern of the Y/SiC composite under the sodium form is reported in Fig. 1 and compared with those of the bare β -SiC support and of its NaY analogue obtained without β -SiC. The diffraction lines could be assigned to three different phases. Beside peaks corresponding to the β -SiC support, comparing the diagram with that of the pure NaY zeolite evidenced the presence of diffraction peaks attributed to the zeolite with a faujasite structure.²⁵ An additional and broad peak at around 7.5° could be assigned, without any exclusivity, to a sub-stoichiometric highly defective silicon oxide (Si_xO_y) phase. This badly-crystallized phase could correspond to a transition phase between the β -SiC (and its mixed SiO_xC_y - SiO_2 surface) and the zeolite crystals. The particular stoichiometry of this transition intermediate phase could allow the anchorage of two phases with totally different structures to be effective, by acting as a glue or allowing a progressive structural change to take place from the support to the supported crystals. The broadness of the peak could derive from a continuous change of both stoichiometry and structure from the support surface to the crystals with the faujasite structure.

Fig. 2 displays scanning electron microscopy images of the bare β -SiC support, the NaY zeolite and the β -SiC supported HY composite. The inset shows that the gross morphology of the β -SiC grains remained unchanged, confirming the shape-memory nature of the coating process. The zeolite crystals in the composite material displayed both similar morphology and size to those of the bulk NaY zeolite, with no specific shapes such as flat particles. The support was assumed not to play any significant role in the morphological aspect of the zeolite crystals, but it should play an active role in the anchorage process. The role of the support was already reported by Candamano *et al.* during the growth of a Y zeolite on a cordierite support.²⁹ The authors explained that the cordierite ceramic played an active role in the crystallisation process during the partial dissolution of the cordierite, thus allowing a

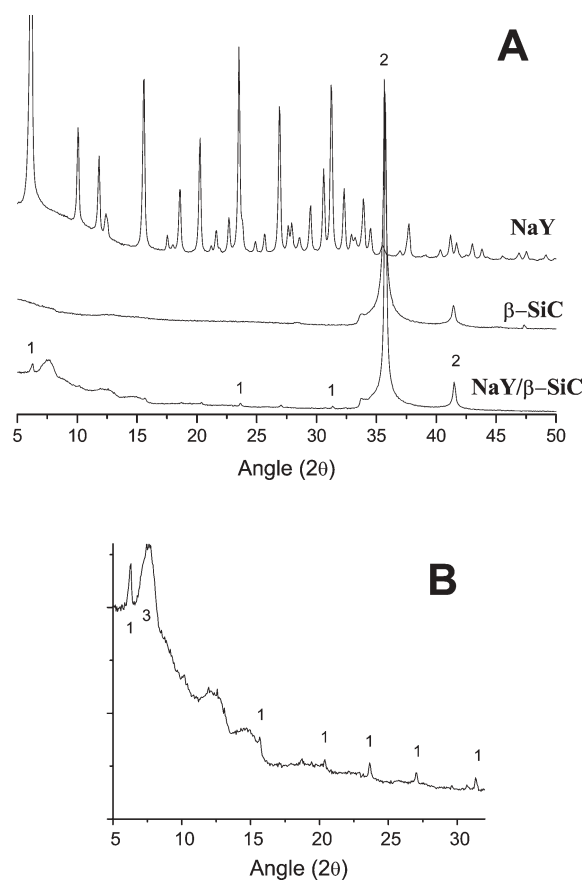


Fig. 1 (A) XRD diagrams of the bulk NaY zeolite, the bare β -SiC support and the NaY/ β -SiC composite material. (1) Y zeolite, (2) β -SiC, (3) undetermined phase. (B) Zoom in the $5\text{--}30^\circ$ range for the NaY/ β -SiC composite material.

real chemical anchorage of the zeolite at the surface of the cordierite surface. A similar mechanism was proposed by Winé on the β -SiC supported BEA zeolite material, with the partial dissolution of the oxide layer located at the surface of the β -SiC after the high temperature air treatment, and further reorganisation to form $(\text{SiO}_4)_{\text{SiC}}\text{--}(\text{SiO}_4)_{\text{zeolite}}$ bindings, allowing the anchorage of the zeolite on the support to be efficient.²⁶ This chemical anchorage allowed a real composite material to be prepared, since a post-synthesis ultra-sound treatment only resulted in the removal of bulk zeolite crystals trapped within the porosity of the β -SiC material. A similar explanation has been put forward by Ivanova *et al.*, the nanoscopic layer of SiO_2 at the support surface ensuring a strong interaction between the support and the gel during the preparation of ZSM-5 coatings on β -SiC monoliths through a superficial dissolution–precipitation sequence.²³

The nitrogen adsorption–desorption isotherms showed the modifications in term of specific surface area resulting from the zeolite coverage of the β -SiC support (Fig. 3). The BET specific surface area of the HY/ β -SiC composite increased from $8.6 \text{ m}^2 \text{ g}^{-1}$ for the micropore-free bare β -SiC support up to $20 \text{ m}^2 \text{ g}^{-1}$ with a $17.4 \text{ m}^2 \text{ g}^{-1}$ micropore contribution, derived from the *t*-plot measurement. By comparison, the bulk HY zeolite had a BET surface area of $400 \text{ m}^2 \text{ g}^{-1}$ with a total microporous content of $380 \text{ m}^2 \text{ g}^{-1}$. This strong increase in

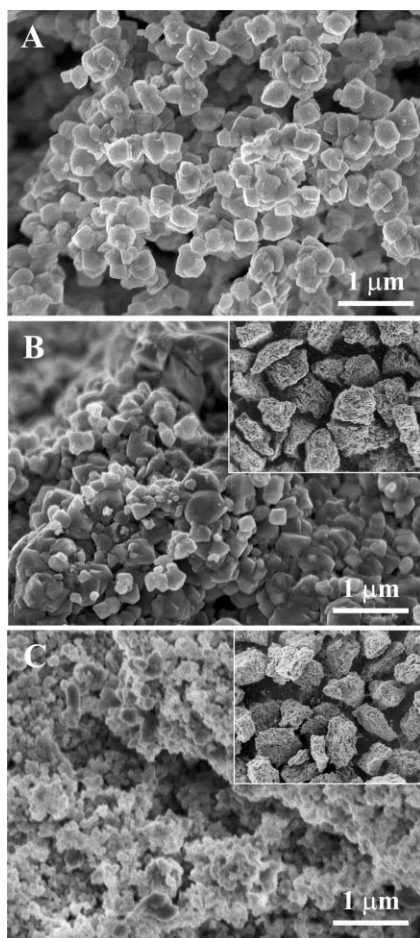


Fig. 2 SEM images of (A) the bulk NaY zeolite, (B) the NaY/ β -SiC composite material, and (C) the bare β -SiC support. Inset: low magnification images of 0.4–1 μ m diameter β -SiC and NaY/ β -SiC grains.

surface area, and especially the appearance of an important microporosity while β -SiC was free of micropores, was in close agreement with the anchorage of zeolite crystals on the SiC support surface. The initial mesoporous nature of the SiC

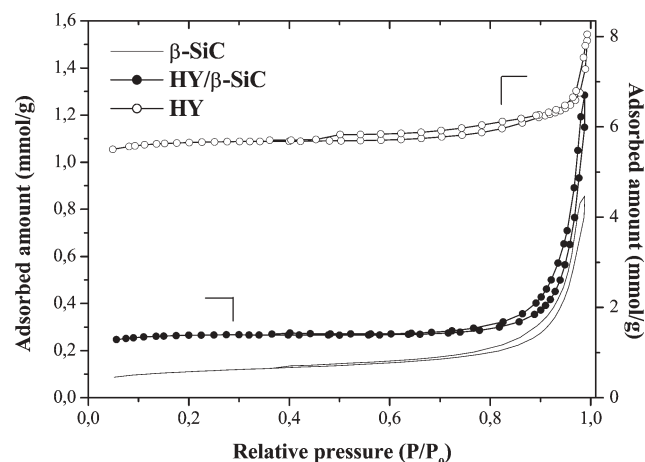


Fig. 3 Nitrogen adsorption–desorption isotherms of pure bulk HY zeolite, β -SiC and β -SiC supported HY zeolite materials.

material gave place to a mainly microporous HY/ β -SiC material.

The amount of zeolite deposited on β -SiC was determined by dissolving the β -SiC support in a hydrofluoric acid solution and by subsequently measuring the resulting weight loss. Taking into account that the zeolite amounted to 8 wt.% of the Y/ β -SiC composite material, the surface area of the composite should thus increase to a level close to 40 $\text{m}^2 \text{g}^{-1}$. The surface area of 20 $\text{m}^2 \text{g}^{-1}$ exhibited by the composite could thus confirm that during the synthesis of the supported zeolite the gel was penetrating inside the mesopores of the β -SiC, leading to formation of the zeolite crystals within the mesoporous network of the support, thus blocking a fraction of the mesopores. This led to a strong increase in the microporosity of the material, whereas part of the SiC surface in the mesopores was blocked by zeolite crystals, and thus was not available for gaseous molecules (nitrogen during BET analysis and also reactants during catalysis) any more.

3.2. Catalytic results

It has been found that, under the given reaction conditions, the two main parameters to control were the temperature and the exchange rate of copper within the zeolite. The exchange rate of the Y zeolite was calculated from the theoretical number of exchangeable cationic sites and from the elemental analysis performed by atomic absorption spectroscopy (CNRS, Vernaison, France). For a total exchange rate, each acidic site of the zeolite would be exchanged by one copper(I) ion. On both bulk Y zeolite and SiC supported Y zeolite materials, a similar exchange rate of 84% was obtained for the zeolite, corresponding to a 13.5 wt.% and a 1 wt.% copper content in the bulk and composite materials, respectively. The incomplete exchange could be explained by a selective exchange resulting from the acidic site strength, as reported by Zechina *et al.*, which showed that the copper exchange directly increased with increasing acidity.³⁰ This led Spoto *et al.* to surmise that only the most acidic sites of the Y zeolite, such as Al–OH–Si and Al–OH, could be exchanged with copper, while by contrast no exchange occurred at this temperature on the weakly acidic Si–OH silanol groups.^{25,31} The vapour phase exchange led to a decrease in the specific surface area of the Y zeolite from 400 $\text{m}^2 \text{g}^{-1}$ down to 320 $\text{m}^2 \text{g}^{-1}$, mainly with a microporosity loss as reported by Hernandez-Maldonado *et al.*³² This loss of surface area could be assigned to a loss of microporosity, attributed by Trigueiro *et al.* to the presence of extra-framework aluminium inside the pores and the channels of the zeolite, and to the blockade of micropores by hydrated species of the exchange cation.³³

The copper exchange rate of the Y zeolite was of high importance, since the DMC formation was first directly related to the copper content, and therefore to the exchange efficiency, as evidenced by means of the STY level obtained on a Cu–Y catalyst (Fig. 4). Furthermore, the DME formation occurred on the acidic sites of the HY zeolite, and therefore on the residual non-exchanged sites of the Cu–Y zeolite, pointing out the importance of the acid site exchange. However, being thermally activated, the DME production remained negligible at a temperature of 130 $^{\circ}\text{C}$, but drastically increased for higher

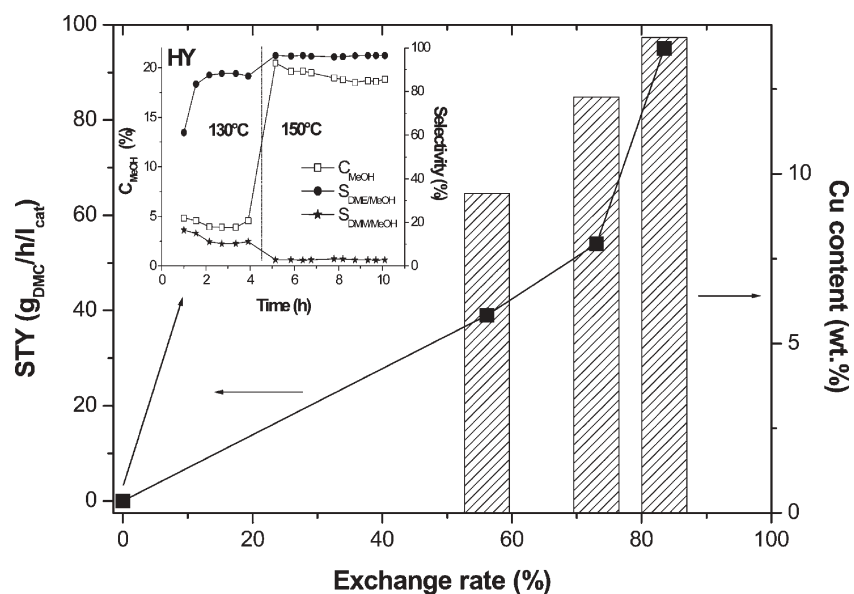


Fig. 4 Influence of the copper exchange rate of the Y zeolite on the STY and on both DMC and DME selectivities. (■) STY to DMC in $\text{g}_{\text{DMC}} \text{h}^{-1} \text{l}_{\text{cat}}$ and (▨) copper content in wt.%. The inset shows the influence of the temperature on the DME formation occurring on the non-exchanged acidic sites of a HY zeolite.

temperatures, as highlighted in Fig. 4 over a non-exchanged HY zeolite. The use of bulk Cu–Y zeolite as catalysts for the DMC synthesis thus remains limited by low methanol conversions, resulting from low reaction temperatures, which cannot be increased for DMC selectivity studies. It should be noted that no carbon residue deposition could be observed, either by microscopy or by temperature-programmed oxidation.

The amount of DMC produced at 130 °C over the supported zeolite reached a stable $\text{g}_{\text{DMC}} \text{h}^{-1} \text{l}_{\text{cat}}$ level, with a stable methanol conversion close to 3% and a selectivity to

DME lower than 3% (Fig. 5). By comparison, the inset of Fig. 5 shows the stable performances obtained on the bulk Cu–Y zeolite catalyst, with a methanol conversion around 17% and a STY to DMC of $95 \text{ g}_{\text{DMC}} \text{h}^{-1} \text{l}_{\text{cat}}$. However, considering the low zeolite content of the SiC supported Y zeolite composite, *i.e.* 8 wt.%, the yield of DMC amounted to $137.5 \text{ g}_{\text{DMC}}$ per h and per litre of zeolite. It should be noted that the bare β -SiC material was totally inactive for synthesizing dimethyl carbonate. This value was higher than that observed on the Cu–Y catalyst, *i.e.*, $95 \text{ g}_{\text{DMC}} \text{h}^{-1} \text{l}_{\text{cat}}$. This interesting space time yield to DMC was obtained with no ΔT temperature

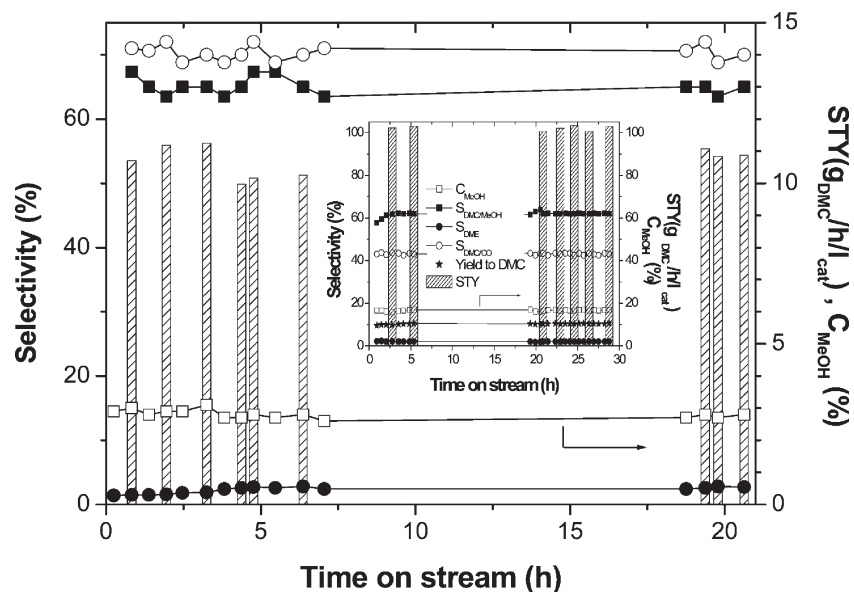


Fig. 5 Catalytic on-stream behaviour of the β -SiC supported Cu–Y zeolite composite catalyst (Cu exchange rate of 84%) for DMC production at 130 °C, in terms of methanol conversion, selectivities and STY to DMC. (□) Methanol conversion, (■) $S_{\text{DMC}/\text{MeOH}}$, (●) $S_{\text{DME}/\text{MeOH}}$, (○) $S_{\text{DMC}/\text{CO}}$ and (▨) STY to DMC in $\text{g}_{\text{DMC}} \text{h}^{-1} \text{l}_{\text{cat}}$. Inset: stable performances obtained on the bulk Cu–Y zeolite at a similar exchange rate of 84%.

overshoot compared with the temperature overshoot of +8 °C occurring at 130 °C over the bulk Cu–Y zeolite, and thus the reaction was performed on the Cu–Y/ β -SiC catalyst at a lower temperature than on its bulk analogue due to a considerably better temperature control with no temperature overshoot resulting from the thermoconductive nature of the β -SiC support. The beneficial high thermal conductivity of β -SiC has already been put forward in several applications.^{19–21,34} Amongst them, one could note the recent preparation of an active and stable Ni/ β -SiC catalyst for the exothermic partial oxidation of methane to obtain a synthesis gas, leading to the required and theoretical H₂/CO molar ratio of 2, while its usual Ni/ γ -Al₂O₃ analogue suffered at the beginning of the process from hot spot formation and from a consequent uncontrolled temperature overshoot, resulting in a H₂/CO molar ratio close to 3, *i.e.*, an excess hydrogen production by methane decomposition.³⁴

The positive contribution of the thermoconductive β -SiC support was also demonstrated by performing the DMC synthesis as a function of the temperature (Fig. 6). No temperature overshoot was observed at the temperatures of 130 °C and 140 °C, whereas performing the reaction at 150 °C and 160 °C resulted in a very weak temperature overshoot of +2 °C and +5 °C, respectively. Simultaneously, the methanol conversion increased from 2.7% at 130 °C to 8.9% at 160 °C, corresponding to a STY of 11 g_{DMC} h⁻¹ l_{cat} and 41 g_{DMC} h⁻¹ l_{cat}, respectively, *i.e.* 137.5 and 512.5 g_{DMC} per h and per litre of zeolite. It was worth noting that, together with the increase in the methanol conversion, the selectivities calculated from methanol were not too drastically affected by the temperature increase, and especially the selectivity to DME, which remained lower than 3% whatever the testing temperature. In addition, the selectivity to DMC calculated from CO, S_{DMC/CO}, decreased from 70% down to 40% when increasing

the temperature from 130 °C to 160 °C, the use of β -SiC diminishing the importance of the unwanted exothermic oxidation of CO to CO₂. This overall behaviour contrasted with the temperature dependence of the bulk Y zeolite-based catalyst (not reported), which showed a strong increase of the S_{DME/MeOH} selectivity with temperatures greater than 135 °C, together with a drastic increase of the CO₂ formation by CO oxidation resulting in a strong decrease of the S_{DMC/CO} selectivity.

This confirmed the interest in using β -SiC for supporting Cu–Y zeolite, by allowing the reactor temperature to be increased in order to overcome the limitation resulting from the low methanol conversion over zeolites, without affecting irretrievably the different selectivities of the reaction, as was the case for bulk Cu–Y zeolite catalysts.

4. Conclusion

A β -SiC supported Cu-exchanged Y zeolite composite catalyst was successfully prepared and used for the gas phase oxidative carbonylation of methanol to dimethyl carbonate. The use of β -SiC probably allowed a real chemical binding between the zeolite and the support surface to occur, by simultaneous anchorage and crystallization of the zeolite, thus resulting in the absence of any detrimental zeolite loss compared with a post-synthesis deposition of zeolite crystals.

The use of a thermoconductive material as support allowed a better control of the catalytic bed temperature, and resulted in limited production of DME and CO₂ by-products even at high temperatures, whereas interesting yields of DMC with time were obtained relative to the real amount of supported active phase.

Further work is being undertaken in order to increase the amount of Y zeolite supported on the β -SiC material by

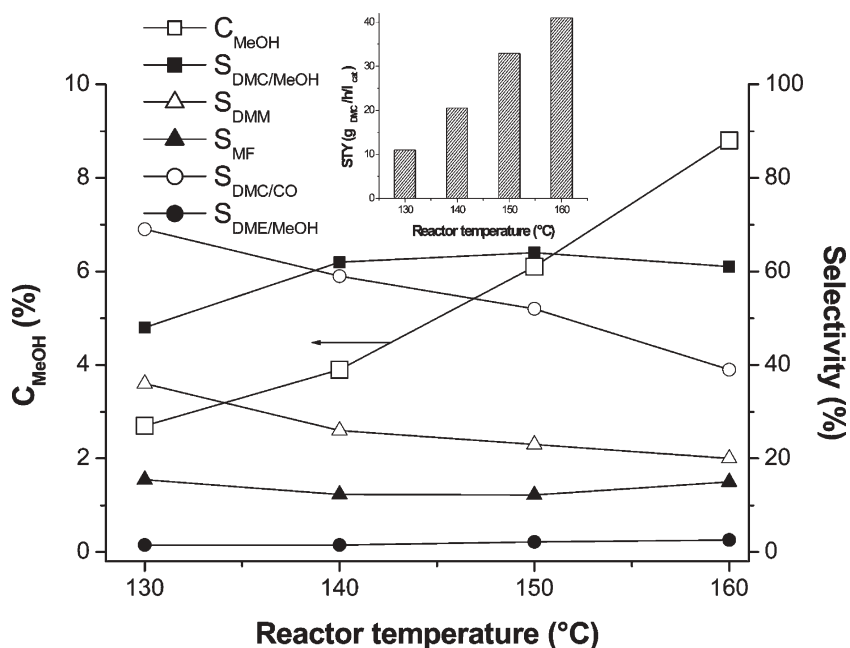


Fig. 6 Influence of the temperature on the performances shown by the β -SiC supported Cu–Y zeolite composite catalyst in terms of methanol conversion, selectivities and STY to DMC.

further coatings, which should allow the STY to be greatly increased, and also to investigate the nature of the badly-crystallized Y–SiC interfacial glue phase and the working state of copper within the Y zeolite framework.

Acknowledgements

The authors are sincerely grateful to the Lürgi AG company for supporting the study. Dr. Thierry Dintzer is acknowledged for performing the SEM analysis. The SICAT company is thanked for synthesizing and providing the β -SiC support material.

References

- 1 D. Delledonne, F. Rivetti and U. Romano, *Appl. Catal., A*, 2001, **221**, 241.
- 2 P. Tundo and M. Selva, *Acc. Chem. Res.*, 2002, **35**, 706.
- 3 (a) M. A. Pacheco and C. L. Marshall, *Energy Fuels*, 1997, **11**, 2; (b) F. Rivetti, *C. R. Acad. Sci.*, 2000, **3**, 497; (c) Y. Ono, *Appl. Catal., A*, 1997, **155**, 133; (d) R. Naejus, R. Coudert and P. Willmann, *Electrochim. Acta*, 1998, **43**, 275.
- 4 H. Babab and A. G. Zeiler, *Chem. Rev.*, 1973, **73**, 75.
- 5 U. Romano, R. Tesel and M. M. Mauri, *Ind. Eng. Chem. Prod. Res. Dev.*, 1980, **19**, 396.
- 6 K. Nishihira, Y. Yamamoto, S. Tanaka, Y. Nishida, T. Matsuzaki, K. Ohdan and A. Nakamura, *J. Chem. Soc., Faraday Trans.*, 1997, **93**(20), 3721.
- 7 G. L. Curnutt and D. L. Harley, in *Oxygen Complexes and Oxygen Activation by Transition Metals*, Plenum Publishing Co., New York, 1988, p. 215.
- 8 (a) M. S. Han, B. G. Lee, B. S. Ahn, D. J. Moon and S. I. Hong, *Appl. Surf. Sci.*, 2003, **211**, 76; (b) M. S. Han, B. G. Lee, I. Suh, H. S. Kim, B. S. Ahn and S. I. Hong, *J. Mol. Catal. A: Chem.*, 2001, **170**, 225.
- 9 K. Tomishige, T. Sakai, S. Sakai and K. Fujimoto, *Appl. Catal., A*, 1999, **181**, 95.
- 10 Y. Yamamoto, T. Matsuzaki, K. Ohdan and Y. Okamoto, *J. Catal.*, 1996, **161**, 577.
- 11 V. V. Kriventsov, O. V. Klimov, O. V. Kikhtyanin, K. G. Ione and D. I. Kochubey, *Nucl. Instrum. Methods Phys. Res., Sect. A*, 2000, **448**, 318.
- 12 A. Punnoose, M. S. Seehra, B. C. Dunn and E. M. Eyring, *Energy Fuels*, 2002, **16**, 182.
- 13 D. Fang and F. Cao, *Chem. Eng. J.*, 2000, **78**, 237.
- 14 H. Itoh, Y. Watanabe, K. Mori and H. Umino, *Green Chem.*, 2003, **5**, 558.
- 15 (a) S. T. King, *J. Catal.*, 1996, **161**, 530; (b) S. T. King, *Catal. Today*, 1997, **33**, 173.
- 16 (a) S. A. Anderson and T. W. Root, *J. Mol. Catal. A: Chem.*, 2004, **220**, 247; (b) S. A. Anderson and T. W. Root, *J. Catal.*, 2003, **217**, 396; (c) S. A. Anderson, S. Manthata and T. W. Root, *Appl. Catal. A: Chem.*, 2005, **280**, 117.
- 17 (a) M. Richter, M. J. G. Fait, R. Eckelt, E. Schreier, M. Schneider, M. M. Pohl and R. Fricke, *Appl. Catal., B*, 2007, **73**(3–4), 69; (b) M. Richter, M. J. G. Fait, R. Eckelt, M. Schneider, J. Radnik, D. Heidemann and R. Fricke, *J. Catal.*, 2007, **245**(1), 11.
- 18 J. C. Jansen, J. H. Koegler, H. van Bekkum, H. P. A. Calis, C. M. van den Bleek, F. Kapteijn, J. A. Moulijn, E. R. Geus and N. van der Puil, *Microporous Mesoporous Mater.*, 1998, **21**(4–6), 213.
- 19 (a) U.S. Pat. Appl. CL-1097-P1, 1998; (b) N. Keller, C. Pham-Huu and M. J. Ledoux, *Appl. Catal., A*, 2001, **217**, 205; (c) G. Garcia Cervantes, F. J. Cadete Santos Aires and J. C. Bertolini, *J. Catal.*, 2003, **214**, 26; (d) W. Z. Sun, G. Q. Jin and X. Y. Guo, *Catal. Commun.*, 2005, **6**, 135.
- 20 N. Keller, C. Pham-Huu, C. Estournès and M. J. Ledoux, *Appl. Catal., A*, 2002, **234**, 191.
- 21 M. J. Ledoux and C. Pham-Huu, *CATTECH*, 2001, **5**(4), 266.
- 22 (a) G. Winé, J. Matta, J. P. Tessonnier, C. Pham-Huu and M. J. Ledoux, *Chem. Commun.*, 2003, 530; (b) G. Winé, J. P. Tessonnier, C. Pham-Huu and M. J. Ledoux, *Chem. Commun.*, 2002, 2418; (c) G. Winé, J. P. Tessonnier, S. Rigolet, C. Marichal, M. J. Ledoux and C. Pham-Huu, *J. Mol. Catal. A: Chem.*, 2006, **248**, 113.
- 23 S. Ivanova, B. Louis, B. Madani, J. P. Tessonnier, M. J. Ledoux and C. Pham-Huu, *J. Phys. Chem. C*, 2007, **111**(11), 4368.
- 24 (a) US Pat. 4914070, 1990; (b) N. Keller, C. Pham-Huu, S. Roy, M. J. Ledoux, C. Estournès and J. L. Guille, *J. Mater. Sci.*, 1999, **34**(13), 3189.
- 25 H. Robson and K. P. Lillerud, *Linde type Y in Verified Synthesis of Zeolitic Materials*, Elsevier, Paris, New-York, 2nd edn. revised, 2001, p. 156.
- 26 G. Wine, PhD Thesis, Louis Pasteur University of Strasbourg, 2004.
- 27 F. Peng and F. Xiao-Bao, *Catal. Today*, 2004, **93–55**, 451.
- 28 (a) P. Yang, Y. Cao, W. L. Dai, J. F. Deng and K. N. Fan, *Appl. Catal., A*, 2003, **243**(2), 323; (b) R. Jiang, Y. Wang, X. Zhao, S. Wang and C. Jin, *J. Mol. Catal. A: Chem.*, 2002, **185**(1–2), 159.
- 29 S. Candamano, P. Frontera, F. Crea and R. Aiello, *Topics Catal.*, 2004, **30–31**, 369.
- 30 A. Zecchina, S. Bordiga, G. Spoto, D. Scarano, G. Petrini, G. Leofanti, M. Padovan and C. O. Arean, *J. Chem. Soc., Faraday Trans.*, 1992, **88**, 2959.
- 31 (a) D. M. Ginter, A. T. Bell and C. J. Radke, in *Synthesis of Microporous Materials, Molecular Sieves*, ed. M. L. Occelli and H. E. Robson, Van Nostrand Reinhold, New York, 1992, vol. 1, p. 6.
- 32 A. J. Hernandez-Maldonado and R. T. Yang, *J. Am. Chem. Soc.*, 2004, **126**, 992.
- 33 F. E. Trigueiro, D. F. J. Monteiro, F. M. Z. Zotin and E. F. Sousa-Aguiar, *J. Alloys Compd.*, 2002, **344**, 337.
- 34 P. Leroi, B. Madani, C. Pham-Huu, M. J. Ledoux, S. Savin-Poncet and J. L. Bousquet, *Catal. Today*, 2004, **91–92**, 53.

Primary biodegradation of ionic liquid cations, identification of degradation products of 1-methyl-3-octylimidazolium chloride and electrochemical wastewater treatment of poorly biodegradable compounds

Stefan Stolte,^{*a} Salha Abdulkarim,^a Jürgen Arning,^a Anne-Katrin Blomeyer-Nienstedt,^c Ulrike Bottin-Weber,^a Marianne Matzke,^b Johannes Ranke,^a Bernd Jastorff^a and Jorg Thöming^c

Received 28th August 2007, Accepted 30th October 2007

First published as an Advance Article on the web 27th November 2007

DOI: 10.1039/b713095c

We investigated the primary biodegradation of different *N*-imidazoles, imidazolium, pyridinium and 4-(dimethylamino)pyridinium compounds substituted with various alkyl side chains and their analogues containing functional groups principally based on OECD guideline 301 D. For the experiments we used two different types of inocula, a freeze-dried mix of bacteria and activated sludge microorganisms from a wastewater treatment plant. The aim of this study was to improve the knowledge base for the structural design of ionic liquids with respect to an increased biodegradability combined with a reduced (eco)toxicological hazard potential. We found a significant primary biodegradation for (eco)toxicologically unfavourable compounds carrying long alkyl side chains (C6 and C8). In contrast for (eco)toxicologically more recommendable imidazolium ionic liquids with short alkyl (\leq C6) and short functionalised side chains, no biological degradation could be found. The introduction of different functional groups into the side chain moiety thus offering a higher chemical reactivity did not lead to the expected improvement of the biological degradation. After an incubation period of 24 days for the 1-methyl-3-octylimidazolium cation we identified different biological transformation products carrying hydroxyl, carbonyl and carboxyl groups. Furthermore, shortened side chain moieties were identified indicating the degradation of the octyl side chain *via* β -oxidation. Moreover, we propose an electrochemical wastewater treatment as part of an alternative disposal strategy for non-biodegradable ionic liquids. We show for the first time that the 1-butyl-3-methylimidazolium cation was completely destroyed within four hours using an electrolysis double-cell (volume = 1.2 L) equipped with electrodes made of iridium oxide (anode), stainless steel (cathode), and a boron-doped diamond-coated bipolar electrode. The products formed electrochemically were easily accessible to biological degradation.

Introduction

In recent years ionic liquids (ILs) have gained a broad interest because of their applicability as solvents in different fields, *e.g.* in organic synthesis,¹ catalysis,² biocatalysis,³ and electrochemistry.⁴ This wide applicability of ionic liquids is mainly based on the beneficial physico-chemical properties (*e.g.* high thermal and electrochemical stability, high conductivity, extraction behaviour, *etc.*) of certain compounds out of this diverse substance class. Furthermore, the negligible vapour pressure of ionic liquids causes reduced air emission and non-flammability. In this respect, the operational safety of ionic liquids is improved as compared to conventional solvents. In

general, the high structural variability of the head group (positively charged core structure), the substituent(s) and the corresponding anion leads to an enormous number of accessible ionic liquids. The combination of these different structural elements allows – at best – for an optimisation of physico-chemical properties of ionic liquids necessary for a defined technical application.

However, regarding the hazard assessment of ionic liquids this structural variability represents an almost insurmountable problem as it is impossible to generate a profound knowledge of the effects on man and the environment for every single compound. Different studies were conducted to evaluate the (eco)toxicity of certain ionic liquids in *in vitro* assays^{5–10} and in some selected organism studies comprising, for example, bacteria,^{11–14} algae,^{15–18} earthworms,¹⁹ waterfleas,^{18,20–22} and zebrafish.²³ A complete overview of the (eco)toxicological data of ionic liquids has been given by Ranke *et al.*²⁴ and Zhao *et al.*²⁵

These studies indicate that ionic liquids can cause adverse effects on organisms. Especially for cations substituted with long (C \geq 8) alkyl side chains^{16–18} or for anions showing lipophilicity or a susceptibility to hydrolysis^{9,16} partially drastic effects have been observed.

^aUFT – Centre for Environmental Research and Technology, Department 3: Bioorganic Chemistry, University of Bremen, Leobener Straße, D-28359 Bremen, Germany.
E-mail: stefan.stolte@uni-bremen.de

^bUFT – Centre for Environmental Research and Technology, Department 10: Ecology, University of Bremen, Leobener Straße, D-28359 Bremen, Germany

^cUFT – Centre for Environmental Research and Technology, Department 4: Process Integrated Waste Minimisation, University of Bremen, Leobener Straße, D-28359 Bremen, Germany

Nevertheless, by an appropriate choice of (eco)toxicologically favourable structural elements as short and functionalised side chains, avoiding the quinolinium and the 4-(dimethylamino)pyridinium head group and by using, for example, chloride, tetrafluoroborate or octylsulfate as the anion,^{8,16,17,26} the (eco)toxicity of an ionic liquid can be reduced remarkably in the test systems investigated so far. This is an important result for the design of inherently safer and thus more sustainable substances. Additionally, according to principles of green chemistry (Paul Anastas and John Warner), chemicals should also be designed to break down to innocuous substances after their use so that they do not accumulate in the environment.²⁷ In contrast, the tendency of certain ionic liquid cations to be thermally and chemically very stable is mirrored in their stability to biological degradation processes. So far, only a few fundamental studies have investigated the biodegradability of ionic liquids.

In a theoretical study, Jastorff *et al.*²⁸ proposed biodegradation pathways for imidazolium cations and presented cytotoxicity data for some of the presumed and subsequently synthesised metabolites.²⁹ Stepnowski and Storoniak³⁰ calculated the energetic stability of radicals formed during the reaction with the cytochrome P450 enzyme system and identified preferred positions of biological transformation reactions for the 1-butyl-3-methylimidazolium cation. Scammells and co-workers^{22,31,32} examined the degradation potential of different 1-butyl-3-methylimidazolium cations combined with Br⁻, BF₄⁻, PF₆⁻, N(CN)₂, (CF₃SO₂)₂N⁻ and octylsulfate as the counterion according to the Sturm and Closed-Bottle test protocols. No compound exhibited significant levels of biodegradation, and only for the octylsulfate-containing ionic liquid was an increased biodegradability observable. A series of imidazolium compounds substituted with amide side chains were analysed and showed poor levels of biodegradation, whereas for different ester group-containing side chains an enhanced biodegradability could be found.^{31–33} However, no compound could be classified as readily biodegradable. In a later study the combination of the imidazolium moiety substituted with ester side chains and octylsulfate as the counterion resulted in readily biodegradable ionic liquids.³³

Wells and Coombe¹⁸ investigated the biodegradability of ammonium, imidazolium, phosphonium and pyridinium compounds by measuring the biological oxygen demand (BOD). No biodegradability of cations with short chains (C ≤ 4) was observable within this test series. For phosphonium and imidazolium cations with longer chains (C12, C16 and C18) a strong inhibitory potential to the inoculum used was found, indicating the toxicity of these ionic liquids towards the microorganisms used.

Recently, Kulpa and co-workers³⁴ examined the biodegradability of *N*-methylimidazolium and 3-methylpyridinium compounds substituted with butyl, hexyl and octyl side chains and bromide as the anion. In dissolved organic carbon (DOC) die-away tests and in tests monitoring the changes in the total dissolved nitrogen (TDN) concentration a dependency between biodegradability and the side chain length was found. 1-Octylpyridinium bromide meets the OECD criterion for being classified as readily biodegradable, whereas

1-hexylpyridinium bromide exhibited a decreased degradation rate. Compared to the pyridinium ILs the mineralisation of the imidazolium ILs was lower. The 1-methyl-3-octylimidazolium cation showed significant degradation rates, but those were not high enough for a classification as readily biodegradable. For the pyridinium and imidazolium head groups carrying a butyl side chain no significant biodegradation was observable. The fact that only the long octyl side chain in ionic liquids brings about an improved biodegradability creates a conflict of aims between minimizing the toxicity and maximizing the biodegradability. Thus, the biodegradability seems to be a bottle-neck in the development of inherently safer ionic liquids.

Following our strategy of designing safer ionic liquids^{28,29} we aimed to overcome this inherent problem and to enlarge the restricted knowledge in the field of biodegradation of ionic liquids, and we analysed systematically the influence of the structural elements 'head group' and 'side chain' (also containing functional groups) on the biodegradability of 27 compounds. Regarding this issue we follow a T-SAR (thinking in terms of structure–activity relationships) guided strategy to:

- (i) systematically select test compounds and structural elements according to the 'test kit concept',^{29,35}
- (ii) apply a theoretical T-SAR algorithm to propose biological transformation products (metabolites),^{28,36}
- (iii) test the selected substances in biodegradation tests using inocula from a wastewater treatment plant according to a modified OECD test protocol;
- (iv) ascertain the primary biodegradation of compounds and identify transformation products *via* HPLC–UV and HPLC–MS analysis;
- (v) identify substructures in chemicals responsible for an improved or declined biodegradability;
- (vi) incorporate the transformation products formed into the hazard assessment of ionic liquids and investigate the (eco)toxicity of the transformation products using test systems at different levels of biological complexity (*e.g.* enzymes, cells, micro-organisms and organisms);
- (vii) use this knowledge in the prospective design of inherently safer chemical products.

For non-biodegradable ionic liquid cations (tested as halides) we propose an electrochemical wastewater treatment using boron-doped diamond (BDD)-coated electrodes to facilitate their breakdown. This electrochemical process is often applied to eliminate biologically persistent compounds.^{37,38} In general, the BDD coating exhibits a high oxygen overpotential which promotes the electro-oxidation of organics *via* electrogenerated hydroxyl radicals due to their high standard redox potential of 2.8 V and reduces the side reaction of oxygen evolution.³⁹ The formed radicals can effectively transform non-biodegradable organic species to biodegradable organic compounds or final inorganic ones like CO₂ and H₂O.^{37,40,41}

Selection of test kit compounds

The test kit comprises different cations combined with a halide (chloride, bromide or iodide) the as counterion. Three

aromatic head groups [4-(dimethylamino)pyridinium, pyridinium and 1-methylimidazolium] substituted with different alkyl side chains (C2, C4, C6, C8) and some mono-*N*-substituted imidazole compounds are included in the test kit. The pyridinium and imidazolium substances are selected to confirm the results from literature and for a validation of the primary degradation tests used. Furthermore, the HPLC–MS analysis allows for an identification of degradation products of these compounds and expands the currently available data.

The 4-(dimethylamino)pyridinium head group, which is not recommendable from an (eco)toxicological point of view,^{8,17,42} was analysed because of its high lipophilicity. This head group being substituted with a hexyl side chain exhibits the same lipophilicity (corresponding to a HPLC-determined parameter) as an octyl-substituted imidazolium compound.⁸ This fact allows for differentiation whether the side chain length or the lipophilicity of a compound is responsible for an increased biodegradability.

Additionally, the imidazolium core is substituted with short side chains containing ether (in different positions), terminal hydroxyl, carboxyl and nitrile functions. These compounds were selected because of their (eco)toxicological beneficial properties and for investigating if the increased chemical reactivity of these functionalised cations concomitantly increases the biodegradability.

Experimental

Chemicals

All tested ionic liquids were received from Merck KGaA (Darmstadt, Germany). Na₂SO₄, KH₂PO₄, K₂HPO₄, Na₂HPO₄·2H₂O, CaCl₂·2H₂O, MgSO₄·7H₂O, FeCl₃·7H₂O and H₂SO₄ were purchased from the Sigma-Aldrich Cooperation (Deisenhofen, Germany). Acetonitrile (HPLC grade), methanol, HgCl₂, NH₄Cl and sodium benzoate were obtained from Fluka (Buchs, Switzerland).

HPLC systems

The HPLC system used for the determination of primary biodegradation and the electrochemical degradation studies was a VWR Hitachi system containing the L-2130 HTA-pump, L-2130 degasser, L-2200 autosampler, L-2300 column oven, L-2450 diode array-detector and the EZChrom Elite software. The HPLC system utilised for analysing degradation products was a Hewlett Packard system Series 1100, with a gradient pump, online degasser, autosampler and a Bruker esquire ESI-MS ion trap detector.

For both systems a hydrophilic interaction liquid chromatography (HILIC) column (Atlantis HILIC Silica 5 μm, 4.6 × 150 mm) with guard column purchased from Waters (Eschborn, Germany) was used. The mobile phase consisted of 80% acetonitrile (HPLC grade) and 20% aqueous 5 mM HK₂PO₄/H₂SO₄ buffer. The system was operated at a flow rate of 1 mL min⁻¹ and 10 μL portions of the samples were injected. A detection wavelength of 212 nm was used for quantification of the original compounds.

Primary biodegradation

The primary biodegradation test was conducted according to a modified version of OECD guideline 301 D.⁴³ Primary biodegradation of the test compounds was monitored *via* HPLC–UV for 31 days. The inoculum used was derived from the wastewater treatment plant Bremen-Seehausen (Germany). Five gram sludge flocs were suspended in 1 L mineral medium and pre-conditioned for 5 days under aerobic conditions. The mineral medium was composed of 8.5 mg L⁻¹ KH₂PO₄, 21.75 mg L⁻¹ K₂HPO₄, 22.13 mg L⁻¹ Na₂HPO₄·2H₂O, 1.7 mg L⁻¹ NH₄Cl, 36.4 mg L⁻¹ CaCl₂·2H₂O, 22.5 mg L⁻¹, MgSO₄·7H₂O and 0.25 mg L⁻¹ FeCl₃ (pH 7.2). Solutions of the test substances were prepared at a concentration of 200 μM (corresponding to 14–61 mg L⁻¹ depending on the molecular weight of the test substances) in inoculated test media (100 mL total volume). Blank samples (inoculated media without test the substance), abiotic controls (200 μM test substance in inoculated media poisoned with 50 mg L⁻¹ HgCl₂) and positive controls (inoculated media with 200 μM imidazole) were also prepared. Replicates of test samples, blanks, abiotic and positive controls were kept in the dark at 20 ± 1 °C. The 100 mL test vessels were closed but not gas-tight. Losses due to evaporation were determined by weighing and were adjusted by the addition of test media. For every testing day 500 μL of all samples were taken, centrifuged (5000 rpm, 15 min) and subsequently analysed *via* HPLC. The percentage of degradation of each sample was calculated referring to the initial concentration.

Oxygen consumption biodegradation experiment

The biodegradation experiments using the sum parameter oxygen depletion was performed due to the DIN EN 1899-2 guideline.⁴⁴ The test solutions were added to the same test media used for the primary degradation test and were inoculated with a commercially available freeze-dried micro-organism mixture (Dr. Lange BioKIT LZC 555).⁴⁵ All experiments were performed in Karlsruhe-bottles, which are adapted to the oxygen electrode used (StirrOx G). Triplicates of each test solution, blanks and controls (using sodium benzoate) were analysed for each sampling day and were discarded after determination of the oxygen content. The oxygen depletion for the test solutions at a given time was corrected by the oxygen demand of the blank after the same time period.

For the determination of the chemical oxygen demand (COD) the cuvette high-speed tests LCK 314, 414, 514, 614 and 014 (Hach Lange GmbH, Düsseldorf, Germany) were used and measured with a photometer Cadas 200 (Hach Lange GmbH, Düsseldorf, Germany).

Electrochemical treatment

The electrochemical degradation investigations have been carried out with aqueous solutions of 1-butyl-3-methylimidazolium chloride (IM14 Cl) at a concentration of 230 μM (40 mg L⁻¹) which was supplemented with 0.06 M Na₂SO₄ and 0.15 M KOH. The conductivity of the mixture was measured to be 20 mS using a WTW inoLab station with a TetraCon conductivity electrode.

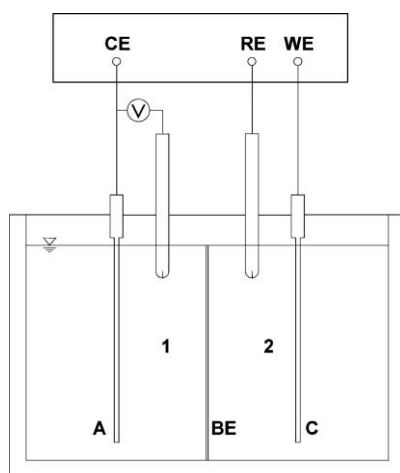


Fig. 1 Electrolysis reactor (A = anode, C = cathode, BE = bipolar BDD- mid-electrode, which divides the reactor into two chambers, RE = reference electrode, WE = working electrode, CE = counter electrode).

The electrochemical degradation experiments were carried out in an electrolysis cell (volume = 1.2 L) equipped with two electrodes made of iridium oxide (anode) and stainless steel (cathode). Additionally, a bipolar mid-electrode – purchased from ‘pro aqua Diamantelektroden Produktion GmbH’ (Niklasdorf, Germany) – made of polyvinylidene fluoride (PVDF) fitted with boron-doped diamonds was used. This electrode arrangement divided the reactor into two chambers (Fig. 1). The distances between the electrodes were 2 cm. The experiments were performed with a constant potential of 2.5 V at the steel cathode adjusted with a reference electrode placed next to the cathode. As the potentiostat an IMP83 PC-10-device of the company ‘Jaisle Elektronik GmbH’ (Waiblingen, Germany) and a power supply unit of the company ‘Statron’ (Zschopau, Germany) were employed.

Results

For biodegradation tests two different types of inocula were used. A commercially available freeze-dried micro-organism mixture (Dr. Lange BioKIT LZC 555) composed for the determination of sewage water qualities⁴⁵ and, secondly, activated sludge from a wastewater treatment plant (Bremen-Seehausen, Germany) was applied.

The freeze-dried bacteria mixture was chosen because this is a standardised product and should allow for a high reproducibility between different test runs. Furthermore, this mixture showed an acceptable biological matrix compared to the activated sludge and therefore caused less interference in the HPLC–UV and HPLC–MS analysis. However, no test substance was metabolised in the primary degradation tests using these freeze-dried bacteria. Thus, all results presented in the following section are related to tests using the activated sludge.

Toxicity and adsorption

None of the test substances inhibited the biodegradability of the reference compound imidazole in the concentration range tested, indicating that the ionic liquids used are not toxic towards the micro-organisms.

The adsorption of the test substances to the activated sludge was checked with an abiotic control (sludge inactivated with HgCl₂). No test compound showed significant sorption to the inoculum. Consequently, an observed concentration decrease of a test substance in biotic samples can be exclusively attributed to biological degradation.

Primary biodegradation

Mono-*N*-substituted imidazole compounds. No decrease in the concentration within the test duration of 31 days could be found for *N*-methylimidazole (IM01), *N*-butylimidazole (IM04), and *N*-octylimidazole (IM08) (Table 1), whereas

Table 1 Structures, acronyms and primary biodegradation rates of alkylimidazoles

Structure	Acronym	Primary biodegradation (%)				
		Day 4	Day 9	Day 17	Day 24	Day 31
	IM00	100	100	100	100	100
	IM01	0	0	0	0	0
	IM01-2Me	0	0	9	93	100
	IM04	0	0	0	0	0
	IM08	0	0	0	0	0

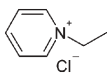
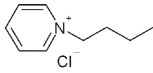
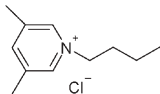
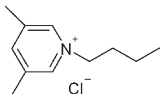
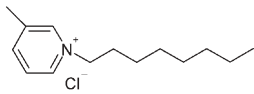
N-methyl-2-methylimidazole (IM01-2Me) was completely degraded after 31 days (Table 1). The positive control, imidazole (IM00), was completely degraded after four days.

Imidazolium ionic liquids. Most of the imidazolium ionic liquids were not metabolised by the activated sludge microbial community (Table 2). In particular, imidazolium cores substituted with short alkyl side chains or short

Table 2 Structures, acronyms and primary biodegradation rates of 1-alkyl-3-methylimidazolium halides

Structure	Acronym	Primary biodegradation (%)				
		Day 4	Day 9	Day 17	Day 24	Day 31
	IM12 Cl	0	0	0	0	0
	IM14 Cl	0	0	0	0	0
	IM16 Cl	0	0	5	8	11
	IM18 Cl	31	40	81	100	100
	IM18OH Br	25	58	100	100	100
	IM17COOH Br	10	18	100	100	100
	IM1-1Ph Cl	0	0	0	0	0
	IM12OH I	0	0	0	0	0
	IM11CN Cl	0	0	0	0	0
	IM13OH Cl	0	0	0	0	0
	IM11O2 Cl	0	0	0	0	0
	IM12O1 Cl	0	0	0	0	0
	IM2O2 Br	0	0	0	0	0
	IM13O1 Br	0	0	0	0	0

Table 3 Structures, acronyms and primary biodegradation rates of *N*-alkylpyridinium chlorides

Structure	Acronym	Primary biodegradation (%)				
		Day 4	Day 9	Day 17	Day 24	Day 31
	Py2 Cl	0	0	0	0	0
	Py4 Cl	0	0	0	0	0
	Py4-3Me-5Me Cl	0	0	0	0	0
	Py8 Cl	0	25	58	100	100
	Py8-3Me Cl	0	25	33	97	100

side chains containing ether, hydroxyl and nitrile functions were highly resistant to biological degradation during the incubation period (Table 2). That also applies to the phenyl-linked imidazolium compound (IM1-1Ph Cl). Small losses (–11%) of 1-hexyl-3-methylimidazolium (IM16) were measured after 31 days compared to the initial concentration (Table 2). A complete primary degradation could be detected for 1-methyl-3-octylimidazolium (IM18) after 24 days, and after 17 days for the hydroxylated (IM18OH) and for the carboxylated (IM17COOH) derivative (Table 2).

Pyridinium ionic liquids. The *N*-ethylpyridinium (Py2) and the *N*-butylpyridinium compounds (Py4 and Py4-3Me-5Me) did not undergo significant biodegradation, whereas

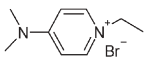
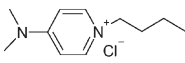
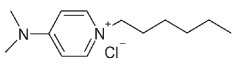
for the *N*-octylpyridinium cations (Py8 and Py8-3Me) a total elimination was observed within 31 days (Table 3).

Dimethylaminopyridinium ionic liquids. In contrast to the *N*-hexyl-substituted 4-(dimethylamino)pyridinium head group (Py6-4NMe2) which was completely degraded within 31 days (Table 4), no biological breakdown could be observed for the *N*-ethyl- and *N*-butyl-derivatives (Py2-4NMe2 and Py4-4NMe2).

Identified transformation products of 1-octyl-3-methylimidazolium

The 24 day sample of the 1-octyl-3-methylimidazolium cation (IM18) was investigated for biodegradation products *via*

Table 4 Structures, acronyms and primary biodegradation rates of *N*-alkyl-4-(dimethylamino)pyridinium halides

Structure	Acronym	Primary biodegradation (%)				
		Day 4	Day 9	Day 17	Day 24	Day 31
	Py2-4NMe2 Br	0	0	0	0	0
	Py4-4NMe2 Cl	0	0	0	0	0
	Py6-4NMe2 Cl	6	12	55	93	100

HPLC–MS analysis. For this sample, no clear UV peaks were seen but different signals within the mass spectrometer were detectable. To ensure that the signals found within this sample correspond to transformation products a blank sample (inoculated test buffer after 24 days) and a sample from the beginning of the test were measured. None of the identified masses in the 24 day sample of IM18 were found in these reference analyses.

The identified transformation products and the concluded pathway for biodegradation of the IM18 compound are shown in Fig. 2. At different retention times the mass-to-charge ratio (m/z^+) 211 was detected, probably belonging to hydroxyl groups at different positions at the side chain of IM18. The observed retention time is similar to the investigated test compound IM18OH (14 min). Furthermore, different signals with $m/z^+ = 209$ could be determined, presumably pertaining to ketones or aldehydes after the oxidation of different hydroxylated compounds. The mass-to-charge ratio of 225 potentially corresponds to a carboxylated product of IM18 (like the test compound IM17COOH; retention time 12.3 min) or to substances containing two functional groups (ketone and hydroxyl). In accordance with this,

$m/z^+ = 225$ occurred in a relatively wide retention time range of 2.5 min, indicating clear structural differences as occur between different carboxylic acids or compounds substituted with both ketone and hydroxyl functions.

Moreover, hydroxylated and/or carboxylated compounds with a reduced number (-2 , -4 or -6) of carbon atoms in the side chain were found (Fig. 2). For these compounds the identified masses occurred as well-defined single peaks suggesting that no isomers with the same mass were formed. The chemical transformations identified were in accordance with the recently predicted ones.²⁸

Adaptation and accumulation of degradation products

After the test period of 31 days the IM18 test bottles were used for a subsequent experiment. To these samples additional IM18 was given (final concentration of 200 μM). For these experiments with pre-adapted inocula an increased biodegradation rate was observed. Within four days a complete primary degradation of IM18 had taken place. This procedure was repeated for two other supplementations of the test compound (all at 600 μM). For all test runs an exhaustive primary degradation was observable after four days. In

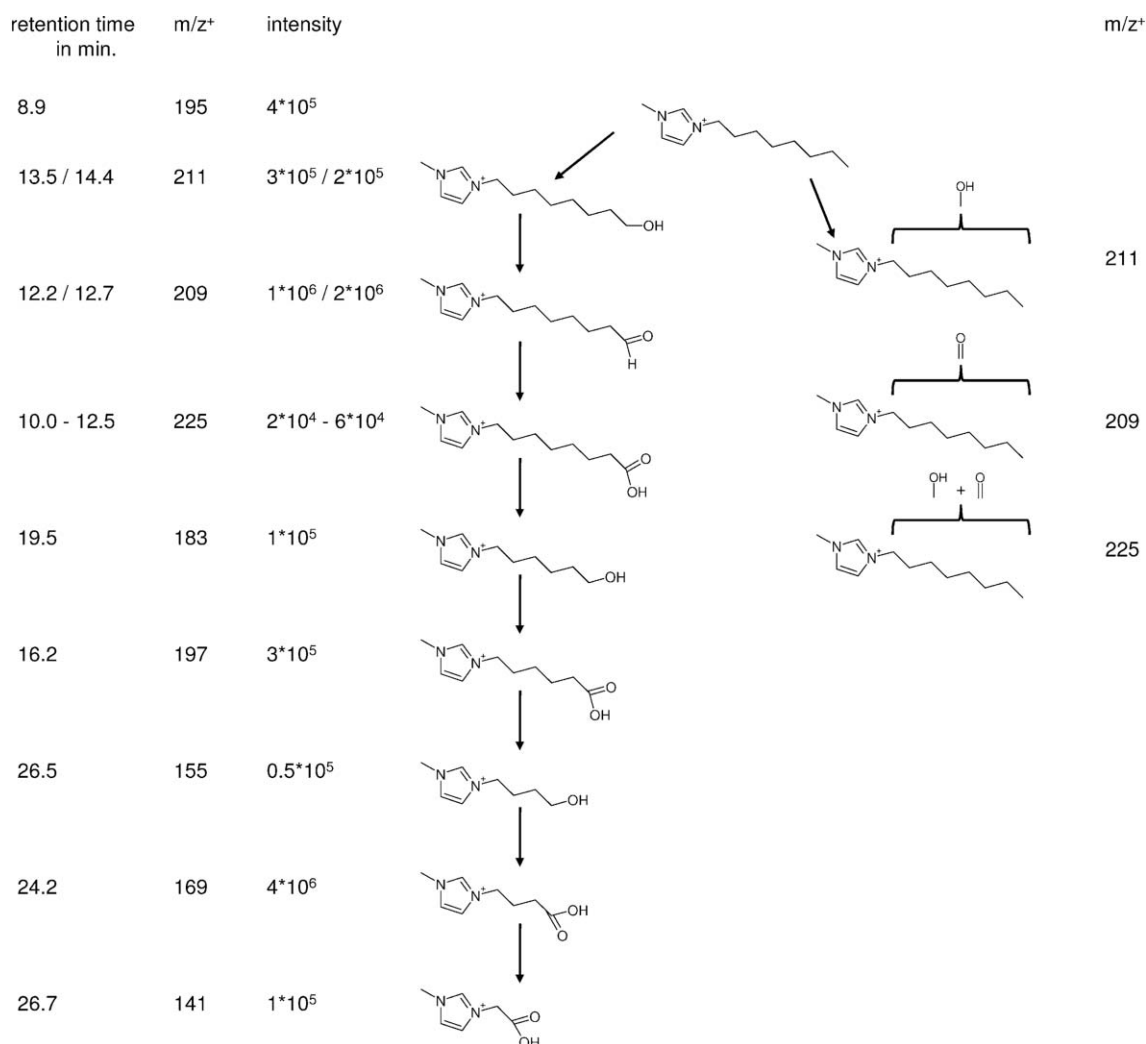


Fig. 2 Retention times, mass-to-charge ratios (positive mode), intensity of signals within the mass spectra and proposed chemical structures.

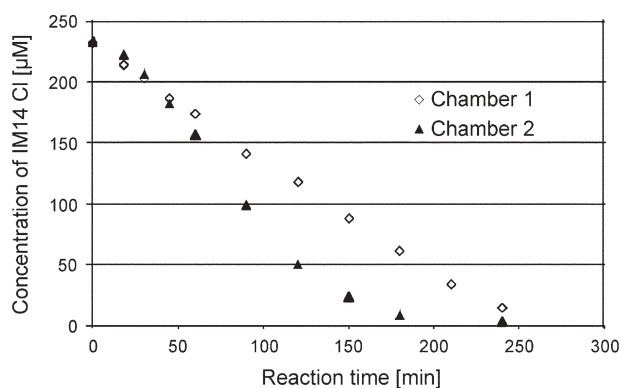


Fig. 3 HPLC-determined degradation of the 1-butyl-3-methylimidazolium cation during the electrolysis experiment.

general, no UV signal within the chromatogram of the spiked samples could be detected except for a peak at approximately 14 min (probably belonging to a hydroxylated product) with a concentration of 220 μM (if calculated as IM18OH). After an additional period of 31 days a remaining concentration of 10 μM was determined.

Electrochemical treatment of 1-butyl-3-methylimidazolium chloride

A nearly complete electrochemical dismantling of the 1-butyl-3-methylimidazolium cation (IM14) within the test duration of 240 min could be observed *via* HPLC–UV measurements (Fig. 3). For chamber 1 (iridium oxide anode/bipolar boron-doped cathode) a linear breakdown of IM14 was observable with a remaining ionic liquid concentration of 14 μM (substance loss 96%). The degradation course in the second chamber (bipolar-doped anode/steel cathode) was sigmoidal and led to a final IM14 concentration of 3 μM (substance loss 99%). The HPLC analysis of the different sampling points revealed various signals for both chambers – mainly with longer retention times on the HILIC column as found for the IM14 cation, indicating more polar chemical entities. After 240 min these signals of breakdown products were not or only marginally detectable. During electrochemical treatment an increasing electrical current (from 1.1 to 5.7 A) and temperature (19 to 58 $^{\circ}\text{C}$) was observed. Furthermore, the chemical oxygen consumption (COD) – used to for indirectly measuring the amount of organic carbon in water – was reduced by around two-thirds for both chambers (chamber 1: $t_0 = 69 \text{ mg L}^{-1}$, $t_{240} = 23 \text{ mg L}^{-1}$; chamber 2: $t_0 = 69 \text{ mg L}^{-1}$, $t_{240} = 24 \text{ mg L}^{-1}$). The biodegradability of the solutions remaining after the electrochemical treatment (pH adjusted at 7 and inoculated with freeze-dried bacteria) was measured by the oxygen depletion assay. The biological oxygen demand (BOD) after 3, 6, and 8 days was determined for both chambers (Fig. 4). An oxygen consumption for both samples was detectable (chamber 1: $4.7 \text{ mg L}^{-1} \approx -60\%$, chamber 2: $4.1 \text{ mg L}^{-1} \approx -55\%$) associated with a decreased COD (chamber 1: $14 \text{ mg L}^{-1} \approx -41\%$, chamber 2: $14 \text{ mg L}^{-1} \approx -42\%$).

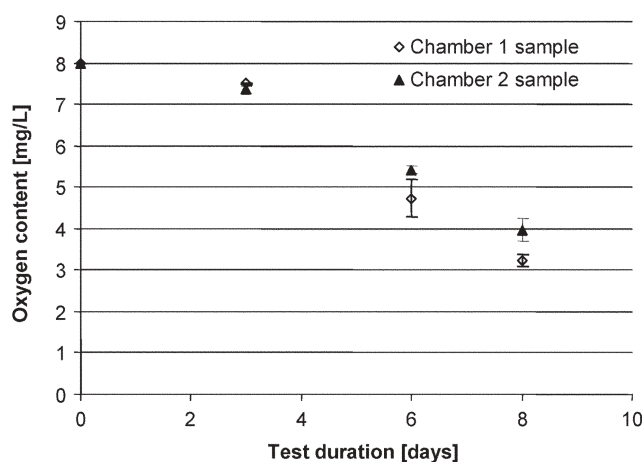


Fig. 4 Biological oxygen consumption of the remaining solutions after electrochemical treatment.

Discussion

Relevance of the primary biodegradation test

The test conditions employed for the primary biodegradation investigations are very similar compared to the ready biodegradability test according to OECD guideline 301 D. This allows for classifying structures as not readily biodegradable, when no clear decrease in the concentration of the test substance was observed.

In contrast, it is not possible within this primary degradation test to term compounds as readily biodegradable, even if a 100% degradation of the test substance is observed, because this 100% degradation is related only to the parent compound (primary degradation) and not to all possibly formed metabolites which might be resistant to further biodegradation.

In general, it is known from biodegradation experiments that after an adaptation period at the beginning of the tests a rapid biodegradation can occur within a few days. In our setup the timeframe between successive sampling points was too long to follow the degradation kinetics in detail.

Primary biodegradation of test compounds

The freeze-dried bacteria mixture was proven not to be suitable for evaluation of the general biodegradability of compounds according to OECD guidelines. This is related to the limited diversity of micro-organisms within this arranged mixture compared to the heterogeneous micro-organism community of the activated sludge.

The results obtained for the wastewater micro-organisms showed that the mono-*N*-substituted imidazole derivatives, which are considered to be poorly biodegradable,^{46,47} could be confirmed for the *N*-alkylated imidazoles investigated here. An exception is *N*-methyl-2-methylimidazole (IM01-2Me), the observed primary degradation of which is unexpected. Either the microbial community used contained a specific micro-organism which could catabolise this substrate or the degradation was just related to the mother compound and not to the transformation products.

For imidazolium ionic liquids with short alkyl ($\leq C6$) and short functionalised side chains no biological degradation could be found. The introduction of functional groups linked to a higher chemical reactivity did not lead to the expected improvement of the biological degradation.

Our study confirmed the results found by Docherty *et al.*,³⁴ that imidazolium and pyridinium compounds with octyl chains are biodegradable. A complete primary degradation was observed within 24 days for IM18 and Py8. On the basis of the identified transformation products of IM18 we propose the breakdown pathway shown in Fig. 2. Here the transformation of the alkyl chain starts with the oxidation of the terminal methyl group (ω -oxidation) catalysed probably by mono-oxygenases, *e.g.* the cytochrome P450 system. The alcohol formed is subsequently oxidised by dehydrogenases *via* aldehydes to carboxylic acids (Fig. 2). The resulting carboxylic acids then can undergo β -oxidation and the two released carbon fragments can enter the tricarboxylic acid cycle as acetylCo-A.

The HPLC–MS results also indicate the formation of different non-terminal hydroxyl groups referring to identical masses but showing varying retention times. These secondary alcohol isomers could not be further degraded *via* β -oxidation. Their transformation process ended either with the formation of ketones or by additional hydroxylation steps. In contrast, for the shortened chain metabolites formed by the β -oxidation steps all identified compounds produced single peak signals, which means that no isomers were formed.

Additionally, we have found that the microbial community was able to adapt to the degradation of IM18. This could be observed by a clear reduction in the degradation time from 24 days down to four days after three additional supplementations of IM18. Potentially, this observation can also be addressed to an increased bacterial concentration within the sample. A total of 800 μM of IM18 was degraded and no transformation products were detected *via* HPLC–UV, indicating a complete biodegradation including the imidazolium core (responsible for UV absorption). Even if IM18 cannot be classified as readily biodegradable it is at least inherently biodegradable. Those results agree with results found by Docherty's group.³⁴

The introduction of $-\text{OH}$ and $-\text{COOH}$ into the octyl chain resulted in an improved primary degradation with a shortened test duration of 17 days. For those compounds an ω -oxidation is not necessary, so the β -oxidation can occur immediately. Therefore, we assume that the ω -oxidation is the rate-limiting step within the biodegradation process of IM18.

Whereas no biodegradation of IM16 occurred, Py6-4NMe2 was totally biodegradable within 31 days. Recently, we investigated the lipophilicity of different compounds using an HPLC-derived parameter (k_0). We found similar lipophilicity values for IM18 ($k_0 = 1.85$)²⁶ and Py6-4NMe2 ($k_0 = 1.80$).²⁶ Therefore, it can be concluded that the chain length ($C = 8$) is not a mandatory criterion for biodegradation, but more important is a certain overall lipophilicity of the compound.

This observation can be explained in at least two ways. First, ionic liquids with longer alkyl chains (higher lipophilicity) have been proven to be more toxic. Therefore, they are able

to produce selective pressure on the microbial community – micro-organisms being capable of degrading ionic liquids with longer alkyl chains are privileged whereas the others that are not able to metabolise ionic liquids are eliminated. This assumption has been proven by Docherty *et al.* who analysed the structure of the microbial community by DNA-PCR DGGE and found an enrichment of few bacteria species in the samples treated with IM18.³⁴

A second explanation is based on an uptake or even an increased uptake into the organisms, which is also related to the lipophilicity of the compounds. Owing to this (higher) uptake the substances can be metabolised by appropriate enzyme systems.

In contrast, IM08 was not degraded even though it is mainly protonated under test conditions ($\text{pH} = 7$) and therefore should possess a similar lipophilicity compared to IM18. Also, the cytotoxicity of IM18 (100 μM) and IM08 (150 μM) is comparable. According to our above-mentioned hypotheses this result was not expected and IM08 should have been biodegradable.

In general, the identified transformation products of IM18 are compounds with shorter side chains and functionalised groups. Previous studies from our group showed that compounds with short and functionalised side chains exhibit lower toxicities towards mammalian cells,⁸ marine bacteria, limnic green algae¹⁷ and duckweed.¹⁷ Therefore, we propose for most of the transformation products lower hazard potentials compared to IM18, which has a high aquatic toxicity (especially to algae)¹⁶. Nevertheless, some restrictions have to be made because the aldehydes, which are intermediates in the oxidation pathway from the $-\text{CH}_2\text{OH}$ group to the $-\text{COOH}$ group, have not been analysed regarding their (eco)toxicity so far and in principle the formation of highly reactive epoxides is thinkable.

Further investigations in this field are desirable to examine the detailed biodegradation pathways, detailed kinetics and the metabolites of ionic liquids showing primary biodegradation. With respect to the design of inherently safer ionic liquids it is necessary to find structural modifications which improve biodegradability without increasing lipophilicity, which correspondingly would increase the toxicity.

Both IM18OH and IM17COOH are biodegradable and they exhibit a reduced cytotoxicity (EC_{50} IM18OH Br = 230 μM ; EC_{50} IM17COOH Br = 3000 μM) as compared to IM18 Cl (EC_{50} IM18 Cl = 60 μM). However, it still has to be investigated if the physico-chemical properties of these ionic liquids ($\text{mp} < 100^\circ\text{C}$) are useful for technical applications and if their toxicities to algae are also in an acceptable range.

The biodegradability of, for example, morpholinium and piperidinium moieties have not been investigated so far, but their *N*-alkylation probably will lead to poorly biodegradable compounds.

Based on the experiences gathered so far, the introduction of oxo-groups into the ring *N*-heterocycles (Fig. 5) should increase biodegradability, because this substructure represents a target site for the cleavage of the C–N bond by an amidohydrolase.⁴⁷ But again, the changes in the physico-chemical properties have to be investigated.

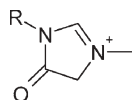


Fig. 5 Introduction of an oxo-group into the core structure represents a potential target site for the cleavage of the C–N bond by an amidohydrolase.

Electrochemical treatment

An electrochemical treatment – as an alternative disposal strategy for non-biodegradable compounds – was applied exemplarily for an aqueous solution of 1-butyl-3-methylimidazolium chloride. An almost complete primary degradation of the IM14 cation was determined *via* HPLC–UV measurements within 4 h. The degradation rate of IM14 in the second chamber was higher compared to the first chamber. This observation is probably caused by an increased formation of hydroxyl radicals at the surface of the anodic side (toward chamber 2) of the bipolar boron electrode. In general, no UV signals after the electrochemical reaction could be found in the chromatogram leading to the conclusion that the positively charged imidazolium core structure (considered mainly to be responsible for the non-biodegradability) has been destroyed. The chemical oxygen demand was decreased in both chambers indicating an electrochemical burning of the test compounds and of the transformation products formed. The remaining solution after the electrolysis process has been analysed in a biodegradation test. For both chambers a clear oxygen consumption through the test micro-organisms used was found after eight days, suggesting an improved biodegradability of the transformation products in comparison to IM14.

These investigations represent a first feasibility study that an electrochemical treatment could be an appropriate technique to remove ionic liquids from wastewater. Detailed examinations evaluating the applicability of this technique – including an optimisation of the performance, the identification of transformation products and a toxicity assessment for the generated solution – are in preparation.

Conclusion

We used a primary biodegradation test to analyse the biodegradability of 27 different compounds with different head groups and side chains. Our results strongly indicate that a certain lipophilicity of the test compounds is an essential criterion for biodegradable ionic liquid cations. However, a high lipophilicity corresponds to an increased (eco)toxicity in different test systems. Thus, a conflict of goals between (eco)toxicologically favourable compounds (short and functionalised side chains) on the one hand and inherently biodegradable substances on the other hand needs to be solved for the development of more sustainable ionic liquids.

The electrochemical wastewater treatment is proposed as an alternative disposal strategy for non-biodegradable ionic liquid cations. Nevertheless, the design of inherently biodegradable ionic liquids should be preferred due to a reduced hazard for man and the environment. Furthermore, here the energy consumption and the need for further chemicals and apparatus

is reduced compared to an electrochemical wastewater treatment.

Acknowledgements

The authors gratefully thank Professor Detmar Beyersmann, Professor Friedrich Widdel, Dr Olav Grundmann, Dr Michael Baune and the whole ionic liquids team in the UFT for helpful discussions. Furthermore, special thanks are given to the Merck KGaA for providing chemicals and for their generous support within our strategic partnership.

References

- 1 S. Chowdhury, R. S. Mohan and J. L. Scott, *Tetrahedron*, 2007, **63**(11), 2363–2389.
- 2 C. Fellay, *Chimia*, 2007, **61**(4), 172–174.
- 3 H. Zhao, *J. Mol. Catal. B: Enzym.*, 2005, **37**, 16–25.
- 4 D. S. Silvester and R. G. Compton, *Z. Phys. Chem.*, 2006, **220**(10–11), 1247–1274.
- 5 J. Ranke, K. Molter, F. Stock, U. Bottin-Weber, J. Poczobutt, J. Hoffmann, B. Ondruschka, J. Filser and B. Jastorff, *Ecotoxicol. Environ. Safety*, 2004, **58**(3), 396–404.
- 6 P. Stepnowski, A. C. Skladanowski, A. Ludwiczak and E. Laczynska, *Hum. Exp. Toxicol.*, 2004, **23**(11), 513–517.
- 7 F. Stock, J. Hoffmann, J. Ranke, R. Stormann, B. Ondruschka and B. Jastorff, *Green Chem.*, 2004, **6**(6), 286–290.
- 8 S. Stolte, J. Arning, U. Bottin-Weber, A. Müller, W. R. Pitner, U. Welz-Biermann, B. Jastorff and J. Ranke, *Green Chem.*, 2007, **9**(8), 760–767.
- 9 S. Stolte, J. Arning, U. Bottin-Weber, M. Matzke, F. Stock, K. Thiele, M. Uerdingen, U. Welz-Biermann, B. Jastorff and J. Ranke, *Green Chem.*, 2006, **8**(7), 621–629.
- 10 R. F. M. Frade, A. Matias, L. C. Branco, C. A. M. Afonso and C. M. M. Duarte, *Green Chem.*, 2007, **9**(8), 873–877.
- 11 M. Matsumoto, K. Mochiduki and K. Kondo, *J. Biosci. Bioeng.*, 2004, **98**(5), 344–347.
- 12 J. Pernak, J. Kalewska, H. Ksycynska and J. Cybulski, *Eur. J. Med. Chem.*, 2001, **36**(11–12), 899–907.
- 13 J. Pernak, K. Sobaszekiewicz and I. Mirska, *Green Chem.*, 2003, **5**(1), 52–56.
- 14 J. Pernak, I. Goc and I. Mirska, *Green Chem.*, 2004, **6**(7), 323–329.
- 15 A. Latala, P. Stepnowski, M. Nedzi and W. Mroziak, *Aquat. Toxicol.*, 2005, **73**(1), 91–98.
- 16 M. Matzke, S. Stolte, K. Thiele, T. Juffernholz, J. Ranke, U. Welz-Biermann and B. Jastorff, *Green Chem.*, 2007, **9**(11), 1198–1207.
- 17 S. Stolte, M. Matzke, J. Arning, A. Bösch, W. R. Pitner, U. Welz-Biermann, B. Jastorff and J. Ranke, *Green Chem.*, 2007, **9**(11), 1170–1179.
- 18 A. S. Wells and V. T. Coombe, *Org. Process Res. Dev.*, 2006, **10**(4), 794–798.
- 19 R. P. Swatloski, J. D. Holbrey, S. B. Memon, G. A. Caldwell, K. A. Caldwell and R. D. Rogers, *Chem. Commun.*, 2004(6), 668–669.
- 20 R. J. Bernot, M. A. Brueseke, M. A. Evans-White and G. A. Lamberti, *Environ. Toxicol. Chem.*, 2005, **24**(1), 87–92.
- 21 D. J. Couling, R. J. Bernot, K. M. Docherty, J. K. Dixon and E. J. Maginn, *Green Chem.*, 2006, **8**(1), 82–90.
- 22 M. T. Garcia, N. Gathergood and P. J. Scammells, *Green Chem.*, 2005, **7**(1), 9–14.
- 23 C. Pretti, C. Chiappe, D. Pieraccini, M. Gregori, F. Abramo, G. Monni and L. Intorre, *Green Chem.*, 2005, **8**(3), 238–240.
- 24 J. Ranke, S. Stolte, R. Störmann, J. Arning and B. Jastorff, *Chem. Rev.*, 2007, **107**, 2183–2206.
- 25 D. B. Zhao, Y. C. Liao and Z. D. Zhang, *CLEAN - Soil, Air, Water*, 2007, **35**(1), 42–48.

- 26 J. Ranke, A. Müller, U. Bottin-Weber, F. Stock, S. Stolte, J. Arning, R. Stormann and B. Jastorff, *Ecotoxicol. Environ. Safety*, 2007, **67**(3), 430–438.
- 27 P. T. Anastas and J. C. Warner, *Green Chemistry: Theory and Practice*; Oxford University Press, New York, 1998.
- 28 B. Jastorff, R. Stormann, J. Ranke, K. Molter, F. Stock, B. Oberheitmann, W. Hoffmann, J. Hoffmann, M. Nuchter, B. Ondruschka and J. Filser, *Green Chem.*, 2003, **5**(2), 136–142.
- 29 B. Jastorff, K. Mölter, P. Behrend, U. Bottin-Weber, J. Filser, A. Heimers, B. Ondruschka, J. Ranke, M. Schaefer, H. Schröder, A. Stark, P. Stepnowski, F. Stock, R. Störmann, S. Stolte, U. Welz-Biermann, S. Ziegert and J. Thöming, *Green Chem.*, 2005, **7**(5), 362–372.
- 30 P. Stepnowski and P. Storonik, *Environ. Sci. Pollut. Res.*, 2005, **12**(4), 199–204.
- 31 N. Gathergood and P. J. Scammells, *Aust. J. Chem.*, 2002, **55**(9), 557–560.
- 32 N. Gathergood, M. T. Garcia and P. J. Scammells, *Green Chem.*, 2004, **6**(2), 166–175.
- 33 N. Gathergood, P. J. Scammells and M. T. Garcia, *Green Chem.*, 2006, **8**(2), 156–160.
- 34 K. M. Docherty, J. K. Dixon and C. F. Kulpa, *Biodegradation*, 2007, **18**, 481–493.
- 35 B. Jastorff, E. G. Abbad, G. Petridis, W. Tegge, R. de Witt, C. Erneux, W. J. Stec and M. Morr, *Nucleic Acids Res., Symp. Ser.*, 1981, **9**, 219–223.
- 36 B. Jastorff, R. Störmann and U. Wölke, *Struktur-Wirkungs-Denken in der Chemie*, Universitätsverlag Aschenbeck & Isensee, Bremen, Oldenburg, 2004.
- 37 C. A. Martinez-Huitle, F. Hernandez, S. Ferro, M. A. Q. Alfaro and A. de Battisti, *Afinidad*, 2006, **62**(521), 26–34.
- 38 V. Linke, M. Baune and J. Thöming, *Vom Wasser*, 2006, **104**(2), 7–11.
- 39 B. Marselli, J. Garcia-Gomez, P. A. Michaud, M. A. Rodrigo and C. Comninellis, *J. Electrochem. Soc.*, 2003, **150**(3), D79–D83.
- 40 L. Gherardini, P. A. Michaud, M. Panizza, C. Comninellis and N. Vatistas, *J. Electrochem. Soc.*, 2001, **148**(6), D78–D82.
- 41 M. A. Rodrigo, P. A. Michaud, I. Duo, M. Panizza, G. Cerisola and C. Comninellis, *J. Electrochem. Soc.*, 2001, **148**(5), D60–D64.
- 42 J. Arning, S. Stolte, A. Bösch, F. Stock, W. R. Pitner, U. Welz-Biermann, J. Ranke and B. Jastorff, *Green Chem.*, 2007, DOI: 10.1039/b712109a.
- 43 OECD 301, Adopted by the Council on 17th July 1992; Ready, 2006.
- 44 DIN EN 1899-2, 1998.
- 45 HACH LANGE GMBH, Dr. Lange BOD5-BioKIT LZC 555, 97/10 edn, 1997.
- 46 E. Rorije, F. Germa, B. Philipp, B. Schink and D. B. Beimbom, *SAR QSAR Environ. Res.*, 2002, **13**(1), 199–204.
- 47 B. Philipp, M. Hoff, F. Germa, B. Schink, D. Beimbom and V. Mersch-Sundermann, *Environ. Sci. Technol.*, 2007, **41**(4), 1390–1398.

A new rationale of reaction metrics for green chemistry. Mathematical expression of the environmental impact factor of chemical processes

Jacques Augé

Received 25th July 2007, Accepted 13th November 2007

First published as an Advance Article on the web 30th November 2007

DOI: 10.1039/b711274b

A rationale of reaction metrics for green chemistry is presented, along with relationships between them. Starting from the definition of mass intensity, it is easy to find the mathematical formula giving the reaction metrics, such as the E-factor, *versus* the parameters of a reaction sequence: yields of each step, atom economy, excess of reactants, mass of auxiliaries and possibly their retrieval. For a complex mixed linear and convergent sequence, such a rationale could be expressed with a mathematical formula as simple as eqn (24). Based on experimental data, the application of such a methodology was proved to be useful to quantify the influence of each parameter of a chemical process on the environmental impact.

Introduction

Chemical processes are currently evaluated under the light of their environmental impact and eco-conception is now integrated in any strategy of synthesis. The twelve principles of green chemistry constitute a basis for such a conception. Quantitative and qualitative assessments of input and output for a particular process were defined by Sheldon with the introduction of the E-factor and the environmental quotient (EQ).¹ Other metrics, such as mass intensity (MI) or reaction mass efficiency (RME) were also proposed for a quantitative evaluation of chemical processes based on the relative mass of raw materials compared to the mass of the product.² In spite of interesting progresses in a formalism associated with these reaction metrics,³ there is a need for a unique and simple mathematical formula which could express such metrics for any single reaction or any reaction sequence.⁴ We are delighted to propose such a formula for a linear and a convergent sequence; the mathematical expression of MI, E-factor or RME clearly shows the influence of parameters, such as yield, global atom economy, excesses of reagents, solvents and additives, which permits a rapid comparison of sustainability of different chemical processes and which actually underlines their specific corner-stone.

Reaction metrics based on mass

Before any determination of reaction metrics based on masses, it is important to define very precisely their meaning.

$$\text{E-factor: } E = \frac{\text{total mass of waste}}{\text{mass of product}}$$

Mass intensity:

$$\text{MI} = \frac{\text{total mass used in a process or process step}}{\text{mass of product}}$$

$$\text{Reaction mass efficiency: } \text{RME} = \frac{\text{mass of product}}{\text{total mass of reactants}}$$

Generalized reaction mass efficiency:

$$\text{gRME} = \frac{\text{mass of product}}{\text{total mass used in a process or process step}}$$

The first 3 definitions have all been used in the past.² Some authors prefer the mass index term instead of mass intensity, but both have the same meaning.⁵ The definition of a generalized reaction mass efficiency (gRME) was recently introduced in order to propose a unification of reaction metrics.³

Total mass used in a process includes all the chemicals used in this process; it concerns reactants, catalysts or any additives such as acids, bases, salts..., solvents of the reaction or solvents required in the work-up (extraction, washing, separation, recrystallization...), chromatographic support if not recycled, *etc.*... If we suppose that: total mass used in a process or process step = total mass of reactants + *S*, then the mass *S* corresponds to all the chemicals used in a process, with the exception of reactants; in the following, *S* will be considered as the total mass of auxiliaries of the process. This is a parameter which has a great importance on the reaction metrics. As a matter of fact this is often the major part of the total waste, which includes by-products, excess of reagents, and reactants not having reacted.

It is easy to see that there are simple relationships between these reaction metrics, so that the determination of MI, E or gRME is in fact a unique problem. RME is of course a less pertinent factor since it does not include *S*.

$$\text{MI} = E + 1 = \frac{1}{\text{gRME}} = \frac{1}{\text{RME}} + \frac{S}{\text{mass of product}}$$

For simplification we have decided to express the mass intensity MI directly from its definition; a mathematical treatment is then easy and the other metrics, such as the well-known E-factor, are then deduced from the expression of MI.

Single reactions

Consider a reaction affording the target product P and a by-product Q, in which v_i are the stoichiometric coefficients

Department of Chemistry, UMR CNRS-ESCOM-University of Cergy-Pontoise, 5 mail Gay-Lussac, Neuville-sur-Oise, 95031, Cergy-Pontoise, France. E-mail: jacques.auge@u-cergy.fr



Scheme 1

(Scheme 1); x is the scale of the reaction. The reagent B could be eventually used in excess.

By definition:

$$\text{MI} = \frac{xM_A + yM_B + S}{\varepsilon x \frac{v_p}{v_A} M_P} \quad (1)$$

where ε is the yield of the reaction, where M_A , M_B and M_P are the molar masses of A, B and P. S is the mass of all the auxiliaries used in a reaction, as mentioned. If a part of these auxiliaries is retrieved or recycled, then the corresponding mass must not be taken into consideration, but the products required for such a regeneration will be included in the overall mass S .

In order to have a general expression of MI, it is useful to introduce the stoichiometric ratio φ .

$\varphi = \frac{y}{v_b} \frac{x}{v_a}$. If the reagent B is used in excess, it means that $\varphi > 1$. Eqn (1) becomes:

$$\text{MI} = \frac{\frac{x}{v_a} (v_a M_A + \varphi v_b M_B) + S}{\varepsilon x \frac{v_p}{v_A} M_P} \quad (2)$$

By dividing each term by $\frac{x}{v_a} (v_a M_A + v_b M_B)$, eqn (2) becomes:

$$\text{MI} = \frac{1 + b + s}{\varepsilon \text{AE}} \quad (3)$$

where $\text{AE} = \frac{v_p M_P}{v_a M_A + v_b M_B}$ is the atom economy of the reaction.

$$b = \frac{(\varphi - 1)v_b M_B}{v_a M_A + v_b M_B} = \frac{\text{mass of the excess of B}}{\text{mass of the reactants in a stoichiometric amount}}$$

$$s = \frac{S}{\frac{x}{v_a} (v_a M_A + v_b M_B)} = \frac{\text{mass of the auxiliaries}}{\text{mass of the reactants in a stoichiometric amount}}$$

From the eqn (3), it is easy to determine the generalized reaction mass efficiency gRME and the environmental factor E.

$$\text{gRME} = \frac{\varepsilon \text{AE}}{1 + b + s} \quad (4)$$

$$E = \frac{1 - \varepsilon \text{AE}}{\varepsilon \text{AE}} + \frac{b}{\varepsilon \text{AE}} + \frac{S}{\varepsilon \frac{x}{v_a} v_p M_P} \quad (5)$$

The Sheldon environmental impact factor (E-factor) is the sum of three terms. The first one is directly correlated to the atom economy AE and to the yield ε of the reaction. The second one is related to the excess of reactants with respect to the stoichiometric ratio. The third one includes the

contributions of all the chemicals besides the reactants and the products. This concerns all the auxiliaries of the reaction if not recycled.

The reaction mass efficiency, s is omitted from eqn (4), so that:

$$\text{RME} = \frac{\varepsilon \text{AE}}{1 + b} \quad (6)$$

At this stage, it is important to wonder what happens if the reactants (either A or B) or the by-products are retrieved. We have to subtract the corresponding amount in the numerator of eqn (3), so that

$$\text{MI} = \frac{1 + b + s - r - q}{\varepsilon \text{AE}} \quad (7)$$

where

$$r = \frac{R}{\frac{x}{v_a} (v_a M_A + v_b M_B)} = \frac{\text{mass of the retrieved reactants}}{\text{mass of the reactants in a stoichiometric amount}}$$

and

$$q = \frac{Q}{\frac{x}{v_a} (v_a M_A + v_b M_B)} = \frac{\text{mass of the retrieved by-products}}{\text{mass of the reactants in a stoichiometric amount}}$$

However, it must be emphasized that the retrieval of the excess of reactants and/or the by-products is normally accompanied by a supplementary use of auxiliaries, which may notably increase s . Of course, this parameter does not affect the reaction mass efficiency, so that

$$\text{RME} = \frac{\varepsilon \text{AE}}{1 + b - r - q} \quad (8)$$

If all the reactants which don't give products are retrieved, then $r = 1 + b - \varepsilon$. If the by-products are totally retrieved, then $q = \varepsilon (1 - \text{AE})$. Thus, if both the excess of reactants and the by-products are retrieved, $\text{RME} = 1$

Taking into account the mass of the auxiliaries, eqn (8) becomes

$$\text{gRME} = \frac{\varepsilon \text{AE}}{\varepsilon \text{AE} + s} \text{ and } E = \frac{s}{\varepsilon \text{AE}} \quad (9)$$

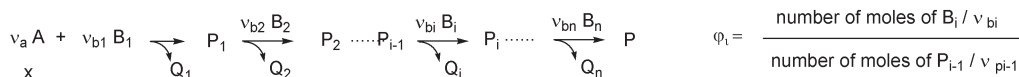
This equation clearly shows that, even if the excesses of reactants and by-products are totally retrieved, the E-factor is affected by the yield and the atom economy of the reaction. Of course, the major part of the environment impact, characterized by the E-factor, arises from the auxiliaries, such as solvents.

Linear sequences

We consider a linear sequence, composed of n reactions (Scheme 2).

Starting from the definition of MI, this becomes

$$\text{MI} = \frac{xM_A + \varphi_1 \frac{x}{v_a} v_{b1} M_{B1} + \dots + \varphi_n (e_1 e_2 \dots e_{i-1}) \frac{x}{v_a} v_{bi} M_{Bi} + \dots + \varphi_n (e_1 e_2 \dots e_{n-1}) \frac{x}{v_a} v_{bn} M_{Bn} + S}{\varepsilon_1 \varepsilon_2 \dots \varepsilon_n \frac{x}{v_a} v_p M_P} \quad (10)$$



Scheme 2

By dividing each term of eqn (10) by x/v_a , we obtain eqn (11):

$$\text{MI} = \frac{v_a M_A + \sum_i \varphi_i (\varepsilon_1 \varepsilon_2 \dots \varepsilon_{i-1}) (v_{bi} M_{Bi}) + \frac{S}{x/v_a}}{v_p M_P \prod_i \varepsilon_i} \quad (11)$$

where $\prod \varepsilon_i$ is the product of the yields of each step of the linear sequence.

We now introduce the overall atom economy of the linear sequence, defined as

$$\text{AE} = \frac{v_p M_P}{v_a M_A + v_{b1} M_{B1} + v_{b2} M_{B2} + \dots + v_{bi} M_{Bi} + \dots + v_{bn} M_{Bn}}$$

We divide each term of eqn (11) by $\sum M = v_a M_A + v_{b1} M_{B1} + v_{b2} M_{B2} + \dots + v_{bi} M_{Bi} + \dots + v_{bn} M_{Bn}$. Therefore

$$\text{MI} = \frac{1 + \sum_i b_i + s}{\text{AE} \prod_i \varepsilon_i} \quad (12)$$

where

$$\begin{aligned}
 b_i &= [\varphi_i (\varepsilon_1 \varepsilon_2 \dots \varepsilon_{i-1}) - 1] \frac{v_{bi} M_{Bi}}{\sum M} = \\
 &= \frac{\text{mass of the excess of the reactants}}{\text{mass of the reactants in stoichiometric amounts}} \\
 s &= \frac{S}{\frac{x}{v_a} \sum M} = \\
 &= \frac{\text{mass of the auxiliaries}}{\text{mass of the reactants in stoichiometric amounts}}
 \end{aligned}$$

S is the total mass of auxiliaries (solvents...) when performing the linear sequence with x moles of the starting material A. This mass must be divided by $\frac{x}{v_a} \sum M$ to obtain s , a dimensionless term which appears in the numerator of the mass intensity.

If a part of the reactants and by-products is retrieved, we must take into account such a retrieval as previously mentioned in eqn (7).

The generalized reaction mass efficiency (gRME) and the E-factor are equal to:

$$\text{gRME} = \frac{\text{AE} \prod_i \varepsilon_i}{1 + \sum_i b_i + s} \quad (13)$$

$$\text{E} = \frac{1 - \text{AE} \prod_i \varepsilon_i}{\text{AE} \prod_i \varepsilon_i} + \frac{\sum_i b_i}{\text{AE} \prod_i \varepsilon_i} + \frac{S}{\frac{x}{v_a} v_p M_P \prod_i \varepsilon_i} \quad (14)$$

As mentioned previously, the Sheldon environmental impact factor (E-factor) is the sum of three terms. The first one is directly correlated to the overall atom economy AE and to the yields of the steps of the linear sequence. The second one is related to the excess of reactants with respect to their partner

in the sequence. The third one includes the contributions of all the chemicals besides the reactants.

In order to decrease the environmental impact, it is important to optimize all the yields, to avoid the use of heavy protecting groups contributing to the decrease of the atom economy, to avoid the use of a large excess of reactants to minimize b_i , and to avoid the use of large quantities of solvents or auxiliaries.

In a reaction sequence in which the global yield is given, it is more advantageous that the last steps are the most efficient ones in terms of yield. Solvents and auxiliaries are then used in smaller quantities, compared to the reverse situation in which the first steps would be the most efficient ones.

The expression of b_i shows that all the yields of the previous steps (steps from 1 to $i - 1$) are involved, which means that the last step is the step for which a large excess of reactant is the less problematic (notice that b_i decreases with the yields of the steps preceding step i).

By omitting s in eqn (13), we obtain the expression of the reaction mass efficiency RME:

$$\text{RME} = \frac{\text{AE} \prod_i \varepsilon_i}{1 + \sum_i b_i} \quad (15)$$

Convergent reactions

In convergent reactions, the target product P arises from two intermediates P_m and P'_m , which are independently prepared (Scheme 3).

Two cases must be considered according to the relative performance of the pathways leading to P_m and P'_m .

In the first case, we consider that the first sequence is more efficient in terms of yields than the second one, so that the overall yield of the product P is calculated from A.

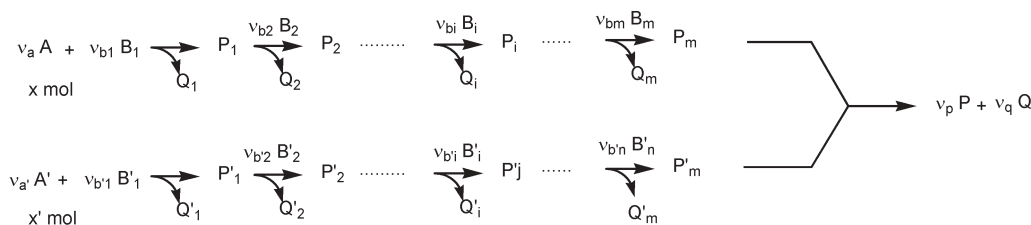
First, consider that P'_m can be possibly used in excess, so that $\frac{x'/v_{a'}}{x/v_a} = \sigma' > 1$

The excess of the reactants is defined as previously:

$$\begin{aligned}
 \varphi_i &= \frac{\text{number of moles of } B_i / v_{bi}}{\text{number of moles of } P_{i-1} / v_{pi-1}} \\
 \varphi'_j &= \frac{\text{number of moles of } B'_j / v_{bj}}{\text{number of moles of } P'_{j-1} / v_{p'j-1}}
 \end{aligned}$$

Starting from the definition of MI, this becomes

$$\text{MI} = \frac{x M_A + \sum_i \varphi_i (\varepsilon_1 \varepsilon_2 \dots \varepsilon_{i-1}) \frac{x}{v_a} v_{bi} M_{Bi} + x' M_{A'} + \sum_j \varphi'_j (\varepsilon'_1 \varepsilon'_2 \dots \varepsilon'_{j-1}) \frac{x'}{v_{a'}} v_{bj} M_{Bj} + S}{\varepsilon_1 \varepsilon_2 \dots \varepsilon_m \varepsilon_n \frac{x}{v_a} v_p M_P} \quad (16)$$



Scheme 3

By dividing each term by x/v_a , we obtain eqn (17):

$$MI = \frac{v_a M_A + \sum_i \varphi_i(\varepsilon_1 \varepsilon_2 \dots \varepsilon_{i-1}) v_{bi} M_{Bi} + \sigma' \left[v_a' M_{A'} + \sum_j \varphi'_j(\varepsilon'_1 \dots \varepsilon'_{j-1}) v_{bj'} M_{Bj'} \right] + \frac{S}{x/v_a}}{\varepsilon_1 \varepsilon_2 \dots \varepsilon_m \varepsilon_n v_p M_P} \quad (17)$$

In this expression of MI, we divide each term by

$$\sum M = v_a M_A + v_a' M_{A'} + v_{b1} M_{B1} + v_{b2} M_{B2} + \dots v_{bm} M_{Bm} + v_{b'1} M_{B'1} + \dots v_{b'm} M_{B'm}$$

Therefore

$$MI = \frac{1 + a' + \sum_i b_i + \sum_j b'_j + s}{\varepsilon_1 \varepsilon_2 \dots \varepsilon_m \varepsilon_n AE} \quad (18)$$

where $AE = \frac{v_p M_P}{\sum M}$ is the overall atom economy of the reaction sequence

$$a' = (\sigma' - 1) \frac{v_a' M_{A'}}{\sum M} = \frac{\text{mass of the excess of } A' \text{ compared to } A}{\text{mass of all the reactants in stoichiometric amounts}}$$

$$b_i = [\varphi_i(\varepsilon_1 \varepsilon_2 \dots \varepsilon_{i-1}) - 1] \frac{v_{bi} M_{Bi}}{\sum M} = \frac{\text{mass of the excess of the reactants } B_i}{\text{mass of all the reactants in stoichiometric amounts}}$$

$$b'_j = [\varphi'_j(\varepsilon'_1 \dots \varepsilon'_{j-1}) - 1] \frac{v_{bj'} M_{Bj'}}{\sum M} = \frac{\text{mass of the excess of the reactants } B'_j}{\text{mass of all the reactants in stoichiometric amounts}}$$

$$s = \frac{S}{\frac{x}{v_a} \sum M} = \frac{\text{mass of the auxiliaries}}{\text{mass of all the reactants in stoichiometric amounts}}$$

What happens if P_m has to be used in excess for the formation of the product P? This will affect the overall yield, so that

$$MI = \frac{1 + a' + \sum_i b_i + \sum_j b'_j + s}{\varepsilon_1 \varepsilon_2 \dots \varepsilon_m \varepsilon_n \rho AE} \quad (19)$$

where $\rho = \frac{\text{number of moles of } P'_m / v_{p'm}}{\text{number of moles of } P_m / v_{pm}} < 1$

However it may occur that $\sigma' < 1$; in that second case, the overall yield must be calculated from the second sequence; x' is then the scale of the overall reaction. We can then introduce a

new ratio $\sigma = \frac{1}{\sigma'}$ so that

$$MI = \frac{1 + a + \sum_i b_i + \sum_j b'_j + s}{\varepsilon'_1 \varepsilon'_2 \dots \varepsilon'_m \varepsilon'_n AE}$$

$$a = (\sigma - 1) \frac{v_a M_A}{\sum M} = \frac{\text{mass of the excess of } A \text{ compared to } A'}{\text{mass of all the reactants in stoichiometric amounts}}$$

$$b_i = [\sigma \varphi_i(\varepsilon_1 \varepsilon_2 \dots \varepsilon_{i-1}) - 1] \frac{v_{bi} M_{Bi}}{\sum M} = \frac{\text{mass of the excess of the reactants } B_i}{\text{mass of all the reactants in stoichiometric amounts}}$$

$$b'_j = [\varphi'_j(\varepsilon'_1 \varepsilon'_2 \dots \varepsilon'_{j-1}) - 1] \frac{v_{bj'} M_{Bj'}}{\sum M} = \frac{\text{mass of the excess of the reactants } B'_j}{\text{mass of all the reactants in stoichiometric amounts}}$$

$$s = \frac{S}{\frac{x'}{v_a'} \sum M} = \frac{\text{mass of the auxiliaries}}{\text{mass of all the reactants in stoichiometric amounts}}$$

The cases leading to eqn (18) are more frequent than those leading to eqn (20). From the more general eqn (18), we can deduce the reaction mass efficiency, the generalized reaction mass efficiency and the E-factor

$$RME = \frac{\varepsilon_1 \varepsilon_2 \dots \varepsilon_m \varepsilon_n AE}{1 + a' + \sum_i b_i + \sum_j b'_j} \quad (21)$$

$$gRME = \frac{\varepsilon_1 \varepsilon_2 \dots \varepsilon_m \varepsilon_n AE}{1 + a' + \sum_i b_i + \sum_j b'_j + s} \quad (22)$$

$$E = \frac{1 - \varepsilon_1 \varepsilon_2 \dots \varepsilon_m \varepsilon_n AE}{\varepsilon_1 \varepsilon_2 \dots \varepsilon_m \varepsilon_n AE} + \frac{a' + \sum_i b_i + \sum_j b'_j}{\varepsilon_1 \varepsilon_2 \dots \varepsilon_m \varepsilon_n AE} + \frac{S}{\varepsilon_1 \varepsilon_2 \dots \varepsilon_m \varepsilon_n \frac{x}{v_a} v_p M_P} \quad (23)$$

It is crucial to evaluate which sequence leads to the overall yield; as previously observed, the E-factor is the sum of three terms.

The first term is correlated to the overall yield and to the overall atom economy; the second one corresponds to the excess of all the reactants and the third term is related to the auxiliaries used.

In this example, the second sequence is less efficient than the first one. The yields of the second sequence do not directly appear in the formula, but it is noteworthy to be reminded that there is a correlation between those yields and the excess of A' with respect to A, which is represented by the parameter a' ; moreover S is of course affected.

Mixed linear and convergent sequence

In Scheme 4 the target product P is derived from P_n , arising from two independent pathways, which is usual in chemical processes.

The overall atom economy becomes: $AE = \frac{v_p M_P}{\sum M}$ where

$$\sum M = v_a M_A + v_{a'} M_{A'} + v_{b1} M_{B1} + \dots + v_{bm} M_{Bm} + v_{b'1} M_{B'1} + \dots + v_{b'm} M_{B'm} + v_{b''1} M_{B''1} + \dots + v_{b''n} M_{B''n}$$

We suppose that the sequence leading to P_m is more efficient than the sequence leading to P'_m , with $x' > x$. Then

$$MI = \frac{1 + a' + \sum_i b_i + \sum_j b'_j + \sum_k b''_k + s}{\varepsilon_1 \varepsilon_2 \dots \varepsilon_m \varepsilon_n \varepsilon''_1 \varepsilon''_2 \dots \varepsilon''_n AE} \quad (24)$$

$$s = \frac{S}{\frac{x}{v_a} \sum M} =$$

mass of the auxiliaries

mass of all the reactants in stoichiometric amounts

$$b_i = [\varphi_i (\varepsilon_1 \varepsilon_2 \dots \varepsilon_{i-1}) - 1] \frac{v_{bi} M_{Bi}}{\sum M} =$$

mass of the excess of the reactants B_i

mass of all the reactants in stoichiometric amounts

$$b'_j = [\sigma'_j \varphi'_j (\varepsilon'_1 \varepsilon'_2 \dots \varepsilon'_{j-1}) - 1] \frac{v_{b'j} M_{B'j}}{\sum M} =$$

mass of the excess of the reactants B'_j

mass of all the reactants in stoichiometric amounts

$$b''_k = [\varphi''_k (\varepsilon_1 \varepsilon_2 \dots \varepsilon_n \varepsilon''_1 \dots \varepsilon''_{k-1}) - 1] \frac{v_{b''k} M_{B''k}}{\sum M} =$$

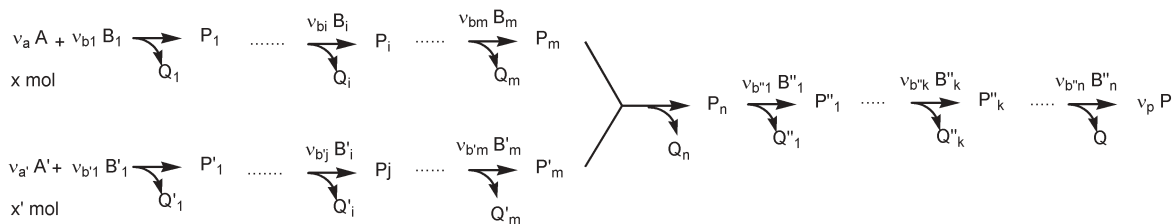
mass of the excess of the reactants B''_k

mass of all the reactants in stoichiometric amounts

$$\varphi''_k = \frac{\text{number of moles of } B''_k / v_{b''k}}{\text{number of moles of } P''_{k-1} / v_{p''k-1}}$$

From eqn (24), we can then deduce gRME and E.

$$gRME = \frac{\varepsilon_1 \varepsilon_2 \dots \varepsilon_m \varepsilon_n \varepsilon''_1 \dots \varepsilon''_n AE}{1 + a' + \sum_i b_i + \sum_j b'_j + \sum_k b''_k + s} \quad (25)$$



Scheme 4

$$E = \frac{1 - \varepsilon_1 \dots \varepsilon_m \varepsilon_n \varepsilon''_1 \dots \varepsilon''_n AE}{\varepsilon_1 \varepsilon_2 \dots \varepsilon_m \varepsilon_n \varepsilon''_1 \dots \varepsilon''_n AE} + \frac{a' + \sum_i b_i + \sum_j b'_j + \sum_k b''_k}{\varepsilon_1 \varepsilon_2 \dots \varepsilon_m \varepsilon_n \varepsilon''_1 \dots \varepsilon''_n AE} \quad (26)$$

$$+ \frac{S}{\varepsilon_1 \dots \varepsilon_m \varepsilon_n \varepsilon''_1 \dots \varepsilon''_n \frac{x}{v_a} v_p M_P}$$

If we exclude the mass S from the calculation, then we may express RME.

$$RME = \frac{\varepsilon_1 \varepsilon_2 \dots \varepsilon_m \varepsilon_n \varepsilon''_1 \dots \varepsilon''_n AE}{1 + a' + \sum_i b_i + \sum_j b'_j + \sum_k b''_k} \quad (27)$$

Application of this methodology to the synthesis of sildenafil

The development of an environmentally attractive synthesis of sildenafil and its assessment by reaction metrics was recently discussed,⁶ so that it is interesting to test our method with this particular example (Scheme 5). Experimental data for the 1997 process were published,⁷ which allows us to determine the reaction mass efficiency of the process. The other metrics were also calculated after discussion of the used auxiliaries.

If we exclude the mass S of the auxiliaries, then we can express the reaction efficiency RME for the process by using eqn (27).

$$RME = \frac{\varepsilon_1 \varepsilon_2 \varepsilon_3 \varepsilon_4 \varepsilon''_1 AE}{1 + a' + b_1 + b_2 + b_{2*} + b_3 + b'_1 + b'_{1*} + b'_2 + b'_3 + b''_1} \quad (28)$$

The overall atom economy is:

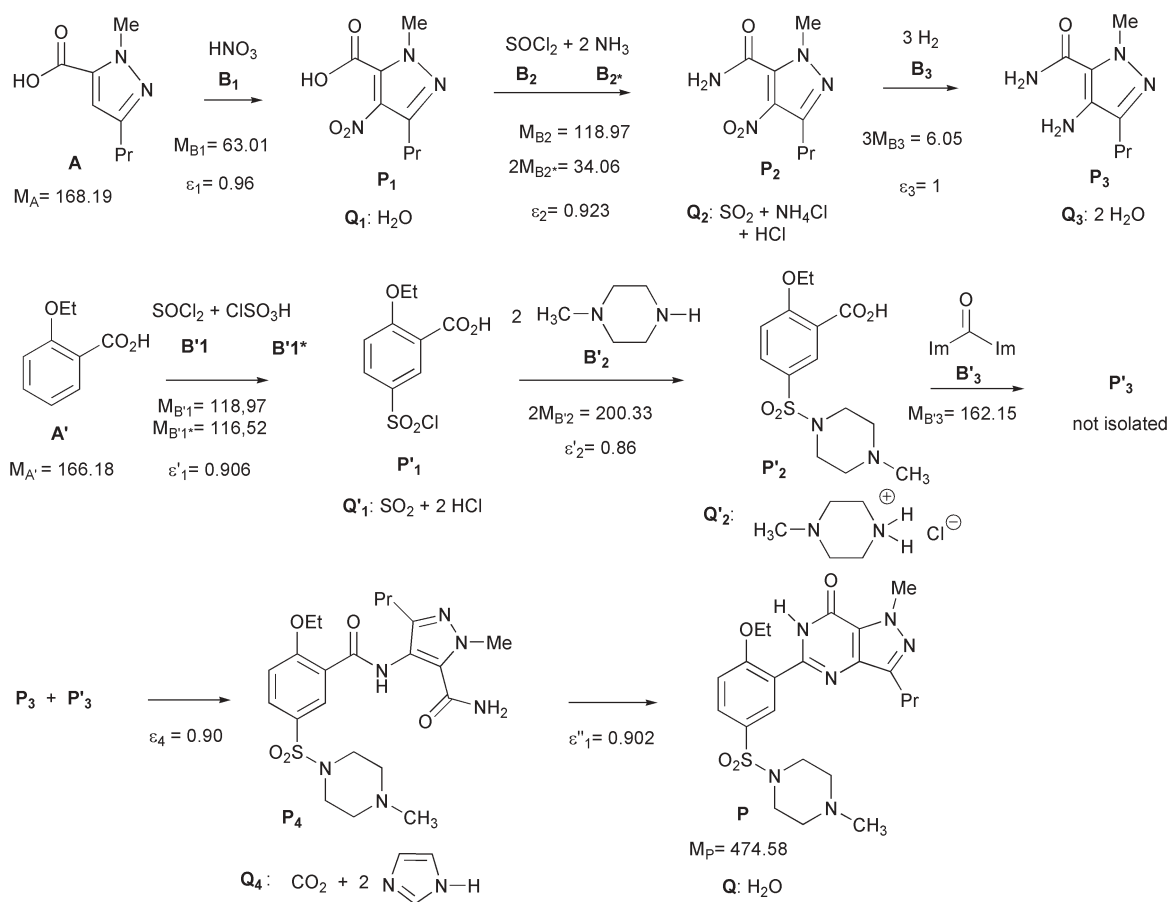
$$AE = \frac{M_P}{\sum M} = \frac{M_P}{M_A + M_{B1} + M_{B2} + 2M_{B2*} + 3M_{B3} + M_{A'} + M_{B'1} + M_{B'1*} + 2M_{B'2} + M_{B'3}}$$

where $\sum M = 1154.43$; therefore $AE = 0.411$

$$a' = (\sigma' - 1) \frac{M_{A'}}{\sum M}$$

The benzoic acid P'_2 (1.24 mol)⁷ was produced from x' moles of A' , such as

$$\varepsilon'_1 \varepsilon'_2 x' = 1.24$$



Scheme 5

The aminopyrazole **P₃** (1.12 mol) was obtained from x moles of **A**, such as

$$\varepsilon_1 \varepsilon_2 \varepsilon_3 x = 1.12$$

Thus $\sigma' = \frac{x'}{x} = 1.259$ and $a' = 0.03728$

Excess of HNO₃ (nitration)

$$\varphi_1 = \frac{11.705}{9.45} = 1.238 \quad b_1 = (\varphi_1 - 1) \frac{M_{B1}}{\sum M} = 0.0130$$

Excess of SOCl₂ (amidation)

$$\varphi_2 = \frac{7.5}{4.69} = 1.599 \quad b_2 = (\varepsilon_1 \varphi_2 - 1) \frac{M_{B2}}{\sum M} = 0.0551$$

Excess of NH₃ (amidation): the concentration of ammonia solution is supposed to be equal to 4 M

$$\varphi_{2^*} = \frac{24}{2 \times 4.69} = 2.5586 \quad b_{2^*} = (\varepsilon_1 \varphi_{2^*} - 1) \frac{2M_{B2^*}}{\sum M} = 0.0430$$

Excess of dihydrogen: if we suppose that a stoichiometric amount of dihydrogen is used in the hydrogenation step, then $\varphi_3 = 1$; however b_3 which is calculated with respect to the stoichiometry of the starting material **A** is negative.

$$b_3 = (\varepsilon_1 \varepsilon_2 \varphi_3 - 1) \frac{3M_{B3}}{\sum M} = -0.0006$$

Excess of SOCl₂ (chlorosulfonation): there is no excess of SOCl₂ with respect to **A'**

$$\varphi'_1 = 1 \quad b'_1 = (\sigma' \varphi'_1 - 1) \frac{M_{B'1}}{\sum M} = 0.0267$$

Excess of chlorosulfonic acid:

$$\varphi'_{1^*} = \frac{0.6213}{0.1504} = 4.131 \quad b'_{1^*} = (\sigma' \varphi'_{1^*} - 1) \frac{M_{B'1^*}}{\sum M} = 0.4240$$

Excess of *N*-methylpiperazine (sulfoamidation)

$$\varphi'_2 = \frac{0.303}{2 \times 0.13} = 1.166 \quad b'_2 = (\sigma' \varphi'_2 \varepsilon'_1 - 1) \frac{2M_{B'2}}{\sum M} = 0.0573$$

Excess of *N,N'*-carbonyldiimidazole (activation of the benzoic acid **P'2**)

$$\varphi'_3 = \frac{1.3}{1.24} \quad b'_3 = (\sigma' \varphi'_3 \varepsilon'_1 \varepsilon'_2 - 1) \frac{M_{B'3}}{\sum M} = 0.0040$$

Cyclization: there is no reactant except **P₄** in the reaction equation. Thus $b''_1 = 0$. In eqn (28), the denominator is equal to 1.66; the overall yield is equal to 0.72 and the overall atom economy is equal to 0.411. Thus RME = 0.178.

In a perfect synthesis, the value of RME is 1. What are the steps which decrease the most strongly the value of RME? Three factors must be considered.

First, the yields have a great influence as indicated by eqn (26), but in that particular case they range from 86 to 96%, which can be considered as very good.

Second, concerning the atom economy, there are two steps which are less performant, the sulfoamidation and the

condensation, since *N*-methylpiperazinium chloride (Q_2) and imidazole (part of Q_4) are respectively formed. In order to measure more precisely their influence, we can express $1/AE$

$$\frac{1}{AE} = \frac{\sum M}{M_p} = \frac{M_p + \sum v_{qi} M_{Qi}}{M_p}$$

$$\sum v_{qi} M_{Qi} = 679.85$$

$M_{Q_2} = 136.63$; Q_2 constitutes 20% of the total by-products

$M_{Q_4} = 180.17$; Q_4 constitutes 26% of the total by-products

Third, we must consider the excess of reactants. The unique parameter b which surpasses 0.1 is b'_{1*} with the high value of 0.424. This is due to the strong excess of chlorosulfonic acid ($\varphi_{1*} = 4.131$) in the chlorosulfonation step. If b'_{1*} could be equal to zero, then RME would be increased up to 0.24, which would correspond to an enhancement of 35% of the reaction mass efficiency!

To determine the mass intensity MI or the E-factor, we need to know the mass S , which is the sum of the masses of the auxiliaries for each step.

$$MI = E + 1 = \frac{1}{RME} + \frac{S}{\text{mass of product}}$$

where $S = S_1 + S_2 + S_3 + S'_1 + S'_2 + S_4 + S''_1$

$$\text{mass of product} = \varepsilon_1 \varepsilon_2 \varepsilon_3 \varepsilon_4 \varepsilon''_1 x M_p$$

The scale x is arbitrary chosen. We took $x = 9.45$ mol because it is the effective scale of the first step of the process which was described in detail.⁷ The masses S_i are evidently proportional to this scale. For each step the waste is calculated from the corresponding amount of starting material with respect to the chosen scale.

Step 1: $S_1 = 14.842$ kg (H_2SO_4)

Step 2: starting from $\varepsilon_1 x$ mol of P_1 , $S_2 = 8.0$ kg (7.940 kg of toluene and 0.060 kg of DMF)

Step 3: starting from $\varepsilon_1 \varepsilon_2 x$ mol of P_2 , $S_3 = 13.976$ kg (13.622 kg of ethyl acetate and 0.254 kg of palladium if not recycled); the unknown amount of ethyl acetate used in the washings is not included in S_3

Step 1': the amount of hexane and toluene used for crystallisation is not mentioned

Step 2': the amount of acetone for crystallization is not mentioned

Step 4: starting from $\varepsilon_1 \varepsilon_2 \varepsilon_3 x$ mol of P_3 , $S_4 = 17.420$ kg (ethyl acetate); the unknown amount of methanol for recrystallization is not included in this term.

Step 1'': starting from $\varepsilon_1 \varepsilon_2 \varepsilon_3 \varepsilon_4 x$ mol of P_4 , $S''_1 = 16.099$ kg (14.251 kg of *t*BuOH, 1.016 kg of *t*BuOK + 0.832 kg of HCl).

If we exclude the solvents of recrystallization, the total mass of auxiliaries when proceeding with 9.45 mol of starting

material, is equal to 70.277 kg, whereas the mass of the final product is equal to 3.226 kg. Thus the third term of eqn (26), which is the contribution of the auxiliaries in the E-factor is equal to 21.52. This value is superior to the value indicated in the literature, which means that a part of the solvents are recycled; besides the catalyst used in the hydrogenation is probably recycled.

We can then deduce the E-factor from the following equation

$$E = \frac{1}{RME} - 1 + \frac{S}{\text{mass of product}} = 26.14$$

It is interesting to note what is the relative weight of each term in the E-factor. The weight of the auxiliaries reaches 82%. The first and the second terms of eqn (26) constitute for each of them 9% of the total E-factor. In other terms, the intra-waste, constituted by the excess of reactants and by the by-products represents 18% of the E-factor, that is 4.62, which is correct compared to other processes.⁶ If b'_{1*} could be equal to zero, then this factor would be reduced to 3.17.

This application allows us to understand that an excess of reactant may be crucial. The importance of the auxiliaries must also be emphasized and there is room for manoeuvre to improve a process by recycling solvents.

Conclusion

We propose in this article a very simple mathematical expression of the mass intensity (MI), and therefore of the E-factor, for a single reaction and for a linear and convergent reaction sequence. In the general case of a mixed sequence, MI is expressed by eqn (24), clearly showing the influence of all the parameters of a process: atom economy, yields, excess of reactants for each individual step and mass of auxiliaries. This should eventually lead one to identify and to quantify the weak link of a process. The application of this methodology to a particular chemical process shows the usefulness of such an approach.

References

- 1 R. A. Sheldon, *Chem. Ind. (London)*, 1992, 903–906; R. A. Sheldon, *Chem. Ind. (London)*, 1997, 12–15; R. A. Sheldon, *CHEMTECH*, 1994, 38–46.
- 2 D. J. C. Constable, A. D. Curzons and V. L. Cunningham, *Green Chem.*, 2002, **4**, 521–527.
- 3 J. Andraos, *Org. Process Res. Dev.*, 2005, **9**, 149–163.
- 4 J. Augé, Symposium Eco-conception, Chimie pour un développement durable, Montpellier, 2007.
- 5 M. Eissen and J. O. Metzger, *Chem. Eur. J.*, 2002, **8**, 3581–3585.
- 6 P. J. Dunn, S. Galvin and K. Hettenbach, *Green Chem.*, 2004, **6**, 43–48.
- 7 D. J. Dale, P. J. Dunn, C. Golightly, M. L. Hughes, P. C. Levett, A. K. Pearce, P. M. Searle, G. Ward and A. S. Wood, *Org. Process Res. Dev.*, 2000, **4**, 17–22.

An alternative method for the regio- and stereoselective bromination of alkenes, alkynes, toluene derivatives and ketones using a bromide/bromate couple†

Subbarayappa Adimurthy,^{*a} Sudip Ghosh,^b Paresh U. Patoliya,^a Gadde Ramachandraiah,^{*a} Manoj Agrawal,^a Mahesh R. Gandhi,^a Sumesh C. Upadhyay,^a Pushpito K. Ghosh^{*a} and Brindaban C. Ranu^{*b}

Received 10th September 2007, Accepted 16th November 2007

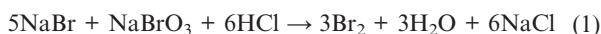
First published as an Advance Article on the web 3rd December 2007

DOI: 10.1039/b713829f

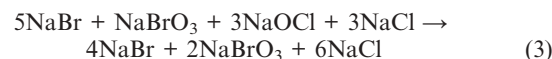
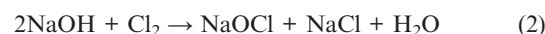
Mixtures of NaBr and NaBrO₃ in two different ratios have been used for highly stereoselective bromination of alkenes and alkynes, and regioselective bromine substitution at the α -carbon of ketones and at the benzylic position of toluene derivatives. The reactions were conducted in an aqueous acidic medium under ambient conditions. The solid reagents were prepared from the intermediate obtained in the “cold process” of bromine manufacture and are stable, non-hazardous and inexpensive to prepare. This procedure provides an efficient and practical alternative to conventional procedures using liquid bromine directly or indirectly.

1 Introduction

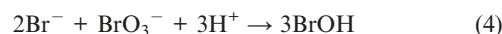
Bromination is a very important process in organic synthesis as bromo derivatives serve as useful intermediates in the manufacture of pharmaceuticals, agrochemicals and other speciality chemicals.¹ Moreover, many pesticides, insecticides, herbicides and fire retardants contain a bromine functionality.² The use of liquid bromine for bromination is still very common in industry as well as in academia, in spite of its hazardous effects, probably due to lack of a suitable alternative. Although, besides liquid bromine, several other safer and user-friendly brominating agents, such as pyridiniumbromide–perbromide,³ quaternary ammonium tribromide,⁴ Amberlyst-A-26 tribromide,⁵ pentylpyridinium tribromide,⁶ 1,2-dipyridiniumbis(tribromide)-ethane (DPTBE),⁷ and *N*-bromosuccinimide (NBS)⁸ have been developed, preparation of all these reagents involves liquid bromine at some stage. As a part of our broad program to explore the desired bromination reaction with minimum by-products or waste generation, as well as elimination of the use of hazardous liquid bromine, we have developed a solid green reagent utilizing the liquid bromine precursor of bromine manufacture.⁹ This precursor comprises a 5:1 molar ratio of NaBr–NaBrO₃ (designated as BR-A) which releases bromine on demand following (*in-situ*) acidification (eqn. 1).¹⁰



On the other hand this reagent (BR-A), when treated with NaOCl [this was generated from the reaction of NaOH and Cl₂ (eqn. 2)], furnished another solid (BR-S) with a composition of 2:1 mole ratio of NaBr–NaBrO₃ (eqn. 3) and was used as such.⁹



This reagent (BR-S) releases BrOH on acidification (eqn. 4).



We report here a simple and efficient bromine addition to alkenes and alkynes using BR-A and bromine substitution to ketones and toluene derivatives by BR-S in aqueous acidic medium (Scheme 1). The rationale for using BR-A for addition and BR-S for substitution reactions is to maintain high atom efficiency as two bromine atoms (Br₂) released from the BR-A (eqn. 1) are consumed in addition to alkenes and alkynes, whereas BrOH generated from BR-S (eqn. 4) is consumed in a substitution reaction of toluenes and ketones.

2 Results and discussion

2.1 Bromination of alkenes and alkynes

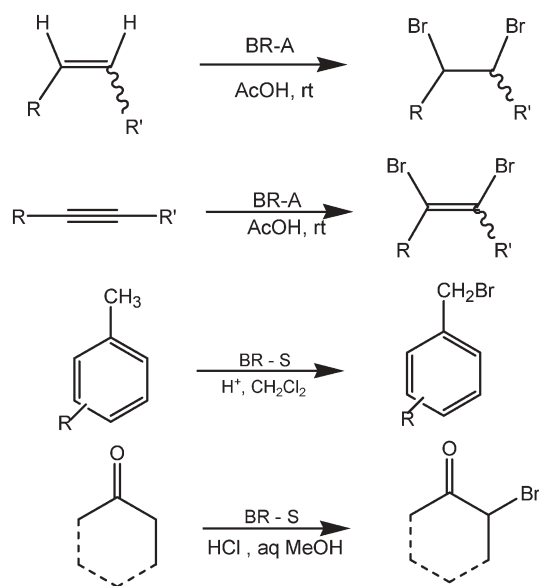
The experimental procedure was very simple. The alkene or alkyne was stirred with the bromide–bromate couple, BR-A, in acetic acid at room temperature for a certain period of time (TLC). Simple work up and purification by column chromatography provided the product.

Several structurally diverse alkenes underwent facile brominations by this procedure to produce the corresponding dibromides. The results are summarized in Table 1. The addition of bromine is completely stereoselective: the *cis* open chain alkenes producing *threo* (or *d,l*) isomers and *trans*

^aCentral Salt and Marine Chemicals Research Institute, Gijubhai Badheka Marg, Bhavnagar–364 002, Gujarat, India. E-mail: sadimurthy@yahoo.com; grama@csmcri.org; pkghosh@csmcri.org; Fax: +91-278-2567562

^bDepartment of Organic Chemistry, Indian Association for the Cultivation of Science, Jadavpur, Kolkata–700 032, India. E-mail: ocher@iacs.res.in

† Electronic supplementary information (ESI) available: spectra (¹H NMR and ¹³C NMR) of all products listed in Tables 1–4 and 6. See DOI: 10.1039/b713829f



Scheme 1

leading to *erythro* (or *meso*) dibromides. The stereochemical assignment was made by the coupling constants (J values) of the adjacent protons at the carbon atoms attached to bromo groups in agreement with the reported values. The cyclic olefins produced exclusively *trans*-dibromides (entries 3 and 4, Table 1). The activated alkenes (entries 7–13) were also smoothly brominated by this procedure. Several functional groups such as CO_2Et , OAc , OMe , ketocarbonyl, methylenedioxy, Cl and NO_2 remained unaffected under the reaction conditions.

A wide range of alkynes also underwent bromination by this reagent to produce the corresponding dibromides. The results are reported in Table 2. As is evident from the results, the alkyl-substituted alkynes provided *trans*-dibromides, while the aryl-substituted ones furnished mixture of *cis* and *trans* isomers with *trans* as the major one. The bromination of alkynes stopped at the dibromide stage and in no reaction was tetrabromide formed. The isolated alkene dibromide also did not undergo further bromination, even after 3 h. This observation is very significant and useful as molecular bromine was found to brominate the alkynes (phenylacetylene, 1-octyne as representative examples) to tetrabromide derivatives. This also demonstrates the contrast of this brominating agent to liquid bromine.¹⁰ This might be due to the slow release of bromine by BR-A in the reaction mixture. However, these addition reactions are possibly following an ionic path as involved with usual brominations by Br_2 .

2.2 Bromination of toluene derivatives (benzylic bromination)

Benzylic brominations are traditionally performed through a radical mechanism using bromine and NBS with radical initiator.¹¹ The other reagents employed for the benzylic bromination include $\text{NaBrO}_3\text{--NaHSO}_3$ ¹² and $\text{HBr--H}_2\text{O}_2$.¹³ These reagents, however, led to a mixture of mono-, di-, and nuclear brominated products. In the course of our studies towards the synthesis of 4-nitrobenzylbromide (abbreviated as PNBBBr) from 4-nitrotoluene (abbreviated as PNT), which is

Table 1 Bromination of alkenes by BR-A

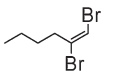
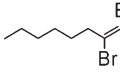
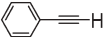
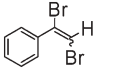
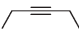
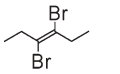
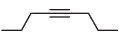
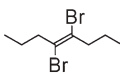
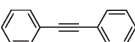
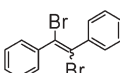
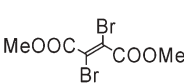
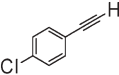
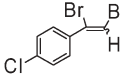
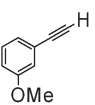
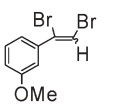
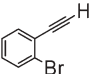
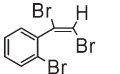
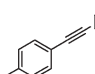
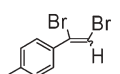
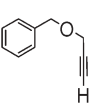
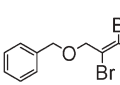
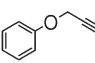
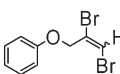
Entry	Alkene	Time/h	Product	Yield (%) ^a	Ref.
1		1.0		90	9
2		1.5		92	9
3		0.5		95	9
4		0.5		98	17
5		1.0		85	18
6		1.0		83	18
7		2.0		78	17
8		1.5		70	19
9		1.0		88	7
10		1.0		85	20
11		1.0		82	21
12		1.5		86	22
13		1.5		79	23

^a Yields refer to those of pure isolated products properly characterized by spectroscopic data (IR, ^1H , ^{13}C NMR).

an important pharmaceutical intermediate,¹⁴ the need for the development of a safe and environmentally benign method encouraged us to investigate the possibility of selective benzylic bromination with BR-S (entry 2, Table 3).¹⁵

Laboratory-scale preparation of PNBBBr initially required a long addition time when the reaction was conducted at room temperature (25–30 °C). Moreover, recovery of product in pure form tended to be low. Subsequently, through several improvements brought about in the process (*vide infra*) it was possible to reduce the reaction time to within 6 h under laboratory conditions. A variety of substituted toluenes and xylenes were obtained by this procedure (Tables 3 and 4). Side product (dibromo compounds/nuclear bromination) formation was low with toluene and substituted toluenes (Table 3). However, bromination of xylenes was accompanied by small

Table 2 Bromination of alkynes by BR-A

Entry	Alkyne	Time/h	Product	Yield (%) ^a	<i>cis:trans</i> ^b	Ref.
1	<chem>C4H9#C</chem>	2.5		85	0:100	24
2	<chem>C6H13#C</chem>	2.5		88	0:100	24
3		2.0		88	35:65	25
4		2.5		86	0:100	24
5		2.5		90	0:100	24
6		2.0		74	50:50	26
7	<chem>MeOOC#CCOOMe</chem>	3.0		76	0:100	27
8		2.0		85	15:85	
9		2.0		78	5:95	28
10		2.0		84	0:100	
11		2.0		83	45:55	29
12		2.5		90	0:100	29
13		2.5		88	30:70	30

^a Yields refer to those of pure isolated products properly characterized by spectroscopic data (IR, ¹H NMR, ¹³C NMR). ^b Ratio was determined by ¹H NMR spectroscopy.

amounts of α,α' -dibromoxylenes (entries 8–10, Table 4). Bromination of *para*- and *ortho*-xylenes gave **1hh** and **1ii** as sole products in 91 and 85% isolated yields, respectively (entries 1 and 2, Table 4), whereas bromination of *m*-xylene offered 52.5% of **1jj** and 45.5% of **1j** (entry 3, Table 4).

A detailed study was undertaken to optimize the reaction conditions for benzylic bromination. For this purpose *p*-nitrotoluene was chosen as the model compound. The reaction was attempted using different solvents (hexane, methanol, dichloromethane, dichloroethane, water). Several complications were encountered in using water and methanol while conversion was low in hexane. In contrast, the reaction was facile in dichloromethane and dichloroethane. The latter has the advantage of a higher boiling point, which can support

a higher reaction temperature leading to faster reaction rates. However, even with dichloromethane as solvent, the reaction could be completed within 6–8 h under reflux conditions and with efficient stirring of the reaction mass. At the end of the reaction, the organic phase could either be evaporated to recover the product and solvent or, preferably, the crude product could be recovered by chilling the reaction mass and re-cycling the mother liquor. Re-crystallization studies were conducted both with methanol and *n*-hexane and both were effective for purification. However, the latter was chosen for scale-up studies to avoid complications due to occluded methanol in the residue. The reaction was scaled up to *ca.* 4.5 mole per batch scale in a 10 L glass reactor and the data is provided in Table 5 for a PNT to Br mole ratio of 1.23:1. The

Table 3 Regioselective benzylic bromination of toluenes and xylenes

Entry	Products	R	Time/h	Yield (%) ^a	Ref.
1	1a	H	1.5	52	16
2	1b	4-NO ₂	12	75	10
3	1c	3-NO ₂	4	61	16
4	1d	2-NO ₂	6	66	16
5	1e	4-Cl	3	84	12
6	1f	3-Cl	3	73	16
7	1g	2-Cl	4	80	16
8	1h	4-CH ₃	5	69 ^b	16
9	1i	2-CH ₃	5	71 ^c	16
10	1j	3-CH ₃	5	66 ^d	16

^a Isolated yields. ^b 12.5% α,α'-dibromoxylene. ^c 9% α,α'-dibromoxylene. ^d 10% α,α'-dibromoxylene.

Table 4 α,α'-Dibromination of xylenes

Entry	Xylene	Time/h	Product	Yield (%) ^a
1	<i>p</i> -Xylene	7	1hh	91
2	<i>o</i> -Xylene	6	1ii	85
3	<i>m</i> -Xylene	9	1jj	98 ^b

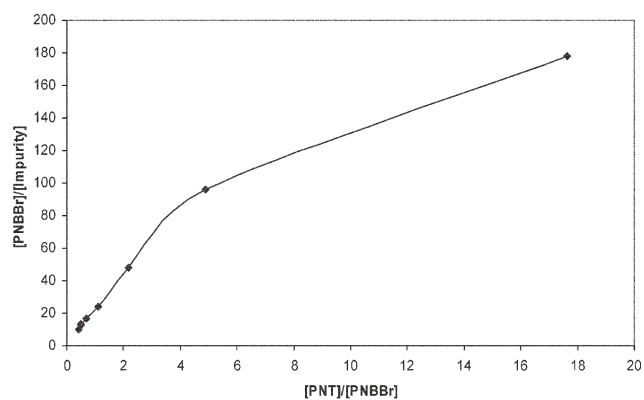
^a Isolated yields. ^b 45.5% **1j** is obtained.

residue remaining after purification of PNBBr and recovery of solvent was re-cycled in the subsequent batch so as to effectively utilize the sizeable amount of PNT and PNBBr remaining in it. This reduced the requirement of fresh PNT while maintaining the total PNT amount constant and also the PNT to solvent ratio constant. Recycling of residue beyond three cycles was found to be not beneficial and alternative means, *e.g.*, vacuum distillation, were necessary to recover PNT and PNBBr from the residue. Over 4 cycles, and accounting for PNT and PNBBr remaining in the residue after fourth cycle, the conversion was found to be 90.1% w.r.t. PNT taken while the selectivity was 90.7%. The combined yield of isolated product was 77.5% (w.r.t. PNT) with 98.1% overall purity. The main impurity formed in the course of PNBBr synthesis was the dibromo impurity, as confirmed through GC-MS. Since such impurity formation would be expected to

Table 5 Scale up data for preparation of *p*-nitrobenzylbromide with recycle of residue^a

Cycle	Fresh PNT/mole	BR-S reagent ^b (Br)/mole	HCl ^c /mole	Recrystallized product ^d /mole	Residue for recycle ^e		
					PNT/mole	PNBBr /mole	Impurities/g
1	4.38	3.56	3.70	2.64	1.23	0.21	31.1
2	3.15	3.56	3.70	2.27	2.05	0.30	50.3
3	2.33	3.65	3.70	1.96	2.21	0.45	92.8
4	2.19	3.65	3.70	2.47	1.22	0.46	179.4

^a All reactions were carried under reflux conditions using 1.8 L CH₂Cl₂, which was recovered and re-used. The reaction time was 8–12 h. ^b 15.8% active Br (w/v). ^c 13.5% (w/v). ^d Re-crystallization with *n*-hexane to achieve product having average purity of 98.1%. ^e Residue as obtained was recycled in the subsequent batch and fresh PNT was taken in a manner so as to keep total PNT input constant.

**Fig. 1** Plot showing the effect of the ratio of PNT to PNBBr on the selectivity of PNBBr formation. Ratios were estimated from GC area per cent data.

depend strongly on the relative concentrations of PNT and PNBBr, an experiment was carried out to study the effect more quantitatively. As can be seen from Fig. 1, the plot of the ratios of PNBBr:impurity *versus* PNT:PNBBr shows a steep increase in the selectivity of PNBBr formation with increasing ratio of PNT to PNBBr. Since this, in turn, is related to the ratio of PNT to BR-S, the latter ratio can be optimally selected to be in the range of 2:1 to 3:1. Reduction in the proportion of impurity will, no doubt, result in enhanced bromine atom efficiency as well.

2.3 Bromination of ketones

The bromide–bromate couple, BR-S, was also very efficiently used for α-monobromination of ketones. The results are presented in Table 6. Cyclic as well as acyclic ketones participated in this reaction.


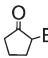
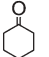
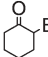

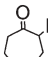
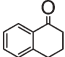
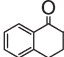
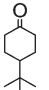
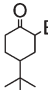
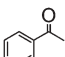
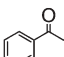
The reactions, in general, are very clean and high yielding. The products were obtained in high purity. Both the reagents, BR-A and BR-S, are non-hazardous and user-friendly.

3 Experimental section

3.1 General procedure. Representative procedure for bromination of alkene (entry 1, Table 1)

To a stirred solution of 1-octene (224 mg, 2 mmol) in acetic acid (4 mL) was added the bromide–bromate couple (5:1) BR-A (600 mg, 2.4 mmol active Br) and the reaction mixture was stirred at room temperature for 1 h (as monitored by TLC).

Table 6 Bromination of ketones by BR-S

Entry	Substrate	Time/h	Product	Yield (%)	Ref.
1		2.0		80	31
2		2.0		85	18
3		2.0		81	32
4		2.0		87	33
5		2.0		76	31
6		1.5		95	33

^a Yields refer to those of pure isolated products properly characterized by spectroscopic data (IR, ¹H NMR, ¹³C NMR).

The acetic acid in the reaction mixture was neutralized by sodium bicarbonate solution. The mixture was then extracted with Et₂O (3 × 10 mL) and the extract was washed with an aqueous solution of Na₂S₂O₃ and brine, and dried (Na₂SO₄). Evaporation of solvent left the crude product, which was purified by column chromatography over silica gel (hexane–ether 95:5) to provide pure 1,2-dibromooctane (489 mg, 90%) as a colourless oil, IR (neat) 2954, 2927, 2856, 1456, 1434 cm⁻¹; ¹H NMR (300 MHz, CDCl₃) δ 0.68 (d, *J* = 6.5 Hz, 3H), 1.07–1.39 (m, 6H), 1.52–1.60 (m, 2H), 1.85–1.93 (m, 2H), 3.36–3.43 (m, 1H), 3.59–3.64 (m, 1H), 3.90–3.98 (m, 1H); ¹³C NMR (75 MHz, CDCl₃) δ 14.4, 22.9, 27.1, 28.8, 31.9, 36.4, 36.7, 53.5. These values are in good agreement with those reported.

This procedure was followed for bromination of all the alkenes and alkynes listed in Table 1 and Table 2. All the products are known compounds except those in entries 8 and 10 in Table 2 and were identified by comparison of their spectroscopic data (¹H and ¹³C NMR) with those reported (see references in Tables 1 and 2). The unknown compounds in entries 8 and 10 in Table 2 were characterized by their spectroscopic data and elemental analysis.

(Table 2, entry 8). Pale yellow viscous oil as mixture of two isomers: IR (neat) 2939, 2936 cm⁻¹; ¹H NMR (300 MHz, CDCl₃) δ 6.82 (s, 0.85H, *trans*), 7.07 (s, 0.15H, *cis*), 7.35–7.47 (m, 4 H); ¹³C NMR (75 MHz, CDCl₃) δ 103.8, 109.6, 120.1, 128.5, 128.6, 128.8, 128.9, 130.2, 130.4, 130.6, 135.40, 135.41. Anal. calcd for C₈H₅Br₂Cl: C, 32.42; H, 1.70; found: C, 32.66; H, 1.98.

(Table 2, entry 10). Yellow viscous oil. IR (neat) 2958, 2932 cm⁻¹. ¹H NMR (300 MHz, CDCl₃) δ 6.87 (s, 1H), 7.24–7.37 (m, 3H), 7.62–7.65 (m, 1H); ¹³C NMR (75 MHz, CDCl₃) δ 107.1, 119.6, 122.2, 127.8, 130.4, 130.7, 133.2, 138.5. Anal. calcd for C₉H₇Br₃: C, 28.19; H, 1.48; found: C, 28.27; H, 1.64.

3.2 General procedure for the benzylic bromination (4-nitrobenzyl bromide is representative)

15.0 g (109.5 mmol) of 4-nitrotoluene, 45 mL of dichloromethane (DCM), 22.0 g of brominating reagent (containing 109.5 mmol available Br) and 50 mL of water were placed in a 500 mL round bottomed flask. To this reaction mixture, 11.5 mL (111 mmol) of 12 M HCl was added dropwise over a period of 12 h under stirring at room temperature. After the complete addition of acid, stirring was continued for a further 30 min. The organic layer was separated: 23.32 g (98.6% yield) of crude material was obtained after removal of solvent. The crude product was purified by crystallization with methanol: 15.25 g (70.6 mmol; 65.4% yield) of 4-nitrobenzyl bromide melts at 100 °C (literature² m.p. 97.5–99 °C). The crude product was purified by crystallization from methanol yielding 15.25 g (70.6 mmol; 65.4% yield) of 4-nitrobenzyl bromide having a melting point of 100 °C (reported m.p. 97.5–99 °C).² The residue (7.9 g) recovered from the mother liquor was recycled in a subsequent batch. 20.0 g (92.6 mmol; 85% yield; m.p. 100 °C) of 4-nitrobenzyl bromide was obtained after crystallization. Average of 75% yield of pure 4-nitrobenzyl bromide (purity >99% by GC) was obtained from two batches. The analytical data of all the products are in good agreement with authentic samples.

This procedure was followed for all the reactions listed in Tables 3 and 4. The products are all known compounds and were identified by comparison of their spectroscopic data (¹H and ¹³C NMR) with those reported (see references in Tables 3 and 4).

Caution. All benzylic bromides are eye irritants. Especially, α,α' -dibromo-*p*- and *o*-xylenes are eye and skin irritants, hence due care must be taken during workup and in handling.

3.3 General procedure. Representative procedure for bromination of ketones (entry 4, Table 6)

To a stirred solution of α -tetralone (730 mg, 5 mmol) in aqueous (1:1) methanol (10 mL), the bromide–bromate couple (2:1) BR-S (1 g, 5 mmol available Br) was added, followed by dropwise addition of dilute HCl (1 N, 10 mL). The reaction mixture was stirred for 2 h (as monitored by TLC). Work up and purification by the same process as in the procedure for bromination of alkene furnished pure α -monobrominated tetralone (967 mg, 86%) as a yellow viscous liquid: IR (neat) 2958, 2929, 2854, 1695, 1467 cm⁻¹; ¹H NMR (300 MHz, CDCl₃) δ 2.51 (m, 2H), 2.91 (m, 1H), 3.28 (m, 1H), 4.7 (t, *J* = 4.2 Hz, 1H), 7.25–7.34 (m, 2H), 7.47–7.53 (m, 1H), 8.06 (d, *J* = 7.8 Hz, 1H); ¹³C NMR (75 MHz, CDCl₃) δ 25.9, 31.7, 50.4, 126.9, 128.3, 128.6, 129.7, 133.9, 142.8, 190.3.

This procedure was followed for all the reactions listed in Table 6. The products are all known compounds and were identified by comparison of their spectroscopic data (¹H and ¹³C NMR) with those reported (see references in Table 6). Although all these representative procedures were based on the mmol scale, gram-scale reactions also produced similar results.

4 Conclusion

We have developed a very simple and efficient procedure for the highly stereo- and regioselective bromination of alkenes, alkynes, toluenes, xylenes and ketones using an alternative solid bromide–bromate couple, avoiding conventional liquid bromine which is highly hazardous and toxic. The primary advantage offered by the present reagent is its calculated release of Br₂ or BrOH on demand in the reaction vessel without polluting the environment. In addition, the selectivity, yield and simplicity of operation associated with this green brominating agent makes it a practical and better alternative to the existing reagents used for these reactions. Further applications of this reagent for other useful reactions are in progress.

Acknowledgements

We gratefully acknowledge the financial support from DST, New Delhi, for this investigation. We thank Professor D. Basavaiah for carrying out exploratory studies on benzylic bromination of toluene with BR-S under a project sponsored by CSMCRI, Bhavnagar. S.G. and M.A. are also thankful to CSIR and UGC, respectively, for their fellowships. The authors acknowledge the valuable comments of the referees which have been incorporated into the manuscript.

References

- (a) R. C. Larock, *Comprehensive Organic Transformations*, Wiley-VCH, New York, 2nd edn., 1999; (b) M. Kuroboshi, Y. Waki and H. Tanaka, *J. Org. Chem.*, 2003, **68**, 3938; (c) C. Gao, X. Tao, Y. Qian and J. Huang, *Chem. Commun.*, 2003, 1444.
- (a) A. Buttler and J. V. Walker, *Chem. Rev.*, 1993, **93**, 1937; (b) G. W. Gribble, *Chem. Soc. Rev.*, 1999, 335.
- J. A. Vona and P. C. Merker, *J. Org. Chem.*, 1949, **14**, 1048.
- S. Naik, R. Gopinath, M. Goswami and B. K. Patel, *Org. Biomol. Chem.*, 2004, **2**, 1670.
- A. Bongini, G. Cainelli, M. Contento and F. Manescalchi, *Synthesis*, 1980, 143.
- J. Salazar and R. Dorta, *Synlett*, 2004, 1318.
- V. Kavala, S. Naik and B. K. Patel, *J. Org. Chem.*, 2005, **70**, 4267.
- J. P. Das and S. Ray, *J. Org. Chem.*, 2002, **67**, 7861.
- (a) S. Adimurthy, G. Ramachandraiah, A. V. Bedekar, S. Ghosh, B. C. Ranu and P. K. Ghosh, *Green Chem.*, 2006, **8**, 916; (b) G. Ramachandraiah, P. K. Ghosh, A. S. Mehta, S. Adimurthy, A. D. Jethva and S. S. Vaghela, U.S. Patent No. 6,740,253 dated 25 May, 2004; (c) G. Ramachandraiah, P. K. Ghosh, A. S. Mehta, S. Adimurthy, A. V. Bedekar and D. B. Shukla, Indian Patent No. 194811 dated 17 Feb, 2006.
- Although the end product of the multi-electron process of eqn. 1 is Br₂, the reaction mechanism is complex (see for example: C. E. S. Côrtes and R. B. Faria, *Inorg. Chem.*, 2004, **43**, 1395) and would inevitably involve formation of reactive intermediates which may also play a role in bromination.
- (a) G. H. Coleman and G. E. Honeywell, *Org. Synth.*, 1943, *Coll. vol. 2*, 443; (b) J. M. Snell and A. Weissberger, *Org. Synth.*, 1955, *Coll. vol. 3*, 788; (c) F. M. Stephenson, *Org. Synth.*, 1963, *Coll. vol. 4*, 984; (d) A. Podgoršek, S. Stavber, M. Zupan and J. Iskra, *Tetrahedron Lett.*, 2006, **47**, 1097; (e) H. Shaw, H. D. Perlmutter and C. Gu, *J. Org. Chem.*, 1997, **62**, 236.
- D. Kikuchi, S. Sakaguchi and Y. Ishii, *J. Org. Chem.*, 1998, **63**, 6023.
- (a) R. Mestres and J. Palenzuela, *Green Chem.*, 2002, **4**, 314; (b) A. Podgoršek, S. Stavber, M. Zupan and J. Iskra, *Tetrahedron Lett.*, 2006, **47**, 7245.
- Know-how has been licensed to Chemcon Speciality Chemical Industry, Vadodara, India, for the bulk production of 4-nitrobenzyl bromide using present technology.
- See Acknowledgement section in ref. 9a.
- C. J. Pauchert and J. Behnke, *The Aldrich Library of ¹³C- and ¹H-FT NMR Spectra*, 1st edn, 1993, vol-II.
- G. W. Kabalka, K. Yang, N. K. Reddy and C. Narayana, *Synth. Commun.*, 1998, **28**, 925.
- Y. Levin, K. Hamza, R. Abu-Reziq and J. Blum, *Eur. J. Org. Chem.*, 2006, **6**, 1396.
- M. Fournier, F. Fournier and J. Berthelot, *Bull. Soc. Chim. Belges*, 1984, **93**, 157.
- M. R. Maharan, W. M. Abdou, M. M. Sidky and H. Wamhoff, *Synthesis*, 1987, 506.
- I. Urasaki and Y. Ogata, *J. Chem. Soc., Perkin Trans. 1*, 1975, 1285.
- J. Schumann, A. Kanitz and H. Hartmann, *Synthesis*, 2002, 1268.
- N. B. Barhate, A. S. Gajare, R. D. Wakharkar and A. V. Bedekar, *Tetrahedron*, 1999, **55**, 11127.
- G. W. Kabalka and K. Yang, *Synth. Commun.*, 1998, **28**, 3807.
- C. Ye and J. M. Shreeve, *J. Org. Chem.*, 2004, **69**, 8561.
- H. A. Muathem, *Synth. Commun.*, 2004, **34**, 3545.
- J. Berthelot, Y. Benammar and B. Desmazieres, *Synth. Commun.*, 1997, **27**, 2856.
- D. B. Bigley, N. A. J. Rogers and J. A. Barltrop, *J. Chem. Soc.*, 1960, 4613.
- L. Shao and M. Shi, *Synlett*, 2006, 1269.
- G. Ariamala and K. K. Balasubramanian, *Tetrahedron*, 1989, **45**, 309.
- B. Das, K. Venkateswarlu, G. Mahender and I. Mahender, *Tetrahedron Lett.*, 2005, **46**, 3041.
- K. Tanemura, T. Suzuki, Y. Nishida, K. Satsumabayashi and T. Horaguchi, *Chem. Commun.*, 2004, 470.
- B. C. Ranu, K. Chattopadhyay and R. Jana, *Tetrahedron*, 2007, **63**, 155.

γ -Valerolactone—a sustainable liquid for energy and carbon-based chemicals

István T. Horváth,*^a Hasan Mehdi,^a Viktória Fábos,^a László Boda^{ab} and László T. Mika^a

Received 21st August 2007, Accepted 13th November 2007

First published as an Advance Article on the web 4th December 2007

DOI: 10.1039/b712863k

We propose that γ -valerolactone (GVL), a naturally occurring chemical in fruits and a frequently used food additive, exhibits the most important characteristics of an ideal sustainable liquid, which could be used for the production of both energy and carbon-based consumer products. GVL is renewable, easy and safe to store and move globally in large quantities, has low melting ($-31\text{ }^{\circ}\text{C}$), high boiling ($207\text{ }^{\circ}\text{C}$) and open cup flash ($96\text{ }^{\circ}\text{C}$) points, a definitive but acceptable smell for easy recognition of leaks and spills, and is miscible with water, assisting biodegradation. We have established that its vapor pressure is remarkably low, even at higher temperatures (3.5 kPa at $80\text{ }^{\circ}\text{C}$). We have also shown by using ^{18}O -labeled water that GVL does not hydrolyze to gamma-hydroxypentanoic acid under neutral conditions. In contrast, after the addition of acid (HCl) the incorporation of one or two ^{18}O -isotopes to GVL was observed, as expected. GVL does not form a measurable amount of peroxides in a glass flask under air in weeks, making it a safe material for large scale use. Comparative evaluation of GVL and ethanol as fuel additives, performed on a mixture of 10 v/v% GVL or EtOH and 90 v/v% 95-octane gasoline, shows very similar properties. Since GVL does not form an azeotrope with water, the latter can be readily removed by distillation, resulting in a less energy demanding process for the production of GVL than that of absolute ethanol. Finally, it is also important to recognize that the use of a single chemical entity, such as GVL, as a sustainable liquid instead of a mixture of compounds, could significantly simplify its worldwide monitoring and regulation.

Introduction

The sustainability of mankind depends on whether we can supply the increasing population with enough energy, food, and chemicals, including carbon-based consumer products, simultaneously, without compromising the long term health of our planet. While it is difficult to predict the exact date of the depletion of fossil fuels,¹ the transition to renewable resources should be accelerated because of the frequently and unexpectedly changing political/economical environments resulting in limited access to and rising costs of fossil fuels.² Since the application of sustainable technologies for energy, including the efficient conversion of solar energy to electricity³ or hydrogen,⁴ might take longer than it is expected, the development of alternative sustainable liquids for energy and the chemical industry should be considered as a key research area in the next few decades. In addition, shifting the production of carbon-based chemicals from fossil fuels to renewable raw materials is also a key issue of sustainability.⁵

Some of the most important characteristics of an ideal sustainable liquid include: the possibility to use it for the production of both energy or carbon-based consumer products, renewable, easy and safe to store and move globally in large quantities, has a low melting point, high boiling and flash points, a definitive but acceptable smell for easy recognition of

leaks and spills, low or no toxicity, and some solubility in water to assist biodegradation. The vapor pressure should be as low as possible to minimize emission. Because of the aqueous and aerobic nature of the environment, it should not react with water and oxygen under ambient conditions. It is also important to recognize that the use of a single chemical entity as a sustainable liquid, instead of a mixture of compounds, could significantly simplify its worldwide monitoring and regulation. We propose and demonstrate here that γ -valerolactone could be considered as a sustainable liquid⁶ for global storage/transportation and a renewable hydrocarbon resource for energy and carbon-based consumer products.

Results and discussions

Although the efficient use of solar energy to produce electricity³ or hydrogen⁴ could solve the energy problem, the production of carbon-based consumer products requires the development of technologies based on renewable carbon sources. While crude oil, liquid natural gas, and coal or natural gas based Fischer–Tropsch liquids⁷ have some of the properties of a sustainable liquid, they are not renewable and therefore cannot be sustainable. Although methyl t-butyl ether (MTBE) was introduced to the gasoline market because of its positive environmental impact on car emission,⁸ its leak to drinking water became a major environmental issue⁹ and no process is known for its direct production from renewable resources,¹⁰ thus it cannot be sustainable as well. Although methanol has attractive properties for fuel-cell applications

^aInstitute of Chemistry, Eötvös University, Pázmány Péter sétány 1/A, H-1117, Budapest, Hungary. E-mail: istvan.t.horvath@att.net

^bMOL Plc, DS Development, Százhalombatta, Hungary

Table 1 Selected physical properties of various oxygenates

	Methanol	Ethanol	MTBE	ETBE	GVL	2-Me-THF
MW/g mol ⁻¹	32.04	46.07	88.15	102.17	100.12	86.13
Carbon (w%)	37.5	52.2	66.1	70.53	60	69.7
Hydrogen (w%)	12.6	13.1	13.7	13.81	8	11.6
Oxygen (w%)	49.9	34.7	18.2	15.66	32	18.7
Boiling point/°C	65	78	55	72–73	207–208	78
Melting point/°C	–98	–114	–109	–94	–31	–136
Density/°C	0.7910	0.8	0.74	0.742	1.05	0.86
Open cup flash point/°C	16.1	14	–33	–19	96	–11
LD ₅₀ , oral for rat/mg kg ⁻¹	5628	7060	4800	5000	8800	N/A

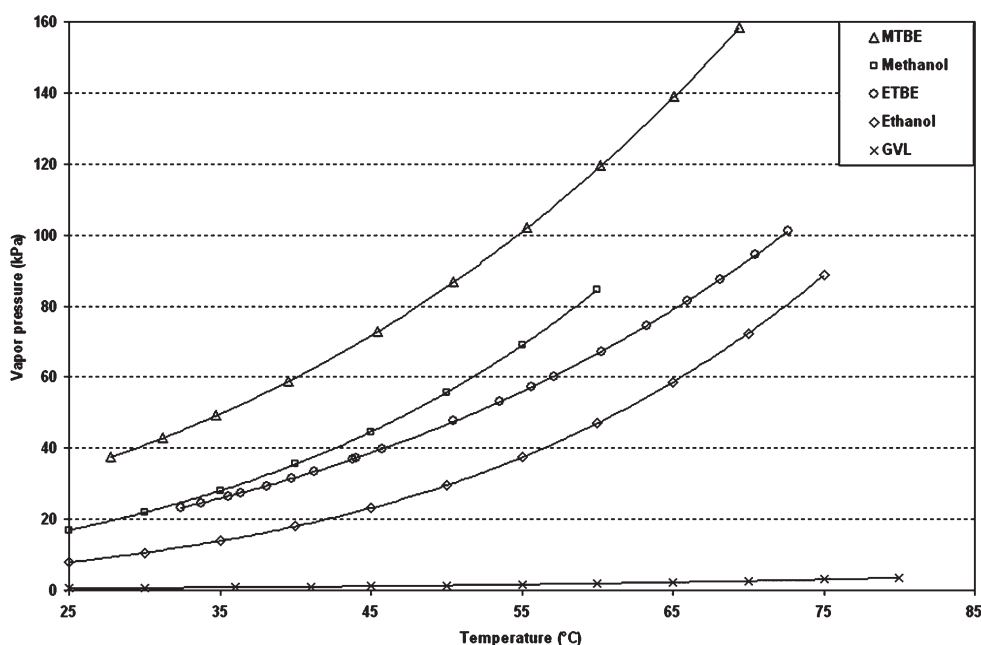
and can be converted to ethylene or propylene,¹¹ its high miscibility with water, combined with its acute toxicity if ingested in larger quantities,¹² could lead to serious environmental problems. In addition, its sustainable production from renewable resources, probably from carbon dioxide or biomass-based syn-gas,¹¹ has to be developed. In the contrary, ethanol is renewable and thus could be considered as a sustainable liquid, however, its low maximum production concentration limits in water,¹³ resulting in serious separation and consequently energy issues,¹⁴ could be a limiting factor. The production of bio-ethanol requires a two-step process; while producing 95% ethanol is straight forward, the removal of the rest of the water requires an energy demanding separation using azeotropic distillation or molecular sieves. Although bio-ethanol has been considered as an environmentally friendly fuel, its sustainability was recently seriously challenged.^{14,15} Finally, ethyl t-butyl ether (ETBE), produced by the reaction of ethanol with iso-butylene,¹⁶ could be considered sustainable only if iso-butylene is made from renewable resources.

We demonstrate here that γ -valerolactone (GVL) could be considered as a sustainable liquid,⁶ since it has several very attractive physical and chemical properties (Table 1), occurs

naturally, has been widely used by the food industry, and has a pleasant smell.¹⁷ In addition, it can be converted to 2-methyl-tetrahydrofuran (2-Me-THF), which has already been considered as the renewable component of an alternative fuel.^{18,19}

Although some of the known physical properties of GVL could make it an excellent candidate to use it as a sustainable liquid (Table 1), some important physical and chemical properties with respect to sustainability have not been reported. We have therefore first established the temperature dependence of the vapor pressure of GVL, a fundamental parameter for controlling VOC emission in general.²⁰ While the vapor pressure of GVL is 0.65 kPa at 25 °C, it only increases to 3.5 kPa at 80 °C (Fig. 1). In comparison to other oxygenates, including methanol,²¹ ethanol,²¹ MTBE,²² and ETBE,²² it appears that GVL has significantly lower vapor pressure.

The possibility that GVL hydrolyzes to gamma-hydroxy-pentanoic acid could result in corrosion problems during storage or transportation in steel equipments.²³ Therefore, the stability of GVL in the presence of water was investigated by treating GVL with an equimolar amount of 95% ¹⁸O-enriched water. No incorporation of ¹⁸O-isotope was observed by GC-MS at room temperature after 3 months and at 60 °C after

**Fig. 1** Temperature dependent vapor pressure of methanol, ethanol, MTBE, ETBE, and GVL.

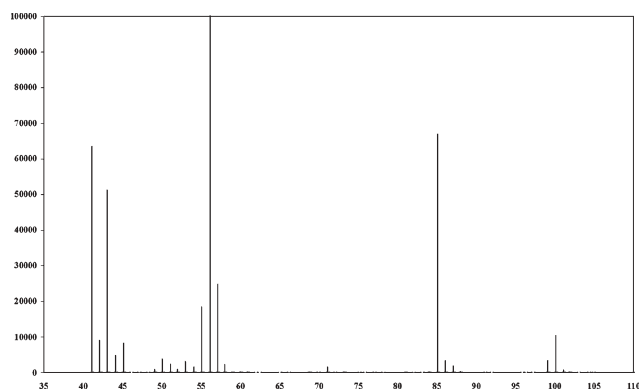


Fig. 2 MS of GVL after the treatment of 2.5 mmol GVL with 2.75 mmol H₂¹⁸O at = 60 °C for 28 days.

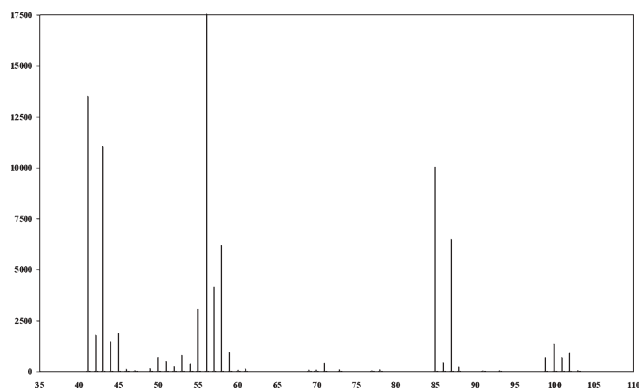


Fig. 3 MS of GVL after treating 2.6 mmol GVL with 2.6 mmol H₂¹⁸O in the presence of 1 mmol of gaseous HCl at 25 °C after 30 min.

28 days (Fig. 2). In contrast, when gaseous HCl was added to the reaction mixture, the incorporation of one ¹⁸O-isotope at room temperature (Fig. 3) and two ¹⁸O-isotopes at 90 °C was detected, indicating the formation of (¹⁸O)-GVL and (¹⁸O)₂-GVL, respectively.²⁴ It should be noted that GVL is miscible with water at room temperature.

The reaction of GVL with aqueous NaOH, resulting in gamma-hydroxypentanoate, has been reported²⁵ and we have confirmed the ring opening reaction by *in situ* NMR.

The stability of GVL under air could be an important issue, especially if peroxide(s) could form under ambient conditions. It has been reported that the reaction of levulinic acid with H₂O₂ results in the formation of gamma-hydroperoxy-GVL in 83% yield.²⁶ We have therefore continuously monitored the peroxide number²⁷ of GVL in a glass flask under air at room temperature. It appears that GVL does not form a measurable amount of peroxides after 35 days, making it a safe material for large scale use for a long time. It should be noted that 2-Me-THF, which can be prepared by the heterogeneous hydrogenation of levulinic acid or GVL,²⁸ readily forms peroxides,† which could be a major safety issue²⁹ for GVL if it

† We were able to prepare peroxide free 2-Me-THF by treating it with an aqueous solution of (NH₄)₂Fe(SO₄)₂, extracting GVL with EtAc, drying it with Na₂SO₄ and finally distilling it. All these operations were performed under nitrogen atmosphere, resulting in 2-Me-THF with no measurable peroxide. Keeping this 2-Me-THF in a closed glass bottle under air for 10 days shows 100 ppm peroxide.

is produced from levulinic acid by non-selective hydrogenation (e.g. over-hydrogenation of GVL to 2-Me-THF).

The application of GVL as a fuel itself has not been investigated yet and we are only aware of one example for its use as an additive to splash-blendable solubilized diesel fuel composition.³⁰ We have evaluated GVL and abs. ethanol as a fuel additive by preparing a mixture of 10 v/v% GVL or EtOH and 90 v/v% 95 octane gasoline (Table 2).³¹ While most of the data for GVL are comparable with ethanol, its lower vapor pressure leads to improved performance indeed.

We have recently demonstrated the multi-step conversion of sucrose to various C5-oxygenates and alkanes by integrating various homogeneous and heterogeneous catalytic systems (Scheme 1).³²

The overall mass and energy balances starting from sucrose to produce either ethanol or GVL are depicted in Scheme 2. While the formation of GVL is more favoured than that of ethanol by 40.6 kcal mol⁻¹, the combustion of the latter will provide more energy with exactly that amount. Since the production of sucrose or other carbohydrate-based feeds will require the same amount of energy for both abs. ethanol and GVL, their sustainability will depend on the conversion and separation technologies to the final product. An important aspect that might favour the route *via* GVL is that the separation of water from the GVL requires less energy than the separation of ethanol from water, since GVL does not form an azeotrope with water, while ethanol does (Fig. 4).

Conclusions

We have demonstrated that γ -valerolactone (GVL) exhibits very attractive physical and chemical properties and could be considered as a sustainable liquid for global storage and transportation, and a renewable hydrocarbon resource for energy and carbon-based consumer products for the chemical industry, provided it could be efficiently produced from biomass, preferentially from ligno-cellulose.³³ Since GVL does not form an azeotrope with water, the latter can be readily removed by distillation, resulting in a less energy demanding process for the production of GVL than that of absolute ethanol.

Experimental

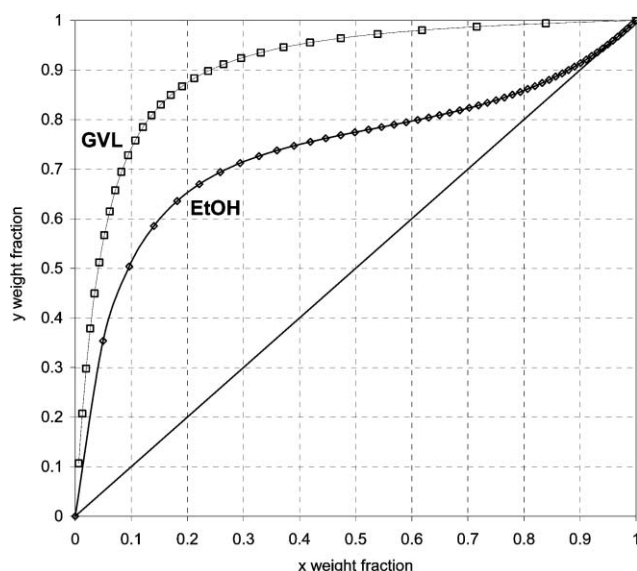
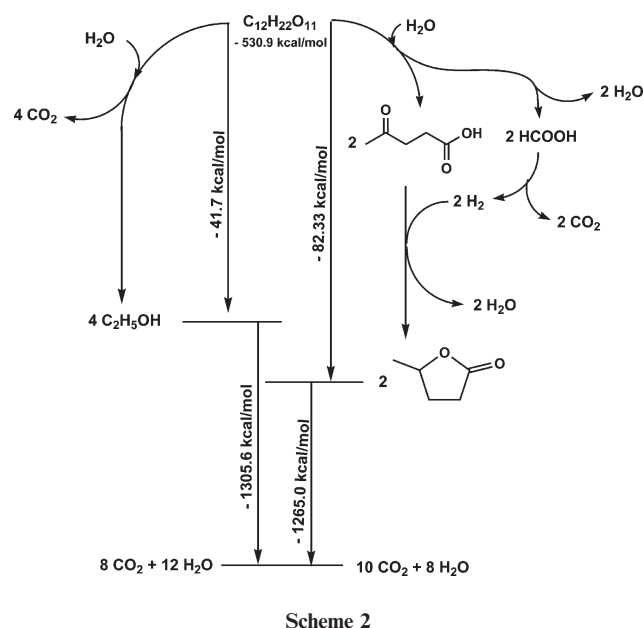
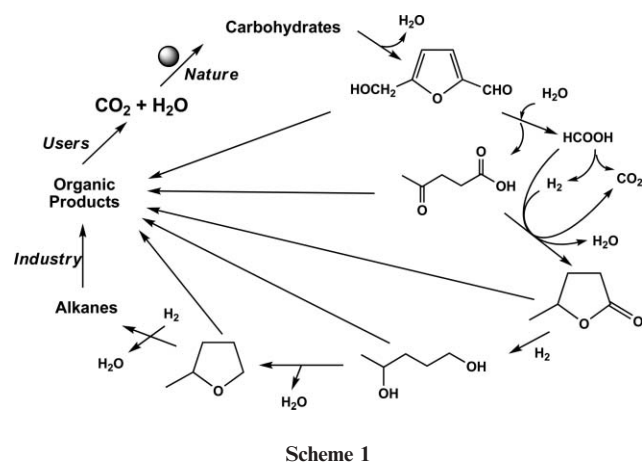
All chemicals were purchased from Aldrich and used without any further purification. Vapor pressure measurements were performed in a 31 mL Hasteloy-C high-pressure Parr reactor connected to a digital gauge. GC-MS spectra were obtained on an Agilent 6890GC instrument (with an 5973 selective mass detector) using a HP-5MS column (30 m \times 0.25 mm \times 0.25 μ m).

Measurement of the vapor pressure at various temperatures

4 mL of a liquid was placed in a 31 mL Hasteloy-C high-pressure reactor under air. The reactor was connected to a gauge and was evacuated at -50 °C for 2–3 min. The temperature was varied between 25–80 °C, and kept the temperature constant until the value of the vapor pressure did not change at all.

Table 2 Selected properties of 90 v/v% 95 octane gasoline and 10 v/v% EtOH or GVL

	MSZ EN 228 requirements	AN-95 gasoline	90 v/v% AN-95 + 10 v/v% EtOH	90 v/v% AN-95 + 10 v/v% GVL
Density (at 15 °C)/kg m ⁻³	720–775	733.5	737.8	765.8
Oxidation stability, min	min. 360	OK	OK	OK
Peroxide number/mg kg ⁻¹	1.75	1.40	1.72	
Vapor pressure (DVPE)/kPa	45–60 (summer) 60–90 (winter)	54.6	65.1	56.6
Vapor pressure (ASVP)/kPa		63.0	71.0	62.2
Evaporated up to 70 °C (v/v%)	20–48 (summer) 22–50 (winter)	27.2	47.9	24.1
Evaporated up to 100 °C (v/v%)	46–71	52.3	57.3	46.2
Evaporated up to 150 °C (v/v%)	min. 75	90.0	90.7	80.0
Final boiling point/°C max.	210	181.9	181.6	202.2
Distillation residue (v/v%)	max. 2	1.0	1.0	0.9
Gum content blown/mg per 100 mL	1.9	1.6	1.9	
Existent gum washed/mg per 100 mL	max. 5	0.5	0.8	0.8
Copper strip	1st class	1A	1A	1A
Motor octane number	min. 85	88.8	89.3	89.2
Research octane number (blending RON)	min. 95	97.2	97.4 (105)	97.3 (105)

**Fig. 4** Calculated equilibrium curves for water–GVL and ethanol–water at 1.01 bar.

Treatment of GVL with ¹⁸O-labeled water

A solution of 50 μL 95% ¹⁸O-enriched H₂O (2.5 mmol) and 265 μL (2.78 mmol) GVL was placed in a vial under air. It was kept at room temperature for 3 months and samples were taken for GC-MS every month. A similar experiment was also performed at 60 °C for 28 days. The GC-MS analysis in all cases showed no incorporation of ¹⁸O to GVL at all ($MW_{\text{GVL}} = 100$).

Treatment of GVL with ¹⁸O-labeled water under acidic conditions

A solution of 51.8 μL 95% ¹⁸O-enriched H₂O (2.6 mmol) and 260 mg (2.6 mmol) GVL ($MW = 100$) was placed in a vial under air. Immediately after the addition of 0.037 g (1.0 mmol) gaseous HCl (prepared by the reaction of NaCl and H₂SO₄) a

sample of 10 μL of liquid was taken and added to 5 mL of ethyl acetate. This sample was dried over sodium sulfate, filtered, and examined by GC-MS. The incorporation of one ^{18}O -labeled oxygen to GVL was observed (MW = 102). 50 μL 95% ^{18}O -enriched H_2O (2.5 mmol) and 0.1 g HCl (2.7 mmol) were added again to the reaction mixture, which was kept at 90 $^\circ\text{C}$. A sample was taken similarly after 3 days for GC-MS. The incorporation of two ^{18}O -labeled oxygens to GVL was observed (MW = 104).

Separation of water from GVL

The distillation of water from the mixture of 250 mL GVL and 250 mL water was performed in a 60 cm glass column packed with Sulzer EX laboratory structured packing with NTP \sim 20. The glass flask was heated up to boiling point (\sim 100 $^\circ\text{C}$) and the product was 99.7% water in one phase, based on GC analysis. No azeotrope formation was observed.

Acknowledgements

This work was funded by the Hungarian National Scientific Research Fund (T047207). We thank Prof. J. Manczinger, (Budapest University of Technology and Economics, Budapest, Hungary) for helping with the separation of water from GVL by distillation.

References

- 1 K. S. Deffeyes, *Beyond Oil: The View from Hubbert's Peak*, Farrar, Straus and Giroux, New York, 2005.
- 2 J. Chow, R. J. Kopp and P. R. Portney, *Science*, 2003, **302**, 1528.
- 3 J.-E. Moser, *Nat. Mater.*, 2005, **4**, 723.
- 4 National Research Council, *The hydrogen economy: opportunities, costs, barriers and R & D needs*, National Academies Press, Washington D. C., 2004.
- 5 M. Schlaf, *Dalton Trans.*, 2006, 4645.
- 6 I. T. Horváth, 10th Annual Green Chemistry & Engineering Conference, Washington, DC, July 26–30, 2006, abstract number 27.
- 7 R. B. Anderson, *The Fischer-Tropsch Synthesis*, Academic Press, Inc., Orlando, 1984.
- 8 Section 211(k) and Section 211(m) of the Clean Air Act, USA.
- 9 A. Keller, J. Froines, C. Koshland, J. Reuter, I. Suffet and J. Last, *Health and Environmental Assessment of MTBE*, report to the Governor and Legislature of the State of California as Sponsored by SB 521, Volume I, Summary and Recommendations, University of California, 1998.
- 10 S. H. Hamid and A. M. Ashraf, *Handbook of MTBE and Other Gasoline Oxygenates*, Marcel Dekker Inc., New York, 2004.
- 11 G. A. Olah, *Angew. Chem., Int. Ed.*, 2005, **44**, 2636.
- 12 Ingestion of 100–250 mL methanol may be fatal or result in blindness.
- 13 A typical fermentation will produce aqueous solutions of up to 8–12% ethanol in water.
- 14 D. Pimentel, *Nat. Resour. Res.*, 2003, **12**, 127.
- 15 T. W. Patzek, *Crit. Rev. Plant Sci.*, 2004, **23**, 519–567; T. W. Patzek, S.-M. Anti, R. Campos, K. W. Ha, J. Lee, B. Li, J. Padnick and S.-A. Yee, *Environ. Dev. Sustain.*, 2005, **7**, 319.
- 16 CDEtbe™ Technology Profile, CDTECH, <http://www.cdtech.com/>.
- 17 Odor description: herbal, sweet, warm, cocoa, and woody, Good Sence Company, Parfumery Raw Materials Information Sheet, <http://www.thegoodscentscompany.com/data/rw1024031.html>.
- 18 S. F. Paul, *US Pat.*, 5 697 987, 1996.
- 19 DOE, Alternative Fuel Transportation Program; P-series fuels (Proposed Rules), *Federal Register*, 1998, **63**, 40202.
- 20 Definition of VOC see 40 C. F. R. (Code of Federal Regulations) 51.100(s).
- 21 K. Nasirzadeh, D. Zimin, R. Neueder and W. Kunz, *J. Chem. Eng. Data*, 2004, **49**, 607.
- 22 M. K. Kriihenbihl and J. Gmehling, *J. Chem. Eng. Data*, 1994, **39**, 759.
- 23 A. Oasmaa and S. Czernik, *Energy Fuel*, 1999, **13**, 914.
- 24 A. Kailan, *Z. Physik. Chem.*, 1921, **94**, 111; A. R. Olson and R. J. Miller, *J. Am. Chem. Soc.*, 1938, **60**, 2687.
- 25 J. B. Umland and S. A. Witkowski, *J. Org. Chem.*, 1957, **22**, 345.
- 26 R. C. P. Cubbon and C. Hewlett, *J. Chem. Soc. C.*, 1968, 2986.
- 27 ASTM_D_3703_99.
- 28 H. S. Broadbent and T. G. Selin, *J. Org. Chem.*, 1963, **28**, 2343; K. Osakada, T. Ikariya and S. Yoshikawa, *J. Organomet. Chem.*, 1982, **231**, 79–90; L. E. Manzer, *U.S. Pat.*, 6 617 464, 2003.
- 29 C. McCloskey, *Plant/Oper. Prog.*, 1989, **8**, 185.
- 30 I. Ahmed, *US Pat.*, 6 190 427 and *US Pat.*, 6 306 184, 2001.
- 31 The 95 octane gasoline contained 32.3% alkylate, 35.47% reformate, 11.65% iC_5 and 20.58% iC_6 components. The RON and MON was 95.5 and 89.0, respectively.
- 32 H. Mehdi, V. Fábos, R. Tuba, A. Bodor, L. T. Mika and I. T. Horváth, *Top. Catal.*, in press.
- 33 I. T. Horváth and P. T. Anastas, *Chem. Rev.*, 2007, **107**, 2169.

Lipase catalysed mono and di-acylation of secondary alcohols with succinic anhydride in organic media and ionic liquids†

Rafał Bogel-Łukasik,^a Nuno M. T. Lourenço,^a Pedro Vidinha,^a Marco D. R. Gomes da Silva,^a Carlos A. M. Afonso,^b Manuel Nunes da Ponte^a and Susana Barreiros^{*a}

Received 22nd May 2007, Accepted 14th November 2007

First published as an Advance Article on the web 29th November 2007

DOI: 10.1039/b707695a

The acylation of the model substrate (*R,S*)-2-octanol with succinic anhydride catalysed by immobilised *Candida antarctica* lipase B was studied in two water-miscible organic solvents, two water-immiscible ones, nine 1-alkyl-3-methylimidazolium ionic liquids (RTILs) and two quaternary ammonium RTILs. From previous reports, the reaction was expected to yield an acidic half ester (hemiester). However, it was found that the diester was also produced, in many cases at an even higher yield. The major reaction products were the (*R*)-hemiester and the (*R,R*)-diester. In some of the solvents, the amount of hemiester formed increased and then remained constant, whereas in others the amount of hemiester first peaked and then decayed. This behaviour could be explained by the coupling of two reaction pathways: the hydrolysis of the hemiester, and the esterification of the hemiester. The solubility limit of succinic acid, produced in the former pathway, was found to be a discriminating parameter, the precipitation of the acid acting as a driving force for the consumption of the hemiester formed. The impact of the choice of solvent on the outcome of the acylation with succinic anhydride was confirmed by conducting the reaction on a preparative scale: in acetonitrile, the reaction produced 32% (w/w) of (*R*)-hemiester and 68% (w/w) of (*R,R*)-diester, whereas in tetrahydrofuran 85% (w/w) of (*R*)-hemiester and 15% (w/w) of (*R,R*)-diester were obtained.

Introduction

The number of industrial processes that involve biotransformations has been increasing steadily.^{1,2} Most biotransformation products are fine-chemicals, pharmaceuticals accounting for the most important share. The use of enzymes as enantioselective catalysts in kinetic resolutions has now become a common method to obtain pure enantiomers. The applicability of this approach has been greatly expanded by replacing the conventional aqueous solutions with nonconventional solvents, not only organic media but also supercritical fluids (sc-fluids) and room-temperature ionic liquids (RTILs). Both sc-fluids and RTILs can comply with the concern for green(er) chemistry.³ Sc-fluids can be vented, leaving no residues, and RTILs have an immeasurably small vapour pressure, at ambient temperature.⁴ The characteristics of both types of systems can also be advantageously combined.^{5–8}

Sec-alcohols account for a large share of the compounds produced in industrial biotransformations.¹ The kinetic resolution of racemic alcohols is very often accomplished *via* a transesterification reaction. The use of enol-esters such as

vinyl esters is a common strategy to make the reaction irreversible due to the formation of vinyl alcohol that tautomerises to acetaldehyde. To avoid possible negative effects of acetaldehyde on enzyme activity, other acylating agents have been researched, such as anhydrides.⁹ In particular, succinic anhydride has been used for the resolution of a wide range of alcohol substrates catalysed by several lipases.^{10–13} In all of these studies, one of the main reasons for the use of succinic anhydride was the fact that the reaction yielded an acidic half ester (hemiester), which could be easily separated from the reaction mixture, *e.g.* by liquid–liquid extraction with an alkaline solution.

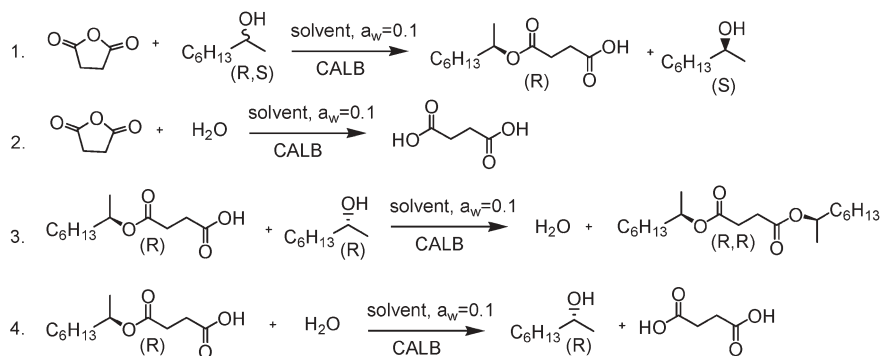
More recently, this reaction–separation strategy has also been applied in 1-butyl-3-methylimidazolium hexafluorophosphate ([bmim][PF₆]).¹⁴ We decided to follow the same approach in the resolution of the substrate model (*R,S*)-2-octanol, catalysed by Novozym 435 in organic solvents and in RTILs. From the previous reports on the use of succinic anhydride as an acylating agent, including that by Terao *et al.*¹⁰ who were able to obtain the two isomers of 2-octanol in high chemical and optical yields, and those by Sorgedraeger *et al.*¹¹ and Bouzemi *et al.*¹² who employed *Candida antarctica* lipase B (CALB) successfully in the resolution of β -nitro alcohols and aryl-alkyl alcohols, we expected to obtain the hemiester alone. However, we found that we were forming the diester as well (Scheme 1).

Also the profiles obtained for the hemiester were not always the same. Here we give a detailed account of our experiments and present a rationalisation of the results obtained.

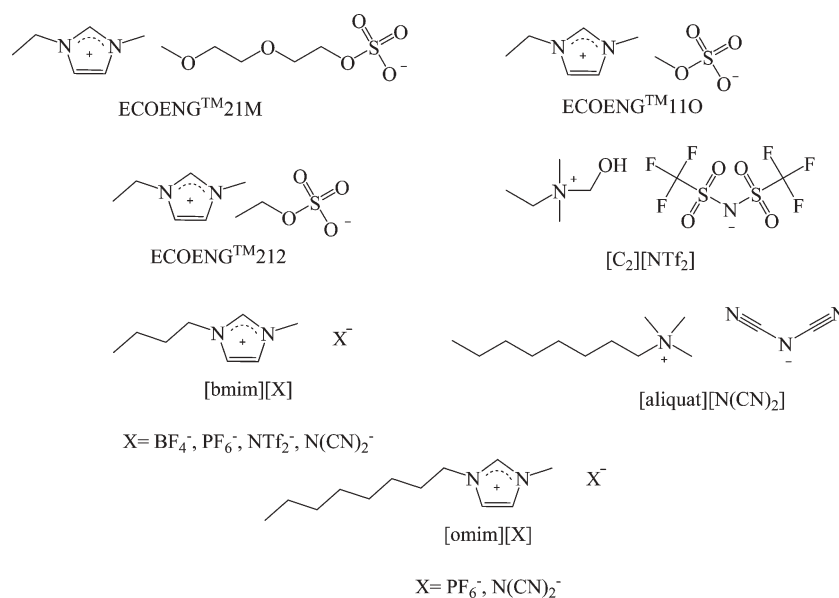
^aREQUIMTE/CQFB, Departamento de Química, Faculdade de Ciências e Tecnologia, Universidade Nova de Lisboa, 2829-516, Caparica, Portugal. E-mail: sfb@dq.fct.unl.pt; Fax: +351 21 2948385; Tel: +351 21 2949681

^bCentro de Química Física Molecular, Instituto Superior Técnico, 1049-001, Lisboa, Portugal

† Electronic supplementary information (ESI) available: Reaction progress in different organic solvents and ionic liquids, conversion of the (*R*)-hemiester in *n*-hexane. See DOI: 10.1039/b707695a



Scheme 1 Reaction pathways.



Scheme 2 Tested ionic liquids.

Results and discussion

Our study began with an optimisation of reaction conditions in [bmim][PF₆] that led to the choice of enzyme concentration, 2-octanol : succinic anhydride molar ratio and water activity (*a_w*). Higher values than indicated for the former two parameters no longer improved 2-octanol conversion. For *a_w* values lower than 0.1, it took longer to reach a steady conversion, whereas for higher *a_w* the maximum conversion obtained was lower. We extended this study to ten other RTILs, as well as two water-miscible and two water-immiscible organic solvents (Scheme 2).

Here we show results for only four of the solvents tested. In most of them, the reaction yielded a mixture of (*R,R*)-diester and (*R*)-hemiester (Figs. 1 and 2).

In some solvents, such as [omim][N(CN)₂] and acetonitrile, the amount of hemiester first peaked and then decayed; in tetrahydrofuran, it first increased and then remained roughly constant, as in more polar solvents like [bmim][PF₆].

To understand these findings, it is important to consider the relevant reaction pathways for the transformation of the substrates. As shown in Scheme 1, in addition to reacting with

the alcohol to form the hemiester (pathway 1), succinic anhydride can also be hydrolysed to give succinic acid (pathway 2). The hemiester can react with an alcohol molecule

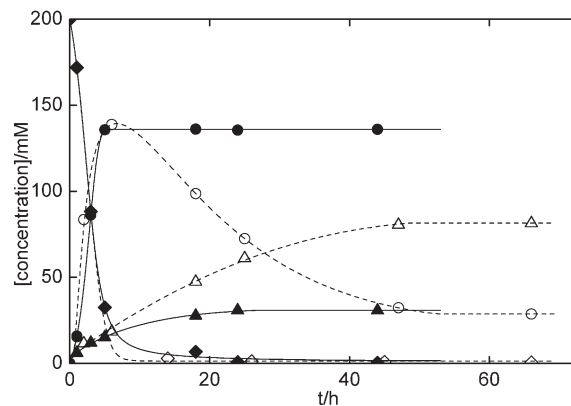


Fig. 1 Reaction progress in tetrahydrofuran (solid lines and full symbols: (*R*)-2-octanol (◆), (*R*)-hemiester (●), (*R,R*)-diester (▲)), and in acetonitrile (dashed lines and open symbols: (*R*)-2-octanol (◇), (*R*)-hemiester (○), (*R,R*)-diester (□)), at 35 °C and *a_w* = 0.1.

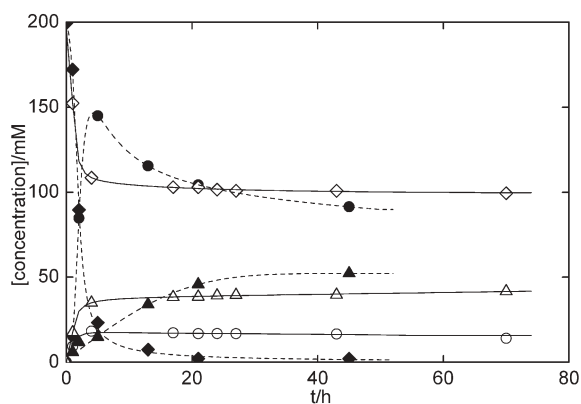


Fig. 2 Reaction progress in [omim][N(CN)₂] (solid lines and full symbols: (*R*)-2-octanol (◆), (*R*)-hemiester (●), (*R,R*)-diester (▲)), and in [bmim][PF₆] (dashed lines and open symbols: (*R*)-2-octanol (◇), (*R*)-hemiester (○), (*R,R*)-diester (□)), at 35 °C and $a_w = 0.1$.

to give the diester (pathway 3), and can also be hydrolysed to give the alcohol and succinic acid (pathway 4). The impact of pathways 3 and 4 on the overall process can be seen in Fig. 3. This figure represents the outcome of a reaction in which only the (*R*)-hemiester was added to [omim][N(CN)₂], at $a_w = 0.1$. The reaction yielded stoichiometric amounts of the diester and of succinic acid, in the same time scale as that depicted in Figs. 1 and 2. Hydrolases such as lipases work *via* a mechanism consisting of an acylation step that leads to the formation of the acyl-enzyme intermediate, followed by deacylation. When only the (*R*)-hemiester and water are present, only pathway 4 can take place. Mechanistically, the serine residue of the catalytic triad attacks the carbon atom on the carbonyl group of the ester bond, leading to the release of the alcohol. The acid is released at the end of the deacylation step. Pathway 3 is an esterification reaction in which the active site serine attacks the carbon atom of the carboxyl group, leading to the release of water and formation of the acyl-enzyme. The diester is the second reaction product. The results from Fig. 3 tell us that immediately after being formed in pathway 4, the alcohol reacts with a second molecule of (*R*)-hemiester to yield the (*R,R*)-diester, *i.e.* pathways 3 and 4 occur virtually simultaneously so that the data points for the diester and the acid are

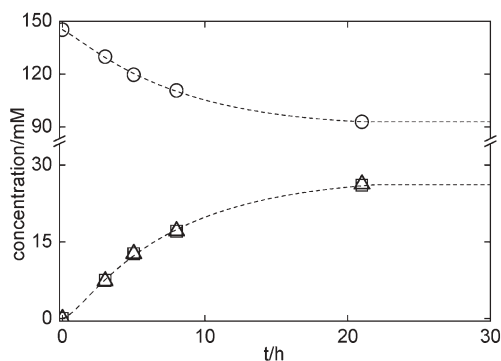


Fig. 3 Conversion of the (*R*)-hemiester (○) in [omim][N(CN)₂], to yield (*R,R*)-diester (△) and succinic acid (□), at 35 °C and $a_w = 0.1$. [(*R*)-hemiester] = 145 mM.

superimposed. Overall the process can be represented as two molecules of (*R*)-hemiester yielding one molecule of (*R,R*)-diester and one molecule of succinic acid, the alcohol and water balancing out, *i.e.* the amounts of (*R*)-hemiester that react through pathways 3 and 4 are exactly the same.

In regular reactions, the alcohol is present at the onset of the process and can influence its outcome. To simulate this situation, an experiment was performed in acetonitrile with initial concentrations of *ca.* 140 mM for the (*R*)-hemiester, and 50 mM for the (*R,S*)-alcohol (the concentration of the (*R*)-alcohol measured at 5 hours of reaction for that solvent, taken from Fig. 2, is 25 mM), as shown in Fig. 4A (full symbols and solid lines). For comparison, this figure includes the results obtained when only the (*R*)-hemiester and water are present, *i.e.* obtained at the same conditions as Fig. 3 (open symbols and dashed lines; again, the curves for the diester and the acid are superimposed). By comparing the two sets of data, one can see that when the alcohol is present at the onset of the process, pathways 3 and 4 are no longer entirely coupled. Due to the initial concentration of the alcohol, there is an additional contribution to the formation of the diester through pathway 3 (full triangles). This means forming the diester at a lower cost in terms of the hemiester, *i.e.* at a stoichiometry of 1 : 1, instead of the 2 : 1 for the coupled process (full circles are below open circles). A mass balance of this data indicates that *ca.* 40% of the (*R*)-hemiester reacts through pathway 4 at these conditions, the remaining 60% reacting through pathway 3. Overall less succinic acid is produced (full squares) and a higher amount of (*R,R*)-diester is generated.

To show that this is approximately what happens in regular reactions, in Fig. 4B we compare the results obtained when only the (*R*)-hemiester and water are present (same open symbols and dashed lines as in Fig. 4A) with data taken from Fig. 1 for acetonitrile (full symbols and solid lines). Fig. 1 shows that the concentration of (*R*)-hemiester reached the value 140 mM at 5 hours of reaction. Thus we extracted the data from Fig. 1 from 5 hours of reaction onwards and superimposed the data on Fig. 4B starting at $t = 0$. Likewise for the (*R,R*)-diester, *i.e.* the data in Fig. 4B taken from Fig. 1 refers only to the (*R,R*)-diester that was formed from 5 hours onwards in the regular reaction. The data for succinic acid was treated in the same way. If we look at the solid lines in Figs. 4A and B, we see that the agreement observed between the two sets of data in what concerns the (*R*)-hemiester and the (*R,R*)-diester is fairly good, thus confirming the coupling of pathways 3 and 4 as the cause for the decrease in the concentration of this ester that is observed in some solvents after the peak. The only significant difference is found for succinic acid (full squares), which can now be produced also in pathway 2, *via* the hydrolysis of succinic anhydride. The hemiester is now generated through pathway 1.

What happens then in the more polar solvents and in tetrahydrofuran? Why does the amount of hemiester produced in pathway 1 remain roughly constant? The answer to this question can be found in the solubility of succinic acid in the solvents. The maximum concentration of (*R*)-hemiester that can be produced in pathway 1 is 200 mM, which means that the maximum concentration of succinic acid that can be generated through the full coupling of pathways 3 and 4 is

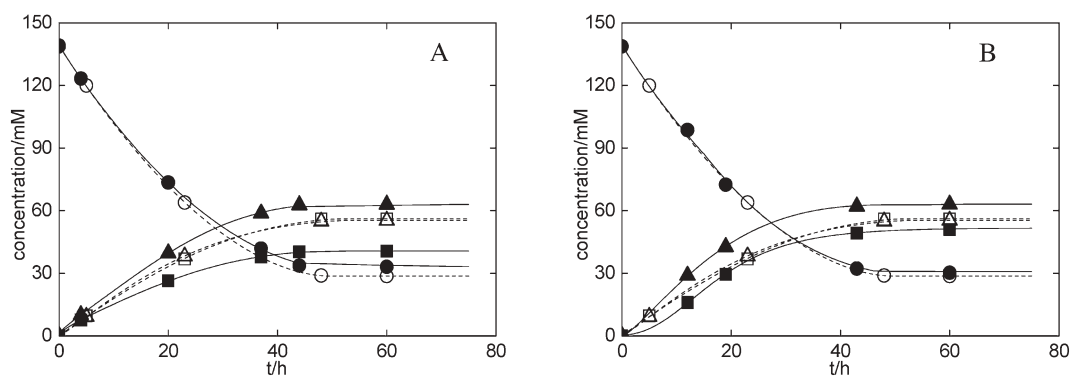


Fig. 4 Conversion of the (*R*)-hemiester (○) in acetonitrile, to yield (*R,R*)-diester (△) and succinic acid (□), at 35 °C and $a_w = 0.1$. [(*R*)-hemiester] = 145 mM. Additional data on A, in full symbols and solid lines: Conversion of the (*R*)-hemiester (139 mM) in acetonitrile, in the presence of (*R,S*)-2-octanol (50 mM)—(*R*)-hemiester (●); (*R,R*)-diester (▲); succinic acid (■). Additional data on B, in full symbols and solid lines: Reaction profile taken from Fig. 1 for acetonitrile, as explained in the text—(*R*)-hemiester (●); (*R,R*)-diester (▲); succinic acid (■).

Table 1 Solubility data for succinic acid, obtained in the present work

Solvent	$C_{\text{succinic acid}}/\text{mM}$
[bmim][PF ₆]	152
[omim][PF ₆]	72
[omim][N(CN) ₂]	97
Di-isopropyl ether	62
<i>n</i> -Hexane	70
Acetonitrile	63
Tetrahydrofuran	286

100 mM. As shown in Table 1, the solubility of succinic acid in acetonitrile is below 100 mM.

The precipitation of the acid should be a driving force for the consumption of the hemiester through pathway 4. Indeed, in this solvent the decline in the amount of (*R*)-hemiester after the peak is very pronounced, more so than in [omim][N(CN)₂], in which the solubility of the acid is higher. Tetrahydrofuran is an interesting solvent in this respect because it has low polarity in a general sense but the solubility of succinic acid in it is almost 300 mM. [omim][PF₆] is also not a problem in that respect. In any case, in the more polar solvents, the reaction is less favourable and the solubility limit of succinic acid is no longer a discriminating parameter.

These findings are not limited to 2-octanol. Reactions with 2-butanol using succinic anhydride as the acylating agent, catalysed by *Pseudomonas cepacia* lipase or Novozym 435, yielded a mixture of diesters and hemiesters in [bmim][PF₆]. The same applied to the Novozym 435 catalysed conversion of 1-phenylethanol. Katsoura *et al.*¹⁵ and Park and Kazlauskas¹⁶ report findings that are somewhat similar to these, in what concerns a perceived important role of solvation on the outcome of the reactions studied. Katsoura *et al.*¹⁵ looked at the acylation of flavonoid glycosides with vinyl esters in two RTILs and two organic solvents, catalysed by Novozym 435 and two other lipases. They found that the reactions produced not only monoacylated flavonoid derivatives, but also di-substituted ones, upon acylation at an additional position on the glucoside moiety. They compared their results with those of other authors who had used the same enzyme, the same organic solvents but a different acylating agent, and had reported the formation of the monoacylated derivative only.

Katsoura *et al.*¹⁵ suggested that their results could be explained by the differences in solvation of the two esters formed. Park and Kazlauskas¹⁶ have also used an argument based on solvation to explain the differences in regioselectivity of the acylation of glucose catalysed by CALB, in RTILs and in organic solvents. We believe that a similar argument can be used in the present study, in which the mono- and di-acylation of 2-octanol depends on a critical balance of solvent polarity and succinic acid solubility.

To stress the relevance of the choice of solvent on the outcome of the acylation with succinic anhydride, we performed reactions in acetonitrile and in tetrahydrofuran on a preparative scale (0.5 g of 2-octanol). In acetonitrile, we isolated 3% (w/w) of (*R*)-hemiester and 68% (w/w) of (*R,R*)-diester, whereas in tetrahydrofuran we isolated 85% (w/w) of (*R*)-hemiester and 15% (w/w) of (*R,R*)-diester.

Experimental

Materials

Immobilised *Candida antarctica* lipase B (Novozym 435) was a gift from Novo Nordisk Bioindustrial, Spain. *Pseudomonas cepacia* lipase was from Amano, Japan. (*R,S*)-2-octanol (>97% purity) was from Riedel-de Haën, (*R,S*)-2-butanol (>98% purity) was from Fluka, and (*R,S*)-1-phenylethanol (>98% purity) was from Merck. Succinic anhydride (>99% purity), tridecane (>99% purity), sodium chloride (99.5% purity) and tetrahydrofuran (>99% purity from Aldrich), freshly distilled from CaH₂. Di-isopropyl ether (>98% purity) was supplied by Merck. Acetonitrile (>99% purity), potassium acetate (>98% purity) and Hydranal Coulomat A and C Karl-Fischer reagents were from Riedel de Haën. Ionic liquids: ECOENGTM 21 M (98% purity), ECOENGTM 110 (99% purity), ECOENGTM 212 (≥98% purity) were gifts from Solvent Innovation GmbH, Cologne, Germany. Ethyl-(2-hydroxyethyl)-dimethylammonium bis(trifluoromethylsulfonyl)imide -[C₂][NTf₂], (purity: ≥99%) was synthesised by us. [bmim][BF₄] (≥98% purity), [bmim][NTf₂] (≥98% purity), [bmim][PF₆] (≥98% purity), [bmim][N(CN)₂] (≥98% purity), [aliquat][N(CN)₂] (≥98% purity), [omim][PF₆] (≥98% purity), [omim][N(CN)₂] (≥98% purity) were supplied by/gifts from

Solchemar Portugal, Lisbon, Portugal. All RTILs were used without any further purification. Substrates and tridecane were stored over molecular sieves (3 Å beads from Merck).

General procedure for the enzymatic acylation

Reactions were performed in plastic vials (reaction volume up to 1 cm³) placed in a constant temperature (35 °C) orbital shaker set for 400 rpm. The solvent (750 µl) was added to succinic anhydride (800 mM), followed by addition of the amount of water required to reach $a_w = 0.1$, enzyme (40 g L⁻¹) and, finally, (*R,S*)-alcohol (400 mM) to start the reaction. Tridecane (2.91 mM) in acetonitrile was used as external standard for GC analysis. For some solvents, a scale of a_w vs. water concentration was built by equilibrating the solvent with saturated salts solutions or with water at 25 °C for a number of days, to achieve the values 0.22 (potassium acetate) and 0.75 (sodium chloride), taken from the literature,¹⁷ and 1 (saturation); the water concentration at $a_w = 0.1$ was obtained by interpolation. In other cases, we took $a_w = 0.1$ to correspond to half the water concentration obtained after equilibration at $a_w = 0.22$, since the scale is linear at low a_w values (equilibration of some of the solvents with a LiCl saturated salt solution that sets $a_w = 0.11$ ¹⁷ showed that the former procedure was reasonably accurate). In the case of acetonitrile and tetrahydrofuran, we derived values from the data for the Wilson equation presented by Bell *et al.*¹⁸ Water concentration was measured by Karl-Fisher titration. In the absence of enzyme, reaction conversion does not exceed *ca.* 2% after 48 hours.

Analysis

The reactions were followed by GC analysis performed with a Trace 2000 Series Unicam gas chromatograph equipped with a 30 m × 0.32 mm id fused silica capillary column coated with a 0.25 µm thickness film of 20% 2,3-dimethyl-6-*tert*-butyldimethylsilyl-β-cyclodextrin dissolved in BGB-15, from BGB Analytik AG. Oven temperature program: 90 °C–110 °C ramp at 1 °C min⁻¹, 110–180 °C ramp at 7 °C min⁻¹, 180–220 °C ramp at 1 °C min⁻¹, injection temperature: 250 °C. Flame ionization detection (FID) temperature: 250 °C. Carrier gas: helium (0–20 min: 4.0 cm³ min⁻¹, 20–50 min: 1.0 cm³ min⁻¹). Split ratio: 1 : 20. The data given are the average of at least two measurements. Retention times: (*R,S*)-2-octanol: 10.21; succinic acid: 11.16; tridecane: 26.26; (*S*)-hemiester: 45.8; (*R*)-hemiester: 45.99; (*S,S*)-diester: 66.55; (*R,R*)-diester: 66.77; (*R,S*)-diester: 66.98. Response factors: (*R,S*)-2-octanol: 8.9; succinic acid: 14.7; hemiesters: 6.3; diesters: 3.1. The enzyme was usually highly selective towards (*R*)-2-octanol ($ee_p > 0.99$), but enantioselectivity dropped in the less polar solvents, which led also to the formation of the (*S*)-hemiester, the (*S,S*)-diester and the *meso*-(*R,S*)-diester from the start of the reaction.

Preparative scale enzymatic acylation

Reactions were performed as described in the previous section, using tetrahydrofuran or acetonitrile (8.0 mL, $a_w = 0.1$), succinic anhydride (770 mg, 801 mmol), Novozym 435

(384 mg) and (*R,S*)-2-octanol (500 mg, 400 mmol). The enzyme was removed by filtration after 5 and 47 hours for tetrahydrofuran and acetonitrile, respectively. The solvent was evaporated under vacuum and after purification by flash column chromatography (SiO₂, eluent: *n*-hexane: ethyl acetate from 90 : 10 to 30 : 70) the amounts of (*R,R*)-diester obtained were 272 mg (68%) in acetonitrile and 56 mg (15%) in tetrahydrofuran, and of (*R*)-hemiester were 125 mg (32%) in acetonitrile and 313 mg (85%) in tetrahydrofuran.

Preparation of *meso* and racemic standards

A mixture of (*R,S*)-2-octanol (568 µl, 3.54 mmol) and succinic anhydride (354 mg, 3.54 mmol) was stirred for 8 h at 145 °C. After this time, the reaction mixture was quenched with a saturated aqueous solution of sodium carbonate and extracted with dichloromethane (3 × 25 mL). The combined organic phases were dried under MgSO₄ and filtered. The solvent was then removed under vacuum leaving oil. Purification by flash column chromatography (SiO₂, eluent: *n*-hexane : ethyl acetate 95 : 5) gave as an oil (959.0 mg, 76%) racemic and *meso*-dioctan-2-yl succinate (diester); ¹H NMR (CDCl₃) δ 0.88 (t, 6H, *J* = 6.9 Hz, CH₃), 1.20 (d, 6H, *J* = 6.2 Hz, CH₃), 1.27 (m, 16H, (CH₂)₄), 1.44–1.49 (m, 2H, CH₂), 1.55–1.58 (m, 2H, CH₂), 2.59 (s, 4H, (CH₂)₂), 4.90 (sex, 2H, *J* = 6.2 Hz, CHO); ¹³C NMR (CDCl₃) δ 14.0 (CH₃), 19.9 (CH₃), 22.6 (CH₂), 25.3 (CH₂), 29.1 (CH₂), 29.6 (CH₂), 31.7 (CH₂), 35.9 (CH₂), 71.4 (CH), 171.9 (CO ester); IR (NaCl, film) 2931, 2858, 1736, 1462, 1415, 1377, 1338, 1311, 1265, 1169, 1122, 1034, 995, 972, 876 cm⁻¹; HRMS (FAB) Calcd. for C₂₀H₃₉O₄ [MH⁺]: 343.28484. Found 343.28443.

The aqueous phase was acidified with a 10% aqueous HCl solution and extracted with dichloromethane (3 × 25 mL). The combined organic phases were dried under MgSO₄ and filtered. The solvent was then removed under vacuum leaving racemic 4-(octan-2-yloxy)-4-oxobutanoic acid (hemiester) as white solid (85.0 mg, 10%) m.p. rt–29 °C; ¹H NMR (CDCl₃) δ 0.87 (t, 3H, *J* = 7.0 Hz, CH₃), 1.19 (d, 3H, *J* = 6.2 Hz, CH₃), 1.26 (m, 8H, (CH₂)₄), 1.43–1.48 (m, 1H, CH₂), 1.54–1.59 (m, 1H, CH₂), 2.56–2.68 (m, 4H, (CH₂)₂), 4.91 (sex, 1H, *J* = 6.2 Hz, CHO), 10.20 (br, 1H, COOH); ¹³C NMR (CDCl₃) 14.0 (CH₃), 19.8 (CH₃), 22.5 (CH₂), 25.3 (CH₂), 29.0 (CH₂), 29.2 (CH₂), 31.7 (CH₂), 35.8 (CH₂), 71.7 (CH), 171.7 (CO ester), 178.4 (CO acid); IR (NaCl, film) 3491–2700, 2956, 2931, 2859, 1732, 1715, 1421, 1378, 1174, 1122, 1033, 994, 959, 839 cm⁻¹; HRMS (FAB) Calcd. for C₁₂H₂₃O₄ [MH⁺]: 231.15963. Found 231.16044.

Preparation of chiral standards

Following the above procedure, using (*S*)-2-octanol (258 µL, 1.61 mmol) or (*R*)-2-octanol (150 µL, 0.96 mmol) the corresponding diester (9% and 4%) and hemiester (79% and 51%) respectively, were obtained. Identical spectral data to that observed for racemic and *meso* standards.

Conclusions

We have shown that the choice of succinic anhydride as acylating agent may sometimes fall short of the expectation of

facilitated extraction of an acidic half ester. A closer inspection of the literature available suggests that in some cases, the formation of the diester may have been overlooked. In the present study, we showed that the outcome of the acylation of (*R,S*)-2-octanol with succinic anhydride is strongly dependent on the solvent and on the solubility of succinic acid in the latter. The outcome of the process is never the hemiester alone. And if the solubility of succinic acid in the solvent is low, the amount of hemiester rapidly decreases after reaching a peak. Similar findings for 2-butanol and 1-phenylethanol confirm that this is a general phenomenon. In our experiments, water activity was kept constant at 0.1. The amount of water that is present in each solvent at this a_w value is sufficient to promote the occurrence of pathway 4 to a point where nearly 50% of the hemiester is consumed *via* this pathway, even in the presence of the alcohol.

Acknowledgements

This work has been supported by the European Commission in the framework of the Marie Curie Research Training Network 'Green Chemistry in Supercritical Fluids: Phase Behaviour, Kinetics and Scale-up' (EC Contract No: MRTN-CT-2004-504005), Fundação para a Ciência e a Tecnologia (FCT, Portugal) and FEDER through the contracts POCI/BIO/57193/2004, POCI/QUI/57735/2004 and the grants SFRH/BD/18487/2004 (N. Lourenço) and SFRH/BD/2003 (P. Vidinha). The authors thank Prof. Urszula Domańska for help in the synthesis of $[C_2][NTf_2]$.

References

- 1 A. Liese, K. Seelbach and C. Wandrey, *Industrial Biotransformations*, Wiley-VCH, Weinheim, Germany, 2006.
- 2 K. Buchholz, V. Kasche and U. T. Bornscheuer, *Biocatalysts and Enzyme Technology*, Wiley-VCH, Weinheim, Germany, 2005.
- 3 R. A. Sheldon, *Green Chem.*, 2005, **7**, 267–278.
- 4 M. J. Earle, J. M. S. S. Esperanca, M. A. Gilea, J. N. C. Lopes, L. P. N. Rebelo, J. W. Magee, K. R. Seddon and J. A. Widegren, *Nature*, 2006, **439**, 831–834.
- 5 M. T. Reetz, W. Wiesenhöfer, G. Franciò and W. Leitner, *Adv. Synth. Catal.*, 2003, **345**, 1221–1228.
- 6 P. Lozano, T. de Diego, D. Carrié, M. Vaultier and J. L. Iborra, *Biotechnol. Prog.*, 2003, **19**, 380–382.
- 7 P. Lozano, T. de Diego, D. Carrié, M. Larnicol, M. Vaultier and J. L. Iborra, *Biotechnol. Lett.*, 2006, **28**, 1559–1565.
- 8 S. Garcia, N. M. T. Lourenço, D. Lousa, A. F. Sequeira, P. Mimoso, J. M. S. Cabral, C. M. A. Afonso and S. Barreiros, *Green Chem.*, 2004, **6**, 466–470.
- 9 D. Bianchi, P. Cesti and E. Battistel, *J. Org. Chem.*, 1988, **53**, 5531–5534.
- 10 Y. Terao, K. Tsuij, M. Murata, K. Achiwa, T. Nishio, N. Watanabe and K. Seto, *Chem. Pharm. Bull.*, 1989, **37**, 1653–1655.
- 11 M. J. Sorgedraeger, R. Malpique, F. van Rantwijk and R. A. Sheldon, *Tetrahedron-Asymmetry*, 2004, **15**, 1295–1299.
- 12 N. Bouzemi, H. Debbeche, L. Aribi-Zouiouèche and J.-C. Fiaud, *Tetrahedron Lett.*, 2004, **45**, 627–630.
- 13 J.-C. Fiaud, R. Gill, J. Legros, L. Aribi-Zouiouèche and W. A. König, *Tetrahedron Lett.*, 1992, **33**, 6967–6970; A. L. Gutman, D. Brenner and A. Boltanski, *Tetrahedron-Asymmetry*, 1993, **4**, 839–844; A. Ghanem and H. Y. Aboul-Enein, *Tetrahedron-Asymmetry*, 2004, **15**, 3331–3351; A. Zada and E. Dunkelblum, *Tetrahedron-Asymmetry*, 2006, **17**, 230–233.
- 14 M. S. Rasalkar, M. K. Potdar and M. M. Salunkhe, *J. Mol. Catal. B: Enzym.*, 2004, **27**, 267–270.
- 15 M. H. Katsoura, A. C. Polydera, L. Tsironis, A. D. Tselepis and H. Stamatis, *J. Biotechnol.*, 2006, **123**, 491–503.
- 16 S. Park and R. J. Kazlauskas, *J. Org. Chem.*, 2001, **66**, 8395–8401.
- 17 L. Greenspan, *J. Res. Natl. Bur. Stand., Sect. A*, 1977, **81A**, 89–96.
- 18 G. Bell, A. E. M. Janssen and P. J. Halling, *Enzyme Microb. Technol.*, 1997, **20**, 471–477.

Copper catalyzed oxidative alkylation of sp^3 C–H bond adjacent to a nitrogen atom using molecular oxygen in water

Olivier Baslé and Chao-Jun Li

Green Chem., 2007, **9**(10), 1047–1050 (DOI: 10.1039/b707745a)

The authors would like to add the following acknowledgement:

We are grateful to the Canada Research Chair (Tier I) foundation (to CJL), FQRNT and McGill University for support of our research.

Dilute aqueous 1-butyl-3-methylimidazolium hexafluorophosphate: properties and solvatochromic probe behaviour

Maroof Ali, Abhra Sarkar, Mohammad Tariq, Anwar Ali and Siddharth Pandey

Green Chem., 2007, **9**(11), 1252–1258 (DOI: 10.1039/b704843b)

Owing to an error in the late stages of production, Table 2 is missing from the printed version of this article.

Table 2 Density (ρ), viscosity (η), and refractive index (n) of dilute aqueous bmimPF₆ as function of temperature (T/K) at different bmimPF₆ mole fraction (X_{bmimPF_6})

X_{bmimPF_6}	0.000000	0.000318	0.000638	0.000951	0.001286
$[\rho(\text{g cm}^{-3})]^{1/2} = a + bT^{1/2}$					
r^2 (std error of fit)	0.9998 (± 0.0001)	0.9998 (± 0.0001)	0.9999 (± 0.0001)	0.9999 (± 0.0001)	0.9999 (± 0.0001)
a	1.0953	1.1045	1.1033	1.1055	1.1137
b	-5.59×10^{-3}	-6.09×10^{-3}	-5.98×10^{-3}	-6.04×10^{-3}	-6.42×10^{-3}
$\ln \eta(\text{mN m}^{-2} \text{ s}) = a + (b/T)$					
r^2 (std error of fit)	0.9985 (± 0.0052)	0.9966 (± 0.0081)	0.9966 (± 0.0082)	0.9968 (± 0.0079)	0.9966 (± 0.0083)
a	-6.4743	-6.6526	-6.7020	-6.6212	-6.6103
b	1896.05	1953.28	1970.60	1948.86	1947.36
$n = a + bT^3$					
r^2 (std error of fit)	0.9654 (± 0.0002)	0.9958 (± 0.0001)	0.9947 (± 0.0001)	0.9969 (± 0.0001)	0.9911 (± 0.0001)
a	1.3429	1.3441	1.3444	1.3435	1.3442
B	-3.78×10^{-10}	-4.14×10^{-10}	-4.07×10^{-10}	-3.64×10^{-10}	-3.79×10^{-10}

The Royal Society of Chemistry apologises for these errors and any consequent inconvenience to authors and readers.

Additions and corrections can be viewed online by accessing the original article to which they apply.

RSC eBook Collection

Access and download existing and new books from the RSC

- **Comprehensive:** covering all areas of the chemical sciences
- **Fully searchable:** advance search and filter options
- **Wide ranging:** from research level monograph to popular science book

See for yourself –
go online to search
the collection and
read selected
chapters
for free!

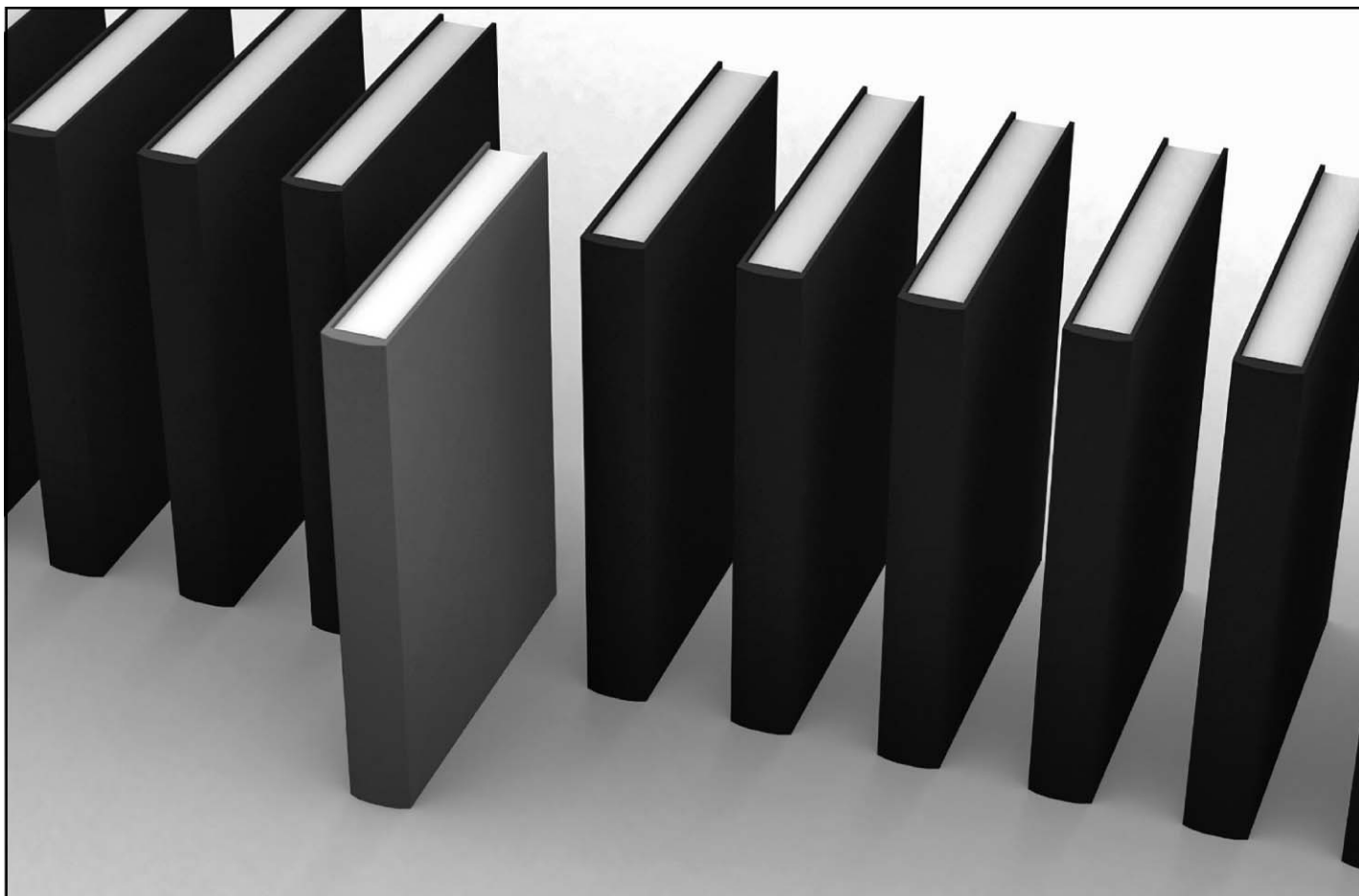


Registered Charity Number 207890

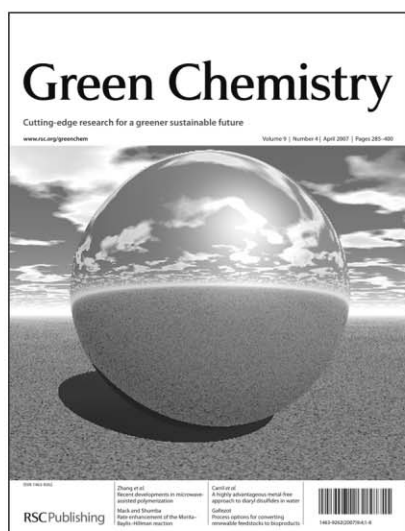
20100654

RSC Publishing

www.rsc.org/ebooks



'Green Chemistry book of choice'



Why not take advantage of free book chapters from the RSC? Through our 'Green Chemistry book of choice' scheme *Green Chemistry* will regularly highlight a book from the RSC eBook Collection relevant to your research interests. Read the latest chapter today by visiting the *Green Chemistry* website.

The RSC eBook Collection offers:

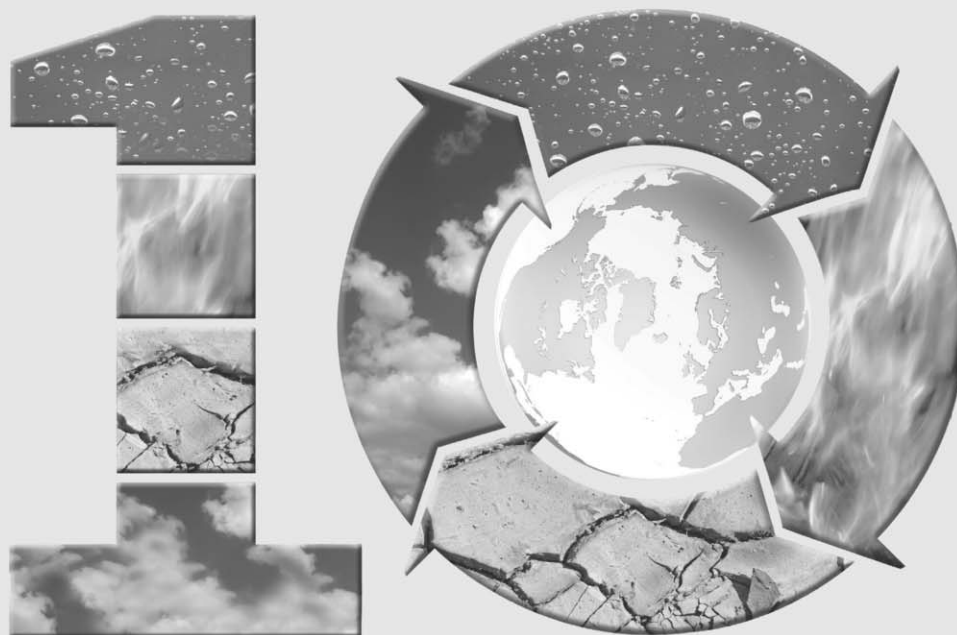
- Over 900 new and existing books
- Fully searchable
- Unlimited access

Why not take a look today? Go online to find out more!

RSC Publishing

www.rsc.org/greenchem

Registered Charity Number 207890



years of publishing!

Journal of Environmental Monitoring...



- Highly visible and cited in MEDLINE
- Accelerated publication rates, typically around 80 days
- Dedicated to the measurement of natural and anthropogenic sources of pollution with a view to assessing environmental and human health effects

Celebrating 10 years of publishing, *Journal of Environmental Monitoring* offers comprehensive and high quality coverage of multidisciplinary, international research relating to the measurement, pathways, impact and management of contaminants in all environments.

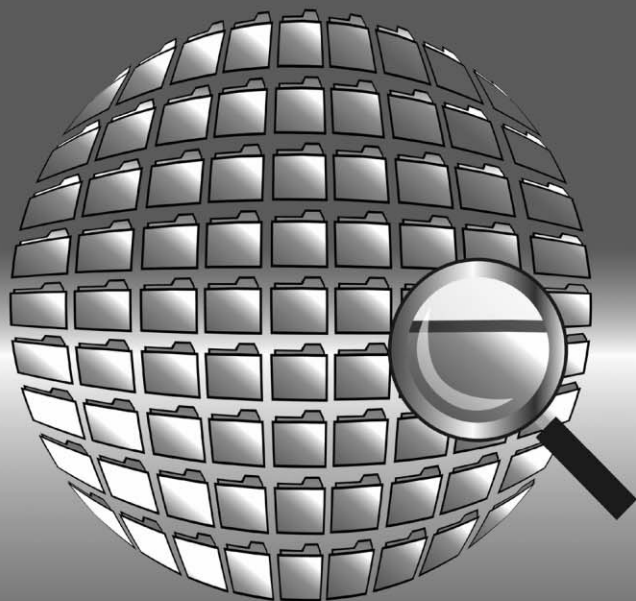
...for environmental processes and impacts!

RSC Publishing

www.rsc.org/jem

Registered Charity Number 207890

RSC Database and Current Awareness Products



- Abstracted from high quality sources
- Easy to use search functions
- Clearly displayed results
- Spanning the chemical sciences

for quick and easy searching

Graphical Databases

present search results in both text and graphical form. Titles include *Catalysts & Catalysed Reactions*, *Methods in Organic Synthesis* and *Natural Product Updates*.

Specialist Databases

review both academic and industrial literature on a wide range of hard to reach and unique information. Titles include *Chemical Hazards in Industry* and *Laboratory Hazards Bulletin*.

Analytical Abstracts

is the first stop for analytical scientists. Offering coverage on all areas of analytical and bioanalytical science. With a fresh new look, including improved search and results features, *Analytical Abstracts* offers an excellent online service.

Find out more at

RSC Publishing

www.rsc.org/databases

Registered Charity Number 207890

Specialised searching

The graphical abstracting services at the RSC are an indispensable tool to help you search the literature. Focussing on specific areas of research they review key primary journals for novel and interesting chemistry.

requires specialised tools

Catalysts & Catalysed Reactions

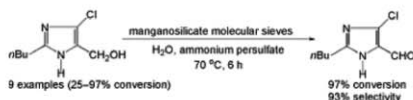
Catalysts and Catalysed Reactions covers all areas of catalysis research, with particular emphasis on chiral catalysts, polymerisation catalysts, enzymatic catalysts and clean catalytic methods.

The online database has excellent functionality. Search by: authors, products, reactants and catalysts, catalyst type and reaction type.

With Catalysts and Catalysed Reactions you can find exactly what you need. Search results include diagrams of reaction schemes. Also available as a print bulletin.



11086 The green catalytic oxidation of alcohols in water by using highly efficient manganosilicate molecular sieves
H. G. Manyar, G. S. Chauré, A. Kumar*
Green Chem., 2006, 8(4), 344-348



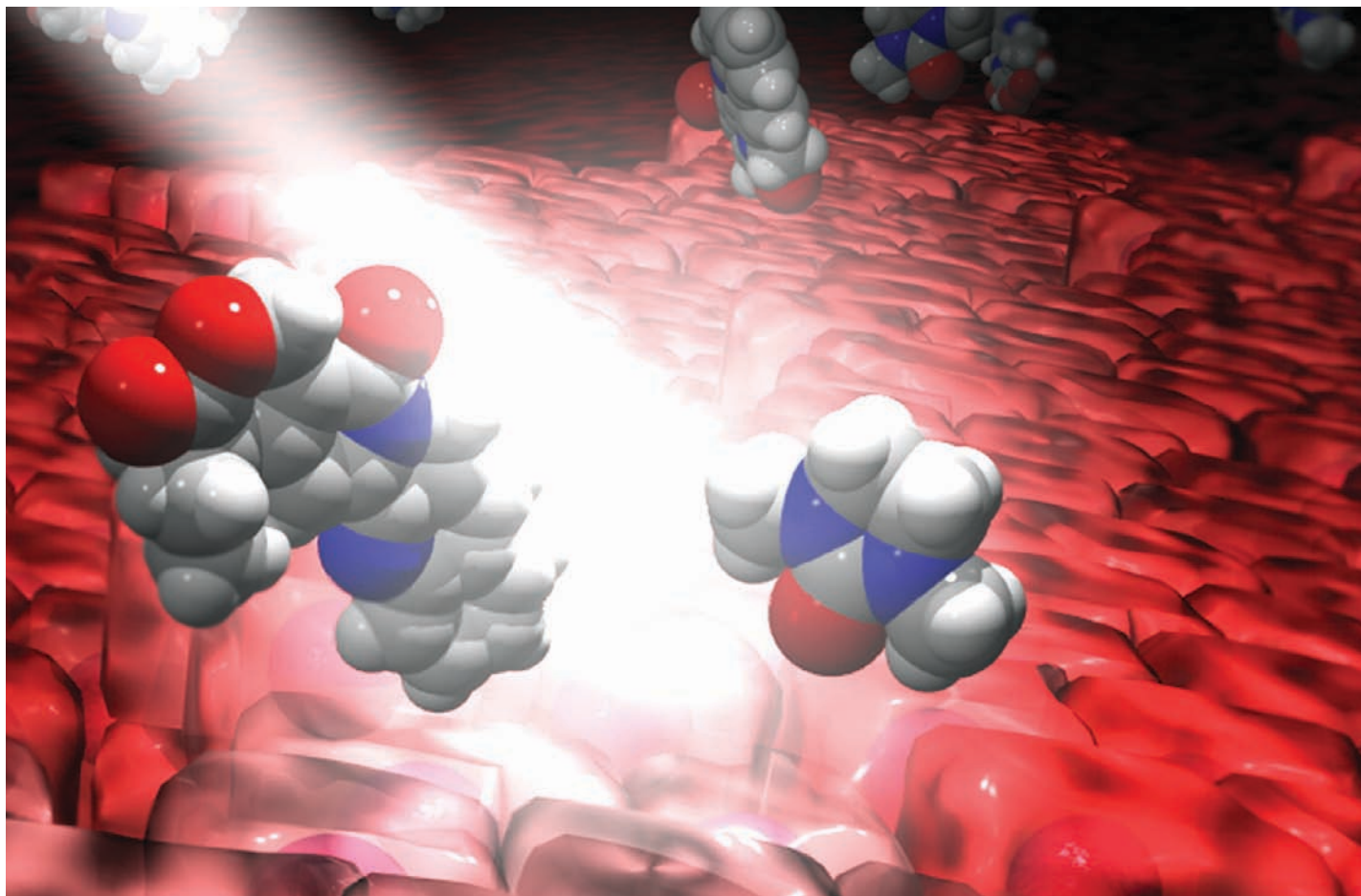
Registered charity Number 207890

For more information visit

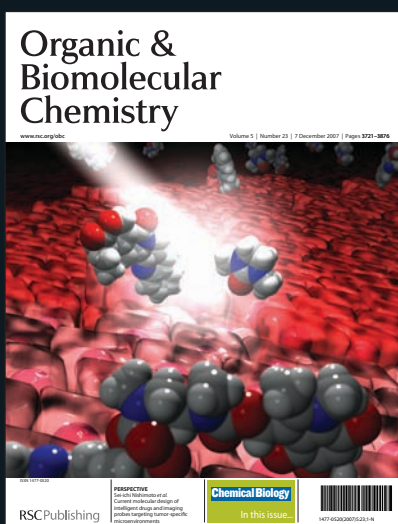
RSC Publishing

www.rsc.org/databases

Registered Charity Number 207890



Organic & Biomolecular Chemistry...



OBC has achieved tremendous success since the first issue was published in January 2003. Can any other 'young' journal boast such highly cited papers, published quickly after independent peer review to such exacting standards?

- Now one of the leading journals in the field, impact factor 2.874*
- Short publication times – average 21 days from acceptance for papers, and 13 days for communications
- Enhanced HTML articles – hyperlinked compound information, ontology terms linked to definitions and related articles, links to IUPAC Gold Book terms, and more . . .

* 2006 Thomson Scientific (ISI) Journal Citation Reports®

... *high quality - high impact!*

RSC Publishing

www.rsc.org/obc

Registered Charity Number 207890



Sit back and relax...

Online shopping is *easy* with the RSC

Whether you're looking for text books, the latest research articles, training courses, conferences or a light read for the commute... online shopping with the RSC couldn't be easier.

24/7 access: The RSC online shop gives you continuous access to class leading products and services, expertly tailored to cater for your training and educational needs.

Browse and buy: Visit our shop to browse over 750 book titles, subscribe or purchase an individual article in one of our journals, join or renew your RSC membership, or register to attend a conference or training event.

Gift ideas: If you're looking for gift ideas, look no further. In our online shop you'll find everything from popular science books like *The Age of the Molecule* and the inspirational *Elegant Solutions* from award winning writer, Philip Ball, to our stunning Visual Elements Periodic Table wall chart and jigsaw.

With secure online payment you can shop online with confidence.

The RSC has so much to offer...**why not go online today?**

RSC Publishing

www.rsc.org/shop

Registered Charity Number 207890

19120654a